



Cape Peninsula  
University of Technology

**MULTIVARIABLE CONTROL OF AN INDUSTRIAL DEBUTANIZER DISTILLATION  
PROCESS**

**by**

**Andisiwe Mbadamana**

**Thesis submitted in fulfilment of the requirements for the degree**

**Master of Engineering: Electrical Engineering**

**in the Faculty of Engineering and the Built Environment**

**at the Cape Peninsula University of Technology**

**Supervisor: Dr. C. Kriger**

**Co-supervisor: Dr. Y. D. Mfoumboulou**

**Bellville**

**November 2021**

**CPUT copyright information**

The dissertation/thesis may not be published either in part (in scholarly, scientific, or technical journals), or as a whole (as a monograph), unless permission has been obtained from the University.

## DECLARATION

I, ANDISIWE MBADAMANA, declare that the contents of this dissertation/thesis represent my own unaided work, and that the dissertation/thesis has not previously been submitted for academic examination towards any qualification. Furthermore, it represents my own opinions and not necessarily those of the Cape Peninsula University of Technology.

  
Andisiwe Mbadamana  
ASTRON ENERGY 70022369  
Technical Service - E & I

March 2022

---

**Signed**

---

**Date**

## **ABSTRACT**

Most processes encountered in the petrochemical industry are coupled and multivariable in nature. Control loops in multivariable control systems tend to interact with one another where a change in one input variable affects multiple other output variables. This is referred to as signal coupling due to process interactions. Control systems capable of providing satisfactory performance for such processes typically require the use of nontrivial multivariable controller design techniques. This thesis discusses the development of two control strategies suitable for multivariable processes; decentralized proportional-integral-derivative (PID) control and centralized model predictive control (MPC).

Among the many control technologies available in the market today, the Proportional-Integral-Derivative (PID) controller is the most widely used controller in industry for its simplicity and ease of implementation with relatively low-cost hardware, providing satisfactory performance for most control applications encountered in industry. The decentralized PID control system is designed using mathematical tools such as the relative gain array (RGA) and the PID controller gain selection is facilitated using the internal model control (IMC) technique. The control loop interactions are compensated by making use of decoupling control techniques. This research presents an opportunity to better understand the important design features offered by the internal model control PID design technique that can be useful for industrial practitioners.

Model predictive control (MPC) is an advanced control technique that makes use of a dynamic process model for prediction and process control. Model predictive control was first introduced in the late 1970s and has since found extensive use in the petrochemical industry, particularly in crude oil refining facilities. Centralized model predictive control is designed to handle process interactions inherently and to incorporate constraints on both the manipulated and controlled variables. This research provides the study of tuning parameter trade-offs that industrial practitioners often must make in designing model predictive controllers.

The work performed in this thesis includes the development of a dynamic transfer function model of a debutanizer column from step response coefficients exported from an industrial real-life operating plant for study in the MATLAB/Simulink environment. Both control strategies developed in this thesis, decentralized PID control and centralized MPC control, are applied on the dynamic model of the industrial debutanizer distillation process that is part of a Gas Recovery Unit (GRU). A GRU forms a major part of a refinery's Fluidized Catalytic Cracking Unit (FCCU). FCCUs convert a low value feedstock mixture into high value product streams. The main purpose of a gas recovery plant in the FCCU is to extract as much valuable liquid product from the overhead vapor stream of the FCCU main fractionator as possible to be treated into Liquefied Petroleum Gas (LPG) and gasoline product streams. The debutanizer distillation process studied in this research is used to separate butane and propane from pentane and heavier hydrocarbons used to produce gasoline.

The work further develops a testbed for real-time implementation of a closed-loop system in a Hardware-in-the-Loop (HiL) configuration. Hardware-in-the-Loop configurations are essential in facilitating learning for process control students in the academic community to aid their understanding of theoretical concepts taught and the work developed in this research furthers such an objective.

*Key words: distillation control, binary distillation control, debutanizer control, proportional-integral-derivative control, decoupling control, multi-loop control, multivariable process control, model predictive control, dynamic matrix control, multivariable predictive control, real-time Hardware-in-the-Loop (HiL).*

## **ACKNOWLEDGEMENTS**

### **I wish to thank:**

- The Executive Management of the Centre for Substation Automation and Energy Management Systems (CSAEMS), for the immense privilege accorded to me to conduct my research under their capable stewardship during the past four years. It has been an enriching experience.
- Dr. Carl Kriger and Dr. Yohan Darcy Mfoumboulou for their supervision and significant contributions they have made to the work done in connection with this thesis.
- Prof. Raynitchka Tzoneva, for her immeasurable contribution to the development of this research. No words can express my gratitude toward her.
- The Management of Astron Energy South Africa for affording me the opportunity and financial support to pursue this research.
- All others not mentioned by name who have in some way rendered their support to the work done in connection with this thesis.

The financial assistance of Astron Energy South Africa towards this research is acknowledged. Opinions expressed in this thesis and the conclusions arrived at, are those of the author, and are not necessarily to be attributed to Astron Energy South Africa.

## **DEDICATION**

To God, the source of all my abilities and to my late grandmother, Lala Ngoxolo Mbongwe.

Declaration	ii
Abstract	iii
Acknowledgements	v
Dedication	vi
Glossary	xxi

## **CHAPTER ONE: INTRODUCTION**

1.1. Introduction	1
1.2. Problem Statement	2
1.2.1. Sub-problem one	2
1.2.2. Sub-problem two	2
1.2.3. Sub-problem three	2
1.2.4. Sub-problem four	3
1.2.5. Sub-problem five	3
1.3. Research Aim and Objectives	3
1.3.1. Aim	3
1.3.2. Objectives	3
1.4. Research Questions	4
1.5. Hypothesis	4
1.6. Delimitation of Research	4
1.6.1. Within the Scope	4
1.6.2. Beyond the scope	5
1.7. Motivation for the Research Project	5
1.8. Assumptions	6
1.9. Thesis Outline	6
1.10. Conclusion	7

## **CHAPTER TWO: LITERATURE REVIEW**

2.1. Introduction	8
2.2. Literature search	8
2.3. Literature review of existing papers on distillation process control	10
2.3.1. Existing papers on distillation process control	10
2.3.2. Comparative analysis and discussion on the developments of the existing literature on distillation process control	16
2.4. Literature review of existing papers on multivariable control	17
2.4.1. Existing papers on multivariable control	18
2.4.2. Comparative analysis and discussion on the developments of the existing literature on multivariable control	23

2.5.	Literature review of existing papers on model predictive control and application on multivariable control systems	24
2.5.1.	Existing papers on model predictive control and application on multivariable control systems	25
2.5.2.	Comparative analysis and discussion on the developments of the existing literature on model predictive control and applications on multivariable control systems	35
2.6.	System development process and system architecture based on literature	39
2.7.	Conclusion	42

### **CHAPTER THREE: CONTROLLER DESIGN CONCEPTS**

3.1.	Introduction	43
3.2.	Relative gain array (RGA)	43
3.3.	Decoupling control	45
3.4.	PID controller design	48
3.4.1.	Model order reduction	48
3.4.2.	IMC-PID controller	49
3.5.	Model predictive control (MPC)	51
3.5.1.	Prediction model for single-input single-output (SISO) systems	54
3.5.2.	Prediction model for multiple-input multiple-output (MIMO) systems	57
3.5.3.	MPC Control Law	58
3.5.4.	Selection of Design Parameters	61
3.6.	Conclusion	62

### **CHAPTER FOUR: DEBUTANIZER DISTILLATION PROCESS IDENTIFICATION AND MODELLING**

4.1.	Introduction	64
4.2.	Debutanizer Distillation Process Description	65
4.2.1.	International Union of Pure and Applied Chemistry (IUPAC) Nomenclature	65
4.2.2.	Gas recovery unit (GRU) and debutanizer distillation process description	65
4.2.3.	Debutanizer distillation process control objectives	66
4.3.	Debutanizer distillation model identification	67
4.4.	Procedure for the development of transfer functions in MATLAB	73
4.5.	Conclusion	92

### **CHAPTER FIVE: DECENTRALIZED PID CONTROLLER DESIGN**

5.1.	Introduction	93
------	--------------	----



5.2.	Reduced second order debutanizer distillation models	93
5.3.	Relative Gain Array (RGA) for the debutanizer second order model	95
5.4.	Decoupling compensators for the second order debutanizer distillation process model	101
5.5.	PID controller design for the second order model with IMC	103
5.5.1.	Model reduction for the second order debutanizer model	103
5.5.2.	IMC controller design for the second order debutanizer model	107
5.6.	Simulation case study	110
5.6.1.	Transient behaviour of the second order debutanizer distillation process	114
5.6.2.	Discussion of the results	122
5.7.	Conclusion	124

## **CHAPTER SIX: MPC CONTROLLER DESIGN METHODS**

6.1.	Introduction	125
6.2.	MPC control system structure	126
6.3.	MPC controller development in MATLAB/Simulink	134
6.3.1.	MPC controller scale factors	134
6.3.2.	Prediction horizon, control horizon and sampling time	135
6.3.3.	Input and output constraints and constraints softening factors	136
6.3.4.	Reference tracking and increment suppression tuning weights	137
6.3.5.	Step-by-step design procedure for MPC controller design in Simulink	138
6.4.	Simulation case study in Simulink	151
6.4.1.	Transient behaviour of the seventh order debutanizer distillation process	152
6.4.2.	Transient behaviour of the seventh order debutanizer distillation process under the influence of unmeasured disturbances	159
6.4.3.	Discussion of the results	166
6.5.	Conclusion	173

## **CHAPTER SEVEN: REAL-TIME IMPLEMENTATION**

7.1.	Introduction	174
7.2.	MATLAB/Simulink	174
7.2.1.	Scaling of decentralized PID controller input and output signals	175
7.2.2.	Simulink model of the second order decentralized PID controllers	176
7.2.3.	Seventh order Simulink model	180
7.3.	TwinCAT	185
7.3.1.	Simulink to Beckhoff TwinCAT 3 model transformation procedure	186

7.4.	LabVIEW	199
7.5.	Hardware-in-the-loop (HiL) configuration for the second order system simulation	201
7.6.	Real-time simulation of the second order debutanizer distillation process model	206
7.6.1.	Performance analysis and discussion of results for the second order system	217
7.7.	Real-time simulation of the seventh order Debutanizer distillation process	218
7.7.1.	Performance analysis and discussion of results for the seventh order system	229
7.8.	Conclusion	231

## **CHAPTER EIGHT: CONCLUSION, THESIS DELIVERABLES, APPLICATIONS AND FUTURE WORK**

8.1.	Introduction	232
8.2.	Thesis aim and objectives	233
8.2.1.	Objectives	233
8.3.	Comprehensive literature review	234
8.4.	Thesis deliverables	235
8.4.1.	Mathematical modelling of the debutanizer distillation process model in the MATLAB/Simulink environment	235
8.4.2.	Design of the dynamic decoupling and decentralized control for the debutanizer distillation process	235
8.4.3.	Design of the model predictive control for the debutanizer distillation process	236
8.4.4.	Development of a transformation procedure for the developed software from the MATLAB/Simulink environment to Beckhoff TwinCAT 3.1 real-time environment for real-time simulation	236
8.4.5.	Development of a hardware-in-the-loop testbed and closed-loop real-time simulation	237
8.5.	Developed software	237
8.6.	Application of the results from this thesis	238
8.7.	Future work	239
8.8.	Publications	239
8.9.	Conclusion	239

<b>REFERENCES</b>	<b>241</b>
-------------------	------------

## LIST OF FIGURES

Figure 2.1: Bar graph of the reviewed publications	9
Figure 2.2: Number of papers per year covering the topic of distillation process control	10
Figure 2.3: Number of papers per year covering the topic of multivariable control	18
Figure 2.4: Number of papers per year covering the topic of model predictive control and application on multivariable control systems	25
Figure 2.5: Proposed system development process and system architecture	41
Figure 3.1: Relative gain of loop pair $M_3-C_3$ (Edgar H Bristol, 1966)	44
Figure 3.2: Second order multivariable system without decoupling (Wade, 1997)	46
Figure 3.3: Incorporating decoupling controllers (Muga, 2015)	47
Figure 3.4: Second order multivariable system without decoupling (Wade, 1997)	48
Figure 3.5: Practical Internal Model Control block diagram with low pass filter $f(s)$ adapted from (Saxena and Hote, 2012)	50
Figure 3.6: Hierarchy of process control activities (Seborg et al., 2004)	52
Figure 3.7: Model predictive control block diagram (Seborg et al., 2004)	53
Figure 4.1: Debutanizer simplified process flow diagram (PFD) (Sadeghbeigi, 2000)	66
Figure 4.2: Summary of the model development process (BluESP, 2018)	68
Figure 4.3: The MATLAB application starting	73
Figure 4.4: Import data	73
Figure 4.5: Select the Excel spreadsheet	74
Figure 4.6: Column vectors	74
Figure 4.7: Successful import	74
Figure 4.8: Imported data in MATLAB workspace	75
Figure 4.9: Creating data object for SIMO coefficients	75
Figure 4.10: Creating data objects validation data	76
Figure 4.11: Opening System Identification app	76
Figure 4.12: System Identification	77
Figure 4.13: Importing data object	77
Figure 4.14: Data object name	78
Figure 4.15: Import validation data	78
Figure 4.16: Successful import of data objects	79
Figure 4.17: Transfer function models	80
Figure 4.18: Number of poles and zeros	80
Figure 4.19: Identification progress	81
Figure 4.20: Model views	82
Figure 4.21: Identified model review and rename	83
Figure 4.22: System identification models to MATLAB workspace	84

<b>Figure 4.23: Comparing the original and matlab models of the debut_diff_press output</b>	92
<b>Figure 5.1: Decoupled second order debutanizer distillation process model (Wade, 1997)</b>	101
<b>Figure 5.2: Process flowchart for the PID controller simulation study</b>	111
<b>Figure 5.3: Second order debutanizer distillation process model in simulink</b>	113
<b>Figure 5.4: Case #5.3.1 dynamic response</b>	115
<b>Figure 5.5: Case #5.3.2 dynamic response</b>	115
<b>Figure 5.6: Case #5.3.3 dynamic response</b>	116
<b>Figure 5.7: Case #5.3.4 dynamic response</b>	116
<b>Figure 5.8: Case #5.3.5 dynamic response</b>	117
<b>Figure 5.9: Simulink model of the decoupled second order multivariable system</b>	118
<b>Figure 5.10: Case #5.4.1 dynamic response</b>	119
<b>Figure 5.11: Case #5.4.2 dynamic response</b>	120
<b>Figure 5.12: Case #5.4.3 dynamic response</b>	120
<b>Figure 5.13: Case #5.4.4 dynamic response</b>	121
<b>Figure 5.14: Case #5.4.5 dynamic response</b>	121
<b>Figure 5.15: LPG c5 concentration (Mol %) exhibiting a -60% undershoot during a -0.04 Mol % step change in the presence of a 5e-06 Mol% White Noise disturbance amplitude</b>	123
<b>Figure 6.1: Seventh order debutanizer distillation process model block diagram</b>	132
<b>Figure 6.2: Closed-loop control structure for the MPC controller</b>	133
<b>Figure 6.3: Simulink application</b>	138
<b>Figure 6.4: Seventh order step response prediction model of the debutanizer distillation process configured in simulink</b>	139
<b>Figure 6.5: Simulink model part 1 - MPC controller</b>	140
<b>Figure 6.6: Simulink model part 2 - DCS regulatory PID controllers</b>	141
<b>Figure 6.7: Simulink model part 3 - ambient temperature disturbance</b>	141
<b>Figure 6.8: Simulink model part 4 - debutanizer distillation process transfer functions</b>	142
<b>Figure 6.9: MPC controller block parameters</b>	143
<b>Figure 6.10: MPC designer app</b>	143
<b>Figure 6.11: MPC controller structure</b>	144
<b>Figure 6.12: Trim model</b>	144
<b>Figure 6.13: Operating point specification</b>	145
<b>Figure 6.14: Trim progress viewer</b>	145
<b>Figure 6.15: View/edit operating point</b>	146
<b>Figure 6.16: Initialize model</b>	146

<b>Figure 6.17: Define and linearize model</b>	<b>147</b>
<b>Figure 6.18: I/O attributes</b>	<b>147</b>
<b>Figure 6.19: Input and output attributes settings</b>	<b>148</b>
<b>Figure 6.20: Prediction horizon, and control horizon</b>	<b>148</b>
<b>Figure 6.21: Constraints</b>	<b>148</b>
<b>Figure 6.22: Constraints settings</b>	<b>149</b>
<b>Figure 6.23: Tuning weights</b>	<b>149</b>
<b>Figure 6.24: Tracking and increment suppression weights</b>	<b>149</b>
<b>Figure 6.25: Closed-loop performance tuning</b>	<b>150</b>
<b>Figure 6.26: Review MPC design</b>	<b>150</b>
<b>Figure 6.27: Update and simulate drop down menu</b>	<b>150</b>
<b>Figure 6.28: Update block and run simulation</b>	<b>150</b>
<b>Figure 6.29: Process flowchart for the mpc controller simulation study</b>	<b>152</b>
<b>Figure 6.30: Case #6.9.1 – dynamic step response</b>	<b>154</b>
<b>Figure 6.31: Case #6.9.2 – dynamic step response</b>	<b>155</b>
<b>Figure 6.32: Case #6.9.3 – dynamic step response</b>	<b>156</b>
<b>Figure 6.33: Case #6.9.4 – dynamic step response</b>	<b>157</b>
<b>Figure 6.34: Case #6.9.5 – dynamic step response</b>	<b>158</b>
<b>Figure 6.35: Disturbance case #6.11.1 – dynamic step response</b>	<b>161</b>
<b>Figure 6.36: Disturbance case #6.11.2 – dynamic step response</b>	<b>162</b>
<b>Figure 6.37: Disturbance case #6.11.3 – dynamic step response</b>	<b>163</b>
<b>Figure 6.38: Disturbance case #6.11.4 – dynamic step response</b>	<b>164</b>
<b>Figure 6.39: Disturbance case #6.11.5 – dynamic step response</b>	<b>165</b>
<b>Figure 6.40: Step response performance metrics adapted from (Nowakova and Pokorny, 2020)</b>	<b>166</b>
<b>Figure 6.41: LGP C5 concentration (Mol %) exhibiting a -140% undershoot during a -0.49 Mol % step change</b>	<b>168</b>
<b>Figure 6.42: Spikes due to interactions on the rest of the controlled outputs at time 200 seconds due to an influence of a -2 kpa step change in the LCN RVP setpoint with all the other setpoints kept constant</b>	<b>169</b>
<b>Figure 6.43: Spikes due to interactions on the rest of the controlled outputs at time 900 seconds due to an influence of a +0.2 Mol% step change in the LPG C5 concentration setpoint with all the other setpoints kept constant</b>	<b>169</b>
<b>Figure 6.44: Spikes due to interactions on the rest of the controlled outputs at time 1100 seconds due to an influence of a +220 kPa step change in the overhead drum pressure setpoint with all the other setpoints kept constant</b>	<b>170</b>

<b>Figure 6.45:</b> Spikes due to interactions on the rest of the controlled outputs at time 1300 seconds due to an influence of a +119 kPa step change in the overhead drum pressure SV-PV gap setpoint with all the other setpoints kept constant	170
<b>Figure 6.46:</b> Spikes due to interactions on the rest of the controlled outputs at time 1500 seconds due to an influence of a -8 kPa step change in the debutanizer differential pressure setpoint with all the other setpoints kept constant	171
<b>Figure 6.47:</b> Spikes due to interactions on the rest of the controlled outputs at time 1500 seconds due to an influence of a +42 % step change in the debutanizer reboiler valve position setpoint with all the other setpoints kept constant	171
<b>Figure 6.48:</b> Spikes due to interactions on the rest of the controlled outputs at time 1800 seconds due to an influence of a -7 DegC step change in the tray 24 temperature setpoint with all the other setpoints kept constant	172
<b>Figure 7.1:</b> Simulink second order PID controller model	177
<b>Figure 7.2:</b> Conversion of RVP process value raw input into engineering units in simulink	178
<b>Figure 7.3:</b> Conversion of RVP setpoint value raw input into engineering units in simulink	178
<b>Figure 7.4:</b> Conversion of LPG C5 setpoint value raw input into engineering units in simulink	178
<b>Figure 7.5:</b> Conversion of LPG C5 process value raw input into engineering units in simulink	179
<b>Figure 7.6:</b> Conversion of RVP PID controller manipulated variable engineering output into raw value in simulink	179
<b>Figure 7.7:</b> Conversion of LPG C5 PID controller manipulated variable engineering output into raw value in simulink	179
<b>Figure 7.8:</b> Seventh order step response prediction model of the debutanizer distillation process configured in simulink	181
<b>Figure 7.9:</b> Simulink model part 1 - MPC controller	182
<b>Figure 7.10:</b> Simulink model part 2 - DCS regulatory pid controllers	183
<b>Figure 7.11:</b> Simulink model part 3 - ambient temperature disturbance	183
<b>Figure 7.12:</b> Simulink model part 4 - debutanizer distillation process transfer functions	184
<b>Figure 7.13:</b> Overview of the hardware and software architecture for the seventh order debutanizer closed loop control system	185

<b>Figure 7.14: TwinCAT 3 extended automation engineering (XAE) philosophy (Beckhoff automation, 2020a)</b>	<b>186</b>
<b>Figure 7.15: Flow diagram of the model transformation from Simulink to TwinCAT 3</b>	<b>187</b>
<b>Figure 7.16: Open simulink</b>	<b>187</b>
<b>Figure 7.17: Code generation options in simulink</b>	<b>187</b>
<b>Figure 7.18: Simulink solver</b>	<b>188</b>
<b>Figure 7.19: Target file selection</b>	<b>188</b>
<b>Figure 7.20: System target file browser</b>	<b>189</b>
<b>Figure 7.21: Code generation options complete</b>	<b>189</b>
<b>Figure 7.22: Build model in simulink</b>	<b>190</b>
<b>Figure 7.23: Starting build procedure</b>	<b>190</b>
<b>Figure 7.24: Build successful</b>	<b>190</b>
<b>Figure 7.25: Start TwincCAT</b>	<b>190</b>
<b>Figure 7.26: Open or create new TwinCAT project</b>	<b>191</b>
<b>Figure 7.27: Adding new TcCOM objects</b>	<b>191</b>
<b>Figure 7.28: Expand custom modules</b>	<b>192</b>
<b>Figure 7.29: Inserting simulink model tccom module</b>	<b>192</b>
<b>Figure 7.30: Simulink model block diagram in twincat</b>	<b>193</b>
<b>Figure 7.31: Creating an execution task</b>	<b>193</b>
<b>Figure 7.32: Rename task</b>	<b>194</b>
<b>Figure 7.33: Task has been successfully created</b>	<b>194</b>
<b>Figure 7.34: Linking the tccom object to the execution task</b>	<b>194</b>
<b>Figure 7.35: Scanning for PLC I/O hardware</b>	<b>195</b>
<b>Figure 7.36: PLC I/O modules have been successfully loaded</b>	<b>195</b>
<b>Figure 7.37: Opening plc i/o points</b>	<b>196</b>
<b>Figure 7.38: Linking the plc i/o to the model i/o</b>	<b>196</b>
<b>Figure 7.39: PLC I/O have been successfully linked</b>	<b>197</b>
<b>Figure 7.40: Activate configuration</b>	<b>197</b>
<b>Figure 7.41: Simulink model of the seventh order debutanizer distillation process</b>	<b>198</b>
<b>Figure 7.42: Block diagram of the second order debutanizer distillation process model in labview</b>	<b>199</b>
<b>Figure 7.43: Front panel of the second order debutanizer distillation process model in LabVIEW</b>	<b>200</b>
<b>Figure 7.44: Overview of the hardware and software architecture for the second order debutanizer closed loop control system</b>	<b>201</b>
<b>Figure 7.45: Connections between systems in the Beckhoff PLC and the compactrio</b>	<b>202</b>

<b>Figure 7.46: Signal information flow between the interconnected physical systems</b>	203
<b>Figure 7.47: NI-9215 and EI3004 typical wiring diagram</b>	203
<b>Figure 7.48: NI-9263 and EI4034 typical wiring diagram</b>	204
<b>Figure 7.49: Connection of the CP2919 multi-touch control panel to the Beckhoff PLC</b>	204
<b>Figure 7.50: Physical system connected in a hardware-in-the-loop configuration</b>	205
<b>Figure 7.51: Personal computers where the development environments are installed</b>	205
<b>Figure 7.52: Flowchart for the second order system hardware-in-the-loop real-time simulation</b>	206
<b>Figure 7.53: Case #7.5.1 – LCN_RVP dynamic response to a -2 kPa setpoint step change from 65 kPa to 63 kPa and LPG C5 concentration dynamic response to a +0.2 Mol% setpoint step change from 0.1 Mol% to 0.3 Mol% steady state</b>	208
<b>Figure 7.54: Case #7.5.2 – LCN_RVP dynamic response to a -3 kPa setpoint step change from 63 kPa to 60 kPa steady state</b>	209
<b>Figure 7.55: Case #7.5.3 – LCN_RVP dynamic response to a +8 kPa setpoint step change from 60 kPa to 68 kPa steady state and LPG_C5 concentration dynamic response to a -0.55 Mol% setpoint step change from 0.6 Mol % to 0.05 Mol % steady state</b>	210
<b>Figure 7.56: Case #7.5.4 – LCN_RVP dynamic response to a +5 kPa setpoint step change from 68 kPa to 73 kPa steady state and LPG_C5 concentration dynamic response to a -0.04 Mol% setpoint step change from 0.05 Mol % to 0.01 Mol % steady state</b>	211
<b>Figure 7.57: Case #7.5.5 – LCN_RVP dynamic response to a -7.5 kPa setpoint step change from 73 kPa to 65.5 kPa steady state and LPG_C5 concentration dynamic response to a +0.14 Mol% setpoint step change from 0.01 Mol % to 0.15 Mol % steady state</b>	212
<b>Figure 7.58: Second order debutanizer process model block diagram with disturbances</b>	213
<b>Figure 7.59: Sase #7.6.1 – LCN RVP dynamic response to a -2 kPa setpoint step change from 65 kPa to 63 kPa steady state with an input disturbance amplitude of 1 and output disturbance amplitude of 0.01 and LPG_C5 concentration dynamic response to a +0.2 Mol% setpoint step change from 0.1 Mol % to 0.3 Mol % steady state with an input disturbance amplitude of 10 and output disturbance amplitude</b>	214
<b>Figure 7.60: Case #7.6.2 - LCN RVP dynamic response to a -2 kPa setpoint step change from 65 kPa to 63 kPa steady state with an input disturbance</b>	



amplitude of 2 and output disturbance amplitude of 0.1 and LPG_C5 concentration dynamic response to a +0.3 Mol% setpoint step change from 0.3 Mol % to 0.6 Mol % steady state with an input disturbance amplitude of 20 and output disturbance amplitude of 0.01	215
<b>Figure 7.61:</b> Case #7.6.3 – LCN RVP dynamic response to a +8 kPa setpoint step change from 60 kPa to 68 kPa steady state with an input disturbance amplitude of 3 and output disturbance amplitude of 1 and LPG_C5 concentration dynamic response to a -0.55 Mol% setpoint step change from 0.6 Mol % to 0.05 Mol % steady state with an input disturbance amplitude of 30 and output disturbance amplitude of 0.1	216
<b>Figure 7.62:</b> Flowchart for the seventh order system real-time simulation	219
<b>Figure 7.63:</b> Case #7.10.1 – dynamic step response to a -2 kPa step change in the LCN RVP setpoint; a +0.2 Mol% step change in the LPG_C5 concentration setpoint; a +220 kPa step change in the overhead drum pressure setpoint; a +119 kPa step change in the overhead drum pressure SV-PV gap setpoint; a -8 kPa step change in the debutanizer differential pressure setpoint; a +7 % step change in the debutanizer reboiler valve position setpoint and a -7 DegC step change in the tray 24 temperature setpoint	221
<b>Figure 7.64:</b> Case #7.10.2 – dynamic step response to a -3 kPa step change in the LCN RVP setpoint; a +0.2 Mol% step change in the LPG C5 concentration setpoint; a -300 kPa step change in the overhead drum pressure setpoint; a -200 kPa step change in the overhead drum pressure SV-PV gap setpoint; a -4 kPa step change in the debutanizer differential pressure setpoint; a +35 % step change in the debutanizer reboiler valve position setpoint and a -4 DegC step change in the tray 24 temperature setpoint	222
<b>Figure 7.65:</b> Case #7.10.3 – dynamic step response to a +3 kPa step change in the LCN RVP setpoint; a -0.49 Mol% step change in the LPG C5 concentration setpoint; a -100 kPa step change in the overhead drum pressure setpoint; a -120 kPa step change in the overhead drum pressure SV-PV gap setpoint; a +14 kPa step change in the debutanizer differential pressure setpoint; a -25 % step change in the debutanizer reboiler valve position setpoint and a +14 DegC step change in the tray 24 temperature setpoint	223
<b>Figure 7.66:</b> Case #7.10.4 – dynamic step response to a +3 kPa step change in the LCN RVP setpoint; a +0.4 Mol% step change in the LPG C5 concentration setpoint; a +120 kPa step change in the overhead drum pressure setpoint;	

a -25 kPa step change in the overhead drum pressure SV-PV gap setpoint;  
a +4 kPa step change in the debutanizer differential pressure setpoint; a -  
20 % step change in the debutanizer reboiler valve position setpoint and a  
+4 DegC step change in the tray 24 temperature setpoint 224

**Figure 7.67:** Case #7.10.5 – dynamic step response to a -1 kPa step change in the LCN RVP setpoint; a -0.31 Mol% step change in the LPG C5 concentration setpoint; a +60 kPa step change in the overhead drum pressure setpoint; a +226 kPa step change in the overhead drum pressure SV-PV gap setpoint; a -6 kPa step change in the debutanizer differential pressure setpoint; a +3 % step change in the debutanizer reboiler valve position setpoint and a -7 DegC step change in the tray 24 temperature setpoint 225

**Figure 7.68:** Disturbance case 7.11.1 – dynamic step response to a -2 kPa step change in the LCN RVP setpoint; a +0.2 Mol% step change in the LPG C5 concentration setpoint; a +220 kPa step change in the overhead drum pressure setpoint; a +119 kPa step change in the overhead drum pressure SV-PV gap setpoint; a -8 kPa step change in the debutanizer differential pressure setpoint; a +7 % step change in the debutanizer reboiler valve position setpoint and a -7 Degc step change in the tray 24 temperature setpoint 227

**Figure 7.69:** Disturbance case 7.11.2 – dynamic step response to a -2 kPa step change in the LCN RVP setpoint; a +0.2 Mol% step change in the LPG C5 concentration setpoint; a +220 kPa step change in the overhead drum pressure setpoint; a +119 kPa step change in the overhead drum pressure sv-pv gap setpoint; a -8 kPa step change in the debutanizer differential pressure setpoint; a +7 % step change in the debutanizer reboiler valve position setpoint and a -7 DegC step change in the tray 24 temperature setpoint 228

## LIST OF TABLES

Table 2.1: Existing papers on distillation process control	11
Table 2.2: Existing papers on multivariable control	19
Table 2.3: Existing papers on model predictive control and applications on multivariable control systems	26
Table 3.1: MPC design parameters	61
Table 4.1: Alkane hydrocarbons (Flowers et al., 2016)	65
Table 4.2: Step response models for the debutanizer distillation process	70
Table 4.3: List and descriptions of variables used in the model	72
Table 4.4: Step response models from the MATLAB transfer functions	89
Table 4.5: Steady state gain comparisons between original model and MATLAB system identification model results	90
Table 5.1: Second order debutanizer distillation process model	94
Table 5.2: IMC PID controller tuning parameters	110
Table 5.3: Simulation case study to investigate the system transient behaviour	114
Table 5.4: Simulation case study to investigate the influence of unmeasured disturbances	119
Table 5.5: Analysis of the performance indicators for each of the setpoint variations without disturbances	122
Table 5.6: Analysis of the performance indicators for each of the setpoint variations with addition of disturbances	123
Table 6.1: Seventh order debutanizer distillation process model	130
Table 6.2: Manipulated variable scale factors	134
Table 6.3: Controlled outputs scale factors	134
Table 6.4: Prediction horizon, control horizon and sampling time	135
Table 6.5: Controlled output constraints	136
Table 6.6: Constraint softening	136
Table 6.7: Controlled output reference tracking weights	137
Table 6.8: Control input tracking and increment suppression weights	137
Table 6.9: Case study of set points for the seventh order system	153
Table 6.10: Simulation case study to investigate the influence of unmeasured disturbances	159
Table 6.11: Analysis of the performance metrics for each of the setpoint variations	167
Table 7.1: Simulink model input scaling	176
Table 7.2: Model output scaling	176
Table 7.3: LabVIEW block diagram object descriptions	200
Table 7.4: Summary of the system hardware and software components	202
Table 7.5: Case study of set points for the second order system	207

<b>Table 7.6: Pulse generator input disturbance parameters</b>	<b>213</b>
<b>Table 7.7: Random noise generator output disturbance parameters</b>	<b>213</b>
<b>Table 7.8: Case study of disturbance rejection for the second order system</b>	<b>213</b>
<b>Table 7.9: Analysis of the performance indicators for each of the setpoint variations for the second order system</b>	<b>217</b>
<b>Table 7.10: Case study of set points for the seventh order system without disturbances</b>	<b>220</b>
<b>Table 7.11: Case study of set points for the seventh order system with disturbances</b>	<b>226</b>
<b>Table 7.12: Analysis of the performance indicators for each of the setpoint variations for the seventh order system</b>	<b>229</b>
<b>Table 8.1: Software developed in this thesis</b>	<b>237</b>

## **APPENDICES**

<b>Appendix A – MATLAB model transfer functions script file</b>	<b>249</b>
<b>Appendix B – MATLAB script file for the second order debutanizer model and IMC controller design</b>	<b>252</b>
<b>Appendix C – Hardware Specifications</b>	<b>255</b>

## GLOSSARY

<b>Terms/Acronyms/Abbreviations</b>	<b>Definition/Explanation</b>
APC	Advanced Process Control
COM	Component Object Model
CX-5020 PLC	Programmable Logic Controller (Beckhoff Automation)
cRIO	CompactRio
DCS	Distributed Control System
DMC	Dynamic Matrix Control
FCCU	Fluid Catalytic Cracking Unit
GRU	Gas Recovery Unit
HiL	Hardware-in-the-Loop
IEC	International Electrotechnical Commission
IMC	Internal Model Control
kPa	Kilopascal
LabVIEW	Laboratory Virtual Instrument Engineering Workbench
IO	Input Output
LCN	Light Cracked Naphtha
LPG	Liquified Petroleum Gas
LTI	Linear time-invariant
MIMO	Multi-Input Multi-Output
MISO	Multiple-Input Single-Output
MOR	Model Order Reduction
MPC	Model Predictive Control
MV	Manipulated Variable
NI	National Instruments
PI	Proportional Integral
PID	Proportional Integral Derivative
PLC	Programmable Logic Controller
PV	Process Variable
RGA	Relative Gain Array
ROT	Real-Time Optimization
SCADA	Supervisory Control and Data Acquisition
SIMO	Single-Input Multiple-Output
SISO	Single-Input Single-Output
SV	Set Value
TcCOM	TwinCAT Object Models
TF	Transfer Functions
TITO	Two-Input Two-Output
Twin CAT	The Windows Control Automation
V	Voltage
VI	Virtual Instrument
XAE	Extended Automation Engineering
XAR	Extended Automation Runtime

# CHAPTER ONE: INTRODUCTION

## 1.1. Introduction

Distillation control has been the subject of numerous research publications for decades and the increased research interest can be attributed to the important role distillation processes fulfil in the petrochemical industry as a separation technique for separating multicomponent fluid mixtures into separate individual streams. Good process control and operation of industrial distillation columns offers significant economic incentives since distillation columns use considerable amounts of energy and are one of the most widely used processes, especially in oil refining facilities (Buckley et al., 1985). However, distillation columns present process control challenges due to their coupled multivariable structure and often exhibit nonlinear dynamic behaviour (Buckley et al., 1985). Most processes encountered in the petrochemical industry like distillation columns are coupled and multivariable in nature. Coupling occurs when a single process variable's dynamic behaviour influences other process variables giving rise to variable interactions (Seborg et al., 2004). Control systems capable of providing satisfactory performance for such processes typically require the use of nontrivial multivariable controller design techniques suitable for multiple-input-multiple-output (MIMO) processes and that can effectively deal with process variable interactions.

This thesis discusses the development of two control strategies suitable for multivariable processes; decentralized proportional-integral-derivative (PID) control and centralized model predictive control (MPC). The decentralized PID control system is designed using tools such as the relative gain array (RGA) introduced in (Edgar H Bristol, 1966) and the PID controller gain selection is facilitated using the internal model control (IMC) technique introduced by (Garcia and Morari, 1982). The control loop interactions are compensated for by making use of decoupling control techniques. On the other hand, centralized model predictive control, as a multivariable control technique, handles process interactions inherently and is designed to incorporate constraints on both the manipulated and controlled variables.

The work performed in this thesis includes the development of a dynamic transfer function model of a debutanizer column from step response coefficients exported from an industrial real-life operating plant for study in the MATLAB/Simulink environment. Both control strategies, decentralized PID control and centralized MPC control, developed in this thesis are applied on the dynamic model of the industrial debutanizer distillation process. The debutanizer distillation process studied in this research is a part of a fluid catalytic cracking converter's (FCCU) gas recovery plant and is used to separate butane (C4's) and propane (C3's) from pentane (C5's) and heavier hydrocarbons used to produce gasoline as part of the gas recovery unit (GRU)

(Sadeghbeigi, 2000). The work further develops a testbed for a real-time implementation of a closed loop system in a Hardware-in-the-Loop (HiL) configuration.

This chapter provides the problem being addressed by the outcomes of this thesis in Section 1.1. The research problem is outlined in Section 1.2. The aims, and objectives are presented in Section 1.3. The research questions are given in Section 1.4 and the hypothesis in Section 1.5. The scope of the research is presented in Section 1.6 and the motivation of this research is presented in Section 1.7. Section 1.8 presents the assumptions considered in the development of this thesis. This chapter ends with an outline of the thesis that provides the overview of the work presented in the rest of the thesis in Section 1.9 and concluding remarks are provided in Section 1.10.

## **1.2. Problem Statement**

The focus of this research is to develop a methodology for the design and implementation of control techniques suited for coupled, interacting and multivariable processes such as debutanizer distillation processes. Process control systems capable of providing satisfactory performance for coupled and multivariable processes require the use of multivariable controller design techniques. The debutanizer distillation process control problem is used in this research as a case study to test the developed control algorithms. The above-mentioned problem can be further divided into five sub-problems as follows:

### **1.2.1. Sub-problem one**

Develop linear-time-invariant (LTI) continuous-time transfer function models from empirical model data of an industrial debutanizer distillation process and perform open-loop simulations in the MATLAB/Simulink environment.

### **1.2.2. Sub-problem two**

Develop mathematical descriptions for the design of a decentralized PID control system using design and analysis tools such as the relative gain array (RGA), the Niederlinski index, ideal decoupling control, model order reduction (MOR) and the internal model control (IMC) technique for PID controller tuning and perform closed-loop simulation case studies in the MATLAB/Simulink environment for various set points and process disturbances.

### **1.2.3. Sub-problem three**

Develop a model predictive control (MPC) system based on a linear step response prediction model and perform closed-loop simulation case studies in the MATLAB/Simulink environment for various set points and process disturbances.

#### **1.2.4. Sub-problem four**

Transform the developed models as portable software modules from the MATLAB/Simulink environment to the Beckhoff TwinCAT 3.1 real-time simulation environment. Perform closed-loop and real-time simulations of a seventh order MPC control system in the TwinCAT 3.1 environment for various set points and process disturbances.

#### **1.2.5. Sub-problem five**

Implement a second order debutanizer distillation process model in the LabVIEW simulation environment and decentralized PID controllers in the TwinCAT 3.1 environment and configure the system in a Hardware-in-the-Loop (HiL) testbed and perform closed-loop and real-time simulation case studies for various set points and process disturbances.

### **1.3. Research Aim and Objectives**

#### **1.3.1. Aim**

The aim of this research is to develop multivariable controller design methodologies for an industrial debutanizer distillation process model and implement a closed-loop control system in a Hardware-in-the-Loop (HiL) configuration and simulated in real-time.

#### **1.3.2. Objectives**

The objectives of this research are broken down into theoretical analysis and real-time practical implementation.

##### **1.3.2.1. Theoretical Analysis**

- a) To review existing literature in the fields of distillation process control, debutanizer column control, multivariable control, model predictive control and its applications on multivariable control systems.
- b) To develop the debutanizer distillation process transfer function model from an industrial empirical model in the MATLAB/Simulink software environment.
- c) To perform a detailed investigation of the mathematical formulation for decoupling compensators for the decentralized PID controller design.
- d) To design controller strategies and analysis methodologies for effective loop pairing and tuning for satisfactory closed-loop performance and perform closed loop simulations to verify the effective elimination of process variable interactions.
- e) To develop a model predictive control system in the MATLAB/Simulink environment and perform simulation studies in closed-loop for set point tracking, constraint handling and disturbance rejection.



### **1.3.2.2. Real-Time Practical Implementation**

- a) To develop software methods and algorithms in the MATLAB/Simulink, TwinCAT 3.1 and LabVIEW environments to investigate the various models developed.
- b) To perform a transformation of the developed models as portable software modules from the MATLAB/Simulink environment to the Beckhoff TwinCAT 3.1 simulation environment.
- c) To configure a testbed for the real-time implementation of the closed loop system in a Hardware-in-the-Loop (HiL) configuration.
- d) To perform real-time simulation case studies for set point tracking, constraint handling and disturbance rejection for the developed controller design methodologies.

## **1.4. Research Questions**

- a) **Question 1:** Does a centralized multivariable MPC control structure perform better in eliminating process interactions than decoupling compensators do for a decentralized PID control structure?
- b) **Question 2:** Does closed-loop control performance significantly differ between a simulation environment and real-time Hardware-in-the-Loop (HiL) testbed?

## **1.5. Hypothesis**

The centralized model predictive control structure is expected to produce superior performance compared to the decentralized PID control structure for the control of a coupled debutanizer distillation process model since model predictive control is inherently a multivariable controller that incorporates process interactions and constraints in the formulation of the control law. Furthermore, the closed-loop control performance is expected to be not different between the simulation environment and the real-time Hardware-in-the-Loop (HiL) testbed.

## **1.6. Delimitation of Research**

### **1.6.1. Within the Scope**

- a) Literature review on distillation and debutanizer process control, multivariable and multi-loop control, model predictive control and its applications on multivariable control systems.
- b) Development and open-loop simulations of the debutanizer distillation process model in the MATLAB/Simulink software environment.
- c) Development of mathematical descriptions for the decentralized PID controller design and closed-loop simulations.

- d) Development of model predictive controller design using the Model Predictive Control Toolbox in the MATLAB/Simulink software environment and closed-loop simulations.
- e) Real-time simulations in real-time and in a Hardware-in-the-Loop (HiL) configuration for various set points and process disturbances.

### **1.6.2. Beyond the scope**

- a) Development of a first principles debutanizer distillation process model.
- b) Detailed review of the debutanizer distillation process model ill-conditioning.
- c) Non-linear controller design techniques.
- d) Detailed review and analysis of the MPC mathematical equations of the MATLAB/Simulink Model Predictive Control Toolbox.
- e) Detailed review of commercial model predictive control model development processes.
- f) Implementation of the developed control algorithms in a real-life operating process plant.

### **1.7. Motivation for the Research Project**

This research focuses on three main important subjects; PID control, MPC control, and Hardware-in-the-Loop implementation.

Firstly, among the many control technologies available in the market today, the PID controller is the most widely used controller in industry for its simplicity and ease of implementation with relatively low-cost hardware providing satisfactory performance for most control applications encountered in industry (Seborg et al., 2004). This research presents an opportunity to better understand important design features offered by the internal model control PID design technique that can be useful for industrial practitioners.

Secondly, model predictive control techniques have been proven to provide enormous economic value wherever they have been implemented appropriately (Bullerdiek and Hobbs, 1995), (Masheshri et al., 2000). Model predictive control techniques are widely used to achieve increased profitability in the process industry, especially in oil refining facilities around the world (Qin and Badgwell, 2003). This research investigates the theoretical background of what has become the standard advanced process control technique in the petrochemical industry today. This enables the study of tuning parameter trade-offs that industrial practitioners often must make in designing model predictive controllers.

Finally, Hardware-in-the-Loop configurations are essential in facilitating learning for process control students in the academic community to aid their understanding of theoretical concepts taught and the work developed in this research furthers such an objective.

## **1.8. Assumptions**

- a) The empirical model extracted from an online commercial model predictive control software package is assumed to be a valid representation of the process dynamics prevalent in a typical industrial debutanizer distillation process.
- b) The process model is assumed linear and time invariant around its operating range.
- c) The real-time simulations conducted in this work are assumed to provide accurate results of practical importance to similar real-life system design and testing.

## **1.9. Thesis Outline**

The thesis document consists of eight chapters providing background information with methods developed, simulation results, real-time implementation, and results of this research. The rest of this thesis is outlined as follows:

Chapter 2 presents a review and analysis of existing literature in the fields of distillation process control, debutanizer column control, multivariable control, model predictive control and its application on multivariable control systems are provided. The chapter deals specifically with published work on the common techniques employed in the above-mentioned fields such as the debutanizer distillation composition control, relative gain array (RGA) interaction measuring method, decoupling control techniques for interaction elimination, internal model control (IMC) tuning strategy, model predictive control and its applications in the petrochemical industry and other industries such as the aviation and power electronics sectors. These topics are reviewed based of the gathered literature, analysed, and compared to develop a thorough understanding of the historical developments and current state of the art for each topic.

Chapter 3 presents the multivariable controller design concepts utilized in the development of this thesis. The main concepts covered include the relative gain array (RGA) and the Niederlinski index methods which are used for interaction analysis and control structure selection. The decoupling control techniques used for effective elimination of multivariable process interactions and the model order reduction (MOR) techniques that enable simplified controller tuning are both described. The internal model control (IMC) used to obtain the PID gains, and finally, the multivariable model predictive control (MPC) technique are described. The mathematical formulations for these concepts are provided with explanations of their working principles.

Chapter 4 presents the identification process for the development of the debutanizer distillation process model used in this thesis. The chapter presents the workflow process followed from the collection of raw plant data to the resulting mathematical transfer function models.

Chapter 5 provides the controller design of a decentralized PID control system for the debutanizer distillation process model. Closed-loop simulations in the MATLAB/Simulink environment to test the developed algorithms for closed-loop performance are done.

Chapter 6 presents the development of an MPC control system using the MATLAB/Simulink Model Predictive Control Toolbox and testing the designed controller in the debutanizer distillation process model.

Chapter 7 presents the transitioning of the developed control systems and models from the MATLAB/Simulink simulation environment into a real-time simulation environment.

Chapter 8 provides concluding remarks for the thesis, thesis deliverables, applications, and future work.

## **1.10. Conclusion**

In this chapter, an introduction of the thesis and the problem being addressed by its outcomes are provided. The research aims and objectives, the research questions and hypothesis are presented. The scope of the research, the assumptions considered in the development of the thesis and the motivation of the research are outlined. The scope of the research, the assumptions considered in the development of the thesis and the motivation of the research are provided. This chapter ends with an outline of the thesis that provides the overview of the work presented in the chapters that follow.

The following chapter presents a review of published work in the fields of distillation process control, debutanizer column control, multivariable control, model predictive control and its application on multivariable control systems. The review includes literature on common techniques employed in the above-mentioned fields such as the debutanizer distillation composition control, relative gain array (RGA) interaction measuring method, decoupling control techniques for interaction elimination, internal model control (IMC) tuning strategy, model predictive control and its applications in the petrochemical industry and other industries such as the aviation and power electronics sectors.

## CHAPTER TWO: LITERATURE REVIEW

### 2.1. Introduction

In this chapter, a review and analysis of existing literature in the fields of distillation process control, debutanizer column control, multivariable control, model predictive control and its applications on multivariable control systems are provided. This chapter deals specifically with published work on the common techniques employed in the above-mentioned fields such as the debutanizer distillation composition control, relative gain array (RGA) interaction measuring method, decoupling control techniques for interaction elimination, internal model control (IMC) tuning strategy, model predictive control and its applications in the petrochemical industry and other industries such as the aviation and power electronics sectors. These topics are reviewed based on the gathered literature, analyzed, and compared to develop a thorough understanding of the historical developments and current state of the art for each topic. The obtained literature helps in guiding this research and its execution process to the conclusion.

Section 2.2 provides a description of the focus areas for the research, the selection of key words used for the literature search and a graphical representation of the number of publications found and reviewed. Section 2.3 to 2.5 provides the literature review for each of the topics defined in section 2.2 followed by a comparative analysis on the developments of the found literature. Section 2.6 provides the proposed system development process and system architecture based on literature review, and finally, concluding remarks are provided in Section 2.7.

### 2.2. Literature search

Distillation processes fulfill an important role in the petrochemical industry as one of the most widely used separation techniques (Luyben, 1993). Process control and operation of industrial distillation columns offers significant economic incentives since distillation columns use considerable amounts of energy and are one of the most widely used processes, especially in the refining industry (Buckley et al., 1985). Distillation columns present process control challenges due to their coupled multivariable structure and nonlinear dynamic behavior. Control systems capable of providing satisfactory performance for such processes typically require the use of nontrivial multivariable controller design techniques.

To better understand the challenges involved and available solutions tried and offered by others, a literature search is required followed by a review of the resultant literature with the objectives of this research in mind. To provide a complete review of the subject of distillation control, three focus areas have been devised for research and analysis and these include historical as well as present developments on:

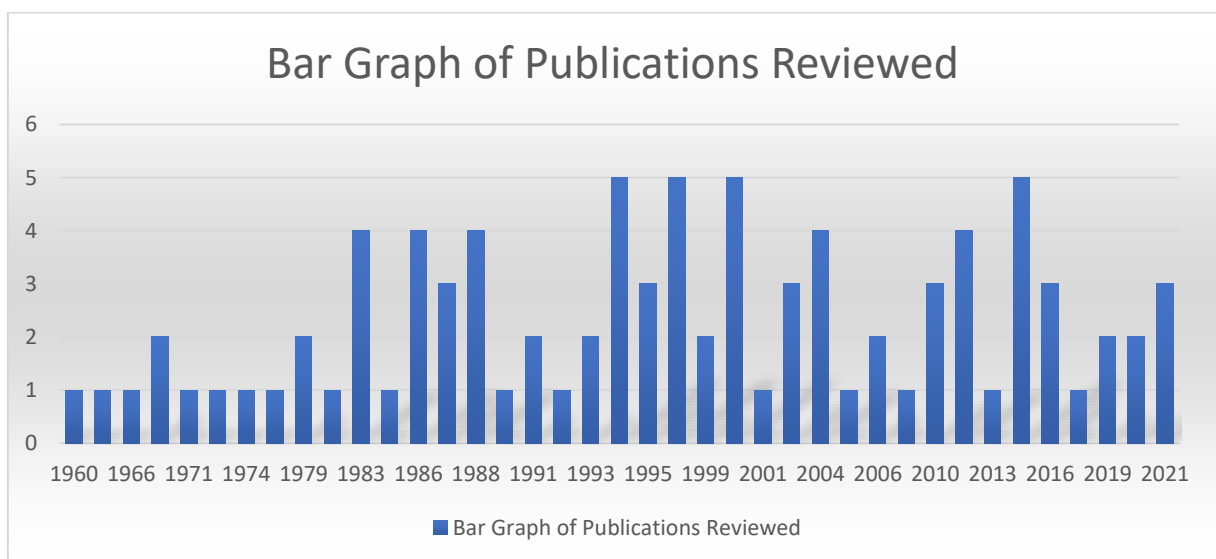
- a) **Distillation process control and debutanizer column control**
- b) **Multivariable control**

c) **Model predictive control and application on multivariable control systems**

To help in finding relevant literature and published work on the above-mentioned topics, a list of keywords has been developed for database and search engine input, these include:

- a) **Distillation process control and debutanizer column control** – distillation control, binary distillation control, debutanizer control
- b) **Multivariable control** - distillation decoupling control, distillation multi-loop control, multivariable process control
- c) **Model predictive control and application on multivariable control systems** - model predictive control, dynamic matrix control, multivariable predictive control

Figure 2.1 provides a graphical representation of the reviewed literature in the development of this chapter illustrating the publication trends over the years. The literature review presented in this chapter surveys the academic research work published in the topics of distillation process control, debutanizer column control, multivariable control and model predictive control and its applications on multivariable control systems together with the methods used under each topic with their reported results.



**Figure 2.1: Bar graph of the reviewed publications**

The Cape Peninsula University of Technology Library Database and Journals search engines were used as the main resources for the gathered literature as outlined in the following sections.

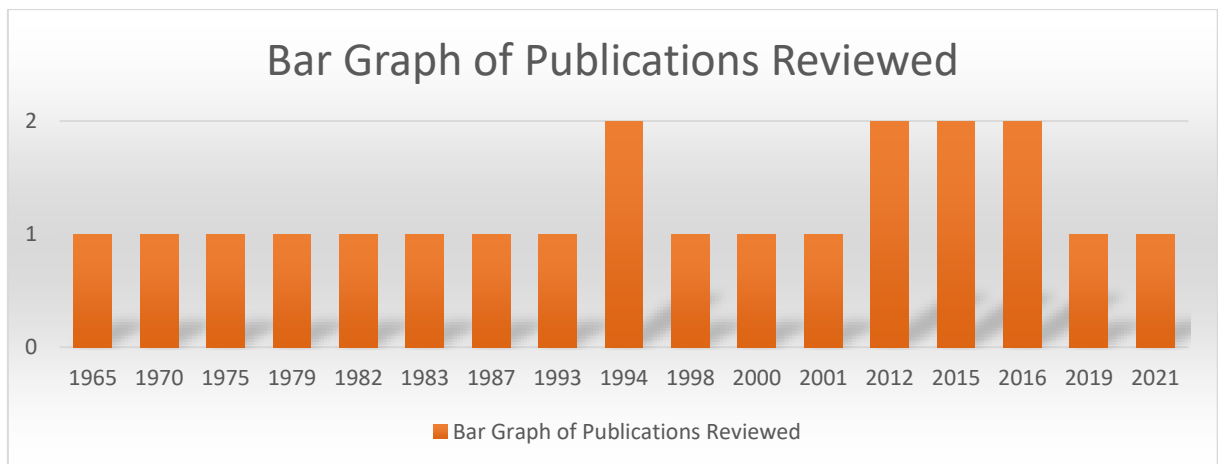
### 2.3. Literature review of existing papers on distillation process control

The first literature review was done on the topic of distillation process control and debutanizer column control. The research was mainly focused on binary distillation control, dual composition control on distillation processes and debutanizer columns.

#### 2.3.1. Existing papers on distillation process control

Figure 2.2 graphically presents the reviewed number of papers arranged by publication year on Distillation process control and debutanizer column control. The publications reviewed were acquired using the keywords: “Distillation Control”, “Binary Distillation Control” and “Debutanizer control”. The criteria for selecting a publication to include in the literature review were:

- a) The work must deal with Distillation process control and debutanizer column control.
- b) The problem or topic being addressed in relation to distillation and debutanizer column control must be clearly stated together with objectives and achieved results.
- c) The type of control system or strategy employed is described.



**Figure 2.2:** Number of papers per year covering the topic of distillation process control

It can be observed that the years of publication on the topic of distillation process control and debutanizer column control span over five decades. Table 2.1 presents the publications reviewed between the years of 1965 and 2021 on distillation process control and debutanizer column control. The table is divided into five columns; the first column indicates the author(s) and the year of publication, the second column describes the principal focus of the work, the third column provides a description of the plant or process considered. The main control strategy discussed is given in column four, and the author’s remarks and conclusions are provided in the last column.

**Table 2.1: Existing papers on distillation process control**

<b>Paper</b>	<b>Principal focus of the work</b>	<b>Plant/process controlled</b>	<b>Main control strategy</b>	<b>Author's conclusions</b>
(Rijnsdorp, 1965)	Provides a measure for quantifying interactions in distillation control systems.	Generic distillation process	Decoupling Multivariable Control	The work presented forms the early foundation in the methods available for measuring interactions of control loops to determine adequate control loop structures and can be extended to systems beyond distillation processes.
(Maarleveld and Rijnsdorp, 1970)	Investigates constraint control - where constraints change as operating conditions change.	De-isopentanizer distillation column	Decoupling Multivariable Control	Practical considerations in the design of control systems for distillation columns are provided in this paper. The work is particularly valuable in the descriptions presented for constraints prevalent in industrial distillation columns.
(Luyben, 1975)	Discusses the business case and implications for dual composition control on distillation columns pursued to achieve energy conservation.	Binary distillation column	Decoupling Multivariable Control	The incentives for attempting dual composition control are challenged considering an alternative of controlling the ratio of either the reboiler or the reflux with the feed flow rate. The author cites complexities brought by dual composition control schemes in the form of closed loop stability, interactions, and instrumentation. The technological advances may have eased some of the complexities associated with dual composition control in the paper over the years, however this is still an important paper for practitioners aiming to reduce distillation energy consumption.
(Tyréus, 1979)	The Inverse Nyquist Array design is proposed as an alternative to dominant interacting and noninteracting control.	Binary distillation column	Inverse Nyquist Array	The work puts forward limitations of multi-loop decoupling control strategies in aiding design decisions. The Inverse Nyquist Array method was applied for loop pairing and design of interaction compensators for an industrial distillation column with results showing better controller performance providing a payback period of less than 3 months.
(Weber and Gaitonde, 1982)	The work proposes controlling the distillation cut point temperatures for dual composition control in distillation columns as an	Binary distillation column	Conventional Multivariable Control	The presented work makes use of ad hoc calculations for the Cut point and Fractionation setpoint to control composition and interactions in the distillate and bottom products. The



Paper	Principal focus of the work	Plant/process controlled	Main control strategy	Author's conclusions
	alternative to reflux-feed ratio, reboiler-feed ratio and single or dual online composition analyzers.			reported results indicate that the strategy is highly limited as interactions are not completely removed although it has the advantage of simple and requires little maintenance once commissioned.
(Fuentes and Luyben, 1983)	The work addresses a common problem in high purity dual composition control brought by dead time in on-line analyzers and high volatility.	High purity binary distillation column	Cascade multivariable PI control	The work reported that high purity columns lead to slow online composition analyzer response times i.e., increased time constant. As such a control scheme that maintains the composition within tolerable variations around the setpoint is proposed. The authors make use of cascade control of the tray temperatures with the composition on both ends of the tower with improved control being reported.
(McDonald and McAvoy, 1987)	Implements an online gain and time constant scheduled dynamic matrix control (DMC) strategy.	High purity binary distillation process	Dynamic Matrix Control	The proposed approach modifies the traditional DMC controller strategy to improve performance in nonlinear high purity dual composition control distillation columns. The proposed approach estimates process parameters to determine appropriate instances to schedule an update of the controller model gains and time constants. The method is reported to be different from adaptive control in that it is open loop but with the benefit of being able to update parameters more quickly compared to adaptive control albeit at a higher computation effort.
(Luyben, 1993)	A book on practical approaches to industrial distillation control systems.	Distillation processes	Multivariable Control	The book covers most aspects that control, and process design engineers may find particularly valuable in selecting the best configuration and control system structures for distillation columns.
(Musch and Steiner, 1994)	The objective of the work is to propose a control strategy for high purity distillation control simple enough to be implemented on an industrial Distributed Control System (DCS).	Distillation process	Decoupling multivariable PID control	The authors propose a decoupling control strategy based on optimally tuned PID controller. Often academic solutions are not easily implementable in industrial platforms such as the DCS. The work proposed in this paper can go a long way in bridging the gap between

Paper	Principal focus of the work	Plant/process controlled	Main control strategy	Author's conclusions
				theoretically validated solutions and practical implementation of such solutions.
(Freitas et al., 1994)	Improving the production of naphtha through better control of the top and bottom temperatures and operating the column near the constraints of the bottom product composition.	Debutanizer column	Decoupling multivariable PID control	The control strategy implemented was decoupling control to eliminate process interactions which were a cause for large variations in the bottom product quality, the Naphtha Reid vapor pressure (RVP). The proposed solution involved importing plant model input/output data into MATLAB and performing simulations to test the various controller tuning strategies prior to implementation. The resulting decoupled PID control system led to an increase in Naphtha production and operating profit margin of the column.
(Ansari and Tadó, 1998)	Improving setpoint tracking on the top and bottom product qualities of the debutanizer by using nonlinear Generic Model Control (NGMC).	Debutanizer column	NGMC	The work implemented a nonlinear GMC on a debutanizer column that was previously under the control of PID controllers. The controller utilized steady state approximate models of the plant and was able to achieve good setpoint tracking results, contrary to the conventional use of dynamic models to achieve good control. The work further implemented inferential models for the LPG C5 concentration and LCN RVP variables instead of depending on the slow responding online analyzer instrumentation.
(Neto et al., 2000)	Improving controller performance under model uncertainty due to varying operating conditions by multi-model predictive control (MMPC).	Debutanizer column	MMPC	The problem of model mismatch that is prevalent in model-based control strategies is addressed using multi-model predictive control (MMPC). In MMPC the most suitable model for existing operating conditions is selected from a preprogrammed set of linear models by minimizing an optimization algorithm for the selection. The robustness for the system is further improved by the addition of a Lyapunov condition in the optimization formulation. The reported results show better controller performance in setpoint tracking for both LPG C5 and Gasoline RVP compared to

Paper	Principal focus of the work	Plant/process controlled	Main control strategy	Author's conclusions
				the conventional single model based MPC.
(Abou-Jeyab et al., 2001)	Simplifying the optimization algorithm of constrained MPC to minimize computational effort.	Distillation process	Simplified Model Predictive Control	The work proposes minimizing only the error of a single point on the prediction horizon when formulating the control inputs instead of minimizing all the points along the prediction horizon as done in traditional MPC control law formulations. The reported results surprisingly indicate equivalent controller performance with the benefit of reduced computation effort due to the simplified optimization algorithm.
(Pitta and Odloak, 2012)	Implementation of closed loop identification to circumvent the operational disturbances and costs associated with open loop identification during model updates.	Debutanizer column	MPC	The paper presents a closed loop re-identification approach implemented in a debutanizer distillation column. The method involves completing plant testing by introducing excitations into the process while in closed loop without affecting production. This is contrary to open loop plant tests that take up large amounts of human resources and time. The reported results showed improvement in the updated model resulting in better MPC controller performance. This method has the potential to save large amounts of money for organizations that employ large scale model predictive controllers such as oil refineries more especially if such a method can be more automated.
(Cecil, 2012)	A practical book on distillation control covering aspects on interest to industrial practitioners.	Distillation process	Various	The work advocates for the use of steady-state separation models to determine what control configuration to use for distillation column control. This contrasts with the widely accepted approaches of either making use of dynamic models or basing such decisions on qualitative assessments during piping and instrumentation diagram (P and ID) development.
(Ramli and Chandra Mohan, 2015)	Improving production of propane or LPG from the debutanizer to be at the target of 30% and Butane to be at the target of 70%.	Debutanizer column	MPC	The methodology involves building a steady state and dynamic model simulation in a software environment (HYSYS) with real plant data and conducting step response

Paper	Principal focus of the work	Plant/process controlled	Main control strategy	Author's conclusions
				tests. The data collected from the step response tests is collected into a System Identification algorithm in MATLAB and simulated to obtain process gains, time constants and time delays to be used for tuning the real-life debutanizer MPC controllers. However, from the paper it is unclear whether the obtained results from the model achieved the stated objectives nor is it clarified how the tuning of the MPC controllers is implemented with the obtained data from MATLAB.
(Paulo Padrão et al., 2015)	Improving control of the C3 concentration in the debutanizer LPG to consistently meet product specifications.	Debutanizer column	PID	The work presented a simple control strategy of finding PID controller gains that minimize the integral of the absolute error (IAE) of the C3 concentration response using an optimization objective function subject to upper and lower constraint limits of the PID gains as constraints. The appropriate tuning parameters are searched for using an optimization algorithm. The results show improved overshoot and settling time of the C3 concentration. The strategy appears simple and implementable on any control loop provided that the correct upper and lower constraint limits are known and set accordingly.
(Ramli et al., 2016)	Improving top and bottom temperature control as well as composition predictions.	Debutanizer column	ANN	Proposed a novel strategy for Debutanizer control using equation-based artificial neural networks (ANN) to improve top and bottom temperature control as well as composition predictions. The paper reported superior performance of the ANN strategy compared to the conventional PID for the cases tested as part of the study.
(Ramli, 2016)	A comparison study of various PID controller tuning strategies for including Internal Model Control, Smith Predictor, Feedback and Feedforward control and Cascade control.	Debutanizer column	PID	The author concluded the IMC method is better than the other tuning strategies in a debutanizer distillation column control application. The criticism that can be levelled against the work is the lack of clarity on the process variables being controlled from Debutanizer column and the

Paper	Principal focus of the work	Plant/process controlled	Main control strategy	Author's conclusions
				process model development was not clearly presented.
(Fatima et al., 2019)	The paper addresses system identification of a debutanizer distillation column.	Debutanizer column	None	The authors developed identification methods based on linear and nonlinear identification. The FOPTD method was used for the linear identification whereas the Nonlinear Autoregressive with Exogenous Input (NLARX) was used for nonlinear identification. The authors concluded that the NLARX better approximated the output behavior of the system compared to the linear FOPTD.
(Fatima et al., 2021)	Proposes the Adaptive neuro-fuzzy inference system (ANFIS) for top and bottom composition soft sensors.	Debutanizer column	None	The primary business case for the proposed technique is based on the unavailability of sufficient data samples to adequately train soft sensors such as the ANN which is based on machine learning. The authors concluded that the ANFIS approach results in better prediction performance and generalization compared to the ANN approach.

### 2.3.2. Comparative analysis and discussion on the developments of the existing literature on distillation process control

The control of distillation columns has been a subject of research articles from the academic community for many years and the literature review conducted reveals that control of distillation columns has not been a trivial task (Luyben, 1993). The main themes that are apparent from the reviewed literature are the control structure selection and alternative design strategies that can be employed in dual composition control of the top and bottom products of binary distillation columns.

Distillation columns are highly nonlinear, and the selection of a suitable control structure is critical for satisfactory control performance. The work by Rijnsdorp (1965) helps in quantifying control loop interactions for a selected control structure, as such, when interactions are quantified and control loops have been paired, decoupling compensators are implemented to eliminate the interactions in multi-loop control systems. Musch and Steiner (1994) used a decoupling control strategy that is based on optimally tuned PID controllers for high purity distillation control that could be implemented on industrial Distributed Control System (DCS) platforms. In contrast, the work by Tyréus (1979) presented limitations of multi-loop decoupling control strategies in aiding design decisions and instead proposed using the Inverse Nyquist

Array method as an alternative for loop pairing and design of interaction compensators for an industrial distillation column. Even though both methods achieve the objective of eliminating control loop interactions, it is the ability to implement the control scheme on a DCS platform that makes the work by Musch and Steiner (1994) particularly important and relevant for industrial practitioners. Luyben (1993) covers important aspects that control engineers and process engineers can use in the selection of the best process equipment configurations and control system structures for distillation columns.

Since the purpose of distillation is to separate fluid mixtures into multiple streams, one of the most important measurements for control is the composition of the separated streams to have the ability to control the achieved degree of separation. In binary distillation columns, the composition of the top and bottom products are often the key indicators of the distillation column performance, and the control objectives are often to maintain the compositions of these two-product streams within predetermined specifications resulting in dual composition control schemes. The main benefit of dual composition control is energy conservation in distillation columns (Tham, 1999). However, dual composition control presents challenges due to nonlinearities and ill-conditioning especially in high purity distillation columns. Although the control strategy implemented by Freitas et al., (1994) worked well for a dual composition application based on decoupling control to deal with process interactions which were causing large variations in a debutanizer's bottom product quality, the incentives for attempting dual composition control were challenged by Luyben (1975). Luyben (1975) instead considered the alternative of controlling a process ratio of either the reboiler heat input with the feed flow rate or the reflux with the feed flow rate to avoid complexities brought by dual composition control schemes such as closed loop stability, interactions, and slow instrumentation measurement responses. Although technological advances over the years may have eased some of the complexities associated with dual composition control, the work is still industry relevant. The challenges with slow instrumentation response times in high purity columns was also reported by Fuentes and Luyben (1983) and they proposed making use of a cascade control scheme using column tray temperatures cascaded with composition on the top and bottom of the column. On the other hand, Weber and Gaitonde (1982) proposed making use of cut points and fractionation setpoint to control compositions and interactions of the top and bottom products. However, their results indicate that their strategy has limitations as interactions are not completely removed.

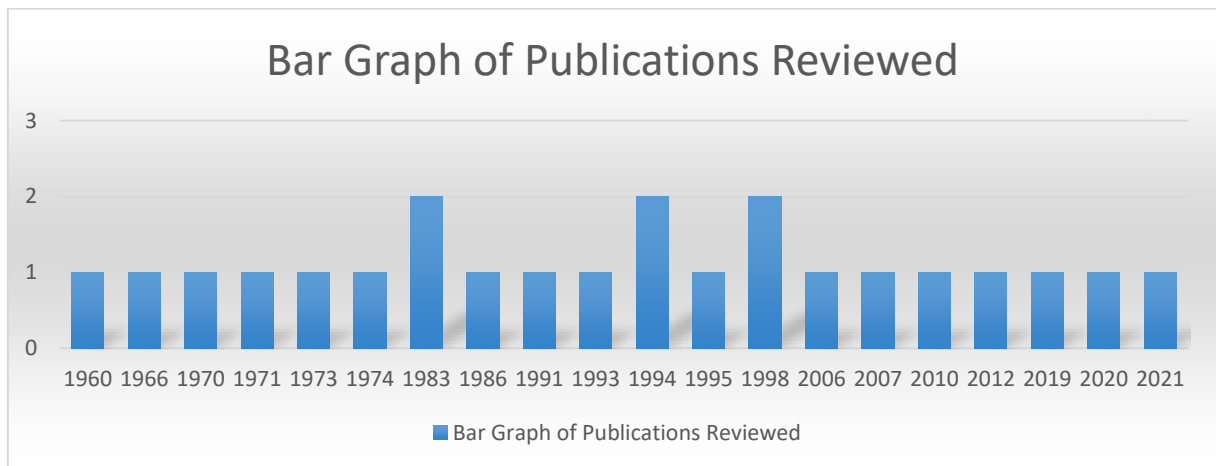
#### **2.4. Literature review of existing papers on multivariable control**

The second literature review was done on the topic of multivariable control. The research was mainly focused on decentralized decoupling control in multivariable control systems.

### 2.4.1. Existing papers on multivariable control

Figure 2.3 graphically presents the reviewed number of papers arranged by publication year on multivariable control. The publications reviewed were acquired using the keywords: “distillation decoupling control”, “distillation multi-loop control”, “multivariable process control”. The criteria for selecting a publication to include in the literature review were:

- a) The work must deal with multivariable control system design.
- b) The problem or topic being addressed in relation to multivariable control must be clearly stated together with objectives and achieved results.
- c) The method used for dealing with process interactions, either through decoupling or a centralized multivariable controller, must be defined.
- d) The type of controller strategy employed is described.



**Figure 2.3: Number of papers per year covering the topic of multivariable control**

It can be observed that the years of publication on the topic of multivariable process control span about six decades. Table 2.2 presents the publications reviewed between 1960 and 2021 on multivariable process control. The table is divided into five columns; the first column indicates the author(s) and the year of publication, the second column describes the principal focus of the work, the third column provides a description of the plant or process considered. The main control strategy discussed is given in column four, and the author’s remarks and conclusions are provided in the last column.

**Table 2.2: Existing papers on multivariable control**

<b>Paper</b>	<b>Principal focus of the work</b>	<b>Plant/process controlled</b>	<b>Main control strategy used</b>	<b>Author's Conclusions</b>
(Chatterjee, 1960)	Design of decoupling compensators	Steam generator and tank blending system	Decoupling multivariable control with compensators	Presents an early treatment of non-interacting control using decoupling compensators in process control systems.
(Edgar H. Bristol, 1966)	Interaction measurement in multivariable systems	None	Decoupling multivariable control	Introduced a measure of interaction between variables called the Relative Gain Array (RGA) for the design of multivariable control systems. The RGA has since become an indispensable part of multivariable control system design.
(Luyben, 1970)	An investigation into two decoupling methods - Ideal and Simplified	High purity binary distillation column	Decoupling multivariable control	The paper determined that simplified decoupling exhibits a more stable closed loop system for high purity distillation columns.
(Niederlinski, 1971)	Introduced the Niederlinski Index (NI) as a tool to determine structural stability of a multivariable control system design.	Generic plant models	Decoupling multivariable PID control	The work proposes another method of determining the most suitable control loop structure. Furthermore, the Niederlinski index has become a valuable method in verifying structural stability of the selected loop pairings to confirm a stable system has been designed.
(Wood and Berry, 1973)	Simplified decoupling and ratio control are implemented in a transfer function model of a Binary distillation column.	Binary distillation column	Decoupling multivariable control with compensators	The paper has become one of the widely reference papers for the distillation column transfer function model.
(Waller, 1974)	Decoupling control for distillation columns.	Generic binary distillation column	Decoupling multivariable control	A further investigation into decoupling and somewhat of a response and further work to work in (Luyben, 1970).
(Cutler and Perry, 1983)	Provides an early treatment and introduction into online process optimization.	None	MPC	The work covers aspects that are still fundamental to any online optimization project in industry and aspects that must be considered include the validity of the process model to be used, the current position of the process relative to constraint limits and a well-designed control system. The paper asserts that optimization models running on offline computers do not often take into consideration the effects of changing design parameters such as physical properties of the process due to



Paper	Principal focus of the work	Plant/process controlled	Main control strategy used	Author's Conclusions
				deterioration of equipment. On the other hand, online computers process real-time data much faster with more accuracy and less errors than human operators. The time it takes for online computers to determine the actual state of the process and provide feedback of where the process is currently operating relative to constraints is much shorter compared to human operators.
(Ogunnaike et al., 1983)	Improving energy efficiency through better control strategies for a pilot plant distillation column.	Pilot plant distillation column with a side stream	PID with time delay compensator	Discusses a multi-delay compensator which could be used with traditional noninteracting design strategies.
(Garcia and Morari, 1985)	Internal model control (IMC).	Distillation process and Fixed Bed Reactor	IMC	Provides a procedure for multivariable control system design with internal model control (IMC).
(Yu and Luyben, 1986)	Multiloop design strategies for multivariable control systems.	Distillation processes	PID	Paper presents options for selection of a multiloop control structure including using the RGA, the Niederlinski index or Morori Indexes of integral controllability methods. The proposed methods are limited to open loop stable systems. Comparison analysis between multiloop control and state-of-the-art multivariable controllers are not undertaken in the paper. However, it is noted that the authors also make no claim of the proposed methods being better than multivariable control methods.
(Nakamoto and Watanabe, 1991)	Control on nonlinear systems with multivariable control strategies.	Tank level, temperature, and pH control	Decoupling multivariable PI control	Proposes a decoupling and linearization control strategy coupled with external PI controllers to compensate for model mismatch that is reported to yield good results even for non-linear, interactive, and uncertain process models.
(Morari, 1993)	A theoretical review of MPC	None	MPC	The work compares the state space formulation of MPC with input/output formulation with the former being preferred for multivariable systems. The work further proposes use of an infinite output horizon to improve system stability. The authors argue that previously cited challenges of using an infinite horizon by researchers

<b>Paper</b>	<b>Principal focus of the work</b>	<b>Plant/process controlled</b>	<b>Main control strategy used</b>	<b>Author's Conclusions</b>
				in the past are no longer a challenge due to modern developments in computing capabilities.
(Mort, 1994)	The design of non-interacting control is briefly presented using decoupling compensators for a lab scale plant model described by transfer functions.	Motor/Alternator Rig (Lab scale)	MPC	The work presents the design of a pre-compensator for the interactions in a DC motor and alternator model. The designed pre-compensator formulation took the form of an ideal decoupling control strategy. The paper did not present any step response results to show the effectiveness of the control system.
(Machacek and Kotyk, 1994)	Adaptive control of a pilot plant binary distillation column	Methanol-Water Distillation	Decoupling multivariable control	An ideal decoupling control strategy is implemented on a methanol-water pilot distillation column. The decoupling compensator coupled with an adaptive controller shows satisfactory performance. This can be a useful strategy where simplicity of control is the goal and where the plant model is uncertain.
(Park and Choi, 1995)	Propose a solution to PID windup	None	None – controller assumed to be already designed	A solution for the problem of controller windup by proposing the use of a compensator is proposed. However, the main drawback is that the authors appear to assume the controller has already been designed and presumably taken care of interactions.
(Chen and Yen, 1998)	Presents a non-linear control strategy based on static decoupling control and decentralized single neural controllers (SNC).	Unknown	Multivariable control with SNC	The paper presents a solution similar in principle to adaptive control where the controller learns and adapts as the process changes. Static decouplers are used to compensate for interactions and the strategy is compared to decentralized PI controllers where it is reported to be a promising solution for multivariable control systems.
(Sågfors and Waller, 1998)	Provides a controller design methodology based on Singular Value Decomposition (SVD) that relies less on an accurate process model and more on process knowledge.	Generic binary distillation column	Multivariable control with SVD	The authors argue that the proposed SVD can achieve satisfactory performance without the difficulty of having to develop a process model. The authors further challenge the justification for process models in some instances by asserting that it quite possible to have an accurate process model and implement a model based multivariable controller

Paper	Principal focus of the work	Plant/process controlled	Main control strategy used	Author's Conclusions
				that ends up being like the proposed SVD in performance.
(Cornieles et al., 2006)	Survey of different decentralized controller tuning strategies and implemented in a Hardware-in-the-Loop (HiL) configuration.	Water reservoir control process	Decoupling multivariable PID control	A virtual plant is simulated in the LabVIEW software environment and a controller in an IBM system coupled together in a HiL configuration. The work makes use of PID control with static decoupling for interactions and comparing performance of the system based on tuning parameters from five different methods including IMC, Ziegler-Nichols, Pole Placement, PI Dual Loop, and the integral of time-weighted absolute error (ITAE).
(Das et al., 2007)	Proposes use of User Datagram Protocol (UDP) for industrial multivariable process control.	None	PID	The paper presents a low latency communication network using UDP for multivariable control instead of the conventional hardwired approach saving ample time on commissioning, maintenance, and financial resource. The use of network infrastructure for industrial process control is an innovative and promising technology in the field of process control if all the issues related to response times can be effectively resolved.
(Shen et al., 2010)	Investigates multiple control structures for PI/PID based control system including decentralized, decoupling, and sparse control.	Generic process models	PID	The work presents a method that unifies the three strategies; decentralized, decoupling, and sparse control, by modifying the structure to achieve either type of control strategy through a simple addition or removal of the respective controllers. The three different strategies have their own advantages and disadvantages individually; this work aimed to unify and simplify practical implementation for industrial process control practitioners.
(Saxena and Hote, 2012)	Theoretical overview of Internal Model Control	None	IMC	A survey of the developments of IMC is provided without a detailed look into IMC for unstable and integrating with time delay, MIMO, and nonlinear systems.
(Li et al., 2019)	The work focuses on improving controller response of a wiped	Wiped film molecular distillation system	PID	A set of linear equations referred to as Colin-Coon formulae are used to obtain the

Paper	Principal focus of the work	Plant/process controlled	Main control strategy used	Author's Conclusions
	film molecular distillation system.			model gains, dead times, and time constants from step response output data. Ideal decoupling was implemented to eliminate interactions and a controller (referred to as Tornambe controller) is designed and compared to the conventional PID controller. The reported results indicate improvement in control loop percentage overshoot. Although the authors claim improvement in settling time as well - such is not evident from the step response comparisons between the conventional PID and Tornambe controllers.
(Dasgupta and Sadhu, 2020)	The authors study decoupling control for multivariable systems with time delays.	Generic binary distillation column	IMC	The work proposes a new method based on inverted decoupling using the structure of IMC control with results reported as superior compared to centralized inverted decoupling presented in (Garrido et al., 2014).
(González et al., 2021)	Decoupling control theoretical overview	Generic binary distillation column	PID	The paper presents an elementary view of the simplified decoupling control technique use in a decentralized PID control structure. The designed control system is shown to have eliminated interactions for a generic second order distillation process model.

#### 2.4.2. Comparative analysis and discussion on the developments of the existing literature on multivariable control

Control loops in multivariable control systems tend to have interactions with one another i.e., a change in one input variable affects multiple other output variables. This is referred to as signal coupling due to process interactions resulting in signals interacting and behaving in ways that may not be expected. To solve this problem, controller design methods using single-input single-output (SISO) architectures may show highly unsatisfactory controller performance if the process interactions are not considered in the design. Instead, multivariable control strategies are required to deal with the process interactions to achieve satisfactory control system performance. The literature review has revealed the existence of numerous control strategies available in the published literature to solve the above-mentioned multivariable control problem. The use of decoupling control in distillation processes had been investigated in the literature for number of decades.

Bristol (1966) introduced the relative gain array (RGA) method as a measure for interactions between variables for the design of multivariable control systems. The RGA has since become one of the most reliable techniques that have found extensive use to quantify interactions and help in developing multivariable control system structures. The work by Yu and Luyben (1986) presented options for the selection of a multiloop control structure including using the RGA and the Niederlinski Index (NI). The Niederlinski Index (NI) was introduced by Niederlinski (1971) as a tool to determine structural stability of multivariable control system designs.

Traditionally, the problem of process variable interactions had been dealt with using heuristic measures that were specific to the control loop under investigation and that could not be generalized. Chatterjee (1960) provided an early treatment of non-interacting control using decoupling compensators in general process control systems. Luyben (1970) investigated the two commonly used decoupling methods today i.e., Ideal and Simplified decoupling. Luyben (1970) determined that simplified decoupling exhibits a more stable closed loop system for high purity distillation columns. However, a further investigation into decoupling and a response and further work to Luyben's work was given by Waller (1974) where more definitive descriptions were provided. The strategy of decoupling has also been applied in a distillation process by Machacek and Kotyk (1994) who implemented an ideal decoupling control strategy on a methanol-water pilot distillation column and noted that this can be a useful strategy where simplicity of control is the goal and when the plant model is uncertain. Decoupling compensators allow controller design to be approached as though they were individual SISO PI/PID controllers, allowing for use of conventional tuning methods. The work by Cornieles et al., (2006) made use of PID control with static decoupling for interactions and compared performance of the system based on tuning parameters from five different conventional tuning methods including internal model control (IMC), Ziegler-Nichols and Pole Placement.

Shen et al., (2010) investigated multiple control structures for PI/PID control systems including decentralized, decoupling, and sparse control strategies. The work presented a method that unified these three strategies; decentralized, decoupling, and sparse control, by modifying the structure of the control system to achieve either type of control strategy through a simple addition or removal of the respective controllers. The three different strategies have their own individual advantages and disadvantages; however, this work aimed to unify and simplify practical implementation for industrial process control practitioners.

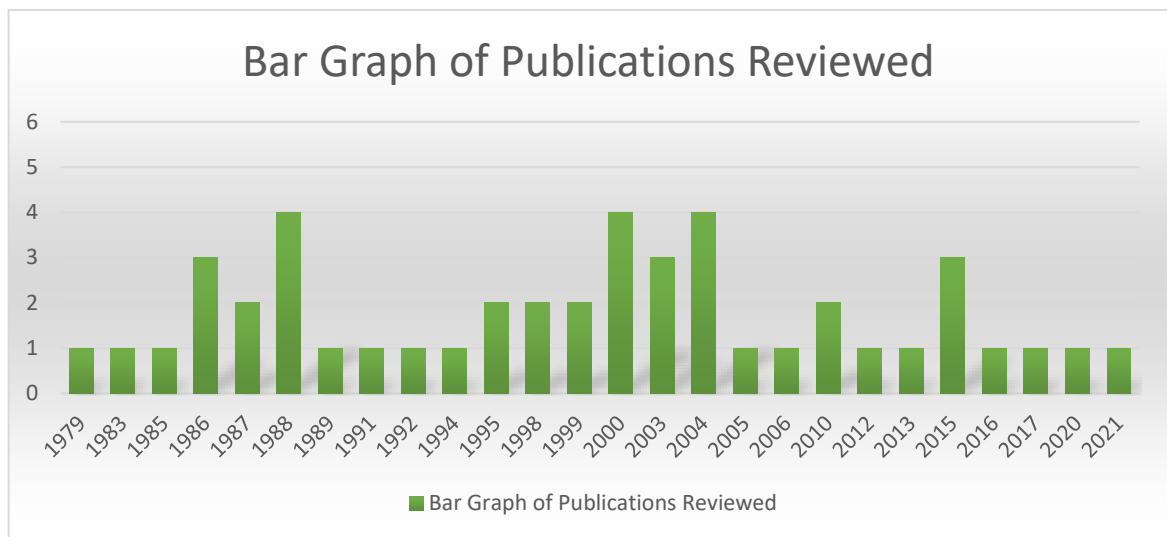
## **2.5. Literature review of existing papers on model predictive control and application on multivariable control systems**

The third and last literature review was done on the topic of model predictive control and application on multivariable control systems. The research was mainly focused on model predictive control's early developments, applications to industrial processes, nonlinear systems, process optimization, as well as its challenges and limitations.

### 2.5.1. Existing papers on model predictive control and application on multivariable control systems

Figure 2.4 graphically presents the reviewed number of papers arranged by publication year on model predictive control and application on multivariable control systems. The publications reviewed were acquired using the keywords: “model predictive control”, “dynamic matrix control”, “multivariable predictive control”. The criteria for selecting a publication to include in the literature review were:

- a) The work must deal with model predictive control and preferably with applications on multivariable control systems.
- b) The problem or topic being addressed in relation to model predictive control, or its application must be clearly stated together with objectives and achieved results.
- c) The type of model predictive control algorithm used must be stated and described.



**Figure 2.4: Number of papers per year covering the topic of model predictive control and application on multivariable control systems**

It can be observed that the years of publication about multivariable process control span nearly four decades. Table 2.3 presents the publications reviewed between 1979 and 2021 on multivariable process control. The table is divided into five columns; the first column indicates the author(s) and the year of publication, the second column describes the principal focus of the work, the third column provides a description of the plant or process considered in the work. The type of model predictive control discussed is given in column four, and the author’s remarks and conclusions are provided in the last column.

**Table 2.3: Existing papers on model predictive control and applications on multivariable control systems**

Paper	Principal focus of the work	Plant/process controlled	MPC type	Summary
(Cutler and Ramaker, 1979)	Introduction of the first application of Dynamic Matrix Control (DMC)	Industrial Furnace	DMC	Dynamic Matrix Control (DMC) was introduced into the literature for the first time in this paper following its implementation at a Shell refinery. DMC has become the most widely used model predictive control algorithm in the petrochemical industry and petroleum refineries around the world. The paper covers in detail the theoretical background of the DMC algorithm at the time of its invention.
(Ray, 1983)	The work provides an overview of the state-of-the-art multivariable control systems.	Various	MPC	Provides valuable insights through a survey on various topics of multivariable control systems including online parameter estimation, adaptive control, and distributed systems that were prevalent at the time of publication.
(Garcia and Prett, 1986)	The work covers the state of the art in model predictive control as of the time of publication.	None	MPC	The work emphasized a need for a unified theory that seeks to standardize model predictive control solutions to limit the use of ad hoc techniques that tend to be application specific in practice.
(Garcia and Morshedi, 1986)	Quadratic dynamic matrix control (QDMC).	Pyrolysis furnace	QDMC	QDMC was introduced to further improve the constraint handling capability of DMC to enable tight constraint control by formulating the constraints as linear inequalities.
(Ogunnaike, 1986)	The author attempts to bring about an explanation of the reasons for the early successes of DMC.	None	DMC	The paper draws parallels between the DMC algorithm formulation and the well-known techniques which are grounded in statistics such as the least squares parameter estimation method.
(Cutler and Hawkins, 1987)	Presents an application of dynamic matrix control in a hydrocracker reactor with the economic benefits obtained from the controller.	Hydrocracker Reactor	DMC	The paper provides a practical overview of the steps taken in the design and implementation of a DMC controller for a hydrocracker reactor with a preheating furnace. Two tuning parameters were used – the move suppression factor and the equal concern factor. The identification procedure and the optimization algorithm are covered in little detail. However, the controller is reported to have performed well with an online factor exceeding 90% and a

Paper	Principal focus of the work	Plant/process controlled	MPC type	Summary
				reduction in energy consumption in the region of 52%.
(Campo and Morari, 1987)	The design of model predictive control for uncertain linear systems is presented.	None	MPC	This addresses the common problem of model mismatch in model predictive control and all other model-based control strategies. The assumption that a single linear model is representative of the process dynamics is challenged. The authors propose an algorithm that minimizes the worst possible tracking error through the selection of the best representative linear model from a set of models at each sampling instant.
(Morari et al., 1988)	The work presents a theoretical overview of MPC formulations.	None	MPC	The paper represents an in-depth review of model predictive control and its ability to address the most demanding process control problems at the time of publication. The various formulations of unconstrained MPC are reviewed and comparisons with other control strategies are presented. The constraint handling capability of MPC makes it an attractive controller to solving industrial process control problems. This is still a relevant statement even in today's process control systems.
(Georgiou et al., 1988)	Proposes nonlinear dynamic matrix control (DMC) for control of a high purity distillation column.	High purity distillation column	Nonlinear DMC	High purity distillation columns are known to have nonlinearities and this work makes use of nonlinear output transformation which results in nonlinear DMC to overcome the nonlinear dynamics of high purity distillation columns that cause DMC regulatory performance to degrade.
(Kelly et al., 1988)	An application of QDMC in Hydrotreater reactor control of Weighted Average Bed Temperatures is presented.	Hydrocracker reactor	QDMC	The paper covers the project implementation of the QDMC to a hydrocracker reactor outlining the model identification and modelling controller design and tuning of the QDMC. The reported results indicated good handling of process interactions, a wide range of process dynamics and process constraints present in hydrocracker reactor control.
(Yocum and Zimmerman, 1988)	Presents an application of DMC on a distillation column temperature control.	Distillation column	DMC	The capability of DMC to model unusual process dynamics is exploited in this control problem and the DMC controller was able to successfully reduce the



Paper	Principal focus of the work	Plant/process controlled	MPC type	Summary
				variations of the column temperature from the setpoint. The distillation column temperature had inverse response dynamics that were previously not well understood by the plant operators which lead them to controlling the column temperature manually resulting in large variations from the setpoint. The authors do not explicitly state the type of distillation column involved nor the location of the temperature measurement.
(García et al., 1989)	The challenges with robustness of model predictive control are investigated.	None	MPC	The authors assert that past controller design techniques had ignored constraints in their formulation leading to ad hoc methods being developed in the process of controller implementation. The challenge that surfaces is that of costs involved with creating heuristic fixes since each process plant is unique, as such, what works in one plant may not work in a different plant without extensive modifications. The costs associated with these heuristic methods have been reported to outweigh their benefits. On the contrary, model predictive control addresses constraints directly in its formulation.
(Yamuna Rani and Gangiah, 1991)	An application of dynamic matrix control to a nonlinear process model.	Exothermic Reactor	DMC	The authors propose the use of a nonlinear version of dynamic matrix control (DMC) to improve controller performance of a nonlinear exothermic reactor by making use of output transformations of the exponential, logarithmic and reaction rate with results indicating that this method provides better controller performance than the linear DMC.
(Allwright and Papavasiliou, 1992)	A quantitative study of the linear programming optimization algorithm of robust model predictive control	None	MPC	The paper develops a quantitative linear programming problem formulation for impulse response models which results in fewer number of constraints with obvious advantages compared to that developed by (Campo and Morari, 1987).
(Froisy, 1994)	Model predictive control survey	None	MPC	Examined what was then the state of the art in model predictive control technology, its past developments from when it was first introduced in the late 1970's to what it was at the

Paper	Principal focus of the work	Plant/process controlled	MPC type	Summary
				writing of the work. The author further provides a projection of five years into the future of how model predictive control was likely to evolve and mature as a technology including areas that were likely to gain more focus in research and industrial application.
(Moro and Odloak, 1995)	Application of model based constrained FCC control	Fluid Catalytic Cracking (FCC) Unit	DMC	Presented that the dynamic matrix controller is less suitable for systems where some of the controlled variables are only required to be controlled around a range instead of a specific setpoint. Such a case is found in plants such as the fluid catalytic cracking (FCC) unit where, for example, the catalyst regenerator temperature is controlled above and below certain limits to ensure adequate coke combustion and avoid mechanical equipment failure, respectively.
(Lundström et al., 1995)	Discusses DMC limitations	None	DMC	Proposes what is termed an Observer Based MPC (OBMPC) to overcome the limitations of DMC brought about two main assumptions in the DMC formulation i.e., 1) the plant can be represented by a stable step response model and 2) the model mismatch can be modelled as a step signal acting on the process outputs. These assumptions are reported to limit the DMC in that processes with slower process dynamics necessitate the use of many parameters and the controller performance suffer when the disturbance acting on the output is a ramp, or the disturbances affects inputs instead of outputs. The proposed OBMPC is reported as to not possess these limitations.
(Gupta, 1998)	Application of DMC for processes with integrating dynamics.	Continuously Stirred Tank Reactor (CSTR) and column level control	DMC	The work proposed a modification to the DMC algorithm to deal directly with processes that possess integrating dynamics such as level control applications. The reported results show the proposed algorithm eliminates the steady state offset better than traditional DMC.

Paper	Principal focus of the work	Plant/process controlled	MPC type	Summary
(Sorensen and Cutler, 1998)	Linear Programming Optimization with DMC	None	MPC	The paper reported that since targets for the model predictive controller are sometimes set by a higher-level optimization linear program, targets that are inconsistent with what is physically realizable may potentially cause stability problems. Stability can be addressed in such a manner that the prediction horizon is long enough to include the prediction of the steady state
(Dai and Johan, 1999)	Application of DMC in a lab process plant with nonlinear and nonminimum phase dynamics.	Lab scale quadruple-tank process	DMC	Dynamic matrix control's ability to model unusual process dynamics with finite impulse response (FIR) is exploited in this paper dealing with nonminimum phase dynamics of a pilot plant with the controller performance results showing good performance compared to the conventional PI controllers.
(Morari and Lee, 1999)	The work covers the origins and the state of the art in model predictive control as of the time of its publication.	None	MPC	The paper noted the use of the prediction and control horizon as tuning parameters for model predictive control (MPC) is generally ineffective – the behavior of the system becomes insensitive to changes in these parameters over a wide range of values.
(Ansari and Tadé, 2000)	Application of nonlinear model predictive control on a fluid catalytic cracking (FCC) process.	Fluid Catalytic Cracking (FCC) Unit	GMC	A constrained nonlinear model of the FCC unit is utilized with a nonlinear model predictive control strategy based on Generic Model Control (GMC) and compared to linear model predictive control. The reported results indicate superior performance compared to linear model predictive control with the added benefit of not having to re-do plant step tests to update the model since it is not based on plant data. This benefit is valuable in saving resources for organizations utilizing model based advance control techniques.
(Roffel et al., 2000)	First principles modelling and multivariable control of a cryogenic distillation column	Cryogenic distillation process	MPC	A linearized rigorous first principles model of a heat-integrated cryogenic distillation process is used with a constrained multivariable model predictive control (MPC) strategy. The MPC controller is compared to PI control with gain scheduling,

Paper	Principal focus of the work	Plant/process controlled	MPC type	Summary
				feed-forward and decoupling and was found to be more superior in performance.
(Mayne et al., 2000)	Survey paper focused on constrained model predictive control for linear and nonlinear dynamic systems	None	MPC	There have been several heuristic approaches reported in literature to solve the problem of stability and robustness for model predictive control algorithms, as a result, a comprehensive review of the issues of stability and robustness of model predictive controllers given in this paper is useful.
(Hugo, 2000)	The paper deals with practical limitations of model predictive controllers in industry	None	MPC	Challenges the claimed advantages and benefits of model predictive control reported by MPC vendors as well as in literature and raises key issues that tend to be overlooked in model predictive control projects. The work highlights that model predictive controllers are not a 'one-size-fits-all' type of controller although they have their place in highly coupled processes.
(Canney, 2003)	Investigation of Real-time Optimization	None	MPC	The work pointed out that model predictive control is routinely recognized as an important enabling optimization control system of top performing refineries. One of the most active areas of research in model predictive control is developments relating to performance monitoring and sustaining value brought by these controllers.
(Hu Guolong and Sun Youxian, 2003)	An overview of advanced control project (APC) execution	Crude unit distillation process	MPC	An overview of a typical advanced process control project which typically refers to an implementation of an MPC controller in a manufacturing facility. The work outlines the key steps involved with an example of a Crude distillation unit in a refinery.
(Qin and Badgwell, 2003)	Presents one of the most comprehensive and widely cited reviews of model predictive control technologies available in the market at the time of its writing.	None	MPC	The paper looks at the history of model predictive control and takes a deep dive into the different model predictive control products commercially offered by different vendors of model predictive control with their salient features. The paper is a good overview of model predictive control with an industrial perspective.

Paper	Principal focus of the work	Plant/process controlled	MPC type	Summary
(Seborg et al., 2004)	Theoretical formulation of model predictive control is provided.	Various	MPC	The authors provide a useful theoretical framework of model predictive control including the formulations of the predictive model and control law for both the constrained and unconstrained optimization algorithms. The authors are light on details of the multiple-input multiple-output theoretical framework which is only presented as an extension of the single-input single-output formulation.
(Wilson and Das Biswas, 2004)	Improvement in control of a solvent extraction process.	Copper Solvent Extraction process.	DMC	Dynamic matrix controller was implemented and an improvement in throughput of 1.6% was realized from reduced product variability of about 50% and increased controller up-time of up to 90%.
(Beautyman, 2004)	Practical methods that can be used to determine the benefits of a real-time optimization project are outlined.	None	MPC	It is suggested that real-time optimization audits completed prior to implementation are crucial to ensuring the expected benefits from optimization projects are realized. For processes that undergo infrequent changes in modes of operation and economics, an offline infrequent optimization methodology may be sufficient. However, for processes with frequent changes in modes of operation, a full online closed loop real-time optimization is said to be recommended.
(Sharpe and Rezabek, 2004)	Embedded model predictive control tools intended to run on control systems such as the distributed control system (DCS) are proposed.	None	MPC	It is reported that the engineering effort and cost of implementing model predictive control solutions can be significantly decreased by using these embedded model predictive control tools. This strategy helps in eliminating standalone supervisory systems that traditionally implement model predictive control functions. However, the disadvantage would be the execution burden placed on the DCS computation resources and most DCS systems have slower scan times which may or may not have an impact on the model predictive control implementation.
(Kim et al., 2005)	Dynamic matrix control (DMC) is applied in a boiler turbine control application.	Boiler Turbine	DMC	The paper implements dynamic matrix controller to two different models of the boiler – one is derived from a theoretical nonlinear model and the other is

Paper	Principal focus of the work	Plant/process controlled	MPC type	Summary
				derived from the plant input and output data. It is worth noting that although the step response curves were similar – one of the step response curves were significantly different and the cause was due to modelling errors in developing the theoretical model. This points to the need for practitioners to have good process knowledge for the models they are developing to pick up such errors. The work offers insights into the importance of model validation in DMC model identification.
(Wojsznis, 2006)	The work provides a theoretical overview of MPC and optimization	None	MPC	The work provides a good theoretical overview and working principles of model predictive control. The development and implementation of a model predictive control project is covered with insights on the selection of tuning parameters such as penalties on errors and control move inputs.
(Adetola and Guay, 2010)	Real-time optimization with MPC.	None	MPC	The work provides a theoretical framework for the integration of RTO and MPC for constrained uncertain nonlinear systems.
(Holkar and Waghmare, 2010)	Covers tuning of model predictive controllers, providing general rules of thumb on the selection of MPC tuning parameters such as prediction and control horizons, weights on inputs and outputs.	None	MPC	The methods provide a starting point and basis for the selection of the tuning parameters. The paper provides a review of various model predictive control algorithms including Dynamic matrix control (DMC), Model algorithmic control (MAC), Predictive functional control (PFC), Extended prediction self-adaptive control (EPSAC), Extended horizon adaptive control (EHAC) and generalized predictive control (GPC). The reported results indicate that GPC was better than the other controllers. Dynamic matrix control was shown to exhibit poor performance when dealing with ramp-like disturbances.
(Joly, 2012)	Investigates plantwide Optimization	None	MPC	Outlined the goal of optimization in a manufacturing facility such as an oil refinery is to drive process operations towards maximum profit or minimal cost until constraints are reached, either due to equipment safety limits, product quality specifications or environmental regulations. The most successful

Paper	Principal focus of the work	Plant/process controlled	MPC type	Summary
				refineries are said to be those that monitor their performance closely, adjust their operations correspondingly, identify their key weaknesses and correct them promptly.
(Matko et al., 2013)	An application of the DMC algorithm on an aircraft autopilot nonlinear model.	Aircraft Autopilot	DMC	This is a good example of the wide applicability of model predictive control outside of the process industry. The main reported benefit is the ease of tuning allowing non-expert users to exploit the full functionalities of the autopilot system.
(Kouro et al., 2015)	Application of model predictive control (MPC) in power electronics.	None	MPC	The paper presents a review of the emergence of MPC in the control of electrical energy with power semiconductors as well as areas for future research. This is an active research area especially with the increase of distributed power generators and computational power of embedded controllers in recent years.
(Hu Xin et al., 2015)	Application of dynamic matrix control (DMC) in ship positioning systems	Dynamic Ship Positioning	DMC	Addresses the problem of required priori knowledge of system dynamics mandatory in the use of conventional dynamic positioning systems in ships. Proposes the use of DMC where it is reported that priori knowledge of the system dynamics is not necessary thereby allowing non-experts to be comfortable with the control system.
(Forbes et al., 2015)	A review of recent developments in model predictive control	None	MPC	The work is less concerned about the research of the MPC algorithms but rather more focused on the practical challenges faced by MPC practitioners in industry such as ease of commissioning and maintenance of MPC controllers with limited expert skills and resources with the goal of sustaining the benefits brought by these controllers.
(Calugaru and Danisor, 2016)	Application of dynamic matrix control (DMC) in an aircraft landing system	Aircraft landing	MPC	Proposed DMC for an aircraft model during its last phase of the flight for the control of landing stabilization. Reported results show the importance of selecting the correct prediction and control horizons where an increase in the prediction horizon led to degraded performance.

Paper	Principal focus of the work	Plant/process controlled	MPC type	Summary
(Chuong and Vu, 2017)	Application of dynamic matrix control (DMC) in an HVAC system	Heating System (HVAC)	DMC	The work identifies the process model from the input-output data using MATLAB System Identification and applies DMC algorithm with a Quadratic cost function to cater for the constraints. Demonstrates suitability of the control system with a model of a heating system.
(Shen et al., 2020)	The focus of the paper is on energy management system on fuel cell powered vehicles.	Fuel Cell Vehicle	RMPC	The work proposes a strategy based on robust model predictive control (RMPC) together with a Takagi–Sugeno (T–S) fuzzy modelling framework to solve a constrained optimal control problem presented by the power control unit design for fuel cell vehicles. The work is once again another example among many that signify a departure from the traditional process industry applications of model predictive control. This another area that can be expected to grow with the introduction of cleaner energy policies around the world to mitigate the effect of global warming on the planet.
(Hu et al., 2021)	The focus of the paper is to present a survey paper on the role played by MPC in microgrids.	Power Electronic Converter	MPC	The role of MPC in microgrids shows a growing trend. The two main strategies where MPC is employed are at the lower converter-level and at the higher grid-level. The works shows how the MPC is used for voltage regulation and frequency control via power electronic converters at the lower level and it is used for supervisory control tasks such as power flow control between microgrids and power planning and scheduling at higher level. This is a fast growing and promising field for MPC given the growing distributed power generation penetration levels across the globe.

### 2.5.2. Comparative analysis and discussion on the developments of the existing literature on model predictive control and applications on multivariable control systems

Model predictive control (MPC) belongs to a class of advanced control techniques that make use of a dynamic process model in formulating a control law to optimally drive controlled variables to their desired set points (Seborg et al., 2004). Model predictive control, in the form



of dynamic matrix control (DMC), was developed by Cutler and Ramaker (1979) at a Shell oil refinery in the 1970's. DMC has since become the most widely used model predictive control algorithm in the petrochemical industry, specifically in petroleum refineries, around the world (Qin and Badgwell, 2003). The paper by Cutler and Ramaker (1979) covers in detail the theoretical background of the DMC algorithm at the time of its invention. The adoption of DMC in the petrochemical industry was immediate and rapid to such an extent that Ogunnalke (1986) published a paper to bring about an explanation of the possible reasons for the early successes of DMC by drawing parallels between the DMC algorithm formulation and the well-known techniques grounded in the field of Statistics such as the least squares parameter estimation method which was well understood even before the development of DMC. Quadratic dynamic matrix control (QDMC) was later introduced by Garcia and Morshedi (1986) to improve the constraint handling capability of the original DMC algorithm to enable tight constraint control. They achieved this by formulating constraints as linear inequalities with a quadratic optimization algorithm in contrast to the original DMC which used the linear least squares method.

Since the early 1980's, there has been a number of research articles published aimed at providing a survey on the developments of model predictive control. These survey articles help in tracking the progression of model predictive control techniques and its applications over the years. Ray (1983) provided valuable insights through a survey on various topics of multivariable control systems including online parameter estimation, adaptive control, and distributed systems that were prevalent at the time of publication. On the other hand, Garcia and Prett (1986) conducted a review of the current state of model predictive control as of the time of publication. Their work emphasized a need for a unified theory to standardize model predictive control solutions to limit the use of ad hoc techniques that tended to be application specific in practice. In the work by Morari et al., (1988), an in-depth review of model predictive control is presented and its ability to address the most demanding process control problems at the time. The various formulations of unconstrained MPC are reviewed and comparisons with other control strategies are presented. The constraint handling capability of MPC was noted in all these surveys as one of the key features that make MPC an attractive controller to solving industrial process control problems. This is still a relevant statement even in today's process control systems. Froisy (1994) examined what was then the state of the art in model predictive control technology, its past developments from when it was first introduced in the late 1970's to what it was up to that point and possibilities for the future. Qin and Badgwell (2003) presented one of the most comprehensive and widely cited surveys of model predictive control technologies available in the market. The paper looks at the history of model predictive control and takes a deep dive into the different model predictive control products commercially offered by different vendors of model predictive control in industry with their salient features.

The paper remains one of the best recent reviews of the state of industrial model predictive control.

With model predictive control being a multivariable controller, it has naturally been used extensively in distillation process applications in industry. High purity distillation columns are known to have nonlinearities that are difficult to control due to ill-conditioning as described by Skogestad et al., (1988). In Georgiou et al., (1988), a nonlinear dynamic matrix control (DMC) is used for control of a high purity distillation column and they make use of nonlinear output transformation which results in nonlinear DMC to overcome the nonlinear dynamics of high purity distillation columns that cause DMC regulatory performance to degrade. Yocum and Zimmerman (1988) on the other hand presented an application of DMC on a distillation column temperature control. The capability of DMC to model unusual process dynamics is exploited in this control problem and the DMC controller was able to successfully reduce the variations from the setpoint of the column temperature. The distillation column temperature had inverse response dynamics that were previously not well understood by the plant operators which led them to resort to controlling the column temperature manually resulting in large variations from the setpoint. However, the authors do not explicitly state the type of distillation column involved nor the location of the temperature measurement used for control. Other reviewed work where MPC was implemented in a distillation process is that by Roffel et al., (2000) where MPC is applied to a cryogenic distillation column with its performance compared to conventional PI control with gain scheduling, feed-forward and decoupling where it was found that MPC is far superior in performance, as well as the work by Hu Guolong and Sun Youxian (2003) who implemented MPC on a refinery crude distillation unit.

The area of nonlinear model predictive control is another area that has had significant active research. Most industrial processes have nonlinear dynamics that cannot be adequately dealt with using linear controller design theory (Mokhatab and Poe, 2012). In the paper by Yamuna Rani and Gangiah (1991), using a nonlinear version of dynamic matrix control to improve controller performance of a nonlinear exothermic reactor is proposed by making use of output transformations of the exponential, logarithmic and reaction rate with results indicating that this method provides better controller performance than the linear dynamic matrix control formulation. This is similar in comparison to the work by Dai and Johan (1999) where dynamic matrix control's ability to model unusual process dynamics with finite impulse response (FIR) prediction models is exploited. The work deals with the control of nonminimum phase dynamics in a pilot plant with the controller performance results showing good performance compared to conventional PI control.

In the paper by Ansari and Tadé (2000), a constrained nonlinear model of the fluid catalytic cracking unit (FCCU) is utilized with a nonlinear model predictive control strategy based on generic model control (GMC) (Lee and Sullivan, 1988). When compared to linear model

predictive control, the reported results indicated superior performance with the added benefit of not having to re-do plant step tests to update the model since it is not based on plant data. This benefit is valuable in saving resources for organizations utilizing model based advanced control techniques. The work by Kim et al., (2005) implemented dynamic matrix control to two models of an industrial drum-type boiler-turbine; one which was derived from a theoretical nonlinear model and the other derived from plant input and output data. It is worth noting that although the step response curves were similar - one of the step response curves was significantly different with the cause attributed to modelling errors in developing the theoretical model. This pointed to the need for practitioners of model-based control systems to have good process knowledge for the models they are developing to be able to identify such errors. The work also offers insights into the importance of model validation during DMC model identification.

Process optimization remains a central justification for most model predictive control projects. Model predictive control is routinely recognized as an important enabling optimization control system of top performing oil refineries and one of the most active areas of research in model predictive control is developments relating to performance monitoring and sustaining value (Canney, 2003). In industrial process control, model predictive control is implemented primarily as a higher-layer optimization control technique manipulating setpoints of lower-layer regulatory controllers. The model predictive control layer introduces optimization by operating at or near process limits and equipment constraints. Process variables chosen for control at the MPC layer are typically variables that determine the overall process unit's profitability, safety limits and/or constraints (Seborg et al., 2004). Practical methods that can be used to determine the benefits of a real-time optimization projects are outlined by Beautyman (2004) who suggested that real-time optimization audits completed prior to project implementation are crucial to ensuring the expected benefits from optimization projects are realized. For processes that undergo infrequent changes in modes of operation and economics, an offline infrequent optimization control scheme may be sufficient. However, for processes with frequent changes in modes of operation, a full online closed loop real-time optimization control scheme is said to be recommended (Beautyman, 2004). Others such as Joly (2012) have also investigated plantwide optimization and outlined the goal of optimization in a manufacturing facility such as an oil refinery as being to drive process operations towards maximum profit or minimal cost until constraints are reached, either due to equipment safety limits, product quality specifications or environmental regulations. The most successful refineries are said to be those that monitor their performance closely, adjust their operations correspondingly and identify their key weaknesses and correct them promptly.

The success and rapid adoption of model predictive control has not come without challenges and limitations. Lundström et al., (1995) discussed dynamic matrix control limitations. The authors proposed what is termed an Observer Based MPC (OBMPC) to overcome the

limitations of dynamic matrix control brought about two main assumptions in the traditional dynamic matrix control formulation i.e., 1) that all plants can be represented by a stable step response model and 2) that the model mismatch can be modelled as a step signal acting on the process outputs. These assumptions are reported to limit dynamic matrix control in that processes with slower process dynamics necessitate the use of many parameters and the controller performance suffers when the disturbance acting on the output is a ramp, or the disturbance affects inputs instead of outputs whereas the proposed OBMPC is reported as to not possess these limitations.

Hugo (2000) dealt with practical limitations of model predictive controllers in industry. The author challenged the advantages and benefits of model predictive control reported by commercial vendors as well as by some authors in literature and raised key issues that tend to be overlooked in model predictive control projects. The work highlights that model predictive controllers are not a 'one-size-fits-all' type of controllers although they have their place in highly coupled processes. Sharpe and Rezacsek (2004) reported on the significant engineering effort and cost of implementing model predictive control projects and offered a solution in the form of embedded model predictive control tools that could run on the same regulatory layer such as the distributed control system (DCS). The proposed strategy could help in eliminating standalone supervisory control systems that traditionally implement model predictive control functions and instead integrate these to run on regulatory control systems. However, the likely disadvantage would be the execution burden placed on DCS computation resources and most DCS have slower scan times which may or may not have an impact on the model predictive control performance. The work by Forbes et al., (2015) provides a review of recent developments in model predictive control. However, the work is less concerned about the research of the model predictive control algorithms but rather more focused on the practical challenges faced by MPC practitioners in industry such as ease of commissioning and maintenance of these controllers with limited expert skills and less resources with the goal of sustaining the benefits brought by these controllers.

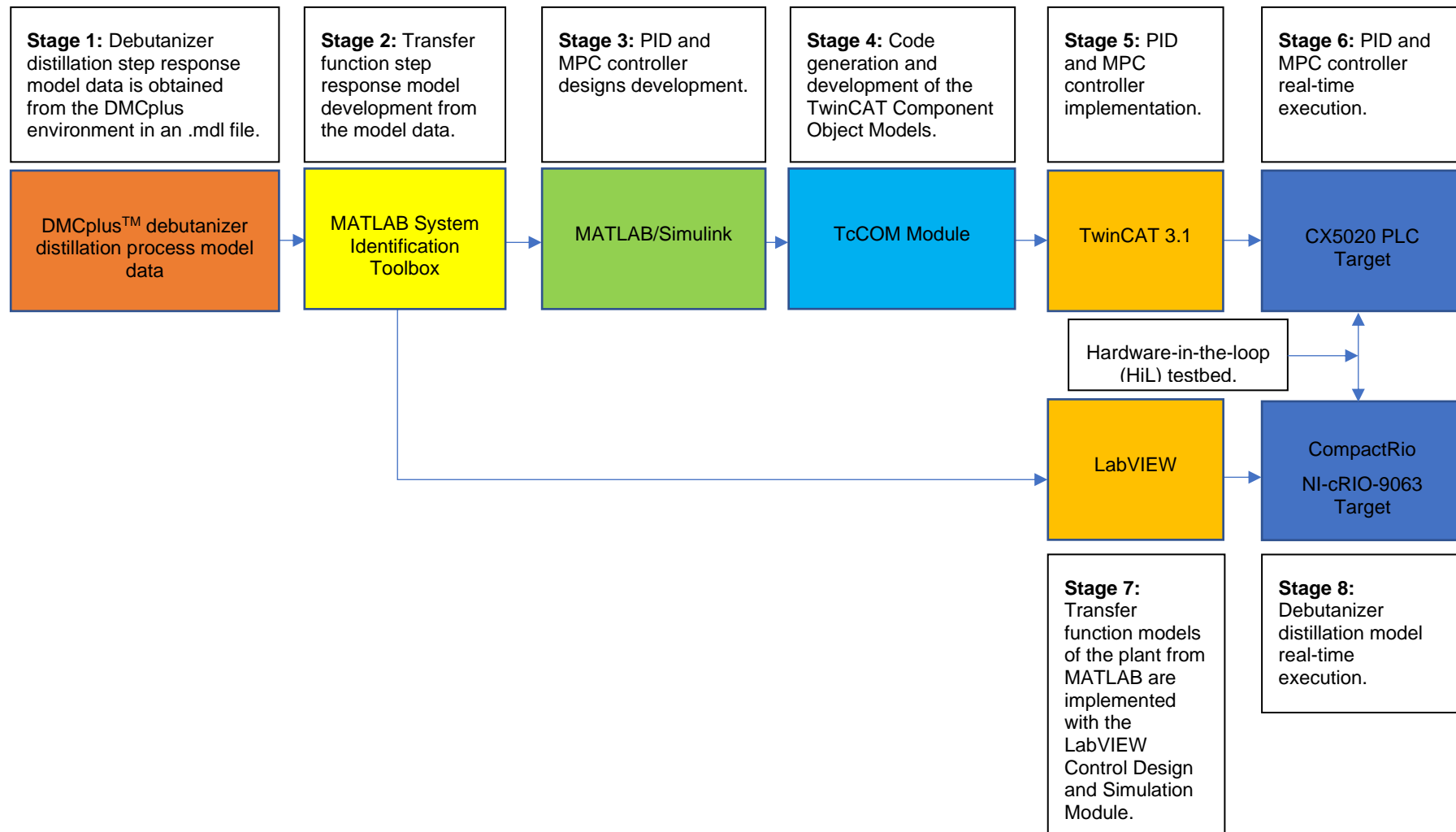
Lastly, model predictive control has also been applied to other industries outside the petrochemical domain. This is indicative of model predictive control's versatility and ability to be adapted to various formulations and applications. Kouro et al., (2015) provided a good review of the emergence of model predictive control in power semiconductor energy control. This is an active research area especially with the increase of distributed power generators and computational power of embedded controllers in recent years. On the other hand, Matko et al., (2013) and Calugaru and Danisor (2016) applied dynamic matrix control in aircraft autopilot systems. This is another good example of the wide applicability of model predictive control outside of the process industry.

## 2.6. System development process and system architecture based on literature

The literature review conducted has shown developments and trends on the topics of distillation process control, debutanizer column control, multivariable control and model predictive control and its applications in multivariable control systems. As a result of the literature reviewed, this research aims to develop multivariable controller design methodologies for a debutanizer empirical model and implement a closed loop control system in a Hardware-in-the-Loop (HiL) configuration and simulate in real-time. According to the reviewed work from the literature, the best way to achieve this objective can be outlined as follows:

- Develop linear-time-invariant (LTI) continuous-time transfer function models from empirical model data of an industrial debutanizer distillation process in the MATLAB environment. A similar approach is demonstrated in (Freitas et al., 1994), (Ramli and Chandra Mohan, 2015) and (Chuong and Vu, 2017).
- Develop mathematical descriptions of the design of decentralized PID controllers using the relative gain array and the Niederlinski index for control loop pairing, ideal decoupling control technique for the elimination of interactions and the internal model control technique for PID controller tuning. These approaches are demonstrated in (Edgar H. Bristol, 1966), (Luyben, 1970), (Niederlinski, 1971), (Garcia and Morari, 1985), (Yu and Luyben, 1986), (Ogunnaike and Ray, 1994) and (Saxena and Hote, 2012).
- Develop an MPC controller based on a linear step response prediction model and its implementation in the MATLAB/Simulink environment. A similar approach is demonstrated in (Kelly et al., 1988), (Seborg et al., 2004) and (Holkar and Waghmare, 2010).
- Finally, implement in the LabVIEW simulation environment the debutanizer distillation process model and the decentralized PID controllers in the Beckhoff's TwinCAT 3 environment and configure a Hardware-in-the-Loop (HiL) testbed and perform simulation case studies in real-time. A similar approach is demonstrated in (Grega, 1999) and (Cornieles et al., 2006).

The findings of the literature review have led to a system development process and system architecture proposal. Figure 2.5 illustrates the proposed system development process and system architecture broken up into 8 stages and arranged to depict the flow of information in flow diagram form and a brief description of each stage is provided.



**Figure 2.5:** Proposed system development process and system architecture

## **2.7. Conclusion**

In this chapter, literature has been reviewed on the fields of Distillation process control and debutanizer column control, multivariable control and model predictive control and its applications on multivariable control systems. The reviewed literature on each of the topics was presented in a tabulated format, analyzed, and compared to develop an understanding of the current state of development for each topic.

The first focus area of Distillation process control and debutanizer column control literature mainly focused on model predictive control's early developments, applications to industrial processes, nonlinear systems, process optimization, as well as its challenges and limitations. The second literature review was mainly focused on decentralized decoupling control in multivariable control systems. The third and last literature review was mainly focused on model predictive control's early developments, applications to industrial processes, nonlinear systems, process optimization, as well as its challenges and limitations. These topics are reviewed based of the obtained literature, derived analysis, and in comparison, to develop a thorough understanding of the current state of development for each topic. The findings of the literature review led to a system development process and system architecture proposal which is presented.

Chapter 3 presents a theoretical background on model predictive control. The general overview and working principle of MPC is outlined and the formulations of the prediction models of both a single-input single-output (SISO) and a multiple-input multiple-output (MIMO) system are provided and the MPC control law formulation with recommended practices in selecting design parameters necessary for MPC controller configuration.

## CHAPTER THREE: CONTROLLER DESIGN CONCEPTS

### 3.1. Introduction

As previously outlined in Chapter 1, good process control and operation of industrial distillation columns offers significant economic incentives since distillation columns consume considerable amounts of energy and are considered one of the most widely used processes, especially in the refining industry (Buckley et al., 1985). Distillation columns present process control challenges due to their coupled multivariable structure and often exhibit nonlinear dynamic behaviour (Buckley et al., 1985). A distillation control problem necessitates the use of control system design techniques that are suitable for multiple-input-multiple-output (MIMO) processes and that can effectively deal with process variable interactions. Most processes encountered in the refining industry are coupled and multivariable in nature. Coupling occurs when a single process variable's dynamic behaviour influences other process variables giving rise to variable interactions (Seborg et al., 2004). Control systems capable of providing satisfactory performance for such processes require the use of nontrivial multivariable controller design techniques.

In this chapter, the multivariable controller design concepts utilized in the development of this thesis are presented. The main concepts covered include the relative gain array (RGA) and the Niederlinski index methods which are used for interaction analysis and control structure selection. The decoupling control techniques used for effective elimination of multivariable process interactions are also described and the model order reduction (MOR) techniques that enable simplified controller tuning. The internal model control (IMC) used to obtain the proportional-integral-derivative (PID) gains, and finally, the multivariable model predictive control (MPC) technique are described. The mathematical formulations for these concepts are provided with explanations of their working principles.

The chapter begins with the relative gain array in section 3.2 followed by decoupling control in section 3.3. In section 3.4, the PID controller design is provided starting with the model order reduction and the IMC-PID controller tuning technique, in section 3.5 the model predictive control strategy is presented with the development of prediction models and control law formulation. Lastly, concluding remarks are provided in section 3.6.

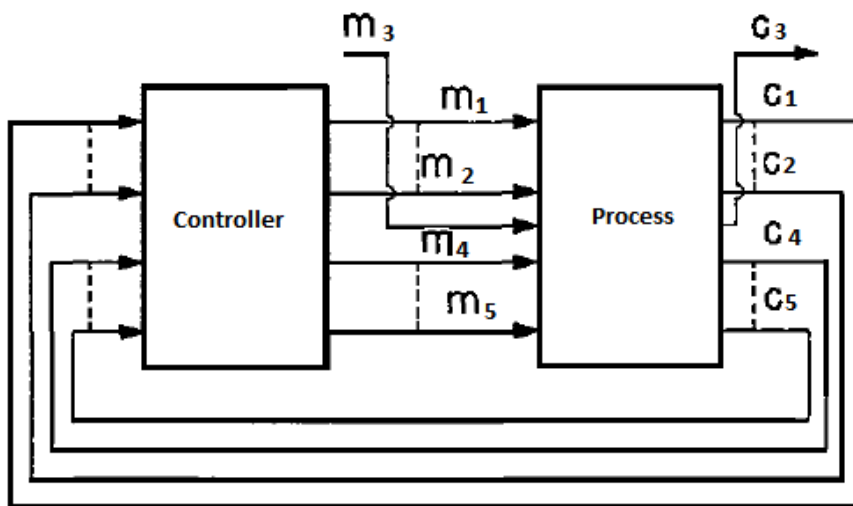
### 3.2. Relative gain array (RGA)

The relative gain array (RGA) is an interaction measure used as a design tool for pairing controlled outputs and control inputs thereby determining the control structure of a system (Edgar H Bristol, 1966). The relative gain of a loop pair can be described as a quantitative measure of the influence a control input has on a controlled output, relative to other control inputs acting on the same system (Ogunnaike and Ray, 1994). The relative gain is given as a



ratio of the open loop steady state gain to the closed loop steady state gain and has been used widely as a design tool (Halvarsson, 2010), (Panwar et al., 2018), (Liang et al., 2020).

To explain the working principle, an example of how the relative gain for a typical input-output pair is determined is illustrated in Figure 3.1, where the relative gain of the loop pair comprised of the control input  $M_3$  and controlled variable  $C_3$  is calculated. Firstly, the open loop steady state gain is determined by opening all the loops in the system and generating a step input change via the control input  $M_3$  and recording the open loop steady state gain of the controlled variable  $C_3$  response. Secondly, the closed loop steady state gain is determined by closing all other control loops leaving only the loop pair  $M_3$  and  $C_3$  open and generating another step input change via the control input  $M_3$  and recording the closed loop steady state gain of the controlled variable  $C_3$  response. It is worth noting that having a control loop open is analogous to having it on manual control in industrial control system terminology. The ratio of the open loop gain to the closed loop gain is referred to as the relative gain for the loop pair  $M_3 - C_3$  (Edgar H Bristol, 1966).



**Figure 3.1: Relative gain of loop pair  $M_3-C_3$**  (Edgar H Bristol, 1966)

The mathematical expression for the relative gain array described above is given by:

$$\lambda_{ij} = \frac{\left(\frac{\partial c_i}{\partial m_j}\right)_{\text{with all other loops open}}}{\left(\frac{\partial c_i}{\partial m_j}\right)_{\text{loop } m_j \text{ open; all other loops closed with perfect control}}} \quad (3.1)$$

The relative gain array for a general second order multivariable system can be represented in matrix form as:

$$\Delta = \begin{bmatrix} \lambda_{11} & \lambda_{12} \\ \lambda_{21} & \lambda_{22} \end{bmatrix} \quad (3.2)$$

where:

$\lambda_{11}$  = Relative gain between input  $M_1$  and output  $C_1$

$\lambda_{12}$  = Relative gain between input  $M_2$  and output  $C_1$

$\lambda_{21}$  = Relative gain between input  $M_1$  and output  $C_2$

$\lambda_{22}$  = Relative gain between input  $M_2$  and output  $C_2$

According to Bristol (1966), the relative gain of a selected pair of the control input and controlled output variables must be as close as possible to a value equal to one (or unity gain). Relative gain values that are negative or much larger than one are considered undesirable and must be avoided (Edgar H Bristol, 1966). Closed loop stability of the selected control structure, more especially for higher order systems, must be confirmed with a check for a positive Niederlinski index (NI) (Ogunnaike and Ray, 1994). Niederlinski (1971) introduced a tool to determine structural stability of multivariable control system designs.

The system is considered unstable if the Niederlinski index is negative, that is if:

$$NI = \frac{|G(0)|}{\prod_{i=1}^n g_{ii}(0)} < 0 \quad (3.3)$$

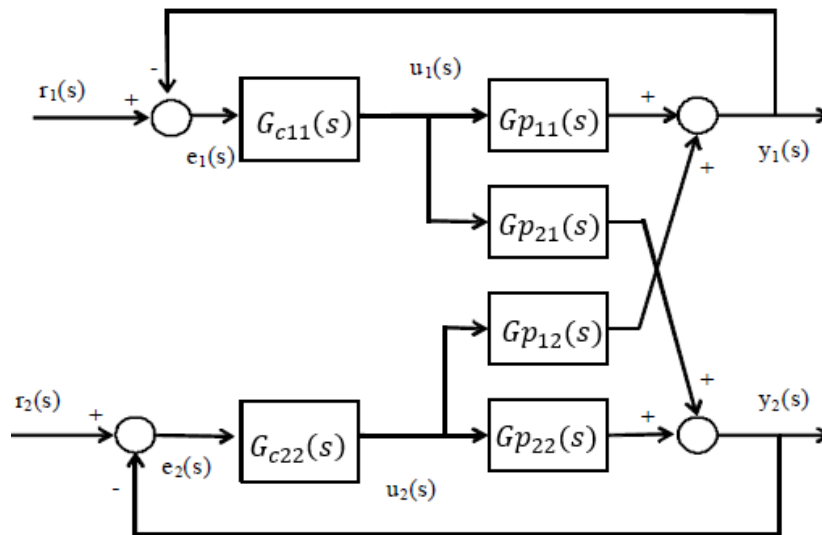
Where  $|G(0)|$  is the determinant of the system's steady state gain matrix and  $\prod_{i=1}^n g_{ii}(0)$  is the product of its diagonal elements (Luyben, 1993).

The objective of the concepts covered in this section is to confirm the input-output pairings of a second order process model and determine structural stability with the Niederlinski Index. These concepts are used in Chapter 5 for the second order debutanizer distillation process model. The following section presents the decoupling control technique that is used in this research to eliminate process variable interactions as will be shown in Chapter 5.

### **3.3. Decoupling control**

Decoupling control refers to the explicit compensation measures that are designed into the system to eliminate the effects caused by undesirable process interactions (Luyben, 1970). In multivariable control systems, process interactions are a common phenomenon where changes in one control variable affects more than the one intended output variable.

An illustrative block diagram of a second order multivariable control system where the outputs appear as being independently controlled without the use of decoupling controllers is shown in Figure 3.2.



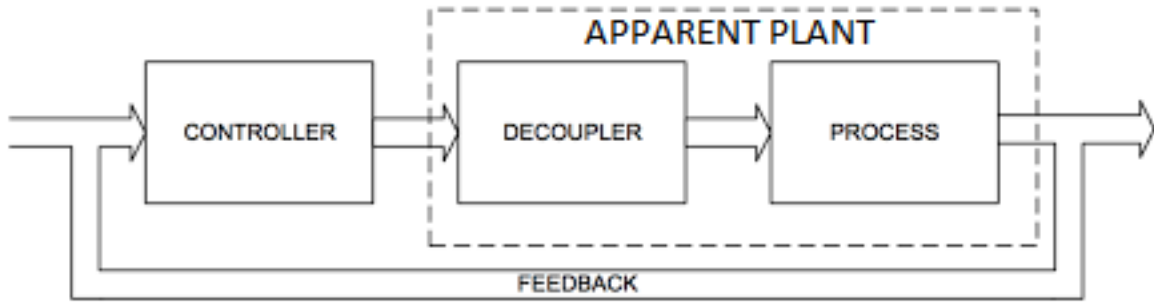
**Figure 3.2: Second order multivariable system without decoupling** (Wade, 1997)

The blocks  $Gp_{11}(s)$ ,  $Gp_{21}(s)$ ,  $Gp_{12}(s)$  and  $Gp_{22}(s)$  represent the transfer function models that relate the system inputs to the system outputs. Process interactions are represented by the  $Gp_{21}(s)$  and  $Gp_{12}(s)$  blocks while the controllers are represented by the blocks  $Gc_{11}(s)$  and  $Gc_{22}(s)$ . Depending on the system properties, it is possible for the system to become unstable and uncontrollable due to the process interactions, represented by the  $Gp_{21}(s)$  and  $Gp_{12}(s)$  blocks in Figure 3.2, with disastrous consequences (Wade, 1997).

Decoupling control is a method of dealing with these process interactions by incorporating decoupling controllers to cancel the effect of the undesired interactions (Luyben, 1970; Morilla et al., 2008; Ogunnaike and Ray, 1994). Two main techniques for implementing decoupling controllers are available: static decoupling and dynamic decoupling. Static decoupling refers to compensation strategies for steady state process interactions. However, this form of decoupling does not compensate for interactions that occur during transient conditions. On the other hand, dynamic decoupling refers to strategies used for compensating for process interactions during both steady state and transient conditions. Therefore, it is more desirable to implement dynamic decoupling in order to ensure process interactions are completely compensated for in the system (Ogunnaike and Ray, 1994).

Two different approaches to conventional dynamic decoupling exist, namely; ideal decoupling, and simplified decoupling (Wade, 1997). The main advantages and disadvantages of each approach can be summarized as being that ideal decoupling yields complicated decoupling transfer functions while offering the benefit of a simpler final apparent process, whereas simplified decoupling yields much simpler decoupling transfer functions while having a relatively more complicated final apparent process (Gagnon et al., 1998; Luyben, 1970; Wade, 1997). Figure 3.3 shows a system block diagram with decoupling compensators incorporated. The block diagram is similar to the conventional closed loop feedback control block diagram

with the exception of the decoupling compensators which are incorporated at the outputs of the controllers before the process.



**Figure 3.3: Incorporating decoupling controllers** (Muga, 2015)

The apparent process as “seen” by the controller becomes a diagonal and for a general second order system can be represented mathematically by the diagonal matrix  $T(s)$ , where:

$$T(s) = G_p(s)D(s) \quad (3.4)$$

$$\begin{bmatrix} T_{11}(s) & T_{12}(s) \\ T_{21}(s) & T_{22}(s) \end{bmatrix} = \begin{bmatrix} Gp_{11}(s) & Gp_{12}(s) \\ Gp_{21}(s) & Gp_{22}(s) \end{bmatrix} \begin{bmatrix} D_{11}(s) & D_{12}(s) \\ D_{21}(s) & D_{22}(s) \end{bmatrix} \quad (3.5)$$

Letting  $T_{12}(s) = T_{21}(s) = 0$  and letting  $D_{11}(s) = D_{22}(s) = 1$  yields a diagonal matrix that represents the decoupled apparent process:

$$\begin{bmatrix} T_{11}(s) & 0 \\ 0 & T_{22}(s) \end{bmatrix} = \begin{bmatrix} Gp_{11}(s) & Gp_{12}(s) \\ Gp_{21}(s) & Gp_{22}(s) \end{bmatrix} \begin{bmatrix} 1 & D_{12}(s) \\ D_{21}(s) & 1 \end{bmatrix} \quad (3.6)$$

Multiplying out the matrices yields:

$$\begin{bmatrix} T_{11}(s) & 0 \\ 0 & T_{22}(s) \end{bmatrix} = \begin{bmatrix} Gp_{11}(s) + Gp_{12}(s)D_{21}(s) & Gp_{11}(s)D_{12}(s) + Gp_{12}(s) \\ Gp_{21}(s) + Gp_{22}(s)D_{21}(s) & Gp_{21}(s)D_{12}(s) + Gp_{22}(s) \end{bmatrix} \quad (3.7)$$

The remainder of the decoupling control problem for a general second order multivariable control system is to solve for  $D_{12}(s)$  and  $D_{21}(s)$  from Equation (3.7). To solve for  $D_{12}(s)$ , let:

$$Gp_{11}(s)D_{12}(s) + Gp_{12}(s) = 0 \quad (3.8)$$

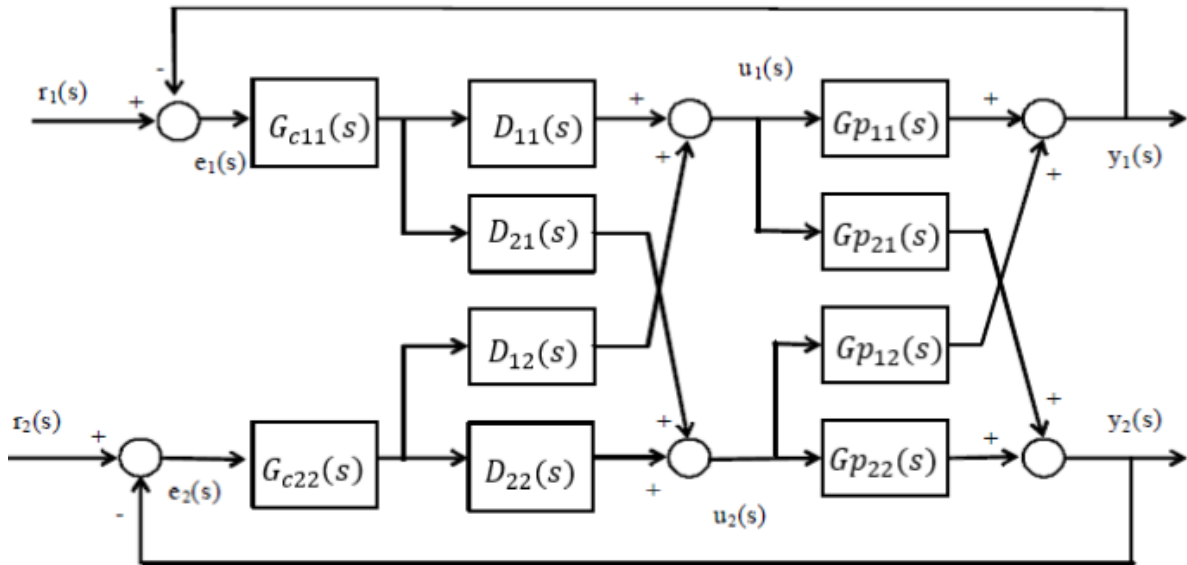
$$\therefore D_{12}(s) = -\frac{Gp_{12}(s)}{Gp_{11}(s)} \quad (3.9)$$

And to solve for  $D_{21}(s)$ , let:

$$Gp_{21}(s) + Gp_{22}(s)D_{21}(s) = 0 \quad (3.10)$$

$$\therefore D_{21}(s) = -\frac{Gp_{21}(s)}{Gp_{22}(s)} \quad (3.11)$$

Finally, as already indicated in Equation (3.6),  $D_{11}(s) = 1$  and  $D_{22}(s) = 1$ . Therefore, the second order multivariable control system block diagram with decoupling compensators incorporated is given in Figure 3.4. Since the values of  $D_{11}(s) = D_{22}(s) = 1$ , their blocks can also be represented as straight lines. The blocks  $D_{12}(s)$  and  $D_{21}(s)$  are the decoupling compensators computed using Equations (3.9) and (3.11), respectively, where  $D_{12}(s)$  compensates for the interactions caused by  $Gp_{12}(s)$  on  $y_1(s)$  and  $D_{21}(s)$  compensates for the interactions caused by  $Gp_{21}(s)$  on  $y_2(s)$ .



**Figure 3.4: Second order multivariable system without decoupling** (Wade, 1997)

The above-mentioned decoupling procedure is used in Chapter 5 to design the decoupling compensators for the second order debutanizer distillation process model used in this research. As shown in Chapter 5, once the decoupling compensators are computed, the decoupled apparent plant models for the two control loops are obtained,  $T_{11}(s)$  representing the decoupled apparent plant of the LCN Reid Vapour Pressure (kPa) loop model and  $T_{22}(s)$  representing the decoupled apparent plant of the LPG  $C_5$  concentration (Mol %) loop model and are further used in the design of the decentralized PID controllers. Since these control loop models can be of a higher order which could complicate the controller design methodology, it is necessary to first implement a form of model order reduction without affecting plant dynamics and such a concept is presented in the next section.

### 3.4. PID controller design

#### 3.4.1. Model order reduction

It is necessary to reduce the given apparent process models to second order by means of model order reduction techniques to simply PID tuning complexity. Reducing high order models enables the controller design to take advantage of the tuning rules available in literature for first order plus time delay (FOPTD) or second order plus time delay (SOPTD) systems

(Visioli, 2005). In PID controller design, model reduction refers to the approximation of a higher order system with a simpler model, using either a first order or second order model. There are two common approaches to model order reduction; designing a controller with the available high order model and reduce the resulting controller to a standard PID form or alternatively to approximate the high order model with a lower order model and proceed with the design of a PID controller for the reduced model (Visioli, 2005), the latter approach is used in this research. Model order reduction techniques have been used successfully for numerous other cases in literature (Isaksson and Graebe, 1999; Skogestad, 2003; Wang et al., 2001; Yongho et al., 1998). In this research, model order reduction is carried out using the method proposed by (Isaksson and Graebe, 1993). The method involves approximating a model by retaining the average dominant poles and zeros as well as the lower order coefficients of the high order model. The reduced model can be written as (Isaksson and Graebe, 1993):

$$\hat{T}(s) = \frac{\hat{B}(s)}{\hat{A}(s)} \quad (3.12)$$

where:

$$\hat{B}(s) = \frac{1}{2}(\hat{B}_1(s) + \hat{B}_2(s)) \quad (3.13)$$

$$\hat{A}(s) = \frac{1}{2}(\hat{A}_1(s) + \hat{A}_2(s)) \quad (3.14)$$

$\hat{B}_1(s)$  and  $\hat{A}_1(s)$  are polynomials obtained by retaining the dominant zeros and poles, respectively, whereas  $\hat{B}_2(s)$  and  $\hat{A}_2(s)$  are polynomials obtained by retaining the lower order coefficients of the numerator and denominator, respectively (Isaksson and Graebe, 1993).

The model order reduction technique presented in this section is relatively simple to understand and is used in Chapter 5 to reduce the obtained apparent plant models of the decoupled debutanizer distillation process to ease of controller design complexity. The controller design methodology adopted in this research which is based on Internal Model Control (IMC) technique is presented in the next section.

### 3.4.2. IMC-PID controller

Internal Model Control (IMC) is a model-based control strategy that can be used for PID controller tuning (Garcia and Morari, 1982; Hepburn and Wonham, 1982; Ming et al., 2020; Seborg et al., 2004). A recent comparison study of various PID controller tuning strategies for including IMC, Smith Predictor, Feedback and Feedforward control and Cascade control concluded the IMC method is better than the other tuning strategies in a debutanizer distillation column control application (Ramli, 2016).

To better elucidate the IMC-PID tuning technique, a single-input single-output (SISO) approximate model  $\tilde{G}_p(s)$  is considered which can be represented as:

$$\tilde{G}_p(s) = \tilde{G}_p(s)_- \tilde{G}_p(s)_+ \quad (3.15)$$

Where  $\tilde{G}_p(s)_-$  is the invertible and minimum phase part of the model and  $\tilde{G}_p(s)_+$  is the non-invertible non-minimum phase part of the model (Isaksson and Graebe, 1999). The IMC controller  $Q_1(s)$  is given by the inverse of the invertible and minimum phase part of the model:

$$Q_1(s) = \tilde{G}_p^{-1}(s)_- \quad (3.16)$$

Where  $Q_1(s)$  is considered stable but not necessarily proper. For closed loop stability, an adjustable low-pass filter  $f(s)$  is incorporated with the inverted model to guarantee that the resulting IMC controller is physically realizable and proper (Morari, 1983).  $f(s)$  is given by:

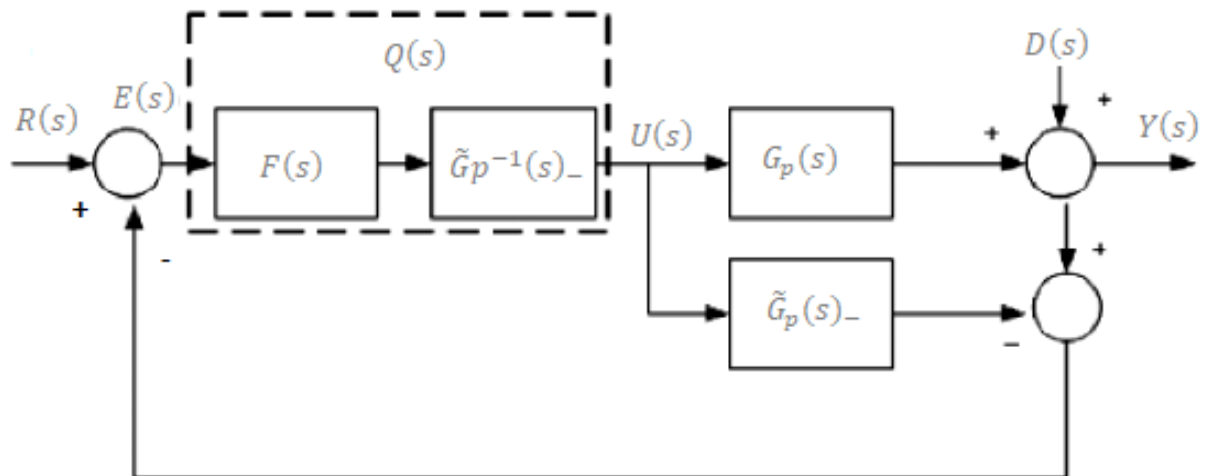
$$f(s) = \frac{1}{(\lambda s + 1)^z} \quad (3.17)$$

Where lambda,  $\lambda$ , is an adjustable tuning filter factor and  $z$  is a factor used to ensure the resulting IMC controller is physically realizable and proper. Therefore, the resulting IMC controller is given by:

$$Q(s) = f(s)Q_1(s) \quad (3.18)$$

$$\therefore Q(s) = \frac{1}{(\lambda s + 1)^z} \tilde{G}_p^{-1}(s)_- \quad (3.19)$$

The complete control structure of IMC is shown in Figure 3.5.



**Figure 3.5: Practical internal model control block diagram with low pass filter  $F(s)$  adapted from (Saxena and Hote, 2012)**

The block diagram shown in Figure 3.5 is similar to the classical feedback control system where  $Q(s)$  represents the IMC controller,  $G_p(s)$  is the plant under control,  $\tilde{G}_p(s)$  represents the plant's approximate model,  $R(s)$  represents the target setpoint,  $Y(s)$  represents the controlled output,  $E(s)$  represents the error between the target setpoint and the controlled output  $Y(s)$ ,  $U(s)$  control inputs into both the physical plant and the plant model and, finally,  $D(s)$  represents the unmeasured disturbances. The difference between the output of the model, which represents the predicted output, and the controlled output is computed and used as bias feedback.

In (Rivera et al., 1986), it is shown that the above-mentioned IMC design procedure naturally yields a PID-type controller. Therefore, the IMC controller obtained from the IMC design procedure above leads to the standard ideal PID feedback controller that can be represented as:

$$G_c(s) = \frac{Q(s)}{1 - Q(s)\tilde{G}_p(s)} := K_p \left( 1 + \tau_I \frac{1}{s} + \tau_D s \right) \quad (3.20)$$

In Chapter 5, the above-mentioned IMC design methodology is used in the design of PID controllers for debutanizer distillation process models. The IMC approach yields controller gains for a PID-type controller that is easy to implement in conventional control system hardware found in industry. As outlined in Chapter 5, the controller gains obtained can be directly implemented and controller performance observed whether it meets the prescribed performance criteria. In cases where the controller performance is not satisfactory, the IMC methodology offers the filter tuning factor, lambda  $\lambda$ , that can be adjusted until the desired control system response is obtained. The next section describes concepts and the theoretical background of another controller design technique which is based on model predictive control (MPC).

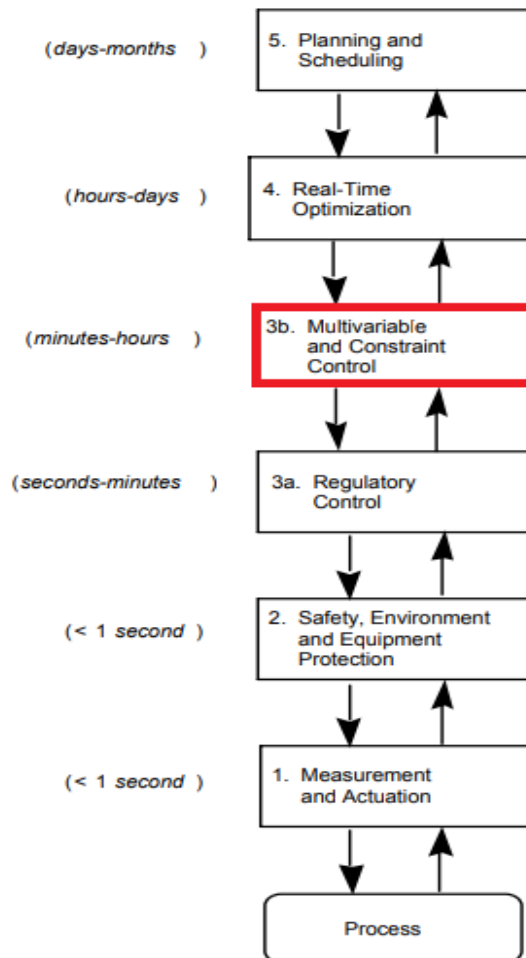
### 3.5. Model predictive control (MPC)

Model predictive control (MPC) is an advanced control technique that makes use of a dynamic process model for prediction and process control. In general, controllers that have the process model integrated within their formulation for control performance purposes are generally referred to as model predictive controllers (Froisy, 1994). Model predictive control was developed in the petrochemical industry as opposed to most control strategies which were developed in academia. Early industrial implementations of MPC are believed to have fuelled the academic theoretical investigations that lead to the broadened knowledge of MPC as it is known today (Froisy, 1994).

In industrial process control, model predictive control is implemented as a constraint handling control technique manipulating setpoints of lower layer regulatory proportional-integral-



derivative (PID) control loops residing in a control system such as a distributed control system (DCS) as illustrated in the hierarchy of process control activities in Figure 3.6 (Morari and Lee, 1999), (Seborg et al., 2004). The first layer of the hierarchy is the measurement and actuation layer where there is the field instrumentation measuring process variables, capturing process data, and making it available to the higher-level layers. This would be instrumentation measuring variables such as pressure, temperature, level, flow, composition, etc. as well the actuators that manipulate the process such as control valves, motors, pumps, etc. with execution frequency of less than one second.

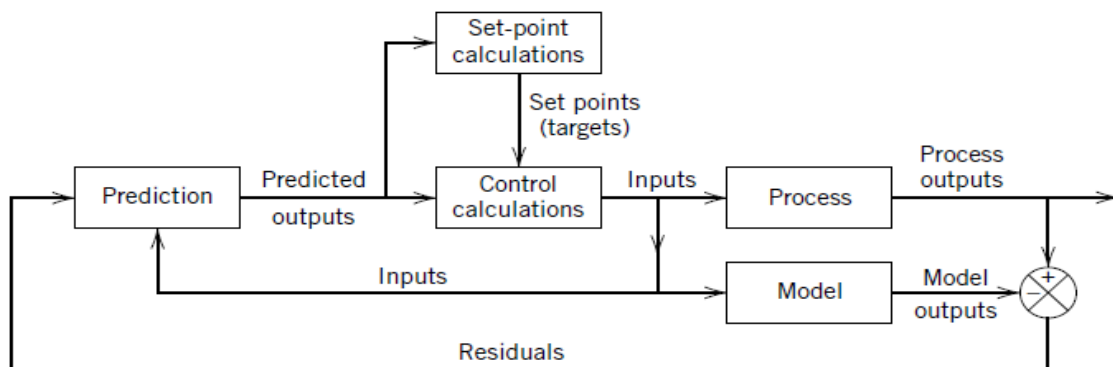


**Figure 3.6: Hierarchy of process control activities** (Seborg et al., 2004)

The second layer in Figure 3.6 is the safety, environment, and equipment protection layer where there is equipment designed to mitigate against process hazardous events from developing beyond equipment design safety limits which may potentially lead to loss of containment of process material with devastating safety and environmental consequences. Equipment in this layer is critical for protecting plant personnel and maintaining safe operations and include process safety alarms and safety instrumented systems (IEC, 2003). The first part of the third layer is the regulatory control layer where the basic process control system resides such as a programmable logic controller (PLC) or the distributed control system (DCS). In this

layer, the regulatory PID controllers reside, and the basic processing of control functions are executed which mainly involve maintaining process variables at their setpoints and ensuring control loop stability as multiple single-input single-output (SISO) control loops with an execution frequency ranging from seconds to a minute. The main role of the regulatory PID controllers is to keep the process stable by maintaining the process variables at their desired setpoints and within design limits with no optimization other than maintaining the process stable (Skogestad, 2007), (Seborg et al., 2004). The second part of the third layer, highlighted in red in Figure 3.6, is the multivariable and constraint control layer. In this layer, advanced control functions with multivariable control techniques such as model predictive control are executed. It is in this layer where optimization is introduced using model predictive control with objectives which include operating the process at or near process limits and equipment constraints. Process variables selected to be part of control by model predictive control are variables that determine the overall unit's profitability, safety limits and/or constraints (Seborg et al., 2004). Model predictive control manipulates the lower-level PID regulatory control loops by adjusting their setpoints in order to effect control (Skogestad, 2007). Finally, the fourth and fifth layers are the real-time optimization layer and the planning and scheduling layer, respectively. Both layers deal with steady state optimization based on market demands, feedstock costs and product prices, with different execution cycles.

A general model predictive control block diagram is illustrated in Figure 3.7 to describe the working principle of model predictive control (Gulzar et al., 2020; Seborg et al., 2004). Figure 3.7 is comprised of five blocks, namely; Prediction, Setpoint calculations, Control calculations, Process and Model. In the prediction block, an accurate dynamic model of the plant is used to predict future values of the controlled outputs. The resulting predicted outputs are sent to the setpoint calculations block and the control calculations block. In the setpoint calculations block, the predicted outputs are used to compute optimal steady-state setpoints. The steady-state setpoints are sent from the setpoint calculations block to the control calculations block for the computation of optimum control moves based on predicted deviations between these setpoints and predicted future values of the controlled outputs (Luyben, 1993).



**Figure 3.7: Model predictive control block diagram** (Seborg et al., 2004)

In computing the control moves an optimization algorithm is used with constraints imposed on the plant explicitly incorporated in the algorithm such as valve travel limits, compressor speed limits, equipment metallurgical limits, etc. Model predictive control's explicit constraint handling capability has been the main reason for its use and success in the refining industry (Morari et al., 1988; Qin and Badgwell, 2003). In Figure 3.7, the computed control moves are sent to three blocks, namely, the feedback to the prediction block, the model block as well as the process block which represent the plant under control. The prediction block utilizes the computed control moves in the next prediction cycle. The control inputs are sent to the process to influence the controlled outputs to move towards their computed setpoint targets. The control moves are also sent to the model. The outputs from the process are compared with model outputs for differences arising from model and plant mismatch and unmeasured disturbances. In cases where the model is a fairly accurate representation of the process and there are no disturbances, the difference between the process outputs and model outputs would be near zero. However, there are unmeasured disturbances and errors in models that result in a non-zero difference. The difference is used as bias to correct the prediction in the next cycle. Control moves are re-calculated at each sampling instant and only one control move is sent to the process and the cycle is repeated. The concepts developed in the following section for model predictive control are used in Chapter 6 in design of an MPC controller for the seventh order debutanizer distillation process model. In the next section, a typical prediction model formulation is described for a single-input single-output (SISO) system.

### 3.5.1. Prediction model for single-input single-output (SISO) systems

A one-step ahead prediction model for a stable single-input single-output (SISO) system can be presented as follows (Seborg et al., 2004):

$$y(k+1) = y_0 + \sum_{i=1}^{N-1} S_i \Delta u(k-i+1) + S_N u(k-N+1) \quad (3.21)$$

where  $k$  represents the sample instant,  $i$  is the standard index of summation for the model horizon,  $N$  represents the limit of summation for the model horizon,  $y(k+1)$  is the predicted future output at  $k+1$  sampling instant,  $y_0$  is the initial condition of the output,  $S_i$  represents the step response coefficients from  $S_1$  to  $S_N$ , and  $\Delta u(k-i+1)$  represents the change in the control input from the previous sampling instant  $(k-i)$  to the next sampling instant  $(k-i+1)$  (Seborg et al., 2004). To differentiate between the predicted output and the actual output, a circumflex symbol ( $\hat{\phantom{y}}$ ) is used to represent the predicted output (Seborg et al., 2004). In Equation 3.21,  $y(k+1)$  is replaced with  $\hat{y}(k+1)$  and zero initial conditions are assumed to be zero ( $y_0 = 0$ ) for simplicity and the resulting equation for the predicted output at  $k+1$  sampling instant can be re-written as:

$$\hat{y}(k+1) = S_1 \Delta u(k) + \sum_{i=2}^{N-1} S_i \Delta u(k-i+1) + S_N u(k-N+1) \quad (3.22)$$

where the first term ( $S_1 \Delta u(k)$ ) represents the effect of the current control action on the predicted output, while the second and third terms:

$$\sum_{i=2}^{N-1} S_i \Delta u(k-i+1) + S_N u(k-N+1)$$

represent the effect of past control actions on the predicted output. From the above formulation, a two-step ahead prediction model can be presented as follows (Seborg et al., 2004):

$$\hat{y}(k+2) = S_1 \Delta u(k+1) + S_2 \Delta u(k) + \sum_{i=3}^{N-1} S_i \Delta u(k-i+2) + S_N u(k-N+2) \quad (3.23)$$

where  $\hat{y}(k+2)$  represents the predicted future output at  $k+2$  sampling instant.

The above formulations can be generalized as follows for a  $J$ -step ahead prediction where  $J$  is a positive integer representing a sampling instant in the future (Seborg et al., 2004):

$$\hat{y}(k+j) = \sum_{i=1}^j S_i \Delta u(k+j-i) + \sum_{i=j+1}^{N-1} S_i \Delta u(k+j-i) + S_N u(k+j-N) \quad (3.24)$$

Equation (3.24) can be broken into two parts – the predicted unforced response:

$$\sum_{i=j+1}^{N-1} S_i \Delta u(k+j-i) + S_N u(k+j-N)$$

and the predicted forced response:

$$\sum_{i=1}^j S_i \Delta u(k+j-i)$$

The unforced response refers to the predicted output due to past control inputs, if no further control inputs were implemented by the controller (Seborg et al., 2004). The predicted unforced response can be replaced by  $\hat{y}^o(k+j)$  such that:

$$\hat{y}^o(k+j) \triangleq \sum_{i=j+1}^{N-1} S_i \Delta u(k+j-i) + S_N u(k+j-N) \quad (3.25)$$

Substituting Equation (3.25) into Equation (3.24):

$$\hat{y}(k+j) = \sum_{i=1}^j S_i \Delta u(k+j-i) + \hat{y}^o(k+j) \quad (3.26)$$

where  $\hat{y}(k+j)$  represents the predicted response due to both previous and future control inputs including the current control input.

Model predictive control compensates for model inaccuracies by computing the difference between the predicted response and the actual measured response. Due to unmeasured disturbances and possible model errors, the predicted response of controlled outputs will not be 100% accurate and thus the incorporation of feedback into the prediction model enables corrections to be made to eliminate the difference between the predicted outputs and actual measured outputs (Morshedi et al., 1979). The output feedback is used to correct for the mismatch between the predicted response and actual response and the computation is updated during each cycle (Luyben, 1993). The resulting output can be represented as:

$$\tilde{y}(k+j) \triangleq \hat{y}(k+j) + b(k+j) \quad (3.27)$$

where  $\tilde{y}(k+j)$  is the corrected output and  $b(k+j)$  represents the bias correction (Seborg et al., 2004), and is defined as:

$$b(k+j) = y(k) - \hat{y}(k) \quad (3.28)$$

Substituting Equation 3.28 into Equation 3.27 results in:

$$\tilde{y}(k+j) \triangleq \hat{y}(k+j) + [y(k) - \hat{y}(k)] \quad (3.29)$$

The preceding formulation can be extended from a single future prediction to multiple future predictions. For simplicity, the formulation of multiple predictions is presented in vector-matrix notation (Seborg et al., 2004):

$$\tilde{\mathbf{Y}}(k+1) \triangleq \text{col}[\tilde{y}(k+1), \tilde{y}(k+2), \dots, \tilde{y}(k+P)] \quad (3.30)$$

where  $\tilde{\mathbf{Y}}(k+1)$  is the vector of the corrected output predictions for the next  $P$  sampling instants where  $P$  is the prediction horizon, and therefore for  $M$  being the control horizon,  $P$  is chosen to be  $P \leq N + M$  and  $M \leq P$ .

$$\hat{\mathbf{Y}}(k+1) = \mathbf{S}\Delta\mathbf{U}(k) + \hat{\mathbf{Y}}^o(k+1) \quad (3.31)$$

where  $\mathbf{S}$  is the  $P \times M$  dynamic matrix comprised of the step response coefficients:

$$\mathbf{S} \triangleq \begin{bmatrix} S_1 & 0 & \dots & 0 \\ S_2 & S_1 & \dots & \vdots \\ \vdots & \vdots & \dots & 0 \\ S_M & S_{M-1} & \dots & S_1 \\ S_{M+1} & S_M & \dots & S_2 \\ \vdots & \vdots & \dots & \vdots \\ S_P & S_{P-1} & \dots & S_{P-M+1} \end{bmatrix} \quad (3.32)$$

Similarly, for the multiple prediction formulation, the addition of the bias correction results in a vector of corrected predictions (Seborg et al., 2004) given by:

$$\tilde{\mathbf{Y}}(k+1) = \mathbf{S}\Delta\mathbf{U}(k) + \hat{\mathbf{Y}}^o(k+1) + [y(k) - \hat{y}(k)]\mathbf{1} \quad (3.33)$$

where  $\mathbf{1}$  is a  $P$ -dimensional vector with all elements having a value of 1. The above formulation is extended to multiple-input multiple-output (MIMO) systems in the next section.

### 3.5.2. Prediction model for multiple-input multiple-output (MIMO) systems

The formulation of the predictive model for SISO systems can be extended to MIMO systems (Seborg et al., 2004). The MIMO formulation is outlined using a general second order two-inputs and two-outputs system as presented in (Seborg et al., 2004). The four step response models for each input-output pair of the system given by:

$$\begin{aligned} \hat{y}_1(k+1) = & \sum_{i=1}^{N-1} S_{11,i} \Delta u_1(k-i+1) + S_{11,N} u_1(k-N+1) \\ & + \sum_{i=1}^{N-1} S_{12,i} \Delta u_2(k-i+1) + S_{12,N} u_2(k-N+1) \end{aligned} \quad (3.34)$$

$$\begin{aligned} \hat{y}_2(k+1) = & \sum_{i=1}^{N-1} S_{21,i} \Delta u_1(k-i+1) + S_{21,N} u_1(k-N+1) \\ & + \sum_{i=1}^{N-1} S_{22,i} \Delta u_2(k-i+1) + S_{22,N} u_2(k-N+1) \end{aligned} \quad (3.35)$$

where  $S_{11,i}$  represents the  $i$ th step response coefficients that relate  $u_1$  and  $y_1$ , and the same convention is followed for the rest of the step response coefficients in  $S_{12,i}$ ,  $S_{21,i}$  and  $S_{22,i}$ .

Like the SISO system formulation, the corrected predictions can be given in dynamic matrix form for a system with  $m$  outputs and  $r$  inputs with a  $P$  prediction horizon and  $M$  control horizon. The resulting formulation is given by (Seborg et al., 2004):

$$\tilde{\mathbf{Y}}(k+1) = \mathbf{S}\Delta\mathbf{U}(k) + \hat{\mathbf{Y}}^o(k+1) + [\mathbf{y}(k) - \hat{\mathbf{y}}(k)] \quad (3.36)$$

where the  $mP$ -dimensional vector of corrected predictions and unforced predicted responses, respectively, is defined as:

$$\tilde{\mathbf{Y}}(k+j) \triangleq \text{col}[\tilde{\mathbf{y}}(k+1), \tilde{\mathbf{y}}(k+2), \dots, \tilde{\mathbf{y}}(k+P)] \quad (3.37)$$

$$\hat{\mathbf{Y}}^o(k+j) \triangleq \text{col}[\hat{\mathbf{y}}^o(k+1), \hat{\mathbf{y}}^o(k+2), \dots, \hat{\mathbf{y}}^o(k+P)] \quad (3.38)$$

and the  $rM$ -dimensional vector for the next  $M$  control moves is defined as:

$$\Delta\mathbf{U}(k) \triangleq \text{col}[\Delta\mathbf{u}(k), \Delta\mathbf{u}(k+1), \dots, \Delta\mathbf{u}(k+M-1)] \quad (3.39)$$

The dynamic matrix  $\mathbf{S}$  containing the step response models ( $m \times r$  matrices) for each input-output pair is defined as:

$$\mathbf{S} \triangleq \begin{bmatrix} \mathbf{S}_1 & \mathbf{0} & \dots & \mathbf{0} \\ \mathbf{S}_2 & \mathbf{S}_1 & \mathbf{0} & \vdots \\ \vdots & \vdots & \ddots & \mathbf{0} \\ \mathbf{S}_M & \mathbf{S}_{M-1} & \dots & \mathbf{S}_1 \\ \mathbf{S}_{M+1} & \mathbf{S}_M & \dots & \mathbf{S}_2 \\ \vdots & \vdots & \ddots & \vdots \\ \mathbf{S}_P & \mathbf{S}_{P-1} & \dots & \mathbf{S}_{P-M+1} \end{bmatrix} \quad (3.40)$$

where the step-response coefficients of the  $i$ th step response model are defined as:

$$\mathbf{S}_i \triangleq \begin{bmatrix} S_{11,i} & S_{12,i} & \dots & S_{1r,i} \\ S_{21,i} & \dots & \dots & S_{2r,i} \\ \vdots & \vdots & \ddots & \vdots \\ S_{m1,i} & \dots & \dots & S_{mr,i} \end{bmatrix} \quad (3.41)$$

The single-input single-output formulation was extended to multiple-input multiple-output (MIMO) systems in this section. The next section outlines the typical formulation of the MPC control law.

### 3.5.3. MPC Control Law

The control law for unconstrained MPC is first provided, then it is followed by the constrained formulation that is more typical in MPC applications. The predicted  $mP$ -dimensional error vector is given by:

$$\hat{\mathbf{E}}(k+1) \triangleq \mathbf{Y}_r(k+1) - \hat{\mathbf{Y}}(k+1) \quad (3.42)$$

where  $\mathbf{Y}_r$  represents the vector of the desired response trajectories and  $\hat{\mathbf{Y}}$  is the vector of predicted responses. The predicted unforced  $mP$ -dimensional error vector if no further control actions are taken is given by:

$$\hat{\mathbf{E}}^o(k+1) \triangleq \mathbf{Y}_r(k+1) - \hat{\mathbf{Y}}^o(k+1) \quad (3.43)$$

and the corrected prediction of the unforced response is given by:

$$\hat{\mathbf{Y}}^o(k+1) \triangleq \hat{\mathbf{Y}}^o(k+1) + \mathbf{I}[y(k) - \hat{y}(k)] \quad (3.44)$$

where the  $\mathbf{I}$  is an identity matrix. Formulation of the control law involves the calculation of control moves for the next  $M$  intervals that minimize an objective function. The  $rM$ -dimensional vector control moves are given by:

$$\Delta\mathbf{U}(k) \triangleq \text{col}[\Delta\mathbf{u}(k), \Delta\mathbf{u}(k+1), \dots, \Delta\mathbf{u}(k+M-1)] \quad (3.45)$$

The quadratic objective function to be minimized is given by:

$$\min_{\Delta\mathbf{U}(k)} J = \hat{\mathbf{E}}(k+1)^T \mathbf{Q} \hat{\mathbf{E}}(k+1) + \Delta\mathbf{U}(k)^T \mathbf{R} \Delta\mathbf{U}(k) \quad (3.46)$$

The  $\mathbf{Q}$  and  $\mathbf{R}$  represent weighting matrices and are positive-definite and positive semi-definite matrices, respectively. The above objective function minimizes deviations in the predicted errors and the magnitude of control moves. The control law that minimizes the objective function is given by:

$$\Delta\mathbf{U}(k) = (\mathbf{S}^T \mathbf{Q} \mathbf{S} + \mathbf{R})^{-1} \mathbf{S}^T \mathbf{Q} \hat{\mathbf{E}}^o(k+1) \quad (3.47)$$

where  $\mathbf{S}$  represents the dynamic matrix comprised of step response coefficients. The control law can be simplified and written as:

$$\Delta\mathbf{U}(k) = \mathbf{K}_c \hat{\mathbf{E}}^o(k+1) \quad (3.48)$$

where  $\mathbf{K}_c$  represents an  $rM \times mP$  controller gain matrix and is defined by:

$$\mathbf{K}_c = (\mathbf{S}^T \mathbf{Q} \mathbf{S} + \mathbf{R})^{-1} \mathbf{S}^T \mathbf{Q} \quad (3.49)$$

MPC makes use of a receding horizon where one computed control move is implemented and the rest are re-calculated at each sampling instant making use of newly available information (Seborg et al., 2004).

The first control move implemented at each sampling instant is calculated with:



$$\Delta \mathbf{u}(k) = \mathbf{K}_{c1} \hat{\mathbf{E}}^o(k+1) \quad (3.50)$$

where  $\mathbf{K}_{c1}$  represents an  $rM \times mP$  controller gain matrix. The above control law formulation is given for unconstrained MPC. However, MPC is typically implemented with system constraints such as valve travels, compressor speeds, equipment metallurgical limits, etc. Constraints can be separated into two categories which are; hard constraints and soft constraints. Hard constraints are those that cannot be violated due to either equipment physical limitations such as valve travel limits or safety limits such as equipment metallurgical limits. Whereas soft constraints are those that are not linked to physical limits and can allow momentary violation such as a steam flow rate constraint set for energy conservation or concentration constraint set to meet product specifications. The constraints are represented in the control law formulation as a set of inequality constraints. The optimization objective function such as that given by Equation 3.46 is solved subject to the system inequality constraints on both the control inputs and controlled outputs. The constraints on  $\mathbf{u}$  and  $\Delta \mathbf{u}$  are generally set as hard constraints given, respectively, by:

$$\mathbf{u}^-(k) \leq \mathbf{u}(k+j) \leq \mathbf{u}^+(k) \quad j = 0, 1, \dots, M-1 \quad (3.51)$$

$$\Delta \mathbf{u}^-(k) \leq \Delta \mathbf{u}(k+j) \leq \Delta \mathbf{u}^+(k) \quad j = 0, 1, \dots, M-1 \quad (3.52)$$

where  $\mathbf{u}^-$  and  $\mathbf{u}^+$  represent the lower and upper limits of  $\mathbf{u}$  respectively and  $\Delta \mathbf{u}^-$  and  $\Delta \mathbf{u}^+$  represent the upper and lower limits of  $\Delta \mathbf{u}$ , respectively. Similarly, the hard constraints on  $\tilde{\mathbf{y}}$  are given by:

$$\mathbf{y}^-(k+1) \leq \tilde{\mathbf{y}}(k+j) \leq \mathbf{y}^+(k+j) \quad j = 0, 1, \dots, P \quad (3.53)$$

where  $\mathbf{y}^-$  and  $\mathbf{y}^+$  represent the lower and upper limits of  $\tilde{\mathbf{y}}$ , respectively. It is common to express constraints on controlled outputs as soft constraints with the use of slack variables. This is to ensure that disturbances on the controlled outputs do not lead to an infeasible solution during the computation of optimization problem. Slack variables provide an acceptable quantity by which the constraints can be violated as such a margin is provided to avoid an infeasible solution. Soft constraints on  $\tilde{\mathbf{y}}$  with slack variables  $\mathbf{s}_j$  can be given by:

$$\mathbf{y}^-(k+1) - \mathbf{s}_j \leq \tilde{\mathbf{y}}(k+j) \leq \mathbf{y}^+(k+j) + \mathbf{s}_j \quad j = 0, 1, \dots, P \quad (3.54)$$

The modified objective function that includes an  $mP$ -dimensional slack variables vector  $\bar{\mathbf{S}} \triangleq \text{col}[s_1, s_2, s_3, \dots, s_p]$  is given by:

$$\min_{\Delta \mathbf{U}(k)} \mathbf{J} = \hat{\mathbf{E}}(k+1)^T \mathbf{Q} \hat{\mathbf{E}}(k+1) + \Delta \mathbf{U}(k)^T \mathbf{R} \Delta \mathbf{U}(k) + \bar{\mathbf{S}}^T \mathbf{T} \bar{\mathbf{S}} \quad (3.55)$$

where  $\mathbf{T}$  is an  $mP \times mP$  weighing matrix for the slack variables.

The typical formulation of the MPC control law for both unconstrained and constrained MPC was outlined. The next section presents the selection of a typical set of parameters necessary in the design of MPC.

### 3.5.4. Selection of Design Parameters

MPC offers a range of parameters to be selected during controller design and configuration. There are several heuristic rules of thumb that exist in literature guiding the selection of MPC parameters (Bemporad et al., 2015; Holkar and Waghmare, 2010; Seborg et al., 2004). The design parameters discussed in this section exclude selection of constraints since constraints are dictated by the plant and equipment limits. The parameters that are necessary to be selected as part of the MPC design process are summarised in Table 3.1.

**Table 3.1: MPC Design Parameters**

MPC Parameters	Symbol
Sample time	$\Delta t$
Model horizon	$N$
Prediction horizon	$P$
Control horizon	$M$
Output weighing matrix	$Q$
Control move weighing matrix	$R$

The sampling time and model horizon are selected based on the process dynamics involved where processes with fast dynamics require short sampling times whereas processes with slower process dynamics, such as most of those found in petrochemical plants and oil refineries, can be configured with longer controller sampling times (Bemporad et al., 2015). A recommended rule of thumb by (Seborg et al., 2004) is to select the sampling time and model horizon such that  $N \times \Delta t = Ts$  where  $N$  is the model horizon or number of parameters,  $\Delta t$  is the sampling period, and  $Ts$  is the process settling time. A useful rule of thumb recommended by (Seborg et al., 2004) is to select the model horizon,  $N$ , such that  $30 \leq N \leq 120$ . The prediction horizon is selected such that the complete dynamic response and the steady state are included in the prediction by the controller (Camacho and Bordons, 2007). As the prediction horizon is decreased, the controller tends to be more aggressive (Seborg et al., 2004). It has been noted that it is advantageous to make the prediction horizon large enough to allow the controller to anticipate constraint violation early and take appropriate action (Bemporad et al., 2015). A recommended rule of thumb by (Seborg et al., 2004) is to select  $P$  such that  $P = M + N$ .

In (Bemporad et al., 2015), it is recommended that the selection of a control horizon be chosen to be between a value of  $1 \leq M \leq P$  whereas a smaller value closer to  $M = 1$  tends to improve the controller execution speed. Whereas the controller increases in its aggressiveness as  $M$  is

increased but the computational burden also increases proportionally (Seborg et al., 2004). A recommended rule of thumb by (Seborg et al., 2004) is to select  $M$  such that  $\frac{N}{3} \leq M \leq \frac{N}{2}$  and  $5 \leq M \leq 20$ . In (Morari and Lee, 1999), it is noted that the use of the prediction and control horizon as tuning parameters for model predictive control (MPC) is generally ineffective i.e. the behaviour of the system becomes insensitive to changes in these parameters over a wide range of values.

The matrix  $Q$  is a  $mP \times mP$ -dimensional positive-definite output weighting matrix containing weighing factors of each controlled output. The weighting factors in  $Q$  aid the controller in defining the priority of the controlled outputs to determine trade-offs. The larger the weighing factor, the more important the controlled variable and the more important it is to keep its reference trajectory deviation at an absolute minimum. It is typical in industrial practice to represent the relative importance of each of the controlled outputs with the inverse of the weighing factor called an equal concern for the relaxation (ECR) or equal concern factor. For example, an ECR of 2 Degrees Celsius (DegC) for a temperature output and an ECR of 10 % for a valve position indicated to the controller that a 2 Degrees Celsius deviation in the temperature output target is of equal concern to a 10 % percent deviation in the valve position target. In this example, temperature out is assigned higher importance than the valve position (Hilton, 1996).

Similarly, the matrix  $R$   $mP \times mP$ -dimensional is a positive semi-definite control move weighting matrix containing weighing factors for the control inputs. The weighting factors in  $R$  aid the controller in determining which inputs are to be moved conservatively i.e., the higher the weighing factor, the more sluggish and robust the controller tends to become, whereas smaller values tend to cause the control moves to exhibit aggressive movements.

This section presented the model predictive control technique theoretical concepts including the rules typically employed in the selection of a typical set of parameters necessary in the design of model predictive control systems in industry. The following section presents the conclusion to this chapter and a brief introduction of what is presented in Chapter 4.

### **3.6. Conclusion**

A theoretical overview of the design techniques utilized in this research has been provided in this chapter. The relative gain array (RGA) mathematical description with an example of a second order system was provided which was followed by the Niederlinski index method. The ideal decoupling control technique utilized in this research is described for second order system. The model order reduction (MOR) technique proposed by Isaksson and Graebe (1993) which involves approximating a model by retaining the average dominant poles and zeros as well as the lower order coefficients of the high order model is described followed by the IMC-PID tuning technique for obtaining the PID controller gains. Finally, the model

predictive control (MPC) technique theoretical concepts are explained including the rules typically employed in the selection of a typical set of parameters necessary in the design of model predictive control systems.

In Chapter 4, the procedure followed in obtaining the transfer function models using the MATLAB System Identification Toolbox is outlined, beginning with the process description of the debutanizer distillation process, its control objectives and control structure. A typical model identification workflow is presented which outlines the key steps involved in the development of the step response models like the model utilized in this research with commercial model predictive control software packages.

## **CHAPTER FOUR: DEBUTANIZER DISTILLATION PROCESS IDENTIFICATION AND MODELLING**

### **4.1. Introduction**

System identification as defined by Ljung (1999) is the building of mathematical models for dynamic systems based on observed input-output data of the system (Ljung, 1999). It is the process by which models representing dynamics of a process plant are developed. System identification is comprised of experimental design, data collection, model structure selection, parameter estimation and model validation (Ljung, 1999). The objective is to obtain a model that represents the system's dynamic response to a level of accuracy dependent on the intended purpose of the model (Ljung, 1999). The plant being investigated as part of this research is a step response model of a debutanizer distillation process. The debutanizer distillation process's step response model was extracted from a commercial model predictive control software package, AspenTech's DMCplus (Goodhart, 1998), which is a representation of the plant dynamics at the time of its identification. The identification process outlined in this chapter is the workflow process followed in producing the step response models for model predictive control applications in industry, from the collection of raw process plant data at the start of the project to the development of the mathematical transfer function models.

This chapter begins with a process description of the debutanizer distillation process and its control objectives presented in section 4.2. In section 4.3, a step response model identification workflow with the use of AspenTech's software package is presented which outlines key typical steps involved in the development of step response curves like the model utilized in this research. The MATLAB procedure for obtaining the transfer function model using the original step response coefficients data exported from AspenTech's software package is outlined in section 4.4 followed by a comparative analysis to determine the accuracy of the estimated transfer functions in terms of how well they represent the original model. Concluding remarks are provided in section 4.5.

## 4.2. Debutanizer Distillation Process Description

### 4.2.1. International Union of Pure and Applied Chemistry (IUPAC) Nomenclature

In organic chemistry a hydrocarbon is defined as a chemical compound made up of hydrogen and carbon atoms found naturally in crude oil (Silberberg, 2015). Properties of hydrocarbons are influenced by the number of carbon atoms present in their molecular structure. In Table 4.1 a list of Alkane hydrocarbons is given with some of their properties such as melting point, boiling point and phase at standard temperature and pressure (STP) (Flowers et al., 2016).

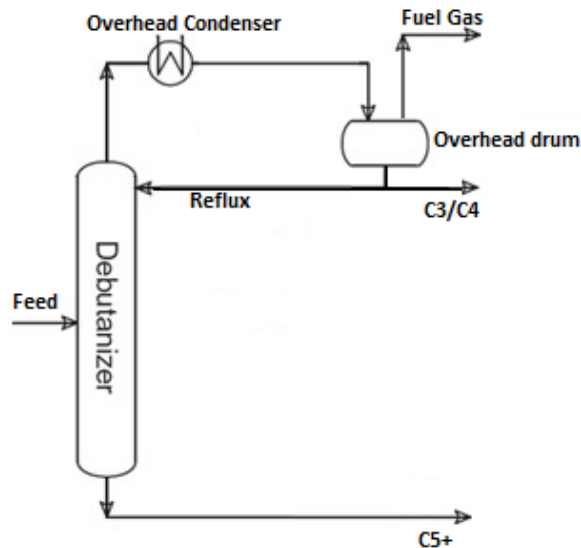
**Table 4.1: Alkane Hydrocarbons** (Flowers et al., 2016)

Alkane	Molecular Formula	Melting Point (°C)	Boiling Point (°C)	Phase at STP
methane	CH <sub>4</sub>	-182.5	-161.5	gas
ethane	C <sub>2</sub> H <sub>6</sub>	-183.3	-88.6	gas
propane	C <sub>3</sub> H <sub>8</sub>	-187.7	-42.1	gas
butane	C <sub>4</sub> H <sub>10</sub>	-138.3	-0.5	gas
pentane	C <sub>5</sub> H <sub>12</sub>	-129.7	36.1	liquid
hexane	C <sub>6</sub> H <sub>14</sub>	-95.3	68.7	liquid
heptane	C <sub>7</sub> H <sub>16</sub>	-90.6	98.4	liquid
octane	C <sub>8</sub> H <sub>18</sub>	-56.8	125.7	liquid
nonane	C <sub>9</sub> H <sub>20</sub>	-53.6	150.8	liquid
decane	C <sub>10</sub> H <sub>22</sub>	-29.7	174.0	liquid

The molecular formula of each hydrocarbon contains information about the quantity of carbon and hydrogen atoms that are present in its molecular structure. In line with the International Union of Pure and Applied Chemistry (IUPAC) nomenclature, it is common practice to refer to hydrocarbons by the prefix of their molecular formula, referring the number of carbon atoms contained in their molecular structure, such as C<sub>3</sub> instead of C<sub>3</sub>H<sub>8</sub> for propane, C<sub>4</sub> instead of C<sub>4</sub>H<sub>10</sub> for butane, and C<sub>5</sub> instead of C<sub>5</sub>H<sub>12</sub> for pentane, etc. This nomenclature is adopted in this research. What follows in the next section is a description for the gas recovery unit (GRU) process plant of which the debutanizer distillation process forms a part.

### 4.2.2. Gas recovery unit (GRU) and debutanizer distillation process description

The gas recovery unit (GRU) forms a major part of a refinery's fluidized catalytic cracking unit (FCCU). FCCUs convert a low value feedstock mixture into high value product streams. The main purpose of a gas recovery plant in the FCCU is to extract as much valuable liquid product from the overhead vapor stream of the FCCU main fractionator as possible to be treated into Liquefied Petroleum Gas (LPG) and gasoline product streams. The debutanizer distillation process studied in this research is a part of an FCCU's gas recovery plant and is used to separate butane (C<sub>4</sub>'s) and propane (C<sub>3</sub>'s) from pentane (C<sub>5</sub>'s) and heavier hydrocarbons used to produce gasoline as part of the gas recovery unit (GRU) (Sadeghbeigi, 2000). Figure 4.1. shows a simplified process flow diagram of debutanizer distillation process.



**Figure 4.1: Debutanizer Simplified Process Flow Diagram (PFD)** (Sadeghbeigi, 2000)

Process feedstock (or simply feed) into the debutanizer distillation column is comprised of a liquid stream from a Stripper column. The composition of the feed is C<sub>3</sub>'s, C<sub>4</sub>'s and C<sub>5</sub>'s and enters in the middle of the debutanizer distillation column as shown in Figure 4.1 (Sadeghbeigi, 2000). The stream is separated in the column into two streams of gas and liquid through a process of fractional distillation. The composition of the gas stream which flows from the top (or overhead) of the column is comprised predominantly of C<sub>3</sub>'s and C<sub>4</sub>'s with small traces of C<sub>5</sub>'s. This overhead gas is condensed by a heat exchanger (also referred to as an overhead condenser) into liquid which gets collected into an overhead drum. Some of the condensed liquid is routed back to the debutanizer distillation column as liquid reflux. The remaining liquid in the overhead produce liquefied drum is routed to other plants as the column top product to be used to petroleum gas (LPG) (Sadeghbeigi, 2000). The by-product of the debutanizer distillation column is fuel gas which is routed to the fuel gas header from the overhead drum during the debutanizer overpressure scenarios. The liquid flowing from the bottom of the debutanizer distillation column, referred to as Light Cracked Naphtha (LCN), is comprised predominantly of C<sub>5</sub>'s and gets routed to other plants as the column bottom product to be used to produce gasoline.

#### **4.2.3. Debutanizer distillation process control objectives**

It is evident from the above description that there are two main product streams from a debutanizer distillation column, and they are the Liquefied Petroleum Gas (LPG) and gasoline, referred to as Light Cracked Naphtha (LCN). An important variable to be controlled is the column's top tray temperature since high top temperature may result in high pressure in the overhead section leading to an over-pressure relief to the fuel gas system. Under normal circumstances, it is undesirable to relieve to the fuel gas system as it results in hydrogen sulphide ( $H_2S$ ) contamination of the fuel gas header. The LPG product quality specifications set limits on the maximum quantity of C<sub>5</sub>'s that may be present in its composition. Furthermore,

C<sub>5</sub>'s is used to produce gasoline which is considered economically more valuable than LPG. Therefore, the objective is to recover C<sub>5</sub>'s from LPG into gasoline (LCN). The quality specification for gasoline limits the range of the Reid Vapour Pressure (RVP) to be between 55 kPa(a) and 75 kPa(a). RVP is a measure of the volatility for products such as gasoline (Stewart and Arnold, 2009). As the RVP of gasoline from the debutanizer distillation column falls below 55 kPa(a), it is an indication that components including C<sub>5</sub>'s are being lifted out the top of the column and, as such, the LPG goes off-specification due to a high concentration of C<sub>5</sub>'s. On the other hand, when the RVP of gasoline goes above 75 kPa(a), the gasoline may be containing a high concentration of undesired light components such as hydrogen sulphide (H<sub>2</sub>S). As such, when a mandatory laboratory test referred to as a copper strip test is conducted on the gasoline it may yield results that are off specification. A copper strip test is used to test the corrosivity of petroleum streams (Kanna et al., 2017). Therefore, the main objectives for the Debutanizer distillation process are summarized as follows (Chevron, 2017):

- 1) Prevent high overhead pressure which may lead to LPG being routed to the fuel gas system from the overhead drum.
- 2) Minimize the concentration of C<sub>5</sub>'s in the overhead stream of Liquefied Petroleum Gas (LPG).
- 3) Control the reid vapor pressure (RVP) of the Light Cracked Naphtha (LCN) stream to meet gasoline specifications.

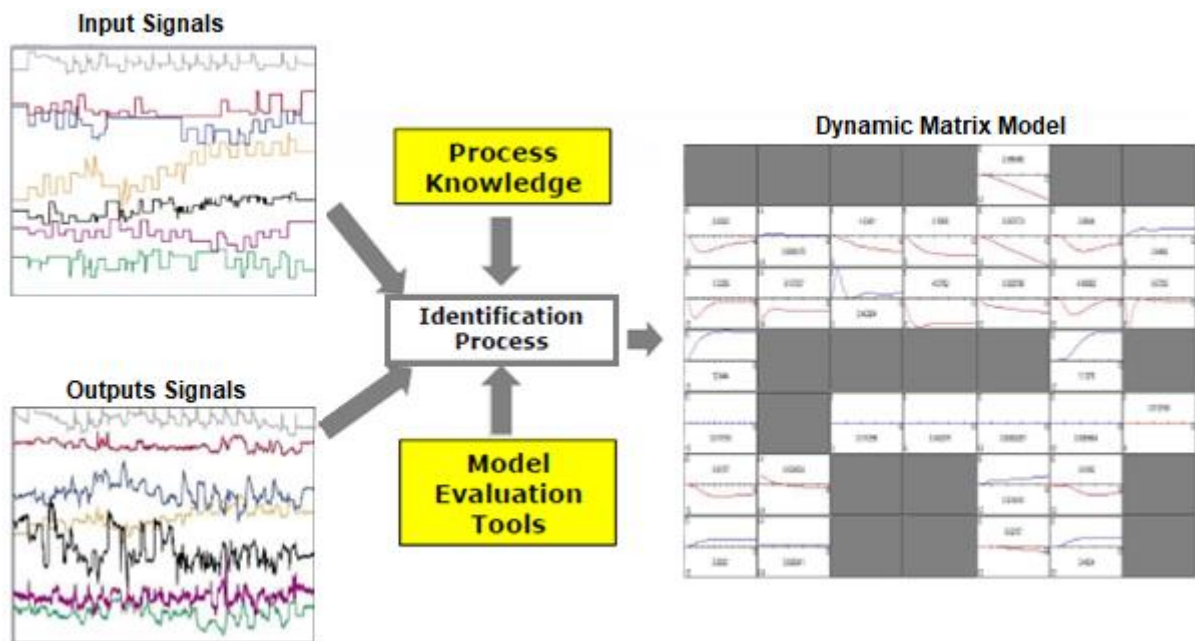
The following section describes a model identification workflow with the use of AspenTech's software package and outlines key typical steps involved in the development of the step response models like the model utilized in this research.

#### **4.3. Debutanizer distillation model identification**

Industry practice to linear model identification is largely carried out with specially designed field experiments rather than rigorous mathematical modelling due to high costs associated with the development of models from first principles (Morari and Lee, 1999). The experiments involve exciting a system with carefully selected input signals and having the system output responses recorded for the development of the models by estimating the finite impulse response (FIR) coefficients from the collected input and output data. The use of a persistently exciting input signals such as the pseudo random binary sequence (PRBS) and cross correlation techniques for system identification has been reported to yield a system's impulse response (Davies, 1967), (Charlton, 1968), (Ljung, 1999).

Figure 4.2 shows a summary of the of the model development process. The process is excited with carefully designed PRBS input signals, the input-output data is collected and analysed with model evaluation tools as part of the identification process together with process knowledge from the process engineers and plant operators resulting in the model response curves representing the dynamic matrix model as shown in Figure 4.2.





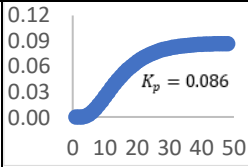
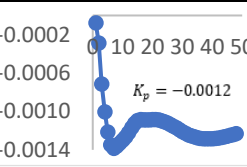
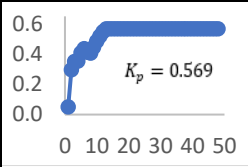
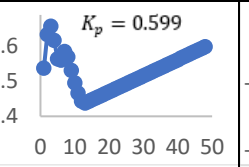
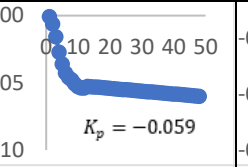
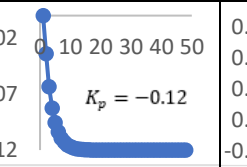
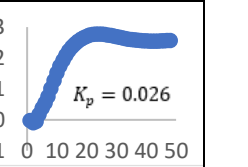
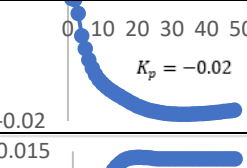
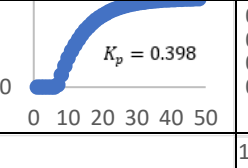
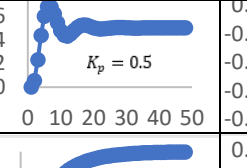
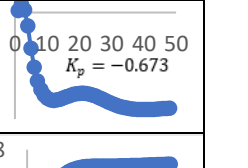
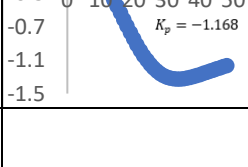
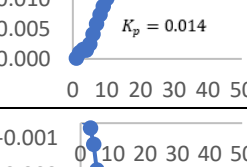
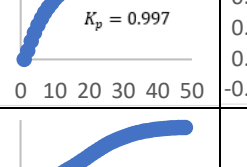
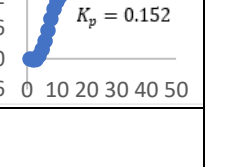
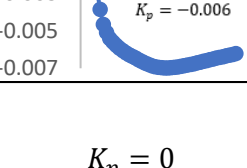
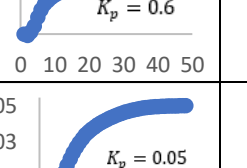
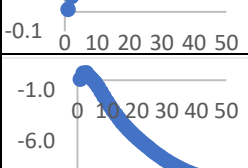
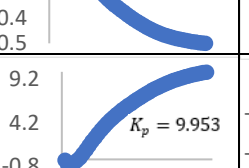
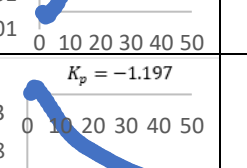
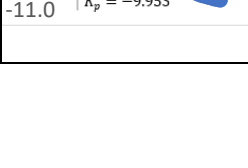
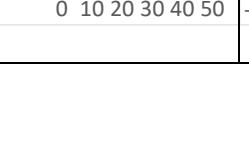

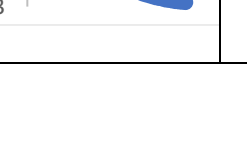
**Figure 4.2: Summary of the model development process** (BluESP, 2018)

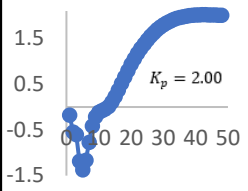
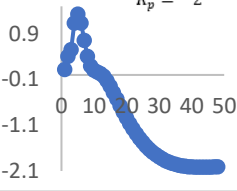
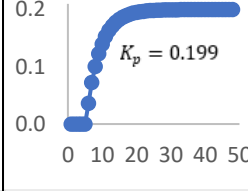
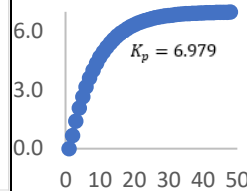
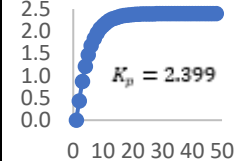
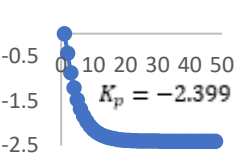
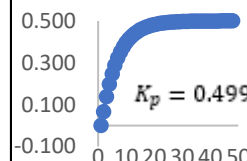
The model used in this research was developed with the use of a commercial software package, AspenTech's DMC3 Builder (Goodhart, 1998). Due to intellectual property and copyright considerations, the model development process described in this section makes use of a publicly available typical example by (Marchionna, 2017). The identification process begins with preparation where all regulatory control loops to be included in the model are tuned and faulty field instrumentation is repaired as poorly tuned and faulty instrumentation has a negative influence on the quality of data collected resulting in inaccurate modelling. The next step is to conduct step response testing. Step response testing involves introducing random perturbations as inputs to the process and collecting dynamic response data. Data points collected during the step testing include PID process variables, setpoint variables and manipulated variables (Marchionna, 2017). The collected data is imported into the software for modelling and creation of step response models. It is necessary to remove corrupted data using interpolation techniques and to select the identification algorithm to be used. The finite impulse response (FIR) algorithm was used in the identification of the model used in this research.

The result of the identification process yields unit step response coefficients presented in plots relating each independent variable with a dependent variable via a dynamic response curve. An approach like the one described above was followed in the development of the step response coefficients for the debutanizer distillation process model studied in this research which is given in Table 4.2. The individual step response models are graphically displayed in a table format in Table 4.2 where the independent variables are arranged as rows of the table and dependent variables are arranged as columns (Seborg et al., 2004). The step response models are normalized to represent unit step responses that are linear. Since the models are linear, the principle of superposition applies, and the scale is preserved. The steady state value

for each step response curve in Table 4.2 represents the steady state gain ( $K_p$ ). It is common practice for the identification process to involve iterations of review and editing to improve the model prior to deployment into the controller model (Marchionna, 2017). The process described above, however, is a description of typical steps undertaken in developing empirical models with AspenTech's DMC3 Builder model predictive control software package in industry which result in a model like the one presented in Table 4.2.

Table 4.2: Step response models for the debutanizer distillation process

	LCN_RVP	LPG_C5	Ovhd_Drum_Press	Ovhd_Drum Press_SV-PV	Debut_Diff_Press	Reboiler_Valve_Pos	Debut_Tray_24_Temp
Ovhd_Press							
Reflux_Flow	$K_p = 0$		$K_p = 0$	$K_p = 0$			
Reboiler_Temp			$K_p = 0$	$K_p = 0$	$K_p = 0$		
Deeth_Feed_Flow	$K_p = 0$		$K_p = 0$	$K_p = 0$	$K_p = 0$		$K_p = 0$
Deeth_Pressure	$K_p = 0$	$K_p = 0$			$K_p = 0$		$K_p = 0$
Deeth_Temp	$K_p = 0$	$K_p = 0$					$K_p = 0$

	LCN_RVP	LPG_C5	Ovhd_Drum_Press	Ovhd_Drum Press_SV-PV	Debut_Diff_Press	Reboiler_Valve_Pos	Debut_Tray_24_Temp
LCN_Recycle_Flow	$K_p = 0$	$K_p = 0$					$K_p = 0$
Ambient_Temp	$K_p = 0$	$K_p = 0$			$K_p = 0$		$K_p = 0$

The list and descriptions of variables used in the model are given in Table 4.3. The first column of Table 4.3 gives the tag names of the variables used for identification, the second column provides the description of the tag name with engineering units, the third column indicates if the variable is a dependent variable, the fourth column indicates the variable is an independent variable, and lastly, the final column indicates whether the variable is a measured disturbance variable.

**Table 4.3: List and descriptions of variables used in the model**

<b>TAG</b>	<b>Description</b>	<b>Dependent Variable</b>	<b>Independent Variable</b>	<b>Disturbance Variable</b>
Ovhd_Press	Overhead Pressure (kPa)		X	
Reflux_Flow	Reflux Flow (m3/h)		X	
Reboiler_Temp	Reboiler Temperature (DegC)		X	
Deeth_Feed_Flow	Deethanizer Feed Flow (m3/h)		X	
Deeth_Pressure	Deethanizer Pressure (kPa)		X	
Deeth_Temp	Deethanizer Temperature (DegC)		X	
LCN_Recycle_Flow	LCN Recycle Flow (m3/h)		X	
LCN_RVP	LCN Reid Vapour Pressure (kPa)	X		
LPG_C5	LPG C5 Concentration (Mol %)	X		
Ovhd_Drum_Press	Overhead Drum Pressure (kPa)	X		
Ovhd_Drum_Press_SV-PV	Overhead Drum Pressure SV-PV Gap (kPa)	X		
Debut_Diff_Press	Debutanizer Differential Pressure (kPa)	X		
Reboiler_Valve_Pos	Reboiler Valve Position (%)	X		
Debut_Tray_24_Temp	Debutanizer Tray 24 Temperature (DegC)	X		
Ambient_Temp	Ambient Temperature Disturbance (DegC)			X

Each of the step response models in Table 4.2 are a discrete time series of step response coefficients. In this research, the conversion to a discrete time series has enabled, among other things, for the models to be exported as a series of step response coefficients encapsulated in a file format referred to as an MDL (.mdl) file (Valve Developer Community, 2006). The step response coefficients contained in the MDL file can then be transferred to an Excel spreadsheet for use in other software platforms such as MATLAB to reproduce and study the model for controller design, as described in Section 4.4.

In conclusion, this section describes the model identification workflow typically followed with AspenTech's DMC3 Builder software package and key steps involved in the development of the step response models are outlined and the step response models for the debutanizer distillation process studied in this research are presented. In the following section, the step-by-step procedure for obtaining the linear time-invariant (LTI) transfer function models using the step response coefficients encapsulated in the MDL (.mdl) file from the AspenTech's DMC3 Builder software package is explained with a comparison of the step MATLAB models with the original models from the AspenTech's DMC3 Builder software package.

#### 4.4. Procedure for the development of transfer functions in MATLAB

The objective of this section is to estimate a transfer function for each of the step response curves in the dynamic model presented in Table 4.2 of the previous section. The MATLAB system identification toolbox was used for the purpose of developing the linear time-invariant (LTI) transfer functions from the step response coefficients obtained from the AspenTech's DMC3 Builder software package as described in the previous section in order to reproduce and study the dynamic model for controller design as part of this research. Single-input multiple-output (SIMO) transfer functions are developed and then combined to form a multiple-input multiple-output (MIMO) dynamic model in the Simulink environment. MATLAB's system identification toolbox is a commercially licensed tool by MathWorks used for building dynamic models from input and output data through its interactive graphical user interface (GUI) which allows end users to drag and drop model data objects during control system design (Ljung, 1988). The step-by-step procedure followed in estimating the transfer functions is described below.

##### Step 1. Start MATLAB

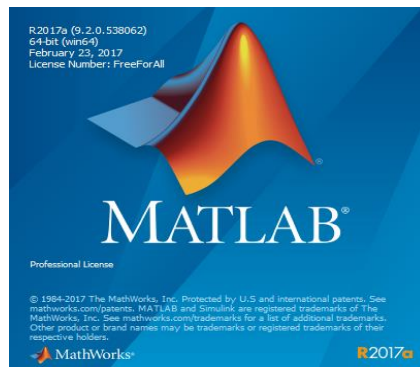


Figure 4.3: The MATLAB application starting

##### Step 2. Select Import Data

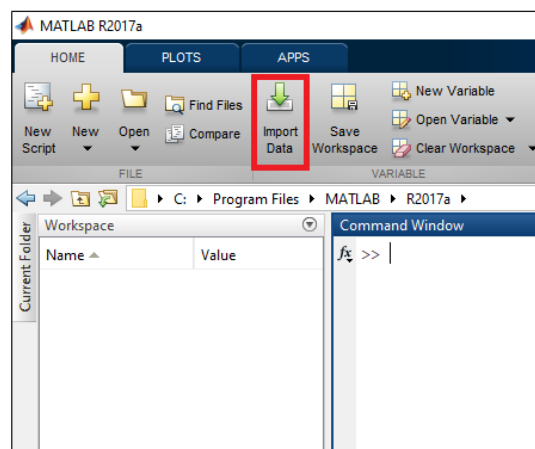
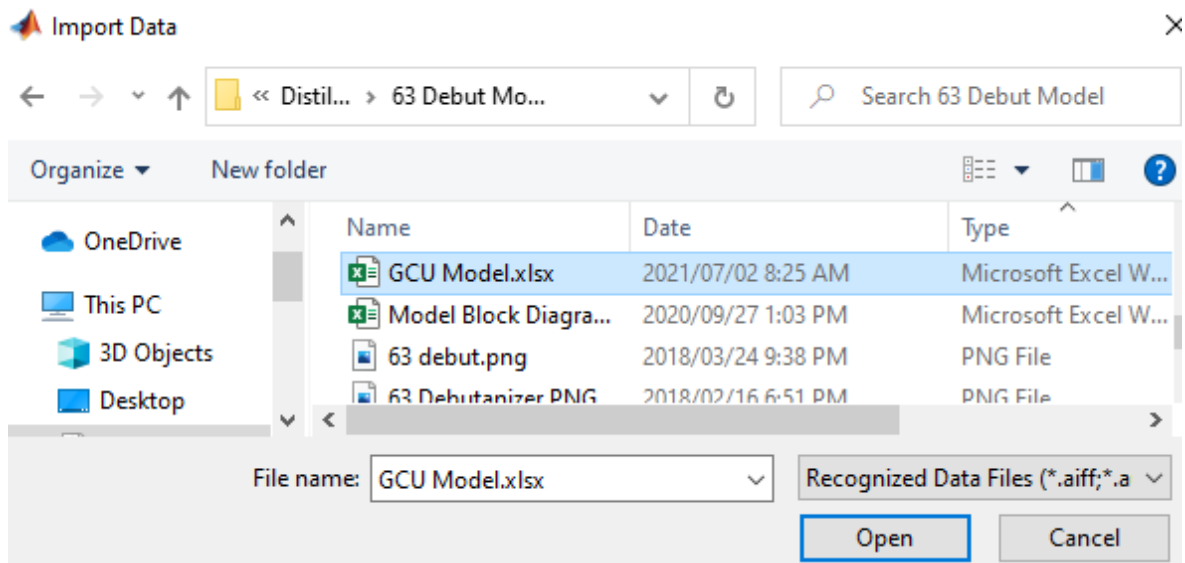


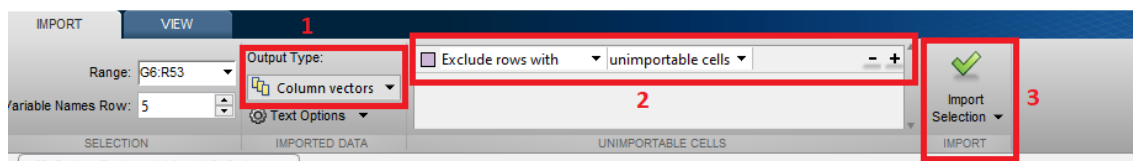
Figure 4.4: Import data

**Step 3.** Select the Excel spreadsheet containing the discrete time data from the MDL file.



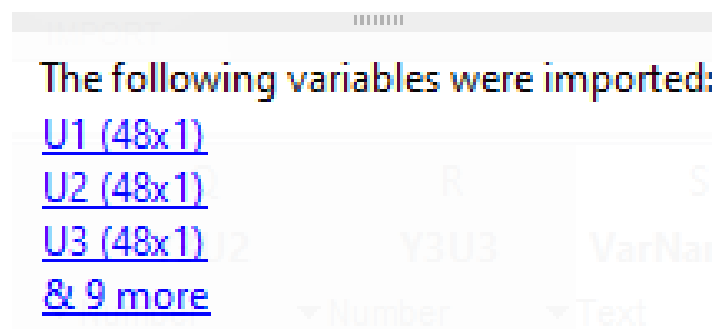
**Figure 4.5: Select the Excel spreadsheet**

**Step 4.** Under Output Type 1) select Column vectors, 2) select Exclude rows with unimportable cells and 3) select Import Selection.



**Figure 4.6: Column vectors**

**Step 5.** A confirmation textbox will momentarily appear indicating the vectors have been successfully imported into the MATLAB Workspace



**Figure 4.7: Successful import**

**Step 6.** The imported column vectors appear in the MATLAB Workspace.

Workspace	
Name ▲	Value
MV1	48x1 double
MV2	48x1 double
MV3	48x1 double
PV1MV1	48x1 double
PV1MV3	48x1 double
PV2MV1	48x1 double
PV2MV2	48x1 double
PV2MV3	48x1 double
PV2UD1	48x1 double
PV3MV1	48x1 double
PV3MV2	48x1 double
PV3UD2	48x1 double
PV3UD3	48x1 double
PV3UD4	48x1 double
PV3UD5	48x1 double
PV4MV1	48x1 double
PV4UD2	48x1 double
PV4UD3	48x1 double
PV4UD4	48x1 double
PV4UD5	48x1 double

**Figure 4.8:** Imported data in MATLAB workspace

**Step 7.** Create the single-input multiple-output (SIMO) time domain data objects for importing into the System Identification Toolbox. The data objects are created with the function **iddata** in the Command Window. This step is repeated for all inputs.

```

Command Window
New to MATLAB? See resources for Getting Started.

>> Ovhd_Press = iddata([PV1MV1 PV2MV1 PV3MV1 PV4MV1 PV5MV1 PV6MV1 PV7MV1], MV1, 1)

Ovhd_Press =

Time domain data set with 48 samples.
Sample time: 1 seconds

Outputs      Unit (if specified)
  y1
  y2
  y3
  y4
  y5
  y6
  y7

Inputs      Unit (if specified)
  u1
  
```

**Figure 4.9:** Creating data object for SIMO coefficients



**Step 8.** Repeat **Steps 4 - 7** for a separate set of coefficients that are used as model validation data to verify the fit of the identified model.

```
Command Window
New to MATLAB? See resources for Getting Started.

>> Ovhd_Press_v = iddata([PV1MV1_v PV2MV1_v PV3MV1_v PV4MV1_v PV5MV1_v PV6MV1_v PV7MV1_v], MV1_v, 1)

Ovhd_Press_v =

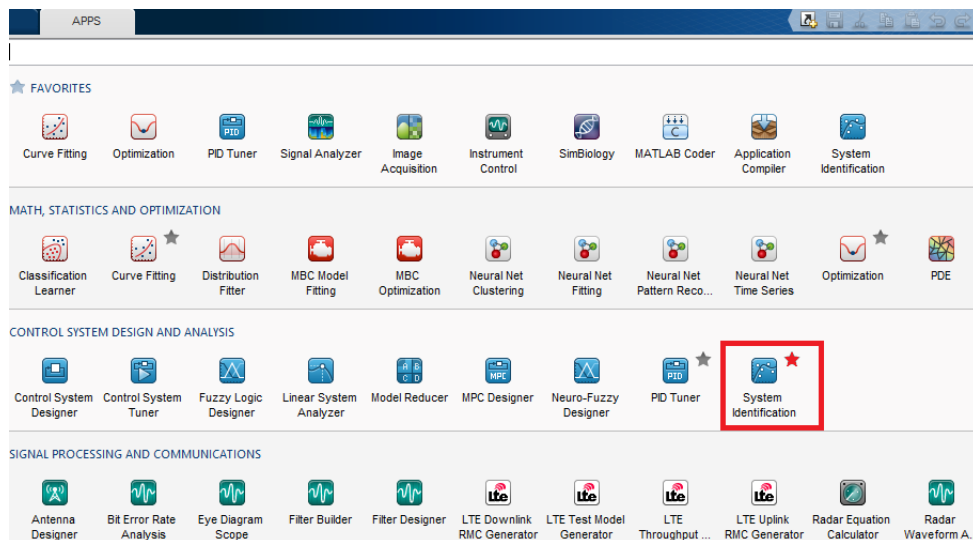
Time domain data set with 48 samples.
Sample time: 1 seconds

Outputs      Unit (if specified)
  y1
  y2
  y3
  y4
  y5
  y6
  y7

Inputs      Unit (if specified)
  ul
```

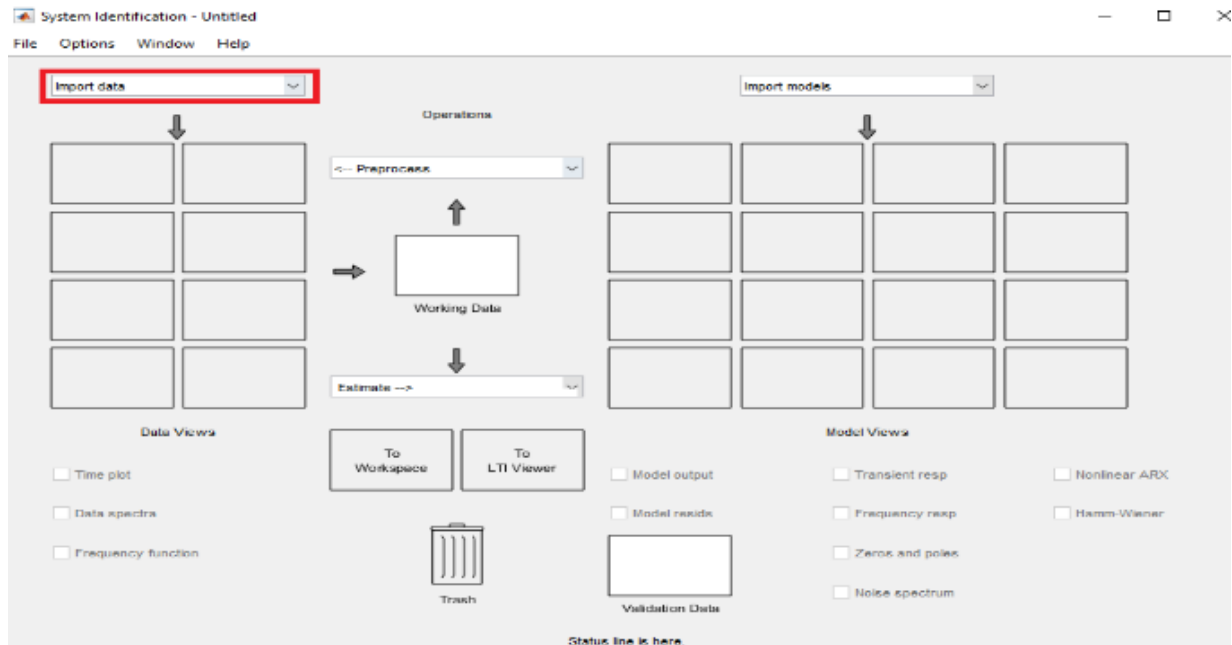
**Figure 4.10:** Creating data objects validation data

**Step 9.** Start System Identification App



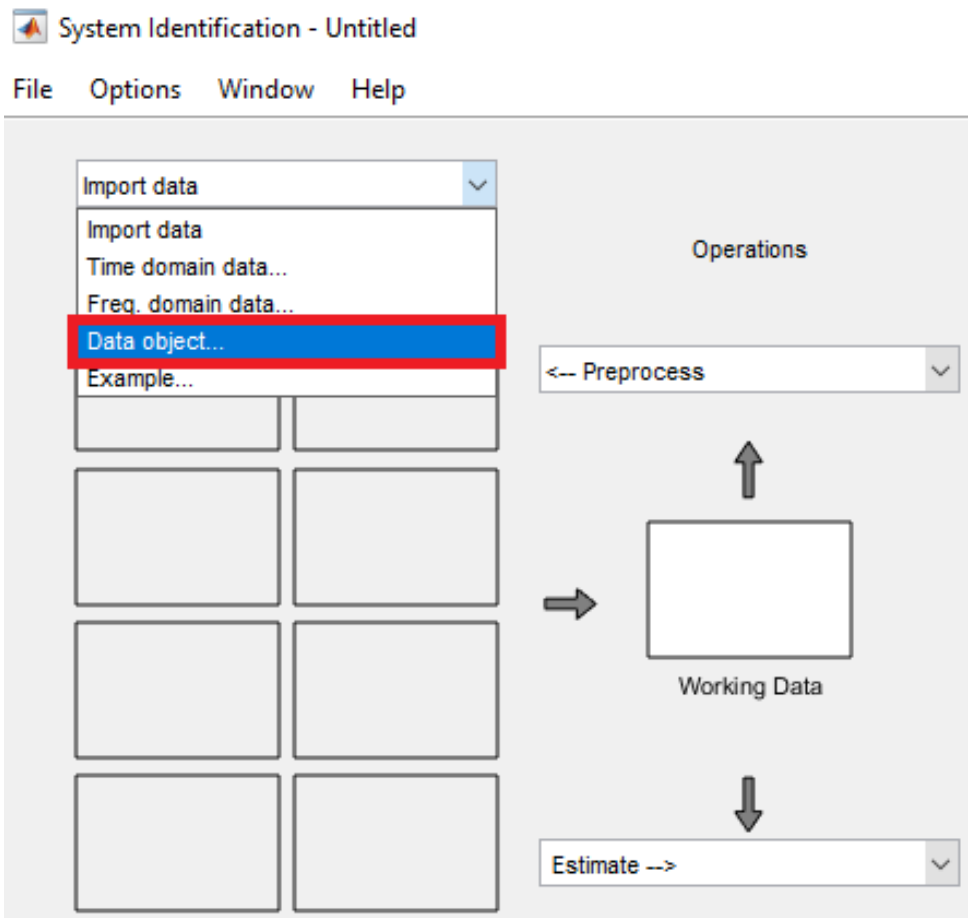
**Figure 4.11:** Opening System Identification App

**Step 10.** Select Import Data



**Figure 4.12: System Identification**

**Step 11.** In the Import Data drop-down menu, select Data object...



**Figure 4.13: Importing data object**

**Step 12.** Enter the data object name under Workspace Variable and click Import. This step is repeated for all three SIMO data objects.

Import Data

Data Format for Signals  
IDDATA or IDFRD/FRD

Workspace Variable  
Object: OVHD\_Press  
Type: IDDATA (Time Domain)

Data Information  
Data name: OVHD\_Press  
Starting time: 1  
Sample time: 1  
More

Import Reset  
Close Help

**Figure 4.14:** Data object name

**Step 13.** Repeat **Steps 11** and **Steps 12** for the validation data.

Import Data

Data Format for Signals  
IDDATA or IDFRD/FRD

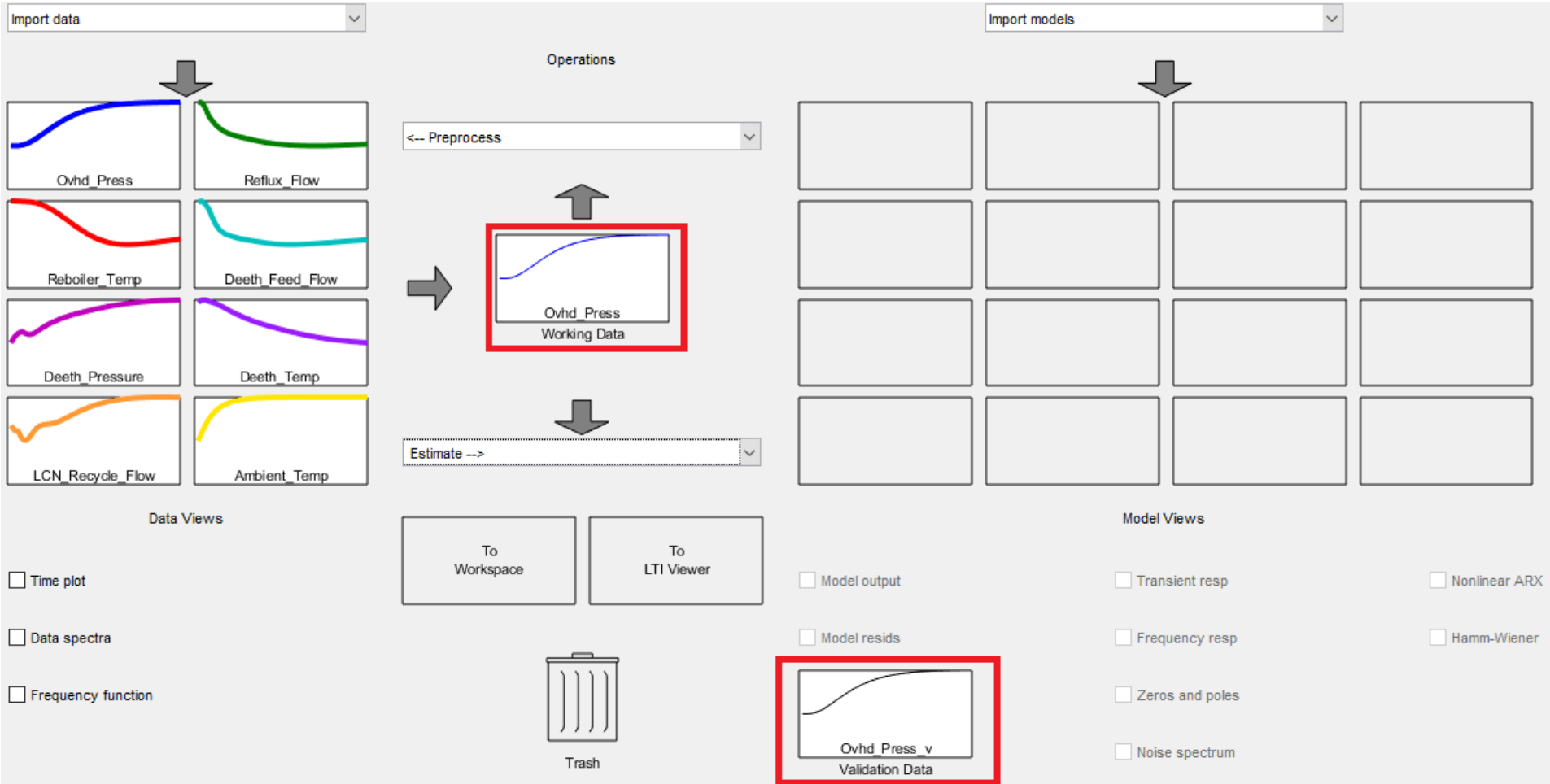
Workspace Variable  
Object: OVHD\_Press\_v  
Type: IDDATA (Time Domain)

Data Information  
Data name: OVHD\_Press\_v  
Starting time: 1  
Sample time: 1  
More

Import Reset  
Close Help

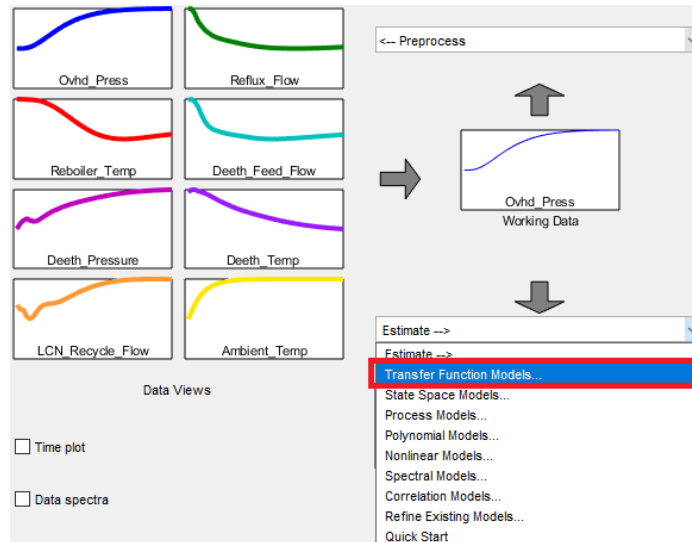
**Figure 4.15:** Import validation data

**Step 14.** Drag and drop the working and validation data objects for the into their respective boxes as shown below from data views.



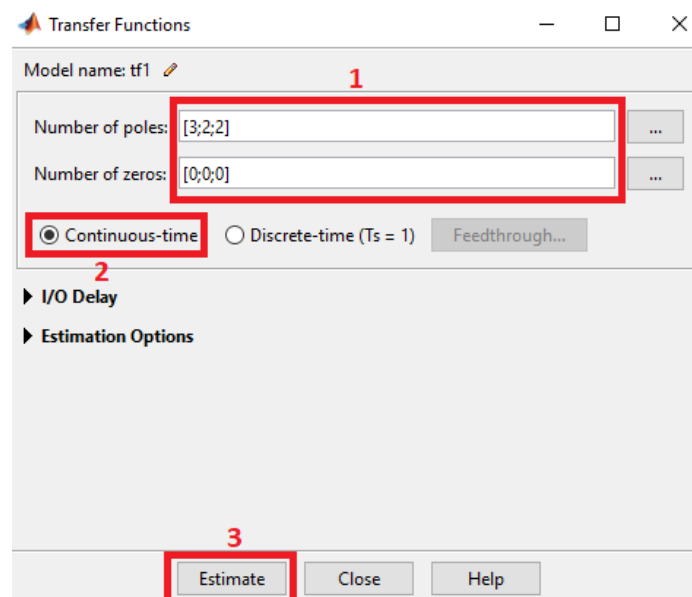
**Figure 4.16:** Successful import of data objects

**Step 15.** In the Estimate drop-down menu, select Transfer Function Models



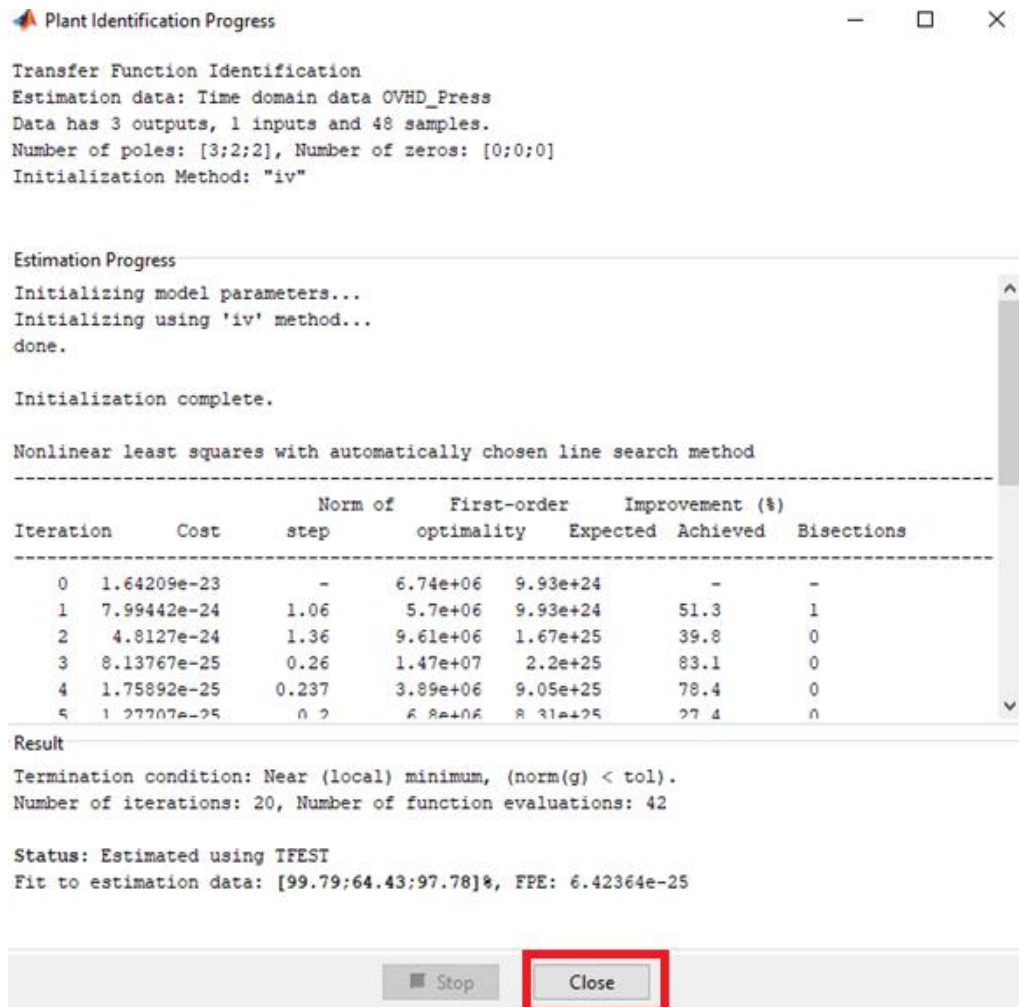
**Figure 4.17: Transfer function models**

**Step 16.** A heuristic approach to select the number of poles and zeros was adopted which was based on a trial and error to obtain a model that best 'fits' the given unit step response curves. As such, 1) select number of poles and zeros, 2) select continuous time and, and 3) click on Estimate.



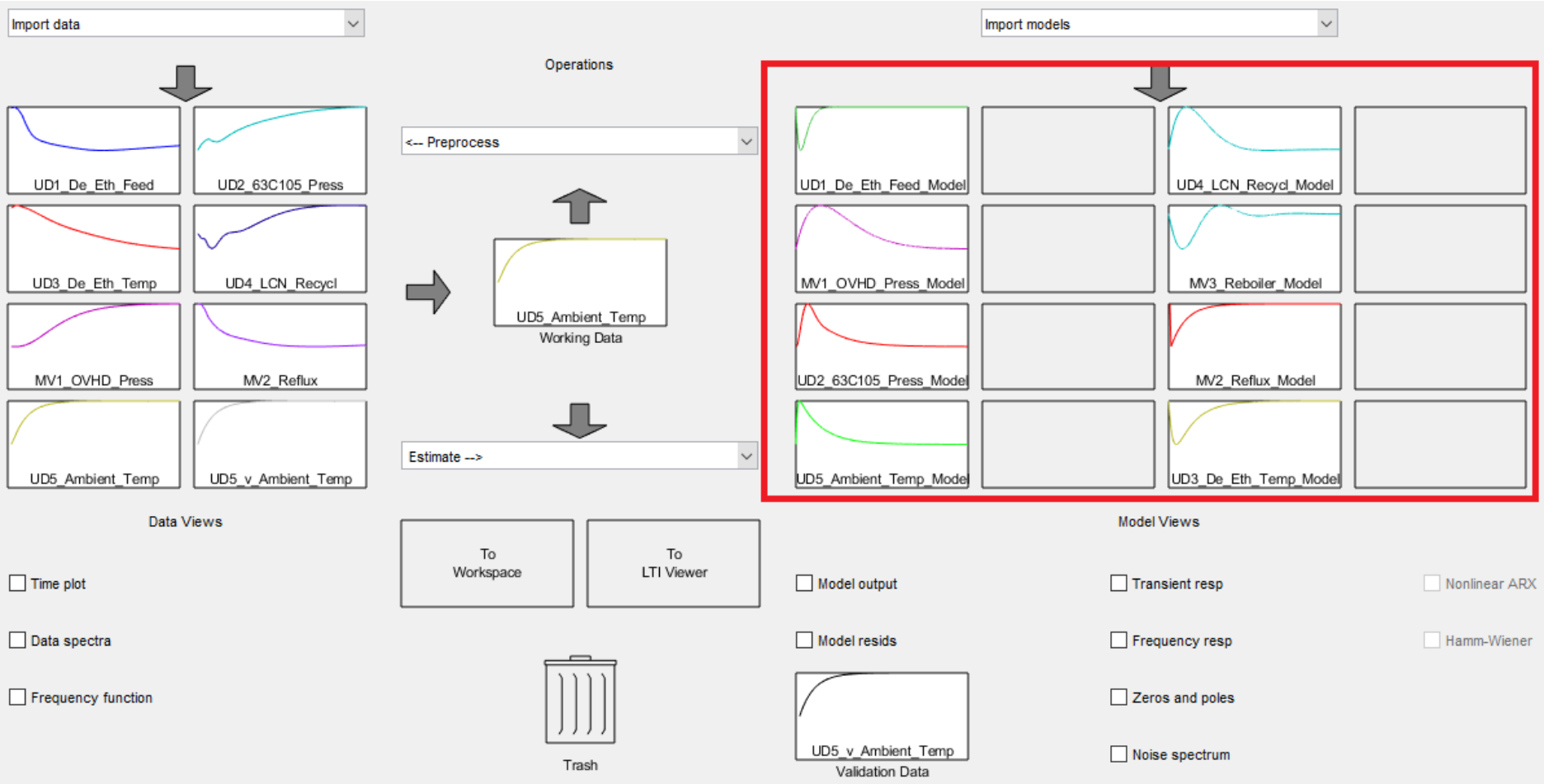
**Figure 4.18: Number of poles and zeros**

**Step 17.** The progress and results of the estimation is displayed in the Plant Identification Progress window. Once the iterations have completed, select Close.



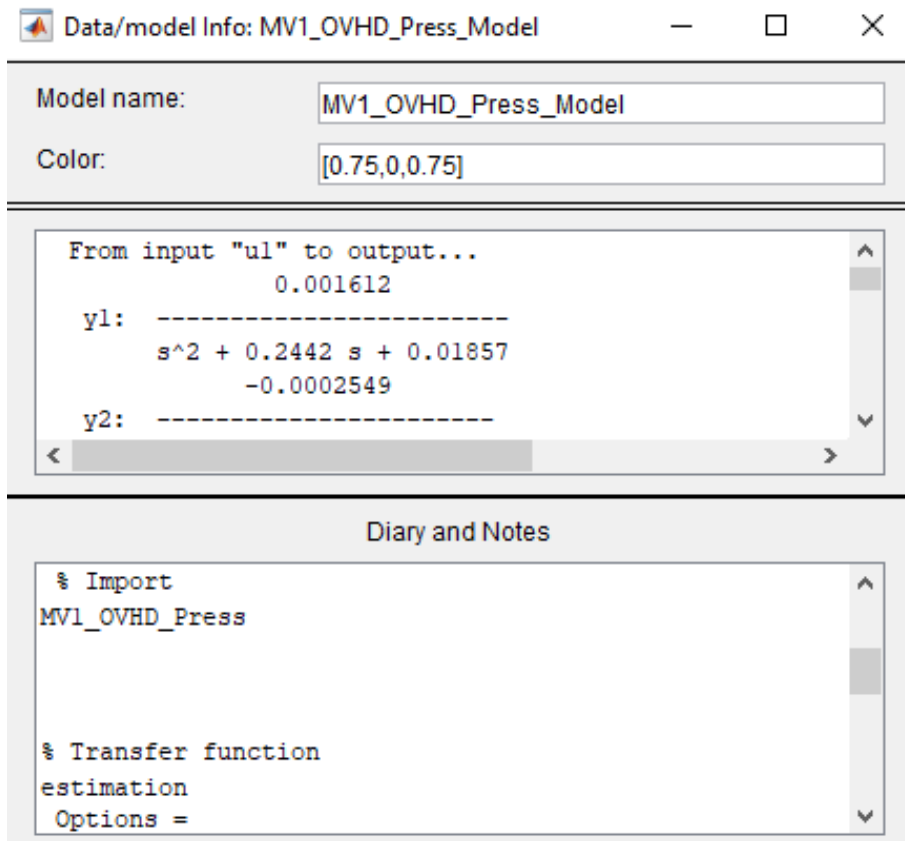
**Figure 4.19:** Identification progress

**Step 18.** Steps 14-17 are repeated for the three SIMO data objects. Once completed, the transfer function SIMO model objects appear under Model Views



**Figure 4.20: Model views**

**Step 19.** To rename the models, right click on each of the transfer function model and change model name. This step is repeated for all the transfer function models.



**Figure 4.21:** Identified model review and rename



**Step 20.** The estimation of the transfer function models is complete. The identified models are still in the system identification toolbox and must be transferred to the MATLAB Workspace. To export the models into the MATLAB Workspace, drag and drop the estimated transfer function SIMO models into the To Workspace box (shown by the red rectangle in Figure 4.22). The model objects will appear in the MATLAB Workspace.



**Figure 4.22: System identification models to MATLAB Workspace**

With the model objects in the MATLAB Workspace, the model data objects are individually called in up in the command window to display the transfer functions for each of the SIMO models. The transfer functions must then be manually typed into a MATLAB script file and assigned variable names. This ensures the transfer functions can be instantiated in the MATLAB/Simulink environment for the configuration of a MIMO model. The MATLAB model transfer functions script file for this research is provided in **Appendix A**. The mathematical formulation showing the input-output relationships of the seventh order debutanizer distillation process transfer function model can be given as:

$$\begin{bmatrix} Y_1 \\ Y_2 \\ Y_3 \\ Y_4 \\ Y_5 \\ Y_6 \\ Y_7 \end{bmatrix} = \begin{bmatrix} TF_{11} & TF_{12} & TF_{13} & TF_{14} & TF_{15} & TF_{16} & TF_{17} \\ TF_{21} & TF_{22} & TF_{23} & TF_{24} & TF_{25} & TF_{26} & TF_{27} \\ TF_{31} & TF_{32} & TF_{33} & TF_{34} & TF_{35} & TF_{36} & TF_{37} \\ TF_{41} & TF_{42} & TF_{43} & TF_{44} & TF_{45} & TF_{46} & TF_{47} \\ TF_{51} & TF_{52} & TF_{53} & TF_{54} & TF_{55} & TF_{56} & TF_{57} \\ TF_{61} & TF_{62} & TF_{63} & TF_{64} & TF_{65} & TF_{66} & TF_{67} \\ TF_{71} & TF_{72} & TF_{73} & TF_{74} & TF_{75} & TF_{76} & TF_{77} \end{bmatrix} \times \begin{bmatrix} U_1 \\ U_2 \\ U_3 \\ U_4 \\ U_5 \\ U_6 \\ U_7 \end{bmatrix} + \begin{bmatrix} 0 \\ 0 \\ TF_{3D1} \\ TF_{4D1} \\ 0 \\ TF_{6D1} \\ 0 \end{bmatrix} \times [D_1] + D_2$$

Where:

$Y_1 =$	LCN_RVP,	LCN Reid Vapour Pressure (kPa)
$Y_2 =$	LPG_C5,	LPG C5 Concentration (Mol %)
$Y_3 =$	Ovhd_Drum_Press,	Overhead Drum Pressure (kPa)
$Y_4 =$	Ovhd_Drum_Press_SV-PV,	Overhead Drum Pressure SV-PV Gap (kPa)
$Y_5 =$	Debut_Diff_Press,	Debutanizer Differential Pressure (kPa)
$Y_6 =$	Reboiler_Valve_Pos,	Debutanizer Reboiler Valve Position (%)
$Y_7 =$	Debut_Tray_24_Temp,	Tray 24 Temperature (DegC)
$U_1 =$	Ovhd_Press,	Overhead Pressure (kPa)
$U_2 =$	Reflux_Flow,	Reflux Flow (m3/h)
$U_3 =$	Reboiler_Temp,	Reboiler Temperature (DegC)
$U_4 =$	Deeth_Feed_Flow,	Deethanizer Feed Flow (m3/h)
$U_5 =$	Deeth_Pressure,	Deethanizer Pressure (kPa)
$U_6 =$	Deeth_Temp,	Deethanizer Temperature (DegC)
$U_7 =$	LCN_Recycle_Flow,	LCN Recycle Flow (m3/h)
$D_1 =$	Ambient_Temp,	Ambient Temperature (DegC)
$D_2 =$	White Noise,	Unmeasured Disturbances

Therefore, the identified transfer function models are given by:

$$TF_{11} = \frac{Y_1}{U_1} = \frac{\text{LCN\_RVP}}{\text{Ovhd\_Press}} = \frac{0.001241}{s^3 + 0.8456 s^2 + 0.1968 s + 0.01438}$$

$$TF_{21} = \frac{Y_2}{U_1} = \frac{\text{LPG\_C5}}{\text{Ovhd\_Press}} = \frac{-0.0001665}{s^2 + 0.3112 s + 0.141}$$

$$TF_{31} = \frac{Y_3}{U_1} = \frac{\text{Ovhd\_Drum\_Press}}{\text{Ovhd\_Press}} = \frac{0.3791}{s^3 + 1.451 s^2 + 4.211 s + 0.6576}$$

$$TF_{41} = \frac{Y_4}{U_1} = \frac{\text{Ovhd\_Drum\_Press\_SV-PV}}{\text{Ovhd\_Press}} = \frac{4.536}{s^2 + 18.06 s + 8.779}$$

$$TF_{51} = \frac{Y_5}{U_1} = \frac{\text{Debut\_Diff\_Press}}{\text{Ovhd\_Press}} = \frac{-0.01348}{s^2 + 1.041 s + 0.2387}$$

$$TF_{61} = \frac{Y_6}{U_1} = \frac{\text{Reboiler\_Valve\_Pos}}{\text{Ovhd\_Press}} = \frac{-0.302}{s^2 + 6.456 s + 2.517}$$

$$TF_{71} = \frac{Y_7}{U_1} = \frac{\text{Debut\_Tray\_24\_Temp}}{\text{Ovhd\_Press}} = \frac{0.0009007}{s^2 + 0.2369 s + 0.0351}$$

$$TF_{12} = \frac{Y_1}{U_2} = \frac{\text{LCN\_RVP}}{\text{Reflux\_Flow}} = 0$$

$$TF_{22} = \frac{Y_2}{U_2} = \frac{\text{LPG\_C5}}{\text{Reflux\_Flow}} = \frac{-0.004903}{s^2 + 1.638 s + 0.2383}$$

$$TF_{32} = \frac{Y_3}{U_2} = \frac{\text{Ovhd\_Drum\_Press}}{\text{Reflux\_Flow}} = 0$$

$$TF_{42} = \frac{Y_4}{U_2} = \frac{\text{Ovhd\_Drum\_Press\_SV-PV}}{\text{Reflux\_Flow}} = 0$$

$$TF_{52} = \frac{Y_5}{U_2} = \frac{\text{Debut\_Diff\_Press}}{\text{Reflux\_Flow}} = \frac{0.008285}{s^2 + 0.2468 s + 0.02035}$$

$$TF_{62} = \frac{Y_6}{U_2} = \frac{\text{Reboiler\_Valve\_Pos}}{\text{Reflux\_Flow}} = \frac{0.1951}{s^2 + 0.3764 s + 0.3902}$$

$$TF_{72} = \frac{Y_7}{U_2} = \frac{\text{Debut\_Tray\_24\_Temp}}{\text{Reflux\_Flow}} = \frac{0.2693 s^3 - 0.1926 s^2 - 0.0219 s - 0.005952}{s^5 + 1.764 s^4 + 1.752 s^3 + 0.5189 s^2 + 0.09789 s + 0.008874}$$

$$TF_{13} = \frac{Y_1}{U_3} = \frac{\text{LCN\_RVP}}{\text{Reboiler\_Temp}} = \frac{-0.004852}{s^3 + 0.3151 s^2 + 0.04709 s + 0.00415}$$

$$TF_{23} = \frac{Y_2}{U_3} = \frac{\text{LPG\_C5}}{\text{Reboiler\_Temp}} = \frac{0.0009339}{s^2 + 0.3965 s + 0.06791}$$

$$TF_{33} = \frac{Y_3}{U_3} = \frac{\text{Ovhd\_Drum\_Press}}{\text{Reboiler\_Temp}} = 0$$

$$TF_{43} = \frac{Y_4}{U_3} = \frac{\text{Ovhd\_Drum\_Press\_SV-PV}}{\text{Reboiler\_Temp}} = 0$$

$$TF_{53} = \frac{Y_5}{U_3} = \frac{\text{Debut\_Diff\_Press}}{\text{Reboiler\_Temp}} = 0$$

$$TF_{63} = \frac{Y_6}{U_3} = \frac{\text{Reboiler\_Valve\_Pos}}{\text{Reboiler\_Temp}} = \frac{0.6714}{s^2 + 5.496 s + 0.6714}$$

$$TF_{73} = \frac{Y_7}{U_3} = \frac{\text{Debut\_Tray\_24\_Temp}}{\text{Reboiler\_Temp}} = \frac{0.01305}{s^2 + 0.5266 s + 0.08758}$$

$$TF_{14} = \frac{Y_1}{U_4} = \frac{\text{LCN\_RVP}}{\text{Deeth\_Feed\_Flow}} = 0$$

$$TF_{24} = \frac{Y_2}{U_4} = \frac{\text{LPG\_C5}}{\text{Deeth\_Feed\_Flow}} = \frac{-0.0007287}{s^2 + 0.6293 s + 0.1123}$$

$$TF_{34} = \frac{Y_3}{U_4} = \frac{\text{Ovhd\_Drum\_Press}}{\text{Deeth\_Feed\_Flow}} = 0$$

$$TF_{44} = \frac{Y_4}{U_4} = \frac{\text{Ovhd\_Drum\_Press\_SV-PV}}{\text{Deeth\_Feed\_Flow}} = 0$$

$$TF_{54} = \frac{Y_5}{U_4} = \frac{\text{Debut\_Diff\_Press}}{\text{Deeth\_Feed\_Flow}} = 0$$

$$TF_{64} = \frac{Y_6}{U_4} = \frac{\text{Reboiler\_Valve\_Pos}}{\text{Deeth\_Feed\_Flow}} = \frac{0.3628}{s^2 + 10.06 s + 0.5412}$$

$$TF_{74} = \frac{Y_7}{U_4} = \frac{\text{Debut\_Tray\_24\_Temp}}{\text{Deeth\_Feed\_Flow}} = 0$$

$$TF_{15} = \frac{Y_1}{U_5} = \frac{\text{LCN\_RVP}}{\text{Deeth\_Pressure}} = 0$$

$$TF_{25} = \frac{Y_2}{U_5} = \frac{\text{LPG\_C5}}{\text{Deeth\_Pressure}} = 0$$

$$TF_{35} = \frac{Y_3}{U_5} = \frac{\text{Ovhd\_Drum\_Press}}{\text{Deeth\_Pressure}} = \frac{0.004934}{s^3 + 0.5241 s^2 + 0.1822 s + 0.00895}$$

$$TF_{45} = \frac{Y_4}{U_5} = \frac{\text{Ovhd\_Drum\_Press\_SV-PV}}{\text{Deeth\_Pressure}} = \frac{-0.004668}{s^3 + 0.47 s^2 + 0.1708 s + 0.008437}$$

$$TF_{55} = \frac{Y_5}{U_5} = \frac{\text{Debut\_Diff\_Press}}{\text{Deeth\_Pressure}} = 0$$

$$TF_{65} = \frac{Y_6}{U_5} = \frac{\text{Reboiler\_Valve\_Pos}}{\text{Deeth\_Pressure}} = \frac{0.002211}{s^2 + 0.4867 s + 0.04347}$$

$$TF_{75} = \frac{Y_7}{U_5} = \frac{\text{Debut\_Tray\_24\_Temp}}{\text{Deeth\_Pressure}} = 0$$

$$TF_{16} = \frac{Y_1}{U_6} = \frac{\text{LCN\_RVP}}{\text{Deeth\_Temp}} = 0$$

$$TF_{26} = \frac{Y_2}{U_6} = \frac{\text{LPG\_C5}}{\text{Deeth\_Temp}} = 0$$

$$TF_{36} = \frac{Y_3}{U_6} = \frac{\text{Ovhd\_Drum\_Press}}{\text{Deeth\_Temp}} = \frac{-0.1775}{s^2 + 0.3455 s + 0.01603}$$

$$TF_{46} = \frac{Y_4}{U_6} = \frac{\text{Ovhd\_Drum\_Press\_SV-PV}}{\text{Deeth\_Temp}} = \frac{0.1785}{s^2 + 0.3471 s + 0.01612}$$

$$TF_{56} = \frac{Y_5}{U_6} = \frac{\text{Debut\_Diff\_Press}}{\text{Deeth\_Temp}} = \frac{-0.001914}{s^3 + 0.1084 s^2 + 0.07097 s + 0.002616}$$

$$TF_{66} = \frac{Y_6}{U_6} = \frac{\text{Reboiler\_Valve\_Pos}}{\text{Deeth\_Temp}} = \frac{-0.04504}{s^2 + 0.649 s + 0.03486}$$

$$TF_{76} = \frac{Y_7}{U_6} = \frac{\text{Debut\_Tray\_24\_Temp}}{\text{Deeth\_Temp}} = 0$$

$$TF_{17} = \frac{Y_1}{U_7} = \frac{\text{LCN\_RVP}}{\text{LCN\_Recycle\_Flow}} = 0$$

$$TF_{27} = \frac{Y_2}{U_7} = \frac{\text{LPG\_C5}}{\text{LCN\_Recycle\_Flow}} = 0$$

$$TF_{37} = \frac{Y_3}{U_7} = \frac{\text{Ovhd\_Drum\_Press}}{\text{LCN\_Recycle\_Flow}} = \frac{0.03129}{s^2 + 0.1977 s + 0.016}$$

$$TF_{47} = \frac{Y_4}{U_7} = \frac{\text{Ovhd\_Drum\_Press\_SV-PV}}{\text{LCN\_Recycle\_Flow}} = \frac{-0.03212}{s^2 + 0.2023 s + 0.01679}$$

$$TF_{57} = \frac{Y_5}{U_7} = \frac{\text{Debut\_Diff\_Press}}{\text{LCN\_Recycle\_Flow}} = \frac{0.0132}{s^2 + 0.4215 s + 0.06652}$$

$$TF_{67} = \frac{Y_6}{U_7} = \frac{\text{Reboiler\_Valve\_Pos}}{\text{LCN\_Recycle\_Flow}} = \frac{6.699}{s^2 + 7.781 s + 0.957}$$

$$TF_{77} = \frac{Y_7}{U_7} = \frac{\text{Debut\_Tray\_24\_Temp}}{\text{LCN\_Recycle\_Flow}} = 0$$

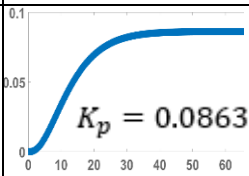
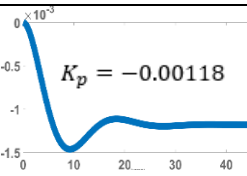
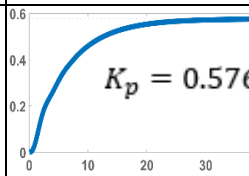
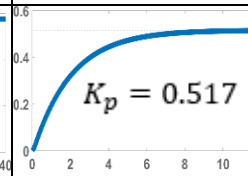
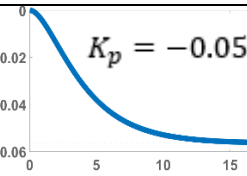
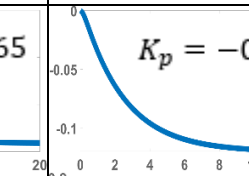
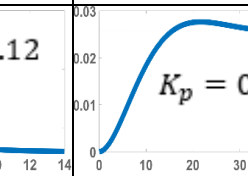
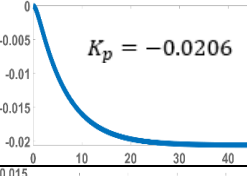
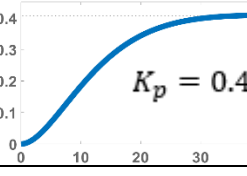
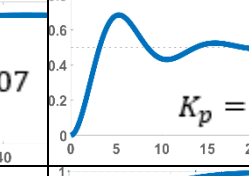
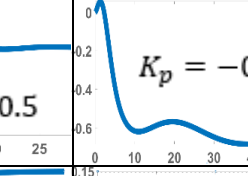
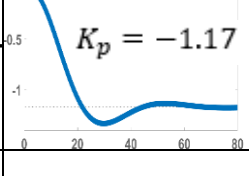
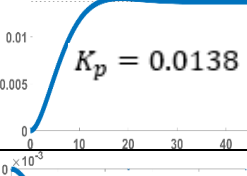
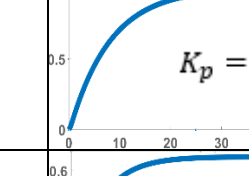
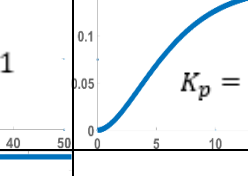
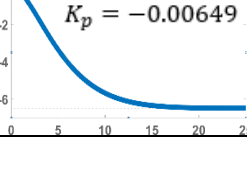
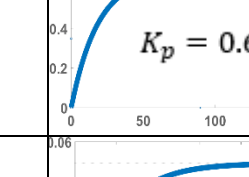
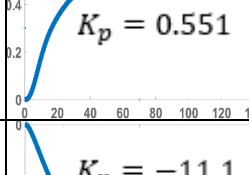
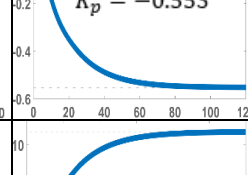
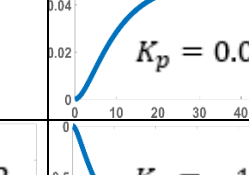
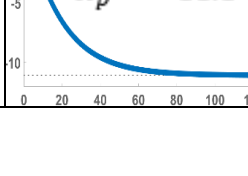
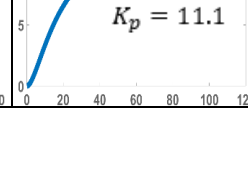
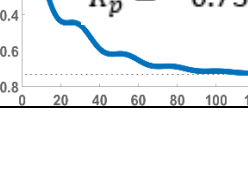
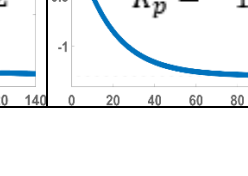
$$TF_{3D1} = \frac{Y_3}{D_1} = \frac{\text{Ovhd\_Drum\_Press}}{\text{Ambient\_Temp}} = \frac{3.061}{s^2 + 5.35s + 1.275}$$

$$TF_{4D1} = \frac{Y_4}{D_1} = \frac{\text{Ovhd\_Drum\_Press\_SV-PV}}{\text{Ambient\_Temp}} = \frac{-3.061}{s^2 + 5.35s + 1.275}$$

$$TF_{6D1} = \frac{Y_6}{D_1} = \frac{\text{Reboiler\_Valve\_Pos}}{\text{Ambient\_Temp}} = \frac{0.4528}{s^2 + 5.249s + 0.9055}$$

The transfer functions given above are estimated with the MATLAB system identification toolbox representing a numerical description for each of the step response curves presented in Table 4.2. In order to determine the accuracy of the estimated transfer functions in terms of how well they represent the original model, a comparative analysis is necessary. For each of the estimated transfer functions given above, the MATLAB function **step (X)**, where **X** represents a transfer function, is used in the command window to obtain the open loop step response curves. The step response curves obtained with the MATLAB transfer functions are presented in Table 4.4 where  $K_p$  represents the steady state gain. Table 4.5 provides the steady state gain comparisons between original model and the MATLAB system identification model results where  $K_{p\_ORIGINAL}$  is the steady state gain of the original model,  $K_{p\_MATLAB}$  is the steady state gain of the MATLAB transfer function model,  $K_{p\_ERROR}$  is the absolute error between the two steady state gains and  $K_{p\%\_ERROR}$  represents the percentage error between the two steady state gains.

Table 4.4: Step response models from the MATLAB transfer functions

	LCN_RVP	LPG_C5	Ovhd_Drum_Press	Ovhd_Drum Press_SV-PV	Debut_Diff_Press	Reboiler_Valve_Pos	Debut_Tray_24_Temp
Ovhd_Press							
Reflux_Flow	$K_p = 0$		$K_p = 0$	$K_p = 0$			
Reboiler_Temp			$K_p = 0$	$K_p = 0$	$K_p = 0$		
Deeth_Feed_Flow	$K_p = 0$		$K_p = 0$	$K_p = 0$	$K_p = 0$		$K_p = 0$
Deeth_Pressure	$K_p = 0$	$K_p = 0$			$K_p = 0$		$K_p = 0$
Deeth_Temp	$K_p = 0$	$K_p = 0$					$K_p = 0$

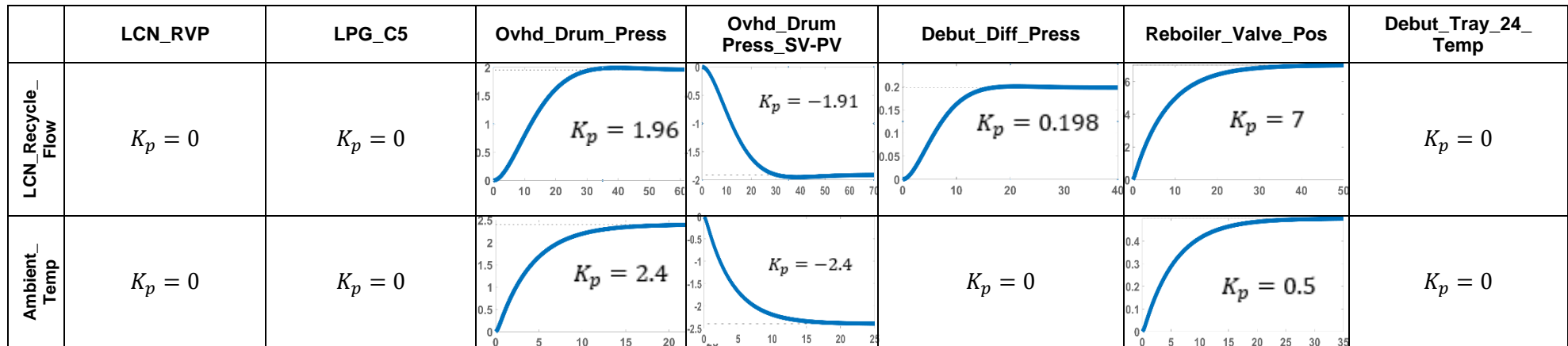


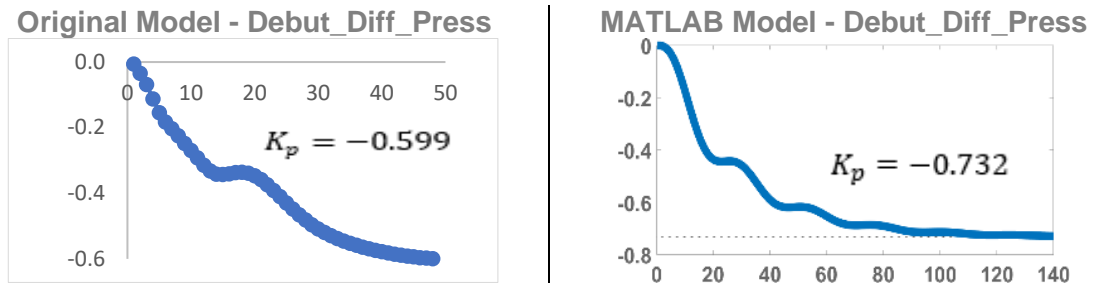
Table 4.5: Steady state gain comparisons between original model and MATLAB system identification model results

	LCN_RVP	LPG_C5	Ovhd_Drum_Press	Ovhd_Drum Press_SV-PV	Debut_Diff_Press	Reboiler_Valve_Pos	Debut_Tray_24_Temp
Ovhd_Press	$K_{p\_ORIGINAL} = 0.086$ $K_{p\_MATLAB} = 0.083$ $K_{p\_ERROR} = 0.003$ $K_{p\_ \%\_ERROR} = 3.5\%$	$K_{p\_ORIGINAL} = -0.0012$ $K_{p\_MATLAB} = -0.00118$ $K_{p\_ERROR} = -0.00002$ $K_{p\_ \%\_ERROR} = 1.7\%$	$K_{p\_ORIGINAL} = 0.569$ $K_{p\_MATLAB} = 0.576$ $K_{p\_ERROR} = -0.007$ $K_{p\_ \%\_ERROR} = 1.2\%$	$K_{p\_ORIGINAL} = 0.599$ $K_{p\_MATLAB} = 0.517$ $K_{p\_ERROR} = 0.082$ $K_{p\_ \%\_ERROR} = 13.7\%$	$K_{p\_ORIGINAL} = -0.059$ $K_{p\_MATLAB} = -0.0565$ $K_{p\_ERROR} = -0.0025$ $K_{p\_ \%\_ERROR} = 4.2\%$	$K_{p\_ORIGINAL} = -0.12$ $K_{p\_MATLAB} = -0.12$ $K_{p\_ERROR} = 0$ $K_{p\_ \%\_ERROR} = 0\%$	$K_{p\_ORIGINAL} = 0.026$ $K_{p\_MATLAB} = 0.0257$ $K_{p\_ERROR} = 0.0003$ $K_{p\_ \%\_ERROR} = 1.2\%$
Reflux_Flow	$K_p = 0$	$K_{p\_ORIGINAL} = -0.02$ $K_{p\_MATLAB} = -0.0206$ $K_{p\_ERROR} = 0.0006$ $K_{p\_ \%\_ERROR} = 3\%$	$K_p = 0$	$K_p = 0$	$K_{p\_ORIGINAL} = 0.398$ $K_{p\_MATLAB} = 0.407$ $K_{p\_ERROR} = -0.009$ $K_{p\_ \%\_ERROR} = 2.3\%$	$K_{p\_ORIGINAL} = 0.5$ $K_{p\_MATLAB} = 0.5$ $K_{p\_ERROR} = 0$ $K_{p\_ \%\_ERROR} = 0\%$	$K_{p\_ORIGINAL} = -0.673$ $K_{p\_MATLAB} = -0.671$ $K_{p\_ERROR} = -0.002$ $K_{p\_ \%\_ERROR} = 0.3\%$
Reboiler_Temp	$K_{p\_ORIGINAL} = -1.168$ $K_{p\_MATLAB} = -1.17$ $K_{p\_ERROR} = 0.002$ $K_{p\_ \%\_ERROR} = 0.2\%$	$K_{p\_ORIGINAL} = 0.014$ $K_{p\_MATLAB} = 0.0138$ $K_{p\_ERROR} = 0.0002$ $K_{p\_ \%\_ERROR} = 1.4\%$	$K_p = 0$	$K_p = 0$	$K_p = 0$	$K_{p\_ORIGINAL} = 0.997$ $K_{p\_MATLAB} = 1$ $K_{p\_ERROR} = -0.003$ $K_{p\_ \%\_ERROR} = 0.3\%$	$K_{p\_ORIGINAL} = 0.152$ $K_{p\_MATLAB} = 0.149$ $K_{p\_ERROR} = 0.003$ $K_{p\_ \%\_ERROR} = 2\%$

	LCN_RVP	LPG_C5	Ovhd_Drum_Press	Ovhd_Drum Press_SV-PV	Debut_Diff_Press	Reboiler_Valve_Pos	Debut_Tray_24_Temp
Deeth_Feed_FI	$K_p = 0$	$K_{p\_ORIGINAL} = -0.006$ $K_{p\_MATLAB} = -0.00649$ $K_{p\_ERROR} = 0.00049$ $K_{p\_ \%\_ERROR} = 8.2\%$	$K_p = 0$	$K_p = 0$	$K_p = 0$	$K_{p\_ORIGINAL} = 0.6$ $K_{p\_MATLAB} = 0.67$ $K_{p\_ERROR} = -0.07$ $K_{p\_ \%\_ERROR} = 11.7\%$	$K_p = 0$
Deeth_Pressur	$K_p = 0$	$K_p = 0$	$K_{p\_ORIGINAL} = 0.499$ $K_{p\_MATLAB} = 0.551$ $K_{p\_ERROR} = -0.052$ $K_{p\_ \%\_ERROR} = 10.4\%$	$K_{p\_ORIGINAL} = -0.499$ $K_{p\_MATLAB} = -0.553$ $K_{p\_ERROR} = 0.054$ $K_{p\_ \%\_ERROR} = 10.8\%$	$K_p = 0$	$K_{p\_ORIGINAL} = 0.05$ $K_{p\_MATLAB} = 0.0509$ $K_{p\_ERROR} = -0.0009$ $K_{p\_ \%\_ERROR} = 1.8\%$	$K_p = 0$
Deeth_Temp	$K_p = 0$	$K_p = 0$	$K_{p\_ORIGINAL} = -9.953$ $K_{p\_MATLAB} = -11.1$ $K_{p\_ERROR} = 1.147$ $K_{p\_ \%\_ERROR} = 11.5\%$	$K_{p\_ORIGINAL} = 9.953$ $K_{p\_MATLAB} = 11.1$ $K_{p\_ERROR} = -1.147$ $K_{p\_ \%\_ERROR} = 11.5\%$	$K_{p\_ORIGINAL} = -0.599$ $K_{p\_MATLAB} = -0.732$ $K_{p\_ERROR} = 0.133$ $K_{p\_ \%\_ERROR} = 22.2\%$	$K_{p\_ORIGINAL} = -1.197$ $K_{p\_MATLAB} = -1.29$ $K_{p\_ERROR} = 0.093$ $K_{p\_ \%\_ERROR} = 7.8\%$	$K_p = 0$
LCN_Re cycle_FI	$K_p = 0$	$K_p = 0$	$K_{p\_ORIGINAL} = 2$ $K_{p\_MATLAB} = 1.97$ $K_{p\_ERROR} = 0.03$ $K_{p\_ \%\_ERROR} = 1.5\%$	$K_{p\_ORIGINAL} = -2$ $K_{p\_MATLAB} = -1.97$ $K_{p\_ERROR} = -0.03$ $K_{p\_ \%\_ERROR} = 1.5\%$	$K_{p\_ORIGINAL} = 0.199$ $K_{p\_MATLAB} = 0.198$ $K_{p\_ERROR} = 0.001$ $K_{p\_ \%\_ERROR} = 0.5\%$	$K_{p\_ORIGINAL} = 6.979$ $K_{p\_MATLAB} = 7$ $K_{p\_ERROR} = -0.021$ $K_{p\_ \%\_ERROR} = 0.3\%$	$K_p = 0$
Ambient_Temp	$K_p = 0$	$K_p = 0$	$K_{p\_ORIGINAL} = 2.399$ $K_{p\_MATLAB} = 2.4$ $K_{p\_ERROR} = -0.001$ $K_{p\_ \%\_ERROR} = 0.04\%$	$K_{p\_ORIGINAL} = -2.399$ $K_{p\_MATLAB} = -2.4$ $K_{p\_ERROR} = 0.001$ $K_{p\_ \%\_ERROR} = 0.04\%$	$K_p = 0$	$K_{p\_ORIGINAL} = 0.499$ $K_{p\_MATLAB} = 0.5$ $K_{p\_ERROR} = -0.001$ $K_{p\_ \%\_ERROR} = 0.2\%$	$K_p = 0$



In comparing the two model graphical representations as shown below in Figure 4.23, it is notable that the dynamic responses are largely similar with the exception of the step response curve relating the `Deeth_Temp` (deethanizer temperature) control input to the `Debut_Diff_Press` (debutanizer differential pressure) controlled output.



**Figure 4.23: Comparing the Original and MATLAB models of the `Debut_Diff_Press` output**

The differences observed in the dynamic responses between the step response curves can be attributed to the complex dynamics that would require a large number of poles and zeros to accurately approximate. It is worth noting that the percentage error considers only differences in the absolute value of the steady state gains, which is equal to 22%, and does not include the dynamic response. Efforts to closely approximate the original model response curve without increasing transfer function complexity, specifically for this step response curve, proved to be unsuccessful. However, for the rest of the step response curves, it can be observed that the differences are negligible, with all being less than 14% and most less than 5% indicating the MATLAB model results are similar to that of the original model. Therefore, it can be reliably concluded that the MATLAB system identification toolbox models are a sufficiently accurate representation of the original models presented in Table 4.2.

#### 4.5. Conclusion

The objectives of this chapter have been fulfilled with the development of a debutanizer distillation process model for use in Chapters 5 and 6. Furthermore, the model developed in this research was originally identified with AspenTech's DMC3 Builder commercial software package using the FIR identification method to estimate the step response coefficients. The identified step response coefficients are then used in this research to estimate transfer function models with MATLAB's system identification toolbox. Finally, open loop step response simulations for each of the estimated transfer functions are conducted to compare the dynamic response curves and steady state gains with the original model with the results indicating that the MATLAB models are a sufficiently accurate representation of the original models.

In the next chapter, the decentralized controller design methods for the second order and third order multivariable models of the debutanizer distillation process transfer function models developed in this chapter, are presented. The decentralized controllers are designed based on the selection of loop pairings and the selection of PID controller gains and the loop interactions are compensated for by making use of decoupling controllers.

## **CHAPTER FIVE: DECENTRALIZED PID CONTROLLER DESIGN**

### **5.1. Introduction**

Among the many control technologies available in the market today, the Proportional-Integral-Derivative (PID) controller is the most widely used controller in industry for its simplicity and ease of implementation with relatively low-cost hardware providing satisfactory performance for most control applications encountered in industry (Seborg et al., 2004). PID controllers are often implemented as part of a basic process control system responsible for the processing of control functions and maintaining process variables at their setpoints in hardware platforms such as programmable logic controllers (PLC) and distributed control systems (DCS) (Seborg et al., 2004). The objective of this chapter is to perform controller design of decentralized PID controllers for the debutanizer distillation process model transfer functions developed in the previous chapter and perform closed-loop simulations in the MATLAB/Simulink environment to test the developed algorithms for closed-loop performance. In this chapter, decentralized controller design methods for a second order model of the debutanizer distillation process are presented. With the controller design concepts presented in Chapter 3, the decentralized PID controllers are designed based on the selection of control loop pairings using the Relative Gain Array (RGA) (Edgar H Bristol, 1966) method, and the PID controller gains are calculated using the Internal Model Control (IMC) method (Garcia and Morari, 1982). The loop interactions prevalent in multivariable systems, such as the debutanizer distillation process models studied in this research, are compensated for by making use of decoupling control techniques. Model reduction techniques are utilized in order to obtain standard PID controller structures, and finally, the resulting controllers for each of the models are simulated in the MATLAB/Simulink software environment to test the developed algorithms for closed loop performance.

This chapter begins with presenting the second order debutanizer distillation process model to be used for the rest of the chapter in section 5.2, the calculation of the RGA for the model is given in section 5.3. Decoupling compensators are derived for the model in section 5.4 and in section 5.5 a model order reduction method to enable simplified controller design is outlined followed by a description of the IMC controller design for the second order debutanizer process model. Section 5.6 presents the MATLAB/Simulink simulation case studies and results for the designed controllers in closed-loop and section 5.7 provides the concluding remarks.

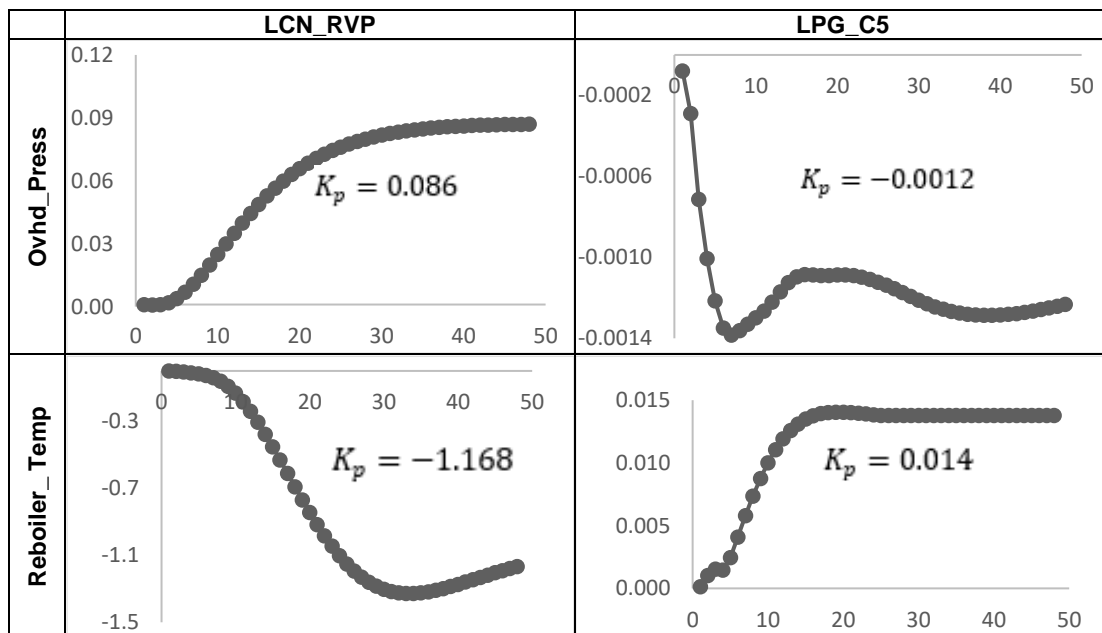
### **5.2. Reduced second order debutanizer distillation models**

The debutanizer distillation process model used in this research is a seventh order process model described by the linear transfer functions developed in Chapter 4. The order or size of the model is determined by the number of inputs and outputs included in the identification and development process of the model. The inputs and outputs included in the model are those that have an impact on the plants' overall profitability. However, it is possible to include or

exclude inputs and outputs from the process model to either increase or decrease the order of the model. Therefore, to reduce computational complexity, the seventh order model is reduced into a second order model. The second order model is given in Table 5.1. The finite impulse response (FIR) algorithm is used in the identification of the model as described in Chapter 4. The model is a representation of unit step response coefficients presented in plots relating each input variable with an output variable via a dynamic response curve. The two inputs are the overhead pressure (kPa) and reflux flow (m<sup>3</sup>/h) whereas the two outputs are the Light Cracked Naphtha (LCN) Reid Vapour Pressure (kPa) and the Liquefied Petroleum Gas (LPG) C<sub>5</sub> concentration (Mol %). The selection of these variables is based on their particular importance in the operation of the debutanizer distillation process since the main objectives, as previously outlined in Chapter 4 are to:

- 1) Prevent high overhead pressure which may lead to LPG being routed to the fuel gas system from the overhead drum.
- 2) Minimize the concentration of C<sub>5</sub>'s in the overhead stream of Liquefied Petroleum Gas (LPG).
- 3) Control the Reid Vapor Pressure (RVP) of the Light Cracked Naphtha (LCN) stream to meet gasoline specifications.

**Table 5.1: Second order debutanizer distillation process model**



The above model is used to perform the design of decentralized PID controllers and carry out closed-loop simulations in the MATLAB/Simulink environment to test the developed algorithms for closed-loop performance. The next section presents the use of the relative gain array to confirm the adequacy of the control structure and loop pairings for the second order debutanizer distillation process model.

### 5.3. Relative Gain Array (RGA) for the debutanizer second order model

The RGA is described in Chapter 3 with an illustrative example of a second order system provided. In this chapter, the RGA is used to confirm the input-output pairings of the second order debutanizer distillation process model to determine whether the existing pairings are desirable according to the properties of the RGA (Edgar H Bristol, 1966) and, as a result, whether there are requirements for the loop pairings to be modified and re-arranged in accordance to improve control system performance. The transfer function model characterizing the second order multivariable debutanizer model given in Table 5.1 can be presented in matrix form as follows:

$$\frac{Y(s)}{U(s)} = \text{TF}(s) = \begin{bmatrix} TF_{11}(s) & TF_{12}(s) \\ TF_{21}(s) & TF_{22}(s) \end{bmatrix} = \dots \quad (5.1)$$

$$\begin{bmatrix} \frac{0.001241}{s^3 + 0.8456s^2 + 0.1968s + 0.01438} & \frac{-0.004852}{s^3 + 0.3151s^2 + 0.04709s + 0.00415} \\ \frac{-0.0001665}{s^2 + 0.3112s + 0.141} & \frac{0.0009339}{s^2 + 0.3965s + 0.06791} \end{bmatrix}$$

It is worth noting that to avoid confusion, the transfer function subscripts are labelled in the standard second order form as follows:

$TF_{11}(s)$  is the transfer function relating LCN\_RVP (output 1) to the Ovhd\_Press (input 1).

$TF_{12}(s)$  is the transfer function relating LCN\_RVP (output 1) to the Reboiler\_Temp (input 2).

$TF_{21}(s)$  is the transfer function relating LPG\_C5 (output 2) to the Ovhd\_Press (input 1).

$TF_{22}(s)$  is the transfer function relating LPG\_C5 (output 2) to the Reboiler\_Temp (input 2).

The objective is to calculate the RGA for this model to determine the suitable input-output pairing. The procedure for calculating the RGA for a general second order system is adopted from (Ogunnaike and Ray, 1994) and outlined below. The steady state gain matrix for the second order multivariable debutanizer model is given by:

$$\text{Steady State Gain Matrix} = \begin{bmatrix} K_{11} & K_{12} \\ K_{21} & K_{22} \end{bmatrix} = \begin{bmatrix} 0.085971550 & -1.16768 \\ -0.00123 & 0.013792 \end{bmatrix} \quad (5.2)$$

The system output expressions are given by:

$$y_1 = K_{11}m_1 + K_{12}m_2 \quad (5.3)$$

$$y_2 = K_{21}m_1 + K_{22}m_2 \quad (5.4)$$

Where:

$K_{11} = 0.085971550$  (Steady state gain of  $TF_{11}(s)$  relating LCN\_RVP to Ovhd\_Press)

$K_{12} = -1.16768$  (Steady state gain of  $TF_{12}(s)$  relating LCN\_RVP to Reboiler\_Temp)

$K_{21} = -0.00123$  (Steady state gain of  $TF_{21}(s)$  relating LPG\_C5 to Ovhd\_Press)

$K_{22} = 0.013792$  (Steady state gain of  $TF_{22}(s)$  relating LPG\_C5 to Reboiler\_Temp)

$m_1 = \text{input 1} = \text{Ovhd\_Press}$

$m_2 = \text{input 2} = \text{Reboiler\_Temp}$

$y_1 = \text{output 1} = \text{LCN\_RVP}$

$y_2 = \text{output 2} = \text{LPG\_C5}$

The preliminary system input-output pairing is such that:

$m_1 = \text{input 1} = \text{Ovhd\_Press}$  controls  $y_1 = \text{output 1} = \text{LCN\_RVP}$

$m_2 = \text{input 2} = \text{Reboiler\_Temp}$  controls  $y_2 = \text{output 2} = \text{LPG\_C5}$

The RGA for a general second order multivariable system as previously presented in Chapter 3 can be given by:

$$\Delta = \begin{bmatrix} \lambda_{11} & \lambda_{12} \\ \lambda_{21} & \lambda_{22} \end{bmatrix} \quad (5.5)$$

Where mathematical expression for the gains is given by:

$$\lambda_{ij} = \frac{\left(\frac{\partial y_i}{\partial m_j}\right)_{\text{all loops open}}}{\left(\frac{\partial y_i}{\partial m_j}\right)_{\text{loop } m_j \text{ open, all other loops closed with perfect control}}} \quad (5.6)$$

To calculate  $\lambda_{11}$ , the partial derivatives in the numerator and the denominator of Equation (5.6) are calculated. Firstly, Equation (5.3) is differentiated with respect to the first input  $m_1$  resulting in:

$$\left(\frac{\partial y_1}{\partial m_1}\right)_{\text{other loop open}} = K_{11} \quad (5.7)$$

To calculate the denominator partial derivative of Equation (5.6), Equation (5.4) is set to zero and the value of  $m_2$  is obtained and substituted into Equation (5.3). This because when the second input is closed it will tend to correct for the deviations in  $y_2$  (or cancel the effect) caused by changes in  $m_1$ . Therefore,  $m_2$  attempts to maintain the change in  $y_2 = 0$  as  $m_1$  changes. Setting  $y_2 = 0$  and solving for  $m_2$  results in:

$$m_2 = -\frac{K_{21}}{K_{22}}m_1 \quad (5.8)$$

Substituting Equation (5.8) into Equation (5.3) and taking the partial derivative with respect to  $m_1$  yields:

$$y_1 = K_{11}m_1 - \frac{K_{12}K_{21}}{K_{22}}m_1 \quad (5.9)$$

$$\left(\frac{\partial y_1}{\partial m_1}\right)_{\text{loop } m_1 \text{ open; loop } m_2 \text{ closed with perfect control}} = K_{11}\left(1 - \frac{K_{12}K_{21}}{K_{11}K_{22}}\right) \quad (5.10)$$

Substituting Equations (5.7) and (5.10) into Equation (5.6) results in:

$$\lambda_{11} = \frac{K_{11}}{K_{11}\left(1 - \frac{K_{12}K_{21}}{K_{11}K_{22}}\right)} = \frac{1}{\left(1 - \frac{K_{12}K_{21}}{K_{11}K_{22}}\right)} \quad (5.11)$$

To obtain  $\lambda_{12}$ , a similar procedure is repeated. Equation (5.3) is differentiated with respect to the second input  $m_2$  resulting in:

$$\left(\frac{\partial y_1}{\partial m_2}\right)_{\text{other loop open}} = K_{12} \quad (5.12)$$

To obtain the denominator partial derivative, Equation (5.4) is set to zero and the value of  $m_1$  is obtained and substituted into Equation (5.3). Setting  $y_2 = 0$  and solving for  $m_1$  results in:

$$m_1 = -\frac{K_{22}}{K_{21}}m_2 \quad (5.13)$$

Substituting Equation (5.13) into Equation (5.3) and taking the partial derivative with respect to  $m_2$  yields:

$$\left(\frac{\partial y_1}{\partial m_2}\right)_{\text{loop } m_2 \text{ open; loop } m_1 \text{ closed with perfect control}} = K_{12}\left(1 - \frac{K_{11}K_{22}}{K_{12}K_{21}}\right) \quad (5.14)$$

Substituting Equations (5.14) and (5.12) into Equation (5.6) results in:

$$\lambda_{12} = \frac{K_{12}}{K_{12}\left(1 - \frac{K_{11}K_{22}}{K_{12}K_{21}}\right)} = \frac{1}{\left(1 - \frac{K_{11}K_{22}}{K_{12}K_{21}}\right)} \quad (5.15)$$

To obtain  $\lambda_{21}$ , Equation (5.4) is differentiated with respect to the first input  $m_1$  resulting in:

$$\left(\frac{\partial y_1}{\partial m_1}\right)_{\text{other loop open}} = K_{21} \quad (5.16)$$

To obtain the denominator partial derivative, Equation (5.3) is set to zero and the value of  $m_2$  is obtained and substituted into Equation (5.4). Setting  $y_1 = 0$  and solving for  $m_2$  results in:

$$m_2 = -\frac{K_{11}}{K_{12}}m_1 \quad (5.17)$$

Substituting Equation (5.17) into Equation (5.4) and taking the partial derivative with respect to  $m_1$  yields:

$$\left(\frac{\partial y_2}{\partial m_1}\right)_{\text{loop } m_1 \text{ open; loop } m_2 \text{ closed with perfect control}} = K_{21}\left(1 - \frac{K_{11}K_{22}}{K_{12}K_{21}}\right) \quad (5.18)$$

Substituting Equations (5.18) and (5.16) into Equation (5.6) results in:

$$\lambda_{21} = \frac{K_{21}}{K_{21}\left(1 - \frac{K_{11}K_{22}}{K_{12}K_{21}}\right)} = \frac{1}{\left(1 - \frac{K_{11}K_{22}}{K_{12}K_{21}}\right)} = \lambda_{12} \quad (5.19)$$

To obtain  $\lambda_{22}$ , Equation (5.4) is differentiated with respect to the second input  $m_2$  resulting in:

$$\left(\frac{\partial y_2}{\partial m_2}\right)_{\text{other loop open}} = K_{22} \quad (5.20)$$

To obtain the denominator partial derivative, Equation (5.3) is set to zero and the value of  $m_1$  is obtained and substituted into Equation (5.4). Setting  $y_2 = 0$  and solving for  $m_1$  results in:

$$m_1 = -\frac{K_{12}}{K_{11}}m_2 \quad (5.21)$$

Substituting Equation (5.21) into Equation (5.4) and taking the partial derivative with respect to  $m_2$  yields:

$$\left(\frac{\partial y_2}{\partial m_2}\right)_{\text{loop } m_2 \text{ open; loop } m_1 \text{ closed with perfect control}} = K_{22}\left(1 - \frac{K_{12}K_{21}}{K_{11}K_{22}}\right) \quad (5.22)$$

Substituting Equations (5.22) and (5.20) into Equation (5.6) results in:

$$\lambda_{22} = \frac{K_{22}}{K_{22}\left(1 - \frac{K_{12}K_{21}}{K_{11}K_{22}}\right)} = \frac{1}{\left(1 - \frac{K_{12}K_{21}}{K_{11}K_{22}}\right)} = \lambda_{11} \quad (5.23)$$

Therefore, the final RGA for the second order multivariable debutanizer distillation model can be calculated using the following equation:

$$\Delta = \begin{bmatrix} \lambda_{11} & \lambda_{12} \\ \lambda_{21} & \lambda_{22} \end{bmatrix} = \begin{bmatrix} \frac{1}{(1 - \frac{K_{12}K_{21}}{K_{11}K_{22}})} & \frac{1}{(1 - \frac{K_{11}K_{22}}{K_{12}K_{21}})} \\ \frac{1}{(1 - \frac{K_{11}K_{22}}{K_{12}K_{21}})} & \frac{1}{(1 - \frac{K_{12}K_{21}}{K_{11}K_{22}})} \end{bmatrix} \quad (5.24)$$

The steady state matrix for the second order multivariable debutanizer distillation model given in Equation (5.2) can be substituted in Equation (5.24) to obtain the RGA. Substituting the steady state gains into Equation (5.24) results in:

$$\Delta = \begin{bmatrix} -4.732905625 & 5.732905625 \\ 5.732905625 & -4.732905625 \end{bmatrix} \quad (5.25)$$

Where:

$$\lambda_{11} = -4.732905625$$

$$\lambda_{12} = 5.732905625$$

$$\lambda_{21} = 5.732905625$$

$$\lambda_{22} = -4.732905625$$

According to the properties of the RGA, it is worth noting that when  $\lambda_{ij} < 0$  it is an indication that the response obtained from the  $i^{th}$  controlled output when manipulated via the  $j^{th}$  control input with all other manipulated variables open, will be opposite in direction when the same is done with all other manipulated variables closed, resulting in completely undesired system responses which may cause the system to be unstable. Therefore, pairing the  $i^{th}$  controlled output with the  $j^{th}$  control input in such a case is not recommended (Edgar H Bristol, 1966), (Ogunnaike and Ray, 1994). It can be observed that pairing the overhead pressure (kPa) with the LCN Reid Vapour Pressure (kPa), as is currently the case, is undesirable according to the properties of the RGA (Edgar H Bristol, 1966). Similarly, pairing the reboiler temperature (DegC) with the LPG C<sub>5</sub> concentration (Mol %) is equally undesirable. The observation leads to the requirement for the loop pairings to be modified such that the overhead pressure (kPa) is paired to control the LPG C<sub>5</sub> concentration (Mol %) and the reboiler temperature (DegC) to be paired to control the LCN Reid Vapour Pressure (kPa). The structure of the second order multivariable debutanizer distillation model is, therefore, re-arranged in accordance with the results obtained from the RGA, as shown below:

$$\begin{bmatrix} Y_1(s) \\ Y_2(s) \end{bmatrix} = \text{TF}(s)U(s) = \begin{bmatrix} \frac{-0.004852}{s^3 + 0.3151s^2 + 0.04709s + 0.00415} & \frac{0.001241}{s^3 + 0.8456s^2 + 0.1968s + 0.01438} \\ \frac{0.0009339}{s^2 + 0.3965s + 0.06791} & \frac{-0.0001665}{s^2 + 0.3112s + 0.141} \end{bmatrix} \begin{bmatrix} \text{Reboiler\_Temp} \\ \text{Ovhd\_Press} \end{bmatrix} \quad (5.26)$$



Where:

$TF_{11}(s)$  is now the transfer function relating the LCN\_RVP (output 1) to the Reboiler\_Temp (input 1)

$TF_{12}(s)$  is now the transfer function relating the LCN\_RVP (output 1) to the Ovhd\_Press (input 2)

$TF_{21}(s)$  is now the transfer function relating the LPG\_C5 (output 2) to the Reboiler\_Temp (input 1)

$TF_{22}(s)$  is now the transfer function relating the LPG\_C5 (output 2) to the Ovhd\_Press (input 2)

The modified steady state matrix reflecting the new control loop pairings is given by:

$$\text{Modified Steady State Gain Matrix} = \begin{bmatrix} K_{12} & K_{11} \\ K_{22} & K_{21} \end{bmatrix} = \begin{bmatrix} -1.16768 & 0.085971550 \\ 0.013792 & -0.00123 \end{bmatrix} \quad (5.27)$$

Equations (5.26) and (5.27) reflect the modified control structure of the second order multivariable debutanizer distillation model following the RGA recommended loop pairings. In order to verify the structural stability of the modified system it is necessary to make use of the Niederlinski Index (Niederlinski, 1971),(Ogunnaike and Ray, 1994). In accordance with the Niederlinski Index properties, the system is considered unstable if the Niederlinski Index is negative, that is if:

$$NI = \frac{|G(0)|}{\prod_{i=1}^n g_{ii}(0)} < 0 \quad (5.28)$$

Where  $|G(0)|$  is the determinant of the system's steady state gain matrix and  $\prod_{i=1}^n g_{ii}(0)$  is the product of its diagonal elements (Luyben, 1993). Therefore, the Niederlinski Index is calculated by first finding the determinant of the modified steady state gain matrix and the product of its diagonal elements as follows:

$$|G(0)| = \det \left( \begin{bmatrix} -1.16768 & 0.085971550 \\ 0.013792 & -0.00123 \end{bmatrix} \right) \quad (5.29)$$

$$= (0.001436246 - 0.001185719) = 0.000250526$$

$$\prod_{i=1}^n g_{ii}(0) = 0.001436246 \quad (5.30)$$

$$\therefore NI = \frac{0.000250526}{0.001436246} = 0.174431072 \quad (5.31)$$

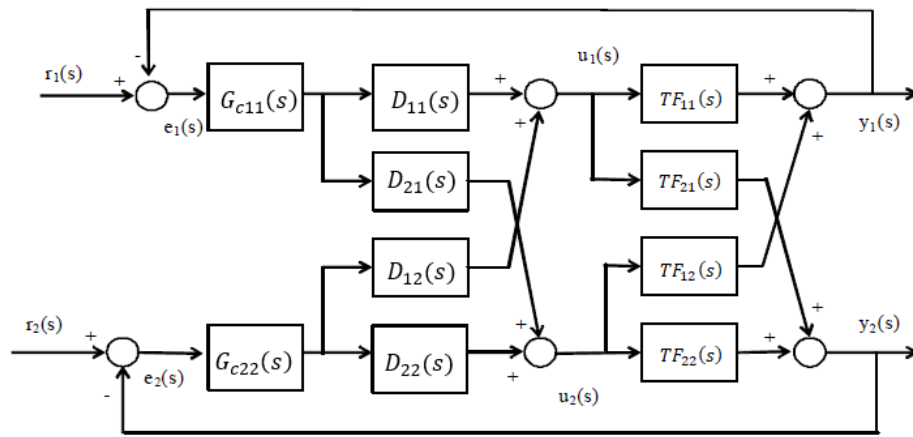
Since the  $NI > 0$  for the chosen pairings, the system can be expected to be stable (Niederlinski, 1971).

The objectives of this section of confirming the input-output pairings of the second order debutanizer distillation process model to determine whether the existing pairings are desirable according to the properties of the RGA (Edgar H Bristol, 1966) have been met. It is found that

there are requirements for the loop pairings to be modified and re-arranged, as such, a modification is made such that the overhead pressure (kPa) is paired to control the LPG C<sub>5</sub> concentration (Mol %) and the reboiler temperature (DegC) is paired to control the LCN Reid Vapour Pressure (kPa) and structural stability is confirmed with the Niederlinski Index. The following section presents the design of decoupling compensators for the newly modified control structure to eliminate the process interactions as described in Chapter 3.

#### 5.4. Decoupling compensators for the second order debutanizer distillation process model

In Chapter 3, decoupling control methods are described and utilized to design decoupling compensators for the second order debutanizer distillation process model to eliminate the process interactions. A block diagram of the decoupled second order multivariable system is shown in Figure 5.1.



**Figure 5.1:** Decoupled second order debutanizer distillation process model (Wade, 1997)

As previously outlined in Chapter 3, since  $D_{11}(s) = D_{22}(s) = 1$ , the decoupling control problem for a general second order multivariable control system is to solve for  $D_{12}(s)$  and  $D_{21}(s)$ .

Recall from Chapter 3 that  $D_{12}(s)$  is given by:

$$D_{12}(s) = -\frac{TF_{12}(s)}{TF_{11}(s)} \quad (5.32)$$

And  $D_{21}(s)$  is given by:

$$D_{21}(s) = -\frac{TF_{21}(s)}{TF_{22}(s)} \quad (5.33)$$

$D_{12}(s)$  and  $D_{21}(s)$  are the decoupling compensators computed using Equations (5.32) and (5.33), respectively, where  $D_{12}(s)$  compensates for the interactions caused by  $TF_{12}(s)$  on  $y_1(s)$

and  $D_{21}(s)$  compensates for the interactions caused by  $TF_{21}(s)$  on  $y_2(s)$ . Substituting the second order debutanizer distillation process model transfer functions  $TF_{11}(s)$ ,  $TF_{12}(s)$ ,  $TF_{21}(s)$ , and  $TF_{22}(s)$  from Equation (5.26) into Equations (5.32) and (5.33) results in:

$$D_{12}(s) = - \frac{\left( \frac{0.001241}{s^3 + 0.8456 s^2 + 0.1968 s + 0.01438} \right)}{\left( \frac{-0.004852}{s^3 + 0.3151 s^2 + 0.04709 s + 0.00415} \right)}$$

$$= \frac{0.001241 s^3 + 0.000391 s^2 + 5.844e-05 s + 5.15e-06}{0.004852 s^3 + 0.004103 s^2 + 0.0009549 s + 6.977e-05} \quad (5.34)$$

$$D_{21}(s) = - \frac{\left( \frac{0.0009339}{s^2 + 0.3965 s + 0.06791} \right)}{\left( \frac{-0.0001665}{s^2 + 0.3112 s + 0.141} \right)}$$

$$= \left( \frac{0.0009339 s^2 + 0.0002906 s + 0.0001317}{0.0001665 s^2 + 6.602e-05 s + 1.131e-05} \right) \quad (5.35)$$

Equation (5.34) and Equation (5.35) are decoupling compensators for the second order debutanizer distillation process model. The decoupling compensators are used in the controller design for the second order system. As previously outlined in Chapter 3, the apparent process as “seen” by the controller becomes a diagonal matrix that can be represented mathematically by the diagonal matrix  $T(s)$ , where:

$$\begin{bmatrix} T_{11}(s) & 0 \\ 0 & T_{22}(s) \end{bmatrix} = \begin{bmatrix} TF_{11}(s) & TF_{12}(s) \\ TF_{21}(s) & TF_{22}(s) \end{bmatrix} \begin{bmatrix} 1 & D_{12}(s) \\ D_{21}(s) & 1 \end{bmatrix} \quad (5.36)$$

Therefore, the decoupled apparent plant is obtained by substituting the dynamic decouplers given by Equations (5.34) and (5.35) into Equation (5.36) resulting in:

$$\begin{bmatrix} T_{11}(s) & 0 \\ 0 & T_{22}(s) \end{bmatrix} = \begin{bmatrix} TF_{11}(s) - \frac{TF_{12}(s)TF_{21}(s)}{TF_{22}(s)} & 0 \\ 0 & TF_{22}(s) - \frac{TF_{21}(s)TF_{12}(s)}{TF_{11}(s)} \end{bmatrix} \quad (5.37)$$

Substituting the second order debutanizer distillation process model transfer functions  $TF_{11}(s)$ ,  $TF_{12}(s)$ ,  $TF_{21}(s)$ , and  $TF_{22}(s)$  from Equation (5.26) into Equation (5.37) yields:

$$T_{11}(s) = \frac{-0.004852}{s^3 + 0.3151 s^2 + 0.04709 s + 0.00415} -$$

$$\dots \frac{\left( \frac{0.001241}{s^3 + 0.8456 s^2 + 0.1968 s + 0.01438} \right) \left( \frac{0.0009339}{s^2 + 0.3965 s + 0.06791} \right)}{\left( \frac{-0.0001665}{s^2 + 0.3112 s + 0.141} \right)}$$

$$= \frac{0.0021088 (s-1.24)(s+0.1788)(s+0.021)(s^2 + 0.2496s + 0.06773)}{(s+0.5207)(s+0.1816)(s^2 + 0.3249s + 0.02762)(s^2 + 0.1335s + 0.02285)(s^2 + 0.3965s + 0.06791)} \quad (5.38)$$

$$\begin{aligned}
T_{22}(s) &= \left( \frac{-0.0001665}{s^2 + 0.3112s + 0.141} \right) - \frac{\left( \frac{0.0009339}{s^2 + 0.3965s + 0.06791} \right) \left( \frac{0.001241}{s^3 + 0.8456s^2 + 0.1968s + 0.01438} \right)}{\frac{-0.004852}{s^3 + 0.3151s^2 + 0.04709s + 0.00415}} \\
&= \frac{7.2364e-05 (s-1.24)(s+0.1788)(s+0.021)(s^2 + 0.2496s + 0.06773)}{(s+0.5207)(s^2 + 0.3249s + 0.02762)(s^2 + 0.3965s + 0.06791)(s^2 + 0.3112s + 0.141)} \quad (5.39)
\end{aligned}$$

Therefore,  $T_{11}(s)$  represents the decoupled apparent plant of the LCN Reid Vapour Pressure (kPa) loop model and  $T_{22}(s)$  represents the decoupled apparent plant of the LPG C<sub>5</sub> concentration (Mol %) loop model. The two apparent plant loop models are used in the remainder of this chapter to design decentralized PID controllers. The apparent plant loop models, as can be observed in Equations (5.38) and (5.39), are both of a higher order which can lead to a nontrivial controller design exercise. Therefore, it is necessary to make use of controller design techniques that implements a form of model order reduction without affecting plant dynamics and controller performance. The next section firstly presents a model order reduction method to enable the determination of PID controller settings and then is followed by the controller design with the IMC method.

## 5.5. PID controller design for the second order model with IMC

### 5.5.1. Model reduction for the second order debutanizer model

To obtain a controller structure that is in the form of PID with the Internal Model Control (IMC) method, it is necessary to reduce the given apparent plant loop models to second order by means of model reduction as proposed by (Isaksson and Graebe, 1993). The model order reduction techniques used in this research are described in Chapter 3 and hereby utilized to reduce the apparent plant loop models given in Equations (5.38) and (5.39). The model reduction is only for the purposes of determining the PID controller settings. It is worth noting that the designed controller still controls the complete apparent plant loop models given in Equations (5.38) and (5.39). The method of Isaksson and Graebe (1993) involves approximating a model by retaining the average dominant poles and zeros as well as the lower order coefficients of the apparent plant loop models. Recall from Chapter 3 that the reduced model can be written as:

$$\hat{T}(s) = \frac{\hat{B}(s)}{\hat{A}(s)} \quad (5.40)$$

Where:

$$\hat{B}(s) = \frac{1}{2} [\hat{B}_1(s) + \hat{B}_2(s)] \quad (5.41)$$

$$\hat{A}(s) = \frac{1}{2}[\hat{A}_1(s) + \hat{A}_2(s)] \quad (5.42)$$

The objective is to determine  $\hat{B}_1(s)$  and  $\hat{A}_1(s)$  which are the polynomials obtained by retaining the dominant zeros and poles, respectively, of the apparent plant loop models whereas  $\hat{B}_2(s)$  and  $\hat{A}_2(s)$  are the polynomials obtained by retaining the lower order coefficients of the numerator and denominator, respectively, of the apparent plant loop models. The number of lower order coefficients is selected to form a second order model since PID controllers are implicitly based on second order models (Graebe and Goodwin, 1992). Furthermore, as asserted in (Isaksson and Graebe, 1993), a second order model results in a PID controller whereas a first order model results in a PI controller.

Recalling the decoupled apparent plant of the LCN Reid Vapour Pressure (kPa) loop model from Equation (5.38):

$$T_{11}(s) = \frac{0.0021088 (s-1.24)(s+0.1788)(s+0.021)(s^2 + 0.2496s + 0.06773)}{(s+0.5207)(s+0.1816)(s^2 + 0.3249s + 0.02762)(s^2 + 0.1335s + 0.02285)(s^2 + 0.3965s + 0.06791)}$$

To obtain  $\hat{B}_1(s)$ , the dominant zero from  $T_{11}(s)$  is the right half plane zero at  $s = 1.24$ . Therefore:

$$\hat{B}_1(s) = s - 1.24 \quad (5.43)$$

To obtain  $\hat{B}_2(s)$ ,  $T_{11}(s)$  is expanded or multiplied out and re-written as:

$$T_{11}(s) = \frac{3.511e-07 s^5 - 2.776e-07 s^4 - 1.531e-07 s^3 - 4.776e-08 s^2 - 6.211e-09 s - 1.107e-10}{0.0001665 s^8 + 0.0002593 s^7 + 0.0001729 s^6 + 6.686e-05 s^5 + 1.66e-05 s^4 + 2.752e-06 s^3 + 3.043e-07 s^2 + 2.083e-08 s + 6.748e-10} \quad (5.44)$$

The polynomial obtained by retaining lower order coefficients in the numerator of  $T_{11}(s)$  is given by:

$$\hat{B}_2(s) = -6.211e - 09 s - 1.107e - 10 \quad (5.45)$$

In order to obtain  $\hat{A}_1(s)$ , the dominant pole from  $T_{11}(s)$  is the complex conjugate set of poles closest to the imaginary axis located at  $s = -0.0667 \pm 0.136i$ . Therefore:

$$\hat{A}_1(s) = s^2 + 0.1335s + 0.02285 \quad (5.46)$$

The polynomial obtained by retaining lower order coefficients in the denominator of  $T_{11}(s)$  is given by:

$$\hat{A}_2(s) = 3.043e - 07 s^2 + 2.083e - 08 s + 6.748e - 10 \quad (5.47)$$

Substituting Equations (5.43) and (5.45) into (5.41) results in:

$$\begin{aligned}
 \hat{B}(s) &= \frac{1}{2}[(s - 1.24) + (-6.211e - 09 s - 1.107e - 10)] \\
 &= \frac{1}{2}(s - 1.24) \\
 &= (0.5s - 0.62) \\
 &= -0.806s + 1
 \end{aligned} \tag{5.48}$$

Substituting Equations (5.46) and (5.47) into (5.42) results in:

$$\begin{aligned}
 \hat{A}(s) &= \frac{1}{2}[(s^2 + 0.1335s + 0.02285) + (3.043e - 07 s^2 + 2.083e - 08 s + \\
 &6.748e - 10)] \\
 &= \frac{1}{2}(s^2 + 0.1342s + 0.0232) \\
 &= (0.5s^2 + 0.0671s + 0.0116) \\
 &= 43.103s^2 + 5.784s + 1
 \end{aligned} \tag{5.49}$$

Substituting Equations (5.48) and (5.49) into (5.40) results in the reduced and decoupled apparent plant of the LCN Reid Vapour Pressure (kPa) loop model given by:

$$\hat{T}_{11}(s) = \frac{-0.806s + 1}{43.103s^2 + 5.784s + 1} \tag{5.50}$$

The above procedure is repeated for the LPG C<sub>5</sub> concentration (Mol %) loop to obtain  $\hat{T}_{22}(s)$ .

Recalling the decoupled apparent plant of the LPG C<sub>5</sub> concentration (Mol %) loop model from Equation (5.39):

$$T_{22}(s) = \frac{7.2364e-05 (s-1.24)(s+0.1788)(s+0.021)(s^2 + 0.2496s + 0.06773)}{(s+0.5207)(s^2 + 0.3249s + 0.02762)(s^2 + 0.3965s + 0.06791)(s^2 + 0.3112s + 0.141)} \tag{5.51}$$

To obtain  $\hat{B}_1(s)$ , the dominant zero from  $T_{22}(s)$  is the right half plane zero at  $s = 1.24$ . Therefore:

$$\hat{B}_1(s) = s - 1.24 \tag{5.52}$$

To obtain  $\hat{B}_2(s)$ ,  $T_{22}(s)$  is expanded or multiplied out and re-written as:

$$T_{22}(s) = \frac{3.511e-07 s^5 - 2.776e-07 s^4 - 1.531e-07 s^3 - 4.776e-08 s^2 - 6.211e-09 s - 1.107e-10}{0.004852 s^7 + 0.007537 s^6 + 0.005471 s^5 + 0.002483 s^4 + 0.0007292 s^3 + 0.000136 s^2 + 1.452e-05 s + 6.681e-07} \quad (5.53)$$

The polynomial obtained by retaining lower order coefficients in the numerator of  $T_{22}(s)$  is given by:

$$\hat{B}_2(s) = -6.211e-09 s - 1.107e-10 \quad (5.54)$$

In order to obtain  $\hat{A}_1(s)$ , the dominant pole from  $T_{22}(s)$  is the complex conjugate poles closest to the imaginary axis located at  $s - 0.156 \pm 0.342i$ . Therefore:

$$\hat{A}_1(s) = s^2 + 0.3112s + 0.141 \quad (5.55)$$

The polynomial obtained by retaining lower order coefficients in the denominator of  $T_{22}(s)$  is given by:

$$\hat{A}_2(s) = 0.000136 s^2 + 1.452e-05 s + 6.681e-07 \quad (5.56)$$

Substituting Equations (5.52) and (5.54) into (5.41) results in:

$$\begin{aligned} \hat{B}(s) &= \frac{1}{2}((s - 1.24) + (-6.211e-09 s - 1.107e-10)) \\ &= \frac{1}{2}(s - 1.24) \\ &= (0.5s - 0.62) \\ &= -0.806s + 1 \end{aligned} \quad (5.57)$$

Substituting Equations (5.55) and (5.56) into (5.42) results in:

$$\begin{aligned} \hat{A}(s) &= \frac{1}{2}((s^2 + 0.3112s + 0.141) + (0.000136 s^2 + 1.452e-05 s + 6.681e-07)) \\ &= \frac{1}{2}(s^2 + 0.321s + 0.1471) \\ &= (0.5s^2 + 0.1605s + 0.07355) \\ &= 6.798s^2 + 2.182s + 1 \end{aligned} \quad (5.58)$$

Substituting Equations (5.48) and (5.49) into (5.40) results in the reduced and decoupled apparent plant of the LPG C<sub>5</sub> concentration (Mol %) loop model given by:

$$\hat{T}_{22}(s) = \frac{-0.806s + 1}{6.798s^2 + 2.182s + 1} \quad (5.59)$$

Therefore, the reduced and decoupled second order apparent plant model of the debutanizer distillation process can be approximated as:

$$\begin{bmatrix} T_{11}(s) & 0 \\ 0 & T_{22}(s) \end{bmatrix} \cong \begin{bmatrix} \hat{T}_{11}(s) & 0 \\ 0 & \hat{T}_{22}(s) \end{bmatrix} \cong \begin{bmatrix} \frac{-0.806s+1}{43.103s^2+5.784s+1} & 0 \\ 0 & \frac{-0.806s+1}{6.798s^2+2.182s+1} \end{bmatrix} \quad (5.60)$$

The IMC controller design method can be applied on the reduced models given in Equation (5.60) to obtain PID controller settings for both of the apparent plant loop models given in Equations (5.38) and (5.39), as demonstrated in the next sub-section.

### 5.5.2. IMC controller design for the second order debutanizer model

As previously described in Chapter 3, the Internal Model Control (IMC) is a model-based control strategy that is used in this section for PID controller tuning as proposed by (Garcia and Morari, 1982). Recall from Chapter 3 that the IMC controller obtained from the IMC design procedure leads to the standard ideal PID feedback controller that can be represented as:

$$G_c(s) = \frac{Q(s)}{1 - Q(s)\tilde{T}(s)_-} := K_p \left( 1 + \tau_I \frac{1}{s} + \tau_D s \right) \quad (5.61)$$

It is the objective of this section to calculate the controller gains; the proportional gain  $K_p$ , the integral gain  $\tau_I$ , and the derivative gain  $\tau_D$ .

For the LCN Reid Vapour Pressure (kPa) loop model, the IMC method is applied as follows:

$$\hat{T}_{11}(s) = \hat{T}_{11}(s)_+ \hat{T}_{11}(s)_- \quad (5.62)$$

Where  $\hat{T}_{11}(s)_+$  contains all nonminimum phase components of the model given by:

$$\hat{T}_{11}(s)_+ = -0.806s + 1 \quad (5.63)$$

and  $\hat{T}_{11}(s)_-$  is the minimum phase part of the model given by:

$$\hat{T}_{11}(s)_- = \frac{1}{43.103s^2 + 5.784s + 1} \quad (5.64)$$

In calculating the PID gains for the LCN Reid Vapour Pressure (kPa) loop model using the IMC method yields:

$$Q(s) = f(s)\hat{T}_{11}(s)_-^{-1} \quad (5.65)$$



$$\hat{T}_{11}(s)^{-1} = \frac{1}{\hat{T}_{11}(s)} = \frac{43.103s^2 + 5.784s + 1}{1} \quad (5.66)$$

$$f(s) = \frac{1}{(-50s+1)} \quad (5.67)$$

Recall from Chapter 3 that  $f(s) = \frac{1}{(\lambda s+1)^z}$  where the tuning parameters have been selected to be  $\lambda = -50$  and  $z = 1$ . The tuning filter factor ( $\lambda$ ) is selected in iterative trial and error to achieve the desired closed loop response. Substituting Equations (5.66) and (5.67) into (5.65) yields:

$$Q(s) = \left( \frac{1}{-50s+1} \right) \left( \frac{43.103s^2 + 5.784s + 1}{1} \right) = \frac{43.103s^2 + 5.784s + 1}{-50s+1} \quad (5.68)$$

Substituting Equation (5.68) into Equation (5.61) results in:

$$\begin{aligned} G_{c11}(s) &= \frac{Q(s)}{1 - \hat{T}_{11}(s)Q(s)} = \frac{\left( \frac{43.103s^2 + 5.784s + 1}{-50s+1} \right)}{1 - \left( \frac{1}{43.103s^2 + 5.784s + 1} \right) \left( \frac{43.103s^2 + 5.784s + 1}{-50s+1} \right)} \\ &= \frac{\left( \frac{43.103s^2 + 5.784s + 1}{-50s + 1} \right)}{1 - \left( \frac{1}{-50s + 1} \right)} \\ &= \frac{43.103s^2 + 5.784s + 1}{-50s + 1 - 1} \\ &= \frac{43.103s^2 + 5.784s + 1}{-50s} \\ &= \frac{43.103s^2}{(-50s)} + \frac{5.784s}{(-50s)} + \frac{1}{(-50s)} \\ &= -0.86206s - 0.11568 - \frac{0.02}{s} \\ \therefore G_{c11}(s) &= -0.11568 \left( 1 + \frac{0.17298}{s} + 7.452s \right) \end{aligned} \quad (5.69)$$

It is worth noting that Equation (5.69) is in the structure of an ideal PID controller:

$$G_c = K_p \left( 1 + \tau_I \frac{1}{s} + \tau_D s \right) \quad (5.70)$$

With the PID controller gains  $K_p = -0.11568$ ,  $\tau_I = 0.17298$  and  $\tau_D = 7.452$  for the LCN Reid Vapour Pressure (kPa) loop controller.

The procedure is repeated to obtain the PID gains for the LPG C<sub>5</sub> concentration (Mol %) loop model. The approximated model is factored out into two parts prior to applying the IMC method as follows:

$$\hat{T}_{22}(s) = \hat{T}_{22}(s)_+ \hat{T}_{22}(s)_- \quad (5.71)$$

Where  $\hat{T}_{22}(s)_+$  contains all nonminimum phase dynamics of the model:

$$\hat{T}_{22}(s)_+ = -0.806s + 1 \quad (5.72)$$

and  $\hat{T}_{22}(s)_-$  is the minimum phase part of the model that is invertible that results in a stable controller:

$$\hat{T}_{22}(s)_- = \frac{1}{6.798s^2 + 2.182s + 1} \quad (5.73)$$

In calculating the PID gains for the LPG C<sub>5</sub> concentration (Mol %) loop model using the IMC method yields:

$$Q(s) = f(s) \hat{T}_{22}(s)_-^{-1} \quad (5.74)$$

$$\hat{T}_{22}(s)_-^{-1} = \frac{1}{\hat{T}_{22}(s)_-} = \frac{6.798s^2 + 2.182s + 1}{1} \quad (5.75)$$

$$f(s) = \frac{1}{(-0.015s + 1)} \quad (5.76)$$

Where the tuning parameters have been selected to be  $\lambda = -0.015$  and  $z = 1$ . The tuning filter factor ( $\lambda$ ) is selected in iterative trial and error to achieve the desired closed loop response. Substituting Equations (5.75) and (5.76) into (5.74) yields:

$$Q(s) = \left( \frac{1}{-0.015s + 1} \right) \left( \frac{6.798s^2 + 2.182s + 1}{1} \right) = \frac{6.798s^2 + 2.182s + 1}{-0.015s + 1} \quad (5.77)$$

Substituting Equation (5.77) into Equation (5.61) results in:

$$\begin{aligned} G_{c22}(s) &= \frac{Q(s)}{1 - \hat{T}_{22}(s)Q(s)} = \frac{\left( \frac{6.798s^2 + 2.182s + 1}{-0.015s + 1} \right)}{1 - \left( \frac{1}{6.798s^2 + 2.182s + 1} \right) \left( \frac{6.798s^2 + 2.182s + 1}{-0.015s + 1} \right)} \\ &= \frac{\left( \frac{6.798s^2 + 2.182s + 1}{-0.015s + 1} \right)}{1 - \left( \frac{1}{-0.015s + 1} \right)} \end{aligned}$$

$$\begin{aligned}
&= \frac{(6.798s^2 + 2.182s + 1)}{-0.015s + 1 - 1} \\
&= \frac{(6.798s^2 + 2.182s + 1)}{(-0.015s)} \\
&= \frac{6.798s^2}{(-0.015s)} + \frac{2.182s}{(-0.015s)} + \frac{1}{(-0.015s)} \\
&= -453.2s - 145.467 - \frac{66.67}{s} \\
\therefore G_{c22}(s) &= -145.466667\left(1 + \frac{0.4583}{s} + 3.1155s\right) \tag{5.78}
\end{aligned}$$

It is again worth noting that Equation (5.78) is in the structure of an ideal PID controller:

$$G_c = K_p\left(1 + \tau_I \frac{1}{s} + \tau_D s\right) \tag{5.79}$$

With the PID controller gains  $K_p = -145.466667$ ,  $\tau_I = 0.4583$  and  $\tau_D = 3.1155$  for the LPG C<sub>5</sub> concentration (Mol %) loop controller. In summary, the IMC PID controller tuning parameters and gains for the LCN Reid Vapour Pressure (kPa) and the LPG C<sub>5</sub> concentration (Mol %) loops are shown in Table 5.2.

**Table 5.2: IMC PID controller tuning parameters**

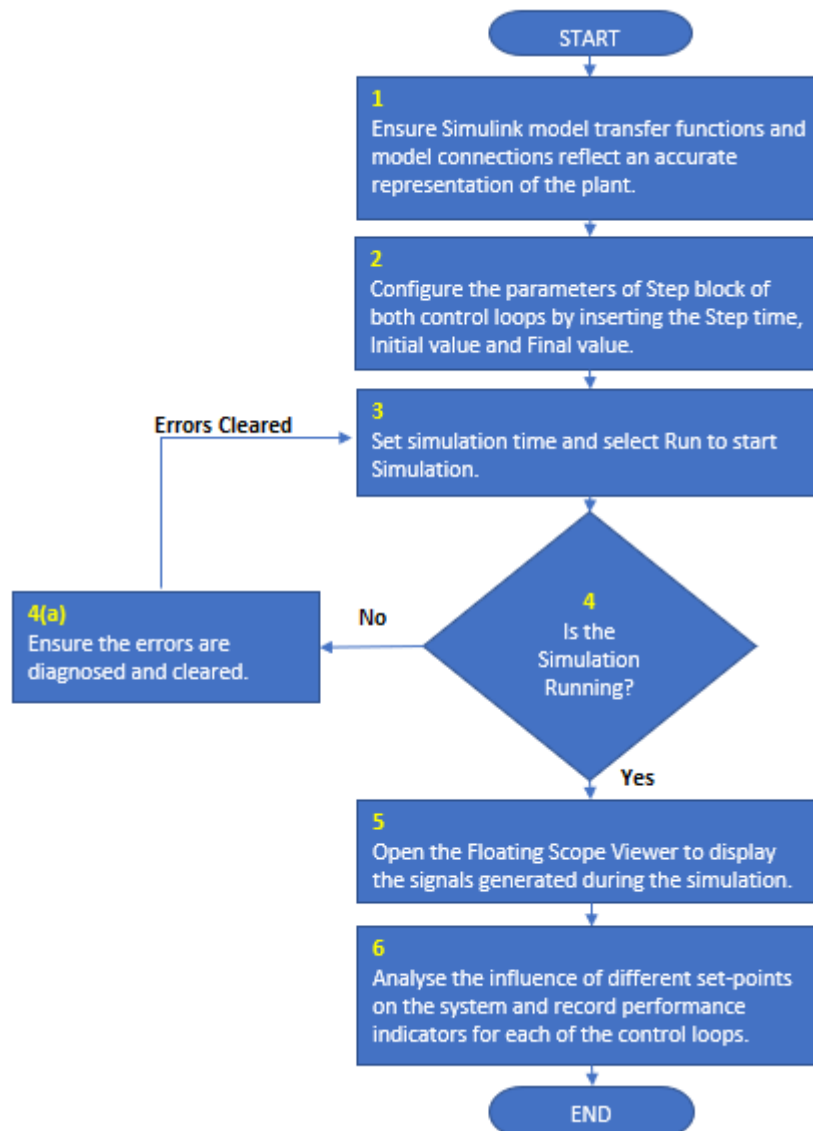
Parameter	LCN Reid Vapour Pressure (kPa)	LPG C <sub>5</sub> concentration (Mol %)
Proportional Gain	-0.11568	-145.466667
Integral Gain	0.17298	0.4583
Derivative Gain	7.452	3.1155
$\lambda$ = filter tuning factor	-50	-0.015
$z$ = filter tuning factor	1	1

The tuning parameters given in Table 5.2 are used in the MATLAB/Simulink environment for the PID controller settings and simulated in closed loop with the second order debutanizer distillation process models. The next section presents the simulation case studies carried out in the MATLAB/Simulink environment to study the effectiveness of the algorithms developed in this chapter.

## 5.6. Simulation case study

The developed PID controllers in the previous section for each of the models are simulated in closed loop with the second order debutanizer distillation process model in the MATLAB/Simulink environment to test the developed algorithms for closed loop performance. The performance indicators of interest observed for both control loops are the percentage overshoot (%), the settling time (seconds) and the absolute steady state error. The control loops are simulated first without disturbances and then followed by simulations with

disturbances included. The simulation study presented in this section follows a pre-defined simulation plan as outlined by the flow chart shown in Figure 5.2. The flow chart consists of six steps. The first step is to ensure that the configured Simulink model transfer functions and model connections reflect an accurate representation of the plant and that all typing errors have been identified and removed. The second step is to configure the parameters of Step input block for the control loops by inserting the Step time, Initial value, and Final value parameters. The third step is to appropriately set the simulation time and select Run to start the Simulation. The fourth step is to ensure that the simulation is running without errors and, if errors are present, to ensure the errors are diagnosed and cleared. The fifth step is to open the floating scope viewer to display the signals generated during the simulation. Lastly, the sixth step is to analyse the influence of different set-points on the system and record performance indicators for each of the control loops.



**Figure 5.2:** Process flowchart for the PID controller simulation study

The flow chart establishes a consistent approach in simulating and observing the performance of the system. The setpoint step changes are entered in the Simulink Step blocks.

The Simulink model of the second order debutanizer distillation process is shown in Figure 5.3 and the MATLAB script file is given in **Appendix B**. The Simulink model is a direct representation of a closed-loop, decoupled, second order multivariable system shown in Figure 5.1. A straight line is used to represent  $D_{11}(s)$  and  $D_{22}(s)$  since  $D_{11}(s) = D_{22}(s) = 1$ . The values of  $D_{12}(s)$  and  $D_{21}(s)$  are given by Equations (5.34) and (5.35), respectively. Lastly, the model transfer functions  $TF_{11}(s)$ ,  $TF_{12}(s)$ ,  $TF_{21}(s)$  and  $TF_{22}(s)$  are that of the re-arranged second order multivariable debutanizer distillation model as given by Equation (5.26). The controllers  $Gc_{11}(s)$  and  $Gc_{22}(s)$  are represented by PID controllers configured in Simulink with the parameters given in Table 5.2.

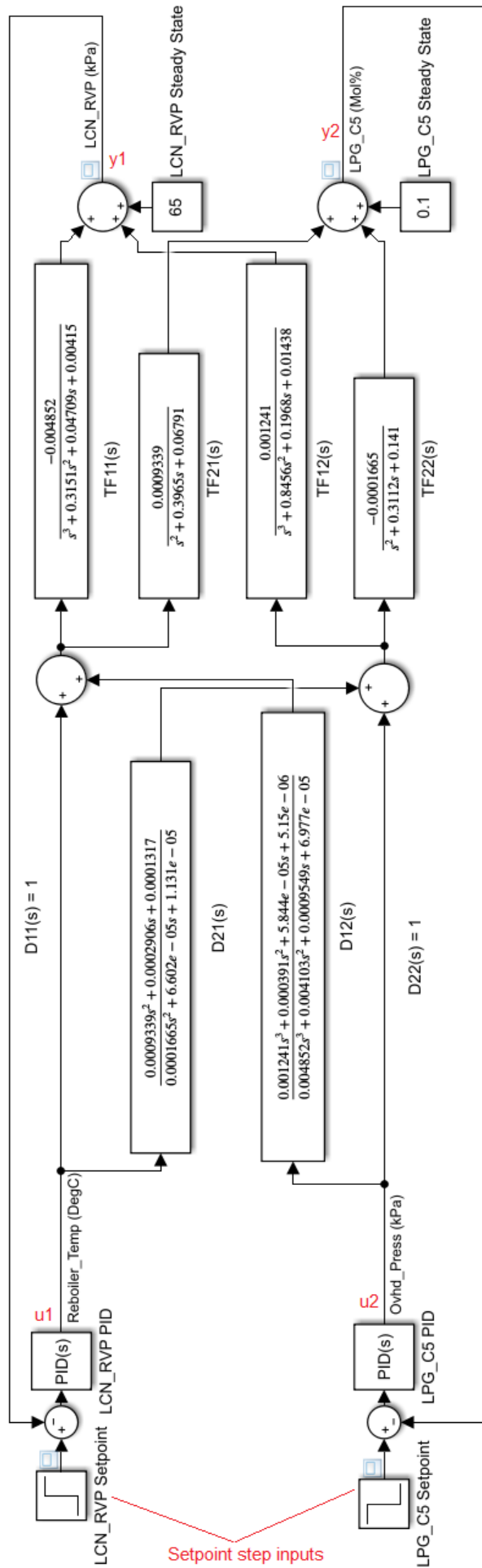


Figure 5.3: Second order debutanizer distillation process model in Simulink

The following sub-section presents the transient behaviour simulation case studies.

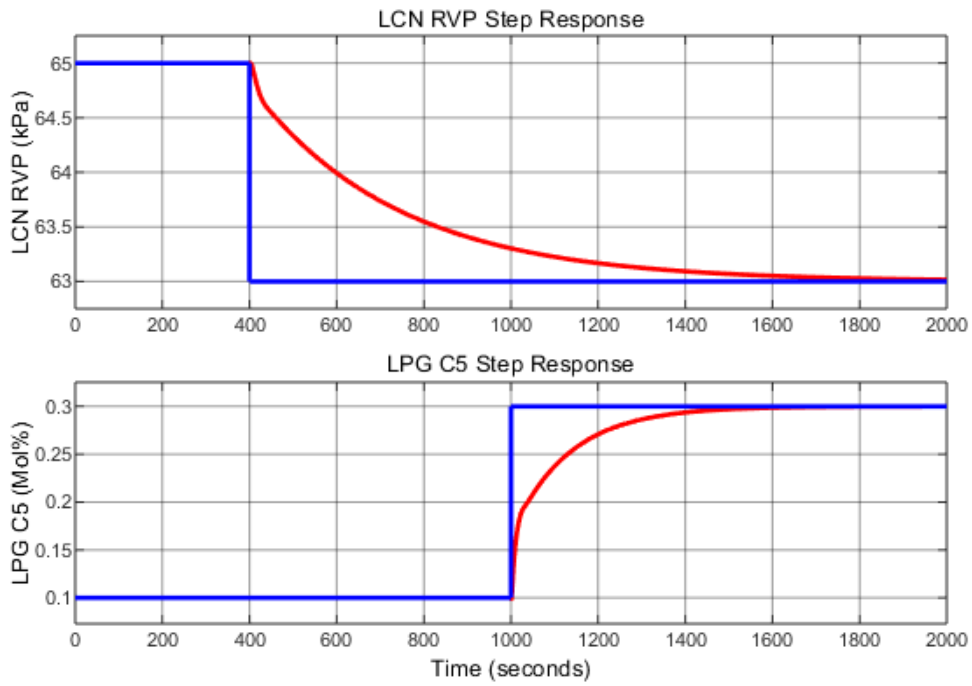
### 5.6.1. Transient behaviour of the second order debutanizer distillation process

The control loops are simulated to observe the two PID controller responses to changes in the controlled output setpoints. The blocks used to input the setpoints are annotated in Figure 5.3 as *Setpoint step inputs* and the outputs observed are annotated as y1 and y2. The PID controller outputs are annotated as u1 and u2. The LCN Reid Vapour Pressure (kPa) loop is varied near its steady state range of 60 kPa to 73 kPa and, similarly, the LPG C5 concentration (Mol %) loop setpoint is varied near its steady state range of 0.01 Mol % to 0.6 Mol %. The setpoint cases for the step response tests to investigate the transient behaviour are presented in the Table 5.3.

**Table 5.3: Simulation case study to investigate the system transient behaviour**

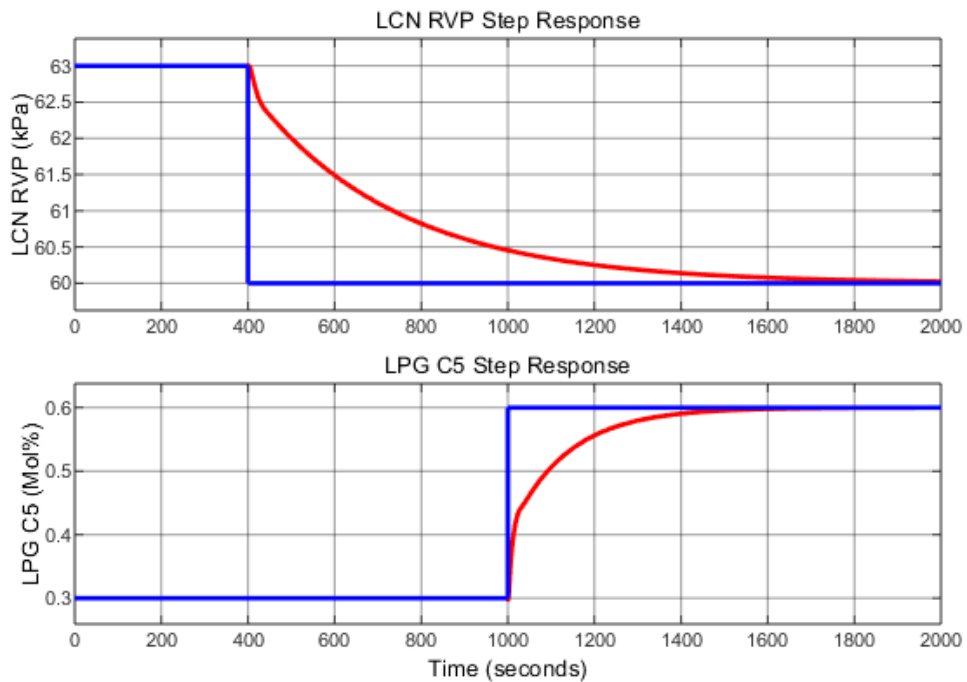
Case #	Loop Name	Initial Setpoint	Final Setpoint	Step Size
5.3.1	LCN_RVP	65 kPa	63 kPa	-2 kPa
	LPG_C5	0.1 Mol%	0.3 Mol%	+0.2 Mol%
5.3.2	LCN_RVP	63 kPa	60 kPa	-3 kPa
	LPG_C5	0.3 Mol%	0.6 Mol%	+0.3 Mol%
5.3.3	LCN_RVP	60 kPa	68 kPa	+8 kPa
	LPG_C5	0.6 Mol%	0.05 Mol%	-0.55 Mol%
5.3.4	LCN_RVP	68 kPa	73 kPa	+5 kPa
	LPG_C5	0.05 Mol%	0.01 Mol%	-0.04 Mol%
5.3.5	LCN_RVP	73 kPa	65.5 kPa	-7.5 kPa
	LPG_C5	0.01 Mol%	0.15 Mol%	+0.14 Mol%

The simulation results showing the closed loop transient behaviour for the two decentralized control loops subjected to the step changes described in Table 5.3 are presented in the Figures 5.4 – 5.8 below. Figure 5.4 shows the LCN RVP dynamic response to a -2 kPa setpoint step change from 65 kPa to 63 kPa and LPG C5 concentration dynamic response to a +0.2 Mol% setpoint step change from 0.1 Mol% to 0.3 Mol% steady state.



**Figure 5.4: Case #5.3.1 dynamic response**

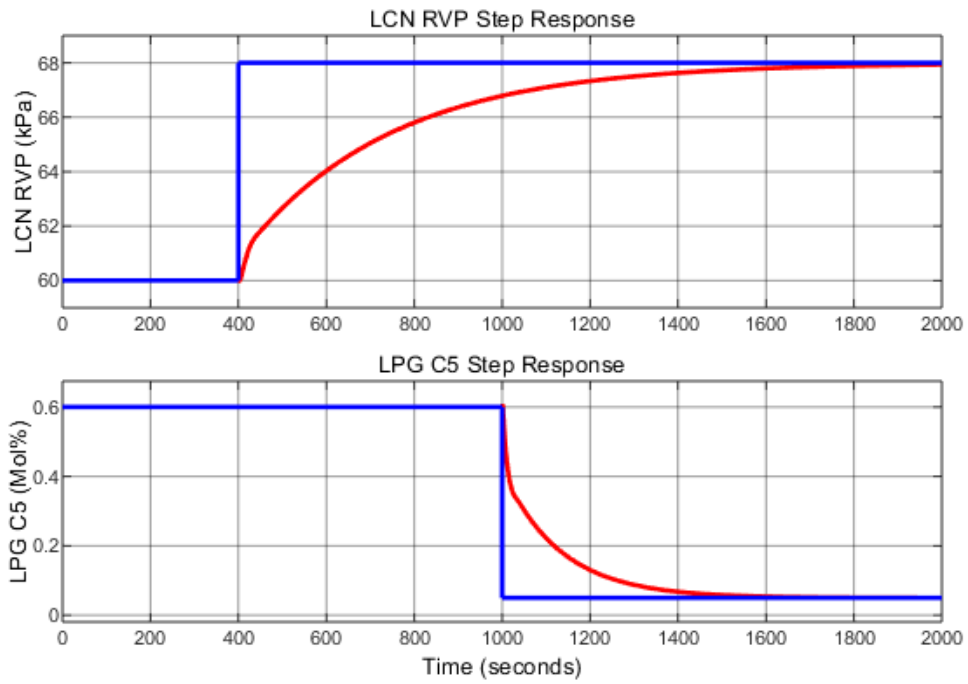
Figure 5.5 shows the LCN RVP dynamic response to a -3 kPa setpoint step change from 63 kPa to 60 kPa steady state and LPG C5 concentration dynamic response to a +0.3 Mol% setpoint step change from 0.3 Mol% to 0.6 Mol % steady state.



**Figure 5.5: Case #5.3.2 dynamic response**

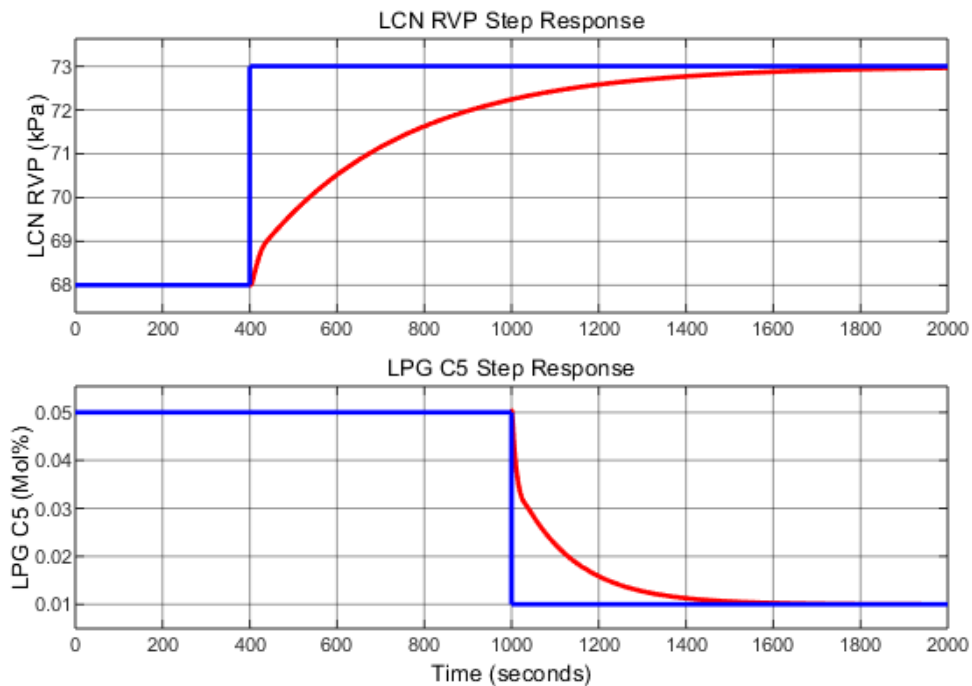
Figure 5.6 shows the LCN RVP dynamic response to a +8 kPa setpoint step change from 60 kPa to 68 kPa steady state and LPG C5 concentration dynamic response to a -0.55 Mol% setpoint step change from 0.6 Mol % to 0.05 Mol % steady state.





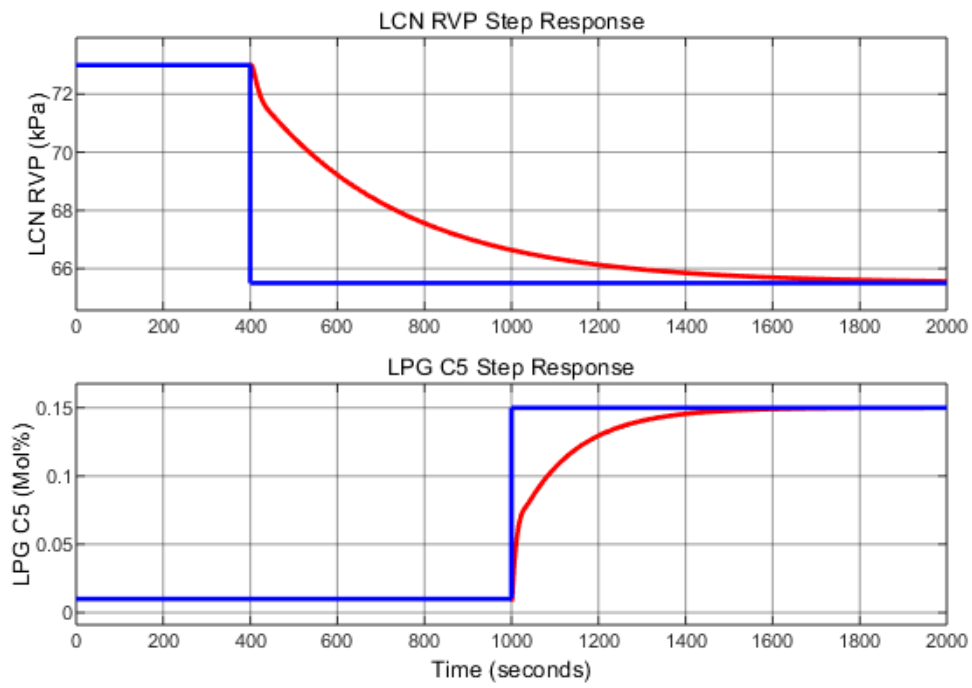
**Figure 5.6: Case #5.3.3 dynamic response**

Figure 5.7 shows the LCN RVP dynamic response to a +5 kPa setpoint step change from 68 kPa to 73 kPa steady state and LPG C5 concentration dynamic response to a -0.04 Mol% setpoint step change from 0.05 Mol % to 0.01 Mol % steady state.



**Figure 5.7: Case #5.3.4 dynamic response**

Figure 5.8 shows the LCN RVP dynamic response to a -7.5 kPa setpoint step change from 73 kPa to 65.5 kPa steady state and LPG C5 concentration dynamic response to a +0.14 Mol% setpoint step change from 0.01 Mol % to 0.15 Mol % steady state.



**Figure 5.8: Case #5.3.5 dynamic response**

The results of the above simulation case study without disturbances are discussed later in Section 5.6.2.

The Simulink model of the second order debutanizer distillation process with the unmeasured output disturbances added at the outputs is shown in Figure 5.9.

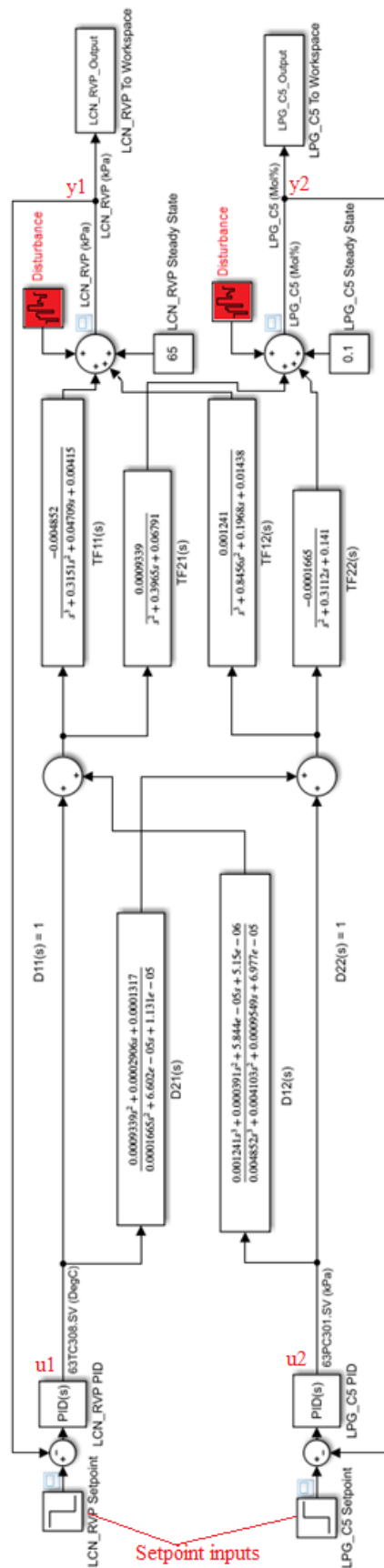


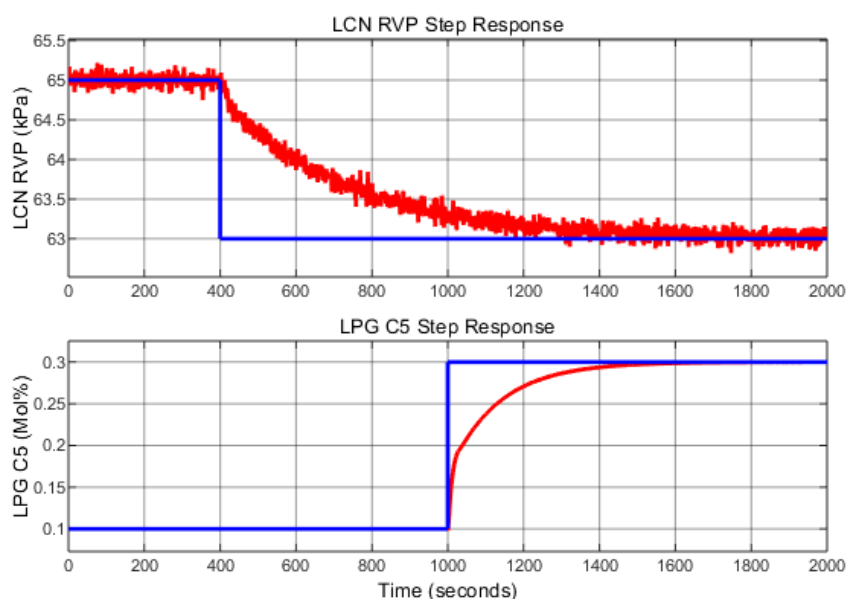
Figure 5.9: Simulink model of the decoupled second order multivariable system

The control loops are further simulated with unmeasured disturbances of random white noise added at both of the system outputs to observe the influence of disturbances on the performance of the PID controllers. The blocks used to input the setpoints are annotated in Figure 5.9 as *Setpoint inputs* and the outputs observed are annotated as y1 and y2. The PID controller outputs are annotated as u1 and u2. The setpoint cases for the step response tests to investigate the influence of unmeasured disturbances on the system transient behaviour are presented in the Table 5.4.

**Table 5.4: Simulation case study to investigate the influence of unmeasured disturbances**

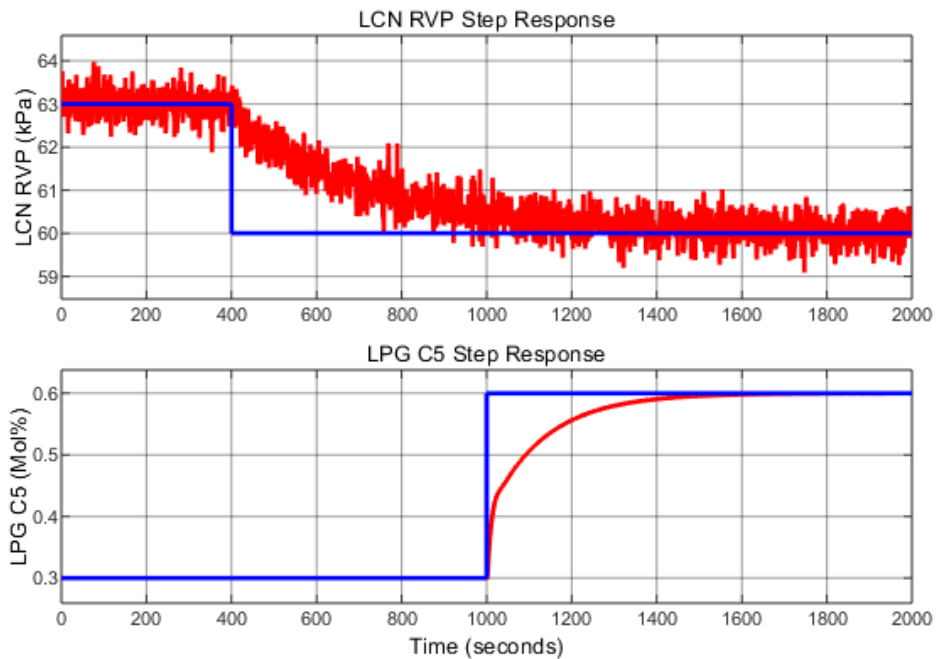
Case #	Loop Name	Initial Setpoint	Final Setpoint	White Noise Amplitude
5.4.1	LCN_RVP	65 kPa	63 kPa	0.005 kPa
	LPG_C5	0.1 Mol%	0.3 Mol%	0 Mol%
5.4.2	LCN_RVP	63 kPa	60 kPa	0.1 kPa
	LPG_C5	0.3 Mol%	0.6 Mol%	0 Mol%
5.4.3	LCN_RVP	60 kPa	68 kPa	0 kPa
	LPG_C5	0.6 Mol%	0.05 Mol%	1E-06 Mol%
5.4.4	LCN_RVP	68 kPa	73 kPa	0 kPa
	LPG_C5	0.05 Mol%	0.01 Mol%	5E-06 Mol %
5.4.5	LCN_RVP	73 kPa	65.5 kPa	0.1 kPa
	LPG_C5	0.01 Mol%	0.15 Mol%	5E-06 Mol %

The simulation results showing the closed loop transient behaviour of the second order debutanizer distillation process under the influence of unmeasured disturbances for the two decentralized control loops subjected to the step changes described in Table 5.4 are presented in the Figures 5.10 – 5.14 below. Figure 5.10 shows the LCN RVP dynamic response to a -2 kPa setpoint step change from 65 kPa to 63 kPa and LPG C5 concentration dynamic response to a +0.2 Mol% setpoint step change from 0.1 Mol% to 0.3 Mol% steady state under influence of 0.005 kPa LCN RVP output disturbance and 0 Mol% LPG C5 output disturbance.



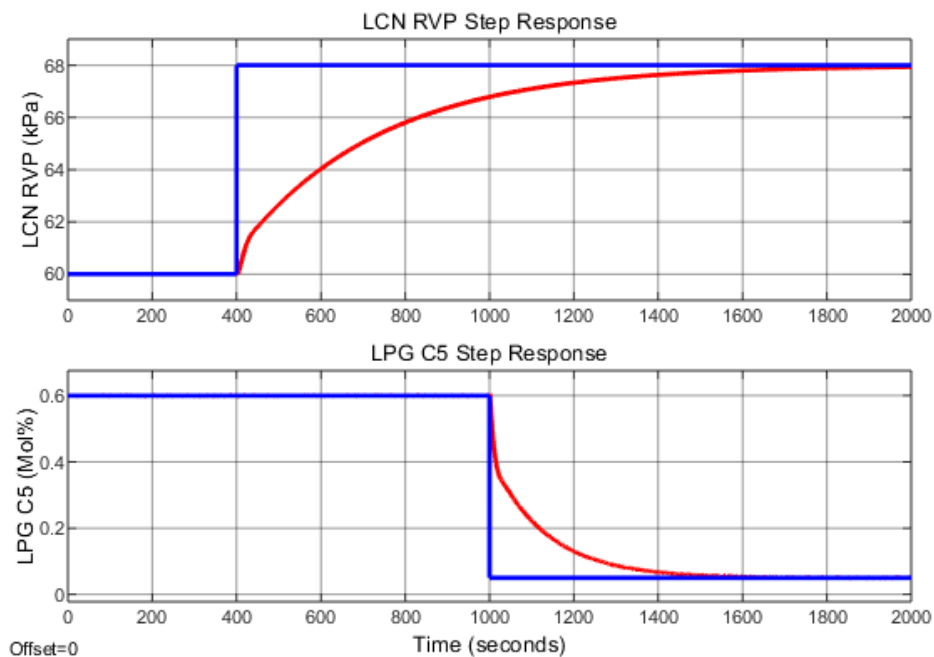
**Figure 5.10: Case #5.4.1 dynamic response**

Figure 5.11 shows the LCN RVP dynamic response to a -3 kPa setpoint step change from 63 kPa to 60 kPa steady state and LPG C5 concentration dynamic response to a +0.3 Mol% setpoint step change from 0.3 Mol% to 0.6 Mol % steady state under influence of 0.1 kPa LCN RVP output disturbance and 0 Mol% LPG C5 output disturbance.



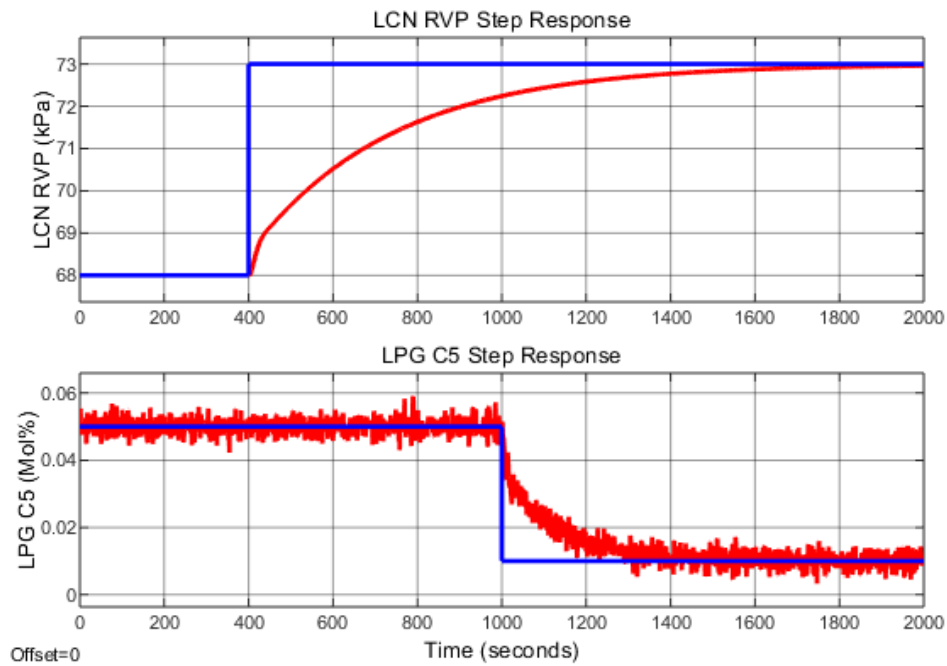
**Figure 5.11: Case #5.4.2 dynamic response**

Figure 5.12 shows the LCN RVP dynamic response to a +8 kPa setpoint step change from 60 kPa to 68 kPa steady state and LPG C5 concentration dynamic response to a -0.55 Mol% setpoint step change from 0.6 Mol % to 0.05 Mol % steady state under influence of 0 kPa LCN RVP output disturbance and 1E-06 Mol % LPG C5 output disturbance



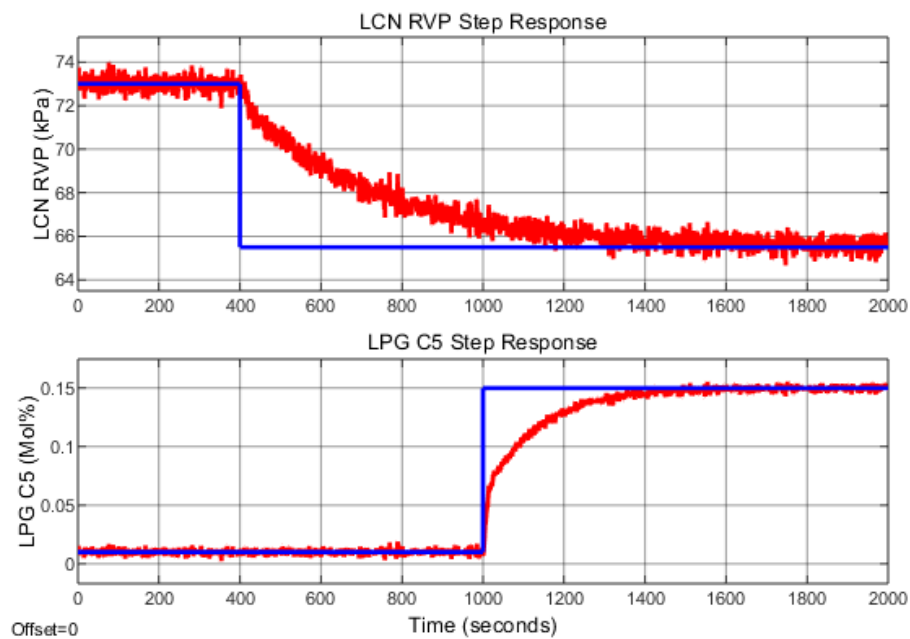
**Figure 5.12: Case #5.4.3 dynamic response**

Figure 5.13 shows the LCN RVP dynamic response to a +5 kPa setpoint step change from 68 kPa to 73 kPa steady state and LPG C5 concentration dynamic response to a -0.04 Mol% setpoint step change from 0.05 Mol % to 0.01 Mol % steady state under influence of 0 kPa LCN RVP output disturbance and 5E-06 Mol % LPG C5 output disturbance



**Figure 5.13: Case #5.4.4 dynamic response**

Figure 5.14 shows the LCN RVP dynamic response to a -7.5 kPa setpoint step change from 73 kPa to 65.5 kPa steady state and LPG C5 concentration dynamic response to a +0.14 Mol% setpoint step change from 0.01 Mol % to 0.15 Mol % steady state under influence of 0.1 kPa LCN RVP output disturbance and 5E-06 Mol % LPG C5 output disturbance.



**Figure 5.14: Case #5.4.5 dynamic response**

The results of the simulation case study are discussed in detail in the following sub-section for both simulations with and without disturbances.

### 5.6.2. Discussion of the results

There are four main observations that are made in the output responses from the simulation case study when disturbances are not considered, namely 1) zero interactions between the two control loops, 2) zero percentage overshoot in the output responses, 3) relatively long settling times, and finally, 4) the zero steady state error. A percentage overshoot metric on time domain step response curves describes a maximum peak value reached by the output response relative to the steady state setpoint and it is representative of the relative stability of the system while the settling time represents the largest time constant of the system and can be defined as the time it takes for the output response to reach and remain within a small range about the target steady state setpoint (Ogata, 2010). The performance metrics of the control loops are given in Table 5.5 for the simulation cases without disturbances. The PID controllers have shown satisfactory closed loop control performances in that there is zero overshoot observed in both the LCN Reid Vapour Pressure (kPa) and the LPG C5 concentration (Mol %) loops when zero disturbances are considered i.e., the response curve profiles observed exhibit that of critically damped control loops.

**Table 5.5: Analysis of the performance indicators for each of the setpoint variations without disturbances**

Loop Name	Initial Setpoint	Final Setpoint	Step Size	Percent Overshoot	Settling Time	Steady State Error	Figure Reference
LCN_RVP	65 kPa	63 kPa	-2 kPa	0%	1600s	0 kPa	Figure 5.4
LPG_C5	0.1 Mol%	0.3 Mol%	+0.2 Mol%	0%	600s	0 Mol%	
LCN_RVP	63 kPa	60 kPa	-3 kPa	0%	1600s	0 kPa	Figure 5.5
LPG_C5	0.3 Mol%	0.6 Mol%	+0.3 Mol%	0%	600s	0 Mol%	
LCN_RVP	60 kPa	68 kPa	+8 kPa	0%	1600s	0 kPa	Figure 5.6
LPG_C5	0.6 Mol%	0.05 Mol%	-0.55 Mol%	0%	600s	0 Mol%	
LCN_RVP	68 kPa	73 kPa	+5 kPa	0%	1600s	0 kPa	Figure 5.7
LPG_C5	0.05 Mol%	0.01 Mol%	-0.04 Mol%	0%	600s	0 Mol%	
LCN_RVP	73 kPa	65.5 kPa	-7.5 kPa	0%	1600s	0 kPa	Figure 5.8
LPG_C5	0.01 Mol%	0.15 Mol%	+0.14 Mol%	0%	600s	0 Mol%	

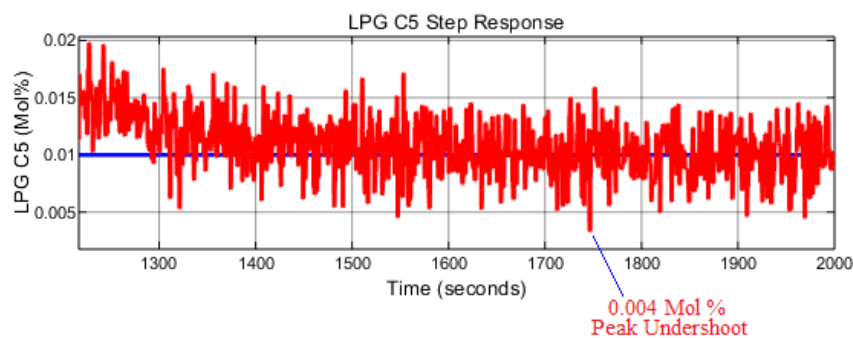
Since the debutanizer distillation process is coupled and multivariable in its structure, without the use of decoupling compensators, the process variable interactions are inevitable where a single process variable's dynamic behaviour influences other process variables. The decoupling compensators designed for the second order debutanizer process model being studied have been able to completely eliminate the effect of interactions to zero. During the simulation studies, the step changes are simultaneously made, and it is observed that the response of the LCN Reid Vapour Pressure (kPa) output does not have an effect on the response of the LPG C5 concentration (Mol %) output, and vice versa. Furthermore, the observed transient responses do not exceed the target steady state setpoint resulting in the zero overshoot of the target. The PID controller gain tuning settings are selected to sacrifice

faster response times to achieve robust responses with zero steady state overshoot and zero oscillations. It is further observed that modifying the internal model control filter parameter results in a modified transient response i.e., a smaller value of the filter parameter leads to a faster transient response with a possibility for overshoot and oscillation whereas a larger filter parameter results in a robust response with no overshoot and oscillations. The outputs of both control loops are observed to closely follow the setpoint step changes with zero steady state error. Since the objective is to ensure the outputs track the command setpoint inputs, a zero steady state error is an indication of the accuracy of the system in meeting this objective. Finally, in the investigation of the influence of random white noise disturbances on the designed system, the observed performance metrics for both control loops are given in Table 5.6 for simulation cases with disturbances added.

**Table 5.6: Analysis of the performance indicators for each of the setpoint variations with addition of disturbances**

Loop Name	Initial Setpoint	Final Setpoint	Output Disturbance Amplitude	Percent Overshoot	Settling Time	Steady State Error	Figure Reference
LCN_RVP	65 kPa	63 kPa	0.005 kPa	0.8%	1600s	±0.5 kPa	Figure 5.10
LPG_C5	0.1 Mol%	0.3 Mol%	0 Mol%	0%	600s	0 Mol%	
LCN_RVP	63 kPa	60 kPa	0.1 kPa	1.7%	1600s	±1 kPa	Figure 5.11
LPG_C5	0.3 Mol%	0.6 Mol%	0 Mol%	0%	600s	0 Mol%	
LCN_RVP	60 kPa	68 kPa	0 kPa	0%	1600s	0 kPa	Figure 5.12
LPG_C5	0.6 Mol%	0.05 Mol%	1E-06 Mol%	-10%	600s	±0.02 Mol%	
LCN_RVP	68 kPa	73 kPa	0 kPa	0%	1600s	0 kPa	Figure 5.13
LPG_C5	0.05 Mol%	0.01 Mol%	5E-06 Mol%	-60%	600s	±0.01 Mol%	
LCN_RVP	73 kPa	65.5 kPa	0.1 kPa	-1%	1600s	±1 kPa	Figure 5.14
LPG_C5	0.01 Mol%	0.15 Mol%	5E-06 Mol%	3%	600s	±0.05 Mol%	

It is observed that as the disturbance amplitude is increased, the controller continues to track the setpoint satisfactorily, however, with increased output overshoot or undershoot and variability. The observed response is due to the increased disturbance amplitude. The undershoot is particularly pronounced in the LPG C5 Concentration (Mol %) output signal reaching a value of -60%. Figure 5.15 provides an enlarged view of the response shown in Figure 5.13 where the undershoot of -60% is observed.



**Figure 5.15: LPG C5 Concentration (Mol %) exhibiting a -60% undershoot during a -0.04 Mol % step change in the presence of a 5E-06 Mol% white noise disturbance amplitude**



The output response is observed to reach 0.004 Mol % which is 0.006 Mol % below the target setpoint of 0.01 Mol %. The cause for the undershoot can be attributed to the magnitude of the step size versus the magnitude of the disturbance signal i.e., the step size of -0.04 Mol % is of such a small magnitude requiring precise control which is proving to be challenging for the controller in the presence of a 5E-06 Mol% white noise disturbance amplitude. In practice, an overshoot or undershoot of a maximum of 10% is considered acceptable and anything beyond 10% can potentially introduce instability in the closed-loop system. Therefore, it is worth noting that small step sizes of a value of -0.04 Mol % are neither practical nor anticipated in practice. For the purposes of this study, such small step changes reveal the limitations of the controller.

The settling times are observed to remain relatively unchanged when compared to the case without disturbances. Overall, the observed control loop responses demonstrate good controller performance for low amplitude disturbances.

The above section provided a summary of the results observed from the simulation case studies for cases with and without disturbances. The following section provides concluding remarks for this chapter.

## **5.7. Conclusion**

In this chapter, a set of decentralized PID controllers tuned using the internal model control (IMC) for a second order debutanizer distillation process model is successfully developed and closed-loop simulation case studies are conducted in the MATLAB/Simulink environment. The controller design methods used included the use of the relative gain array as an interaction measure and designing decoupling compensators to eliminate process variable interactions. In order to ease the PID controller design complexity, a model reduction technique is employed which approximates the original model by retaining its average dominant poles and zeros as well as its polynomial lower order coefficients as proposed by Isaksson and Graebe (1993). It is observed from the simulation studies that the designed and implemented controllers using the Internal Model Control method do achieve good setpoint tracking and that the dynamic decoupling compensators that have been designed and implemented are effective in eliminating process interaction.

In the following chapter, the controller design method for an MPC controller based on the seventh order linear step response prediction model of the debutanizer distillation process which is developed in Chapter 4 is described. The controller development is done using the MATLAB/Simulink Model Predictive Control Toolbox. Furthermore, the process of developing and configuring the model predictive controller in MATLAB/Simulink is outlined. The selection of the controller parameters such as the Scale Factors, Prediction Horizon, the Control Horizon, Sampling Time, input and output constraints, constraint softening factors, reference tracking and increment suppression weights together with a step-by-step procedure are outlined.

## CHAPTER SIX: MPC CONTROLLER DESIGN METHODS

### 6.1. Introduction

Industrial applications of model predictive control (MPC) were first introduced in the late 1970's and have since found extensive use in the petrochemical industry, particularly in crude oil refining facilities (Qin and Badgwell, 2003). There has also been recent specific research aimed at MPC techniques on debutanizer distillation processes such as one presented in (Ramli and Chandra Mohan, 2015). MPC has also been applied to other industries outside the petrochemical domain in the last decade. The work by (Kouro et al., 2015) provided a good review of the emergence of MPC in power semiconductor energy control whereas (Matko et al., 2013) and (Calugaru and Danisor, 2016) applied dynamic matrix control in aircraft autopilot systems. The work by (Chuong and Vu, 2017) applied model predictive control in a Heating, Ventilation, and Air Conditioning (HVAC) system while (Hao and Hau, 2020) presented a liquid level control application. These are exemplary of the wide applicability of MPC outside of the process industry, indicative of its versatility and ability to be adapted to applications. Prior to the era of MPC, multivariable control was implemented using ad hoc strategies such as decoupling controllers, sensors, overrides, time delay compensators, etc. (Morari and Lee, 1999). There are different types of MPC formulations available which differ primarily by the algorithm used to represent the process model (Lopez-guede et al., 2013). It is worth noting that the scope of this chapter is limited to the dynamic matrix control formulation which is an MPC algorithm that makes use of a step response model to represent the process (Cutler and Ramaker, 1979). The objective of this chapter is to develop an MPC control system using the MATLAB/Simulink Model Predictive Control Toolbox and to test the designed controller in an industrial seventh order debutanizer distillation process model.

The breakdown of this chapter is as follows, in section 6.2 the seventh order debutanizer process model and its mathematical transfer functions are recalled and presented as well as the MPC control structure that is used in the remainder of this chapter. Section 6.3 presents the process of configuring the MPC in MATLAB/Simulink including the selection of the controller design parameters such as the scale factors, prediction horizon, the control horizon, sampling time, input and output constraints, constraint softening factors, reference tracking and increment suppression weights. Section 6.3 ends with a MATLAB/Simulink step-by-step procedure followed to configure the controller with the selected design and tuning parameters. Section 6.4 presents the closed-loop simulation case studies to investigate the effectiveness of the parameters configured in the controller and concluding remarks are provided in section 6.5.

## 6.2. MPC control system structure

The objective of this section is to outline the overall control structure that is adopted for the Model Predictive Control (MPC) controller design. In Chapter 4, the development of the seventh order debutanizer distillation process model that is used in this chapter is presented. The model, which is identified with MATLAB's System Identification Toolbox using step response coefficients from AspenTech's DMC3 Builder commercial software package, is given again in Table 6.1 below. Furthermore, as outlined in Chapter 3, typical industrial implementations of MPC have the controller configured to manipulate setpoints of lower layer regulatory proportional-integral-derivative (PID) control loops residing in a control system such as a distributed control system (DCS) as is illustrated in the hierarchy of process control activities in Figure 3.6. Therefore, an MPC controller that manipulates lower level PID control loops to control the seventh order debutanizer distillation process model is presented in this chapter. The MPC controller is designed and implemented using the MATLAB/Simulink Model Predictive Control Toolbox (Bemporad et al., 2015).

The mathematical formulation showing the input-output relationships of the seventh order debutanizer distillation process transfer function model is given as:

$$\begin{bmatrix} Y_1 \\ Y_2 \\ Y_3 \\ Y_4 \\ Y_5 \\ Y_6 \\ Y_7 \end{bmatrix} = \begin{bmatrix} TF_{11} & TF_{12} & TF_{13} & TF_{14} & TF_{15} & TF_{16} & TF_{17} \\ TF_{21} & TF_{22} & TF_{23} & TF_{24} & TF_{25} & TF_{26} & TF_{27} \\ TF_{31} & TF_{32} & TF_{33} & TF_{34} & TF_{35} & TF_{36} & TF_{37} \\ TF_{41} & TF_{42} & TF_{43} & TF_{44} & TF_{45} & TF_{46} & TF_{47} \\ TF_{51} & TF_{52} & TF_{53} & TF_{54} & TF_{55} & TF_{56} & TF_{57} \\ TF_{61} & TF_{62} & TF_{63} & TF_{64} & TF_{65} & TF_{66} & TF_{67} \\ TF_{71} & TF_{72} & TF_{73} & TF_{74} & TF_{75} & TF_{76} & TF_{77} \end{bmatrix} \times \begin{bmatrix} U_1 \\ U_2 \\ U_3 \\ U_4 \\ U_5 \\ U_6 \\ U_7 \end{bmatrix} + \begin{bmatrix} 0 \\ 0 \\ TF_{3D1} \\ TF_{4D1} \\ 0 \\ TF_{6D1} \\ 0 \end{bmatrix} \times [D_1] + D_2 \quad (6.1)$$

Where:

$Y_1 =$	LCN_RVP	LCN Reid Vapour Pressure (kPa)
$Y_2 =$	LPG_C5	LPG C5 Concentration (Mol %)
$Y_3 =$	Ovhd_Drum_Press	Overhead Drum Pressure (kPa)
$Y_4 =$	Ovhd_Drum_Press_SV-PV	Overhead Drum Pressure SV-PV Gap (kPa)
$Y_5 =$	Debut_Diff_Press	Debutanizer Differential Pressure (kPa)
$Y_6 =$	Reboiler_Valve_Pos	Debutanizer Reboiler Valve Position (%)
$Y_7 =$	Debut_Tray_24_Temp	Tray 24 Temperature (DegC)
$U_1 =$	Ovhd_Press	Overhead Pressure (kPa)
$U_2 =$	Reflux_Flow	Reflux Flow (m3/h)
$U_3 =$	Reboiler_Temp	Reboiler Temperature (DegC)
$U_4 =$	Deeth_Feed_Flow	Deethanizer Feed Flow (m3/h)
$U_5 =$	Deeth_Pressure	Deethanizer Pressure (kPa)
$U_6 =$	Deeth_Temp	Deethanizer Temperature (DegC)
$U_7 =$	LCN_Recycle_Flow	LCN Recycle Flow (m3/h)
$D_1 =$	Ambient_Temp	Ambient Temperature (DegC)
$D_2 =$	White Noise	Unmeasured Disturbances:

And where the transfer function models are given by:

$$TF_{11} = \frac{Y_1}{U_1} = \frac{LCN\_RVP}{Ovhd\_Press} = \frac{0.001241}{s^3 + 0.8456 s^2 + 0.1968 s + 0.01438}$$

$$TF_{21} = \frac{Y_2}{U_1} = \frac{LPG\_C5}{Ovhd\_Press} = \frac{-0.0001665}{s^2 + 0.3112 s + 0.141}$$

$$TF_{31} = \frac{Y_3}{U_1} = \frac{Ovhd\_Drum\_Press}{Ovhd\_Press} = \frac{0.3791}{s^3 + 1.451 s^2 + 4.211 s + 0.6576}$$

$$TF_{41} = \frac{Y_4}{U_1} = \frac{Ovhd\_Drum\_Press\_SV-PV}{Ovhd\_Press} = \frac{4.536}{s^2 + 18.06 s + 8.779}$$

$$TF_{51} = \frac{Y_5}{U_1} = \frac{Debut\_Diff\_Press}{Ovhd\_Press} = \frac{-0.01348}{s^2 + 1.041 s + 0.2387}$$

$$TF_{61} = \frac{Y_6}{U_1} = \frac{Reboiler\_Valve\_Pos}{Ovhd\_Press} = \frac{-0.302}{s^2 + 6.456 s + 2.517}$$

$$TF_{71} = \frac{Y_7}{U_1} = \frac{Debut\_Tray\_24\_Temp}{Ovhd\_Press} = \frac{0.0009007}{s^2 + 0.2369 s + 0.0351}$$

$$TF_{12} = \frac{Y_1}{U_2} = \frac{LCN\_RVP}{Reflux\_Flow} = 0$$

$$TF_{22} = \frac{Y_2}{U_2} = \frac{LPG\_C5}{Reflux\_Flow} = \frac{-0.004903}{s^2 + 1.638 s + 0.2383}$$

$$TF_{32} = \frac{Y_3}{U_2} = \frac{Ovhd\_Drum\_Press}{Reflux\_Flow} = 0$$

$$TF_{42} = \frac{Y_4}{U_2} = \frac{Ovhd\_Drum\_Press\_SV-PV}{Reflux\_Flow} = 0$$

$$TF_{52} = \frac{Y_5}{U_2} = \frac{Debut\_Diff\_Press}{Reflux\_Flow} = \frac{0.008285}{s^2 + 0.2468 s + 0.02035}$$

$$TF_{62} = \frac{Y_6}{U_2} = \frac{Reboiler\_Valve\_Pos}{Reflux\_Flow} = \frac{0.1951}{s^2 + 0.3764 s + 0.3902}$$

$$TF_{72} = \frac{Y_7}{U_2} = \frac{Debut\_Tray\_24\_Temp}{Reflux\_Flow} = \frac{0.2693 s^3 - 0.1926 s^2 - 0.0219 s - 0.005952}{s^5 + 1.764 s^4 + 1.752 s^3 + 0.5189 s^2 + 0.09789 s + 0.008874}$$

$$TF_{13} = \frac{Y_1}{U_3} = \frac{LCN\_RVP}{Reboiler\_Temp} = \frac{-0.004852}{s^3 + 0.3151 s^2 + 0.04709 s + 0.00415}$$

$$TF_{23} = \frac{Y_2}{U_3} = \frac{LPG\_C5}{Reboiler\_Temp} = \frac{0.0009339}{s^2 + 0.3965 s + 0.06791}$$

$$TF_{33} = \frac{Y_3}{U_3} = \frac{Ovhd\_Drum\_Press}{Reboiler\_Temp} = 0$$

$$TF_{43} = \frac{Y_4}{U_3} = \frac{Ovhd\_Drum\_Press\_SV-PV}{Reboiler\_Temp} = 0$$

$$TF_{53} = \frac{Y_5}{U_3} = \frac{Debut\_Diff\_Press}{Reboiler\_Temp} = 0$$

$$TF_{63} = \frac{Y_6}{U_3} = \frac{Reboiler\_Valve\_Pos}{Reboiler\_Temp} = \frac{0.6714}{s^2 + 5.496 s + 0.6714}$$

$$TF_{73} = \frac{Y_7}{U_3} = \frac{Debut\_Tray\_24\_Temp}{Reboiler\_Temp} = \frac{0.01305}{s^2 + 0.5266 s + 0.08758}$$

$$TF_{14} = \frac{Y_1}{U_4} = \frac{LCN\_RVP}{Deeth\_Feed\_Flow} = 0$$

$$TF_{24} = \frac{Y_2}{U_4} = \frac{LPG\_C5}{Deeth\_Feed\_Flow} = \frac{-0.0007287}{s^2 + 0.6293 s + 0.1123}$$

$$TF_{34} = \frac{Y_3}{U_4} = \frac{Ovhd\_Drum\_Press}{Deeth\_Feed\_Flow} = 0$$

$$TF_{44} = \frac{Y_4}{U_4} = \frac{Ovhd\_Drum\_Press\_SV-PV}{Deeth\_Feed\_Flow} = 0$$

$$TF_{54} = \frac{Y_5}{U_4} = \frac{Debut\_Diff\_Press}{Deeth\_Feed\_Flow} = 0$$

$$TF_{64} = \frac{Y_6}{U_4} = \frac{Reboiler\_Valve\_Pos}{Deeth\_Feed\_Flow} = \frac{0.3628}{s^2 + 10.06 s + 0.5412}$$

$$TF_{74} = \frac{Y_7}{U_4} = \frac{Debut\_Tray\_24\_Temp}{Deeth\_Feed\_Flow} = 0$$

$$TF_{15} = \frac{Y_1}{U_5} = \frac{LCN\_RVP}{Deeth\_Pressure} = 0$$

$$TF_{25} = \frac{Y_2}{U_5} = \frac{LPG\_C5}{Deeth\_Pressure} = 0$$

$$TF_{35} = \frac{Y_3}{U_5} = \frac{Ovhd\_Drum\_Press}{Deeth\_Pressure} = \frac{0.004934}{s^3 + 0.5241 s^2 + 0.1822 s + 0.00895}$$

$$TF_{45} = \frac{Y_4}{U_5} = \frac{Ovhd\_Drum\_Press\_SV-PV}{Deeth\_Pressure} = \frac{-0.004668}{s^3 + 0.47 s^2 + 0.1708 s + 0.008437}$$

$$TF_{55} = \frac{Y_5}{U_5} = \frac{Debut\_Diff\_Press}{Deeth\_Pressure} = 0$$

$$TF_{65} = \frac{Y_6}{U_5} = \frac{Reboiler\_Valve\_Pos}{Deeth\_Pressure} = \frac{0.002211}{s^2 + 0.4867 s + 0.04347}$$

$$TF_{75} = \frac{Y_7}{U_5} = \frac{Debut\_Tray\_24\_Temp}{Deeth\_Pressure} = 0$$

$$TF_{16} = \frac{Y_1}{U_6} = \frac{LCN\_RVP}{Deeth\_Temp} = 0$$

$$TF_{26} = \frac{Y_2}{U_6} = \frac{LPG\_C5}{Deeth\_Temp} = 0$$

$$TF_{36} = \frac{Y_3}{U_6} = \frac{Ovhd\_Drum\_Press}{Deeth\_Temp} = \frac{-0.1775}{s^2 + 0.3455 s + 0.01603}$$

$$TF_{46} = \frac{Y_4}{U_6} = \frac{Ovhd\_Drum\_Press\_SV-PV}{Deeth\_Temp} = \frac{0.1785}{s^2 + 0.3471 s + 0.01612}$$

$$TF_{56} = \frac{Y_5}{U_6} = \frac{Debut\_Diff\_Press}{Deeth\_Temp} = \frac{-0.001914}{s^3 + 0.1084 s^2 + 0.07097 s + 0.002616}$$

$$TF_{66} = \frac{Y_6}{U_6} = \frac{Reboiler\_Valve\_Pos}{Deeth\_Temp} = \frac{-0.04504}{s^2 + 0.649 s + 0.03486}$$

$$TF_{76} = \frac{Y_7}{U_6} = \frac{Debut\_Tray\_24\_Temp}{Deeth\_Temp} = 0$$

$$TF_{17} = \frac{Y_1}{U_7} = \frac{LCN\_RVP}{LCN\_Recycle\_Flow} = 0$$

$$TF_{27} = \frac{Y_2}{U_7} = \frac{\text{LPG\_C5}}{\text{LCN\_Recycle\_Flow}} = 0$$

$$TF_{37} = \frac{Y_3}{U_7} = \frac{\text{Ovhd\_Drum\_Press}}{\text{LCN\_Recycle\_Flow}} = \frac{0.03129}{s^2 + 0.1977 s + 0.016}$$

$$TF_{47} = \frac{Y_4}{U_7} = \frac{\text{Ovhd\_Drum\_Press\_SV-PV}}{\text{LCN\_Recycle\_Flow}} = \frac{-0.03212}{s^2 + 0.2023 s + 0.01679}$$

$$TF_{57} = \frac{Y_5}{U_7} = \frac{\text{Debut\_Diff\_Press}}{\text{LCN\_Recycle\_Flow}} = \frac{0.0132}{s^2 + 0.4215 s + 0.06652}$$

$$TF_{67} = \frac{Y_6}{U_7} = \frac{\text{Reboiler\_Valve\_Pos}}{\text{LCN\_Recycle\_Flow}} = \frac{6.699}{s^2 + 7.781 s + 0.957}$$

$$TF_{77} = \frac{Y_7}{U_7} = \frac{\text{Debut\_Tray\_24\_Temp}}{\text{LCN\_Recycle\_Flow}} = 0$$

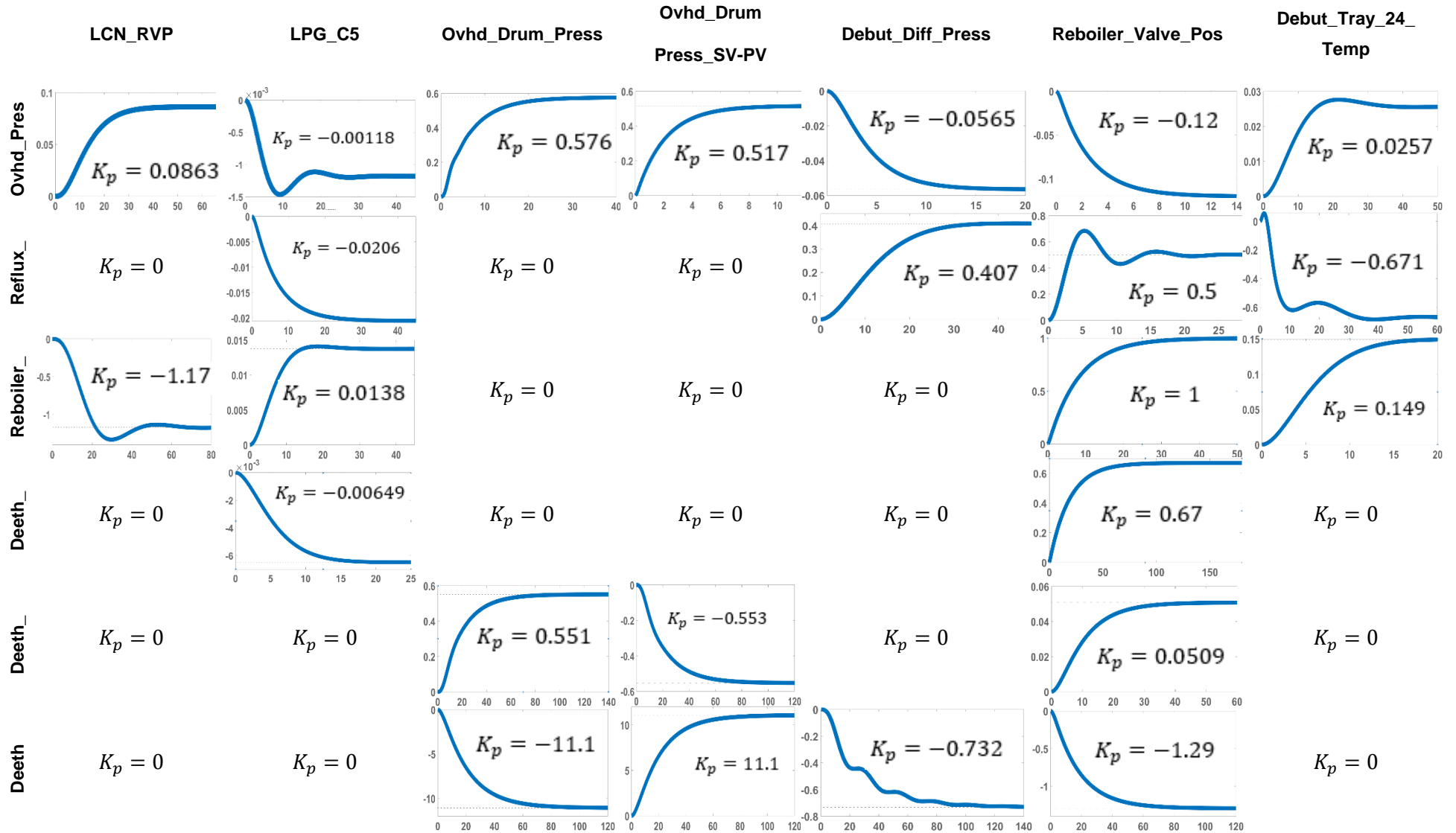
$$TF_{3D1} = \frac{Y_3}{D_1} = \frac{\text{Ovhd\_Drum\_Press}}{\text{Ambient\_Temp}} = \frac{3.061}{s^2 + 5.35 s + 1.275}$$

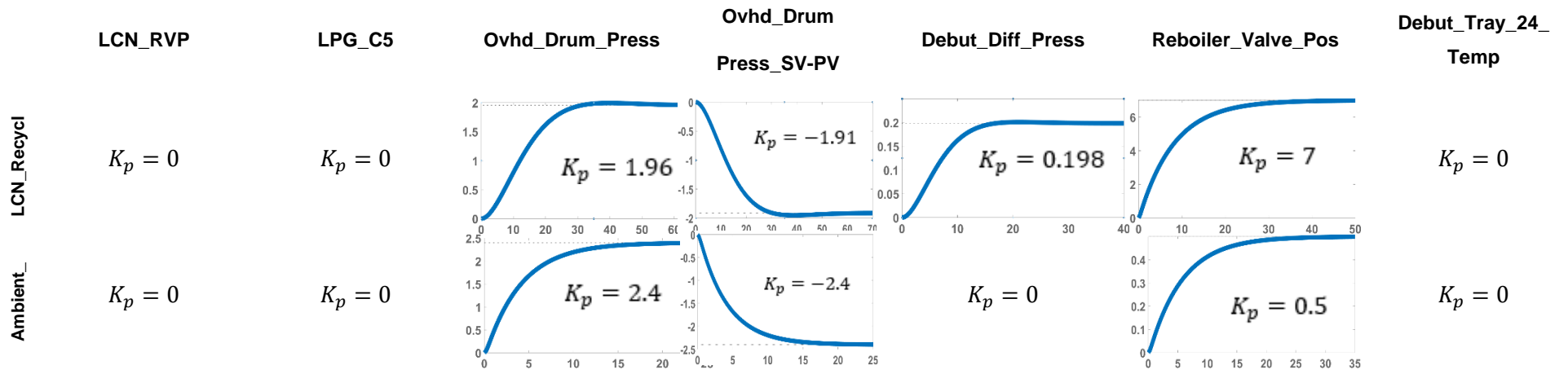
$$TF_{4D1} = \frac{Y_4}{D_1} = \frac{\text{Ovhd\_Drum\_Press\_SV-PV}}{\text{Ambient\_Temp}} = \frac{-3.061}{s^2 + 5.35 s + 1.275}$$

$$TF_{6D1} = \frac{Y_6}{D_1} = \frac{\text{Reboiler\_Valve\_Pos}}{\text{Ambient\_Temp}} = \frac{0.4528}{s^2 + 5.249 s + 0.9055}$$

The process model presented in Table 6.1 and described by the transfer functions above can further be represented in block diagram form given by Figure 6.1.

Table 6.1: Seventh order debutanizer distillation process model







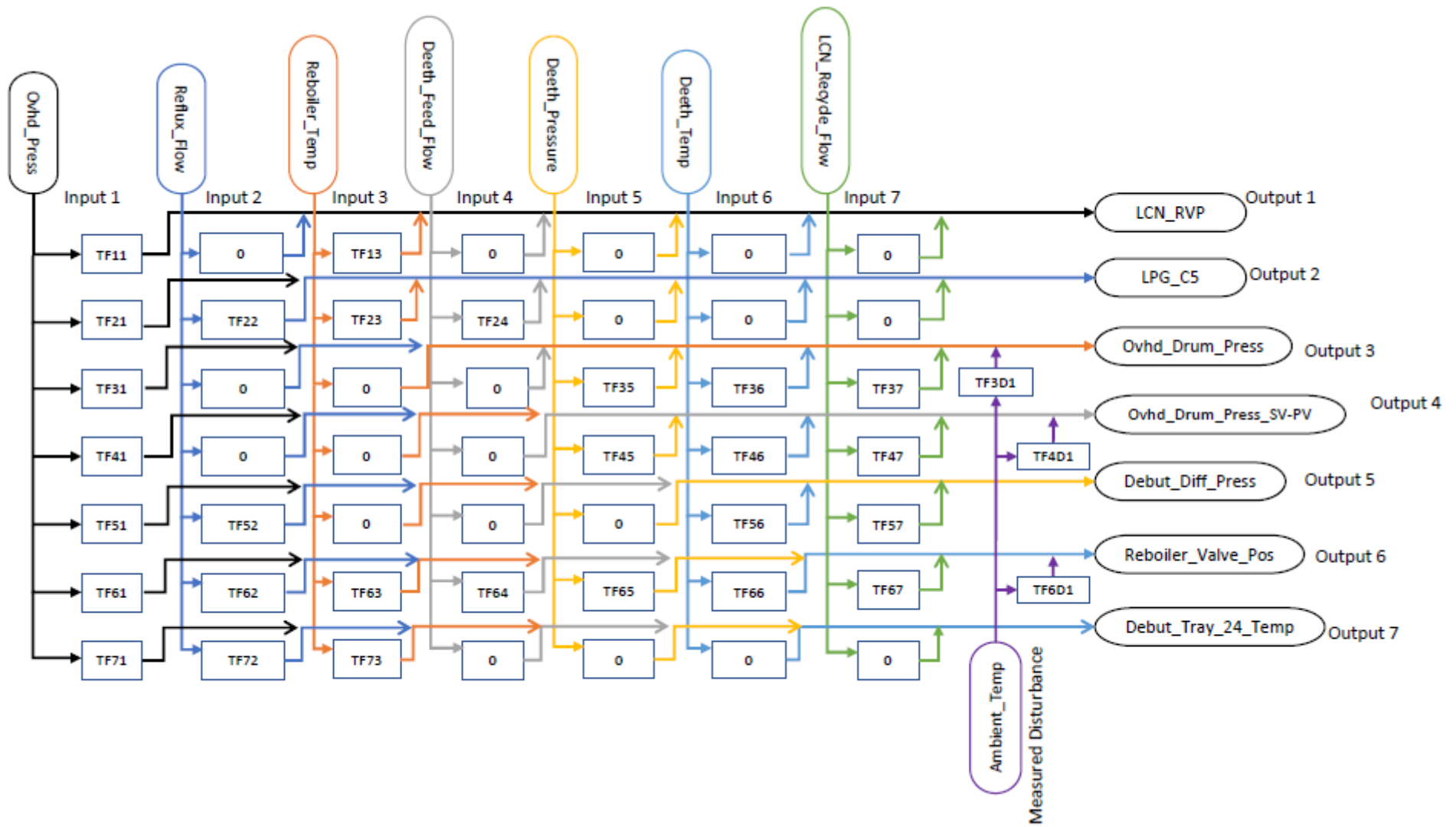
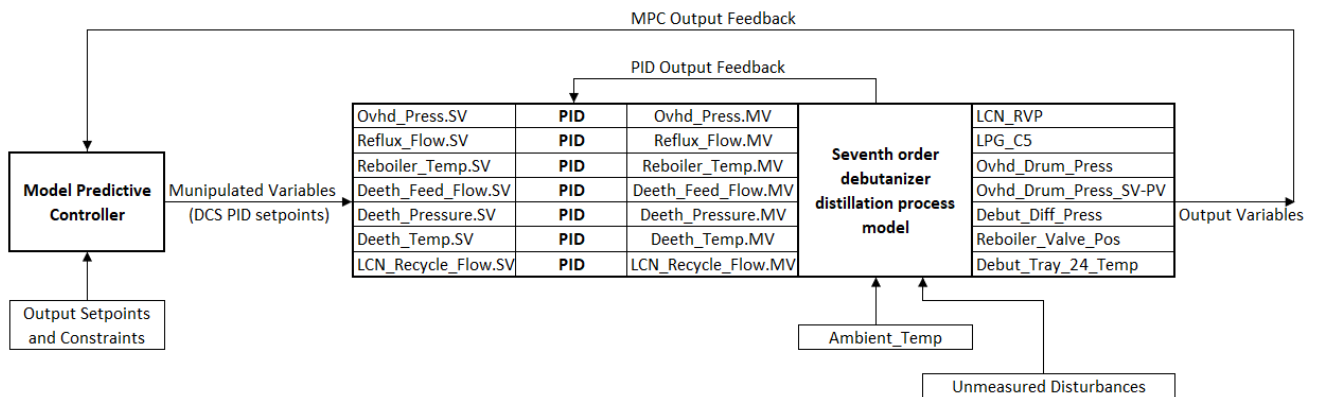


Figure 6.1: Seventh order debutanizer distillation process model block diagram

In Figure 6.1, all the control inputs are listed at the top labelled Input 1 to Input 7, and all the controlled outputs are listed on the labelled Output 1 to Output 7. At the bottom of Figure 6.1, the measured disturbance of ambient temperature is shown. The transfer function blocks are illustrated to show the relationship between the Inputs and Outputs. For example, the relationship between the Deethanizer Pressure (**Deeth\_Pressure**) and the Overhead Drum Pressure (**Ovhd\_Drum\_Press**) is described by the transfer function TF35 which is given by:

$$TF_{35} = \frac{Y_3}{U_5} = \frac{\text{Ovhd\_Drum\_Press}}{\text{Deeth\_Pressure}} = \frac{0.004934}{s^3 + 0.5241 s^2 + 0.1822 s + 0.00895} \quad (6.2)$$

It can be observed from Figure 6.1 that the model structure is coupled, where each control input has an effect on more than one process output (or controlled output). For example, in the case of the Deethanizer Pressure control input, it has an effect not only on the Overhead Drum Pressure but also on the Overhead Drum Pressure SV-PV Gap as described by the transfer function TF45 and on the Debutanizer Reboiler Valve Position as described by the transfer function TF65. Therefore, to effectively control such a coupled multivariable process, a multivariable controller such as an MPC controller is necessary since use of decoupling compensators for such a large system is not feasible. The closed-loop control structure for the MPC controller developed as part of this research is given in Figure 6.2.



**Figure 6.2: Closed-loop control structure for the MPC controller**

The block diagram in Figure 6.2 shows the MPC controller closed-loop system structure that is developed using the Model Predictive Control Toolbox in the MATLAB/Simulink environment. The control inputs used by the MPC controller are the setpoints of regulatory layer PID controllers. The controlled outputs of the PID controllers are assumed to closely track PID setpoints and, therefore, change as the control inputs of the MPC controller are varied.

The process outputs controlled by the MPC controller are in closed-loop and connected back to the MPC controller as measured output feedback.

This section has presented the overall control structure that is adopted for the model predictive control (MPC) controller design. The MPC controller is configured in the MATLAB/Simulink

MPC Toolbox to control the seventh order debutanizer distillation process model by manipulating the setpoints of the regulatory PID controllers. The above-mentioned structure is similar to how MPC is implemented in practice (Seborg et al., 2004). The next section outlines the details of the development and configuration of the MPC controller in the MATLAB/Simulink environment.

### 6.3. MPC controller development in MATLAB/Simulink

Developing the MPC controller using the MPC Toolbox in the MATLAB/Simulink environment can be broken down to two stages 1) setting up the model structure based on the number of inputs and outputs and, 2) selecting and tuning several parameters that describe the desired performance of the controller. The parameters that must be determined and configured in the MPC Toolbox include the 1) scale factors, 2) prediction horizon, 3) the control horizon, 4) sampling time, 5) input and output constraints, 6) constraint softening factors and, 7) reference tracking and increment suppression weights. The process of selection and configuration of each of the above-mentioned parameters is described in this section together with the procedure that is followed in configuring the MPC controller with the MPC Toolbox.

#### 6.3.1. MPC controller scale factors

The MPC controller scale factors are utilized to handle the differences in the ranges of the process variable signals used in the controller structure. The recommended selection for the scale factors is typically to ensure they are equal to the span of the signal being scaled with the span defined as the difference between the maximum and the minimum range values of the signal (Bemporad et al., 2015).

Shown in Tables 6.2 and 6.3 are the scale factors configured for the control inputs and controlled outputs, respectively, together with the range, span, and nominal values for each of the signals for the seventh order debutanizer distillation process model. The nominal values are selected based on the steady state operating conditions of the process.

**Table 6.2: Manipulated Variable Scale Factors**

Name	Range	Span	Nominal Value	Scale Factor
Ovhd_Press	950 – 1110 kPa	160 kPa	1100 kPa	160
Reflux_Flow	18 – 28 m3/h	10 m3/h	20 m3/h	10
Reboiler_Temp	139 – 160 DegC	21 DegC	150 DegC	21
Deeth_Feed_Flow	20 – 90 m3/h	70 m3/h	67 m3/h	70
Deeth_Pressure	1180 – 1280 kPa	100 kPa	1180 kPa	100
Deeth_Temp	88 – 95 DegC	7 DegC	90 DegC	7
LCN_Recycle_Flow	6 – 10 m3/h	4 m3/h	10 m3/h	4

**Table 6.3: Controlled outputs Scale Factors**

Name	Range	Span	Nominal Value	Scale Factor
LCN_RVP	60 – 66 kPa	6 kPa	65 kPa	20
LPG_C5	0 – 0.5 Mol %	0.5 Mol %	0.1 Mol %	0.5
Ovhd_Drum_Press	700 – 1155 kPa	455 kPa	880 kPa	455
Ovhd_Drum_Press_SV-PV	50 – 460 kPa	410 kPa	281 kPa	410

Name	Range	Span	Nominal Value	Scale Factor
Debut_Diff_Press	10 – 30 kPa	20 kPa	23 kPa	20
Reboiler_Valve_Pos	9 – 60 %	51 %	13 %	51
Debut_Tray_24_Temp	60 – 79 DegC	19 DegC	72 DegC	19

The scale factors and nominal values given in Tables 6.2 and 6.3 are configured into the MPC Toolbox during the MPC controller configuration. The next section presents the selection of the prediction horizon, control horizon and sampling time.

### 6.3.2. Prediction horizon, control horizon and sampling time

As previously outlined in Chapter 3, the recommendation for the selection of a control horizon is to choose  $M$  such that  $1 \leq M \leq P$  whereby a smaller value close to  $M = 1$  tends to improve the controller execution speed (Bemporad et al., 2015). A recommended rule of thumb by (Seborg et al., 2004) is to select  $M$  such that  $\frac{N}{3} \leq M \leq \frac{N}{2}$  and  $5 \leq M \leq 20$ . Therefore, the control horizon for this research is selected to be  $M = 16$ . The selection of the prediction horizon is to ensure the complete dynamic response and the steady state are included in the prediction by the controller (Camacho and Bordons, 2007). A rule of thumb by (Seborg et al., 2004) is to select  $P$  such that  $P = M + N$  where  $P$  is the prediction horizon,  $M$  is the control horizon and  $N$  is the model horizon. The model horizon,  $N$ , of the original model is  $N = 48$  since the step response coefficients had a total of 48 data points for each step response curve. Therefore, a value of  $P = 64$  is selected as the prediction horizon for the controller following the rule of  $P = M + N$  proposed in (Seborg et al., 2004) as outlined in Chapter 3.

Finally, the sampling time is typically selected based on the process dynamics involved where processes with fast dynamics require shorter sampling times whereas processes with slower process dynamics, such as majority of those found in petrochemical plants and oil refineries, can be configured with longer controller sampling times (Bemporad et al., 2015) as is outlined in Chapter 3. The sample time selected is  $\Delta t = 1 \text{ second}$  as longer sampling times are observed exhibiting sluggish behaviour.

A summary of the prediction horizon, control horizon and sampling time values used for the controller configuration in this research is provided in Table 6.4.

**Table 6.4: Prediction horizon, control horizon and sampling time**

Name	Value
Prediction Horizon ( $P$ )	64
Control Horizon ( $M$ )	16
Sampling Time ( $\Delta t$ )	1 second

The prediction horizon, control horizon and sampling time values given in Table 6.4 are configured in the MPC Toolbox during the MPC controller configuration. The next section presents the selection of the input and output constraints and constraints softening factors.

### 6.3.3. Input and output constraints and constraints softening factors

Process constraints are dictated by plant and equipment limitations. In this research, a replication of the constraints from the original model is pursued. However, it is observed during the MPC controller configuration that placing constraints on the control inputs results in an infeasible solution. This can be attributed to the controller being forced to give up on one or more of the controlled outputs to satisfy the control input constraints (Froisy, 1994). It is generally recommended to avoid placing constraints on control inputs unless it is absolutely necessary since they are regarded as hard limits that cannot be violated by the controller (Hilton, 1996). Therefore, the constraints are removed on the control inputs for this research by setting their values to negative and positive infinity for the minimum and maximum constraints, respectively. The constraints are, therefore, implemented only on the controlled outputs based on the steady state operating conditions of the original debutanizer distillation column upon which the model used in this research is based on as shown in Table 6.5 below.

**Table 6.5: Controlled output constraints**

Name	Min	Max
LCN_RVP	58	66
LPG_C5	0	0.5
Ovhd_Drum_Press	700	1155
Ovhd_Drum_Press_SV-PV	50	460
Debut_Diff_Press	10	30
Reboiler_Valve_Pos	9	60
Debut_Tray_24_Temp	60	80

Constraint softening values determine the amount by which the controller is permitted to violate the specified constraints. Variables with constraint softening factors set to zero are variables that have hard constraints which shall not be violated by the controller, typically due to safety related or high economic penalty reasons. However, the default values of one for the constraint softening factors is adopted for this research. The summary of the constraint softening factors is provided in Table 6.6.

**Table 6.6: Constraint softening**

Name	Min ECR	Max ECR
LCN_RVP	1	1
LPG_C5	1	1
Ovhd_Drum_Press	1	1
Ovhd_Drum_Press_SV-PV	1	1
Debut_Diff_Press	1	1
Reboiler_Valve_Pos	1	1
Debut_Tray_24_Temp	1	1

The input and output constraints and constraints softening factors given in Tables 6.5 and 6.6 are configured in the MPC Toolbox during the MPC controller configuration. The next section presents the selection of the reference tracking and increment suppression tuning weights.

### 6.3.4. Reference tracking and increment suppression tuning weights

As previously outlined in Chapter 3, the reference tuning weights define the priority of the controlled outputs to determine trade-offs. The larger the weighting factor, the more important the controlled output and the more important it is for the controller to keep its reference trajectory deviation to an absolute minimum. The MPC controller makes use of reference (or setpoint) tuning weights to determine the relative setpoint tracking priority of the controlled outputs and in cases where the reference tracking tuning weight is set to zero, the associated controlled output is provided the lowest priority and will tend to exhibit a steady state error larger than the other controlled outputs (Bemporad et al., 2015). In this research, the reference tuning weights for the controlled outputs are selected on a basis of trial-and-error during the controller tuning where the weights are adjusted until the dynamic response and steady state error are eliminated and then setting the performance tuning slider to Robust. Table 6.7 provides a summary of the final tuning weights for the controlled outputs.

**Table 6.7: Controlled output reference tracking weights**

Name	Initial Weight	Final Robust Tuning Setting Weight
LCN_RVP	60	8.12012
LPG_C5	200	27.0671
Ovhd_Drum_Press	15	2.03003
Ovhd_Drum_Press_SV-PV	15	2.03003
Debut_Diff_Press	60	8.12012
Reboiler_Valve_Pos	20	2.70671
Debut_Tray_24_Temp	25	3.38338

In addition, for increment suppression it is generally recommended to keep the MPC Toolbox tuning weights at their default of zero when the control inputs do not have specific setpoint target values that must be maintained (Bemporad et al., 2015). Therefore, for this research the control inputs are selected to each have a reference tracking weight of zero and an increment suppression (rate) weight left at the default and adjusted by setting the closed-loop performance tuning slider to Robust resulting in a value of 1.47781 as summarised in Table 6.8.

**Table 6.8: Control input tracking and increment suppression weights**

Name	Weight	Rate Weight	Target
Ovhd_Press	0	1.47781	Nominal
Reflux_Flow	0	1.47781	Nominal
Reboiler_Temp	0	1.47781	Nominal
Deeth_Feed_Flow	0	1.47781	Nominal
Deeth_Pressure	0	1.47781	Nominal
Deeth_Temp	0	1.47781	Nominal
LCN_Recycle_Flow	0	1.47781	Nominal

The reference tracking and increment suppression tuning weights given in Tables 6.7 and 6.8 are configured in the MPC Toolbox during the MPC controller configuration. The following section provides a step-by-step procedure to configure the MPC controller in the

MATLAB/Simulink MPC Toolbox followed by a closed-loop simulation case study to investigate the suitability of the selected controller design and tuning parameters .

### **6.3.5. Step-by-step design procedure for MPC controller design in Simulink**

The Simulink MPC Toolbox is a commercial software package by (Bemporad et al., 2015) mainly for analysing and prototyping MPC control systems (Bemporad, 2006). The MPC Toolbox is equipped with an interactive graphical user interface that aides in the configuration of the MPC controller as a MATLAB object that can be instantiated in Simulink simulation models. The MPC controller for this research is based on a seventh order step response prediction model of the debutanizer distillation process which is developed in Chapter 4 and the MPC controller is included as part of the Simulink simulation model for this plant. The step-by-step procedure provided below with illustrations is followed to configure the MPC controller in the MPC Toolbox.

#### **Step 1: Start Simulink**



**Figure 6.3: Simulink application**

## Step 2: Configure the Plant Model Structure

The seventh order step response prediction model of the debutanizer distillation process is configured in Simulink. The model can be broken down into four parts; Part 1) the MPC controller, Part 2) the DCS regulatory PID controllers, Part 3) the ambient temperature disturbance and, Part 4) the debutanizer distillation process transfer functions. The complete Simulink model is given in Figure 6.4 and the four parts are given in Figures 6.5 – 6.8 for clarity of the model details.

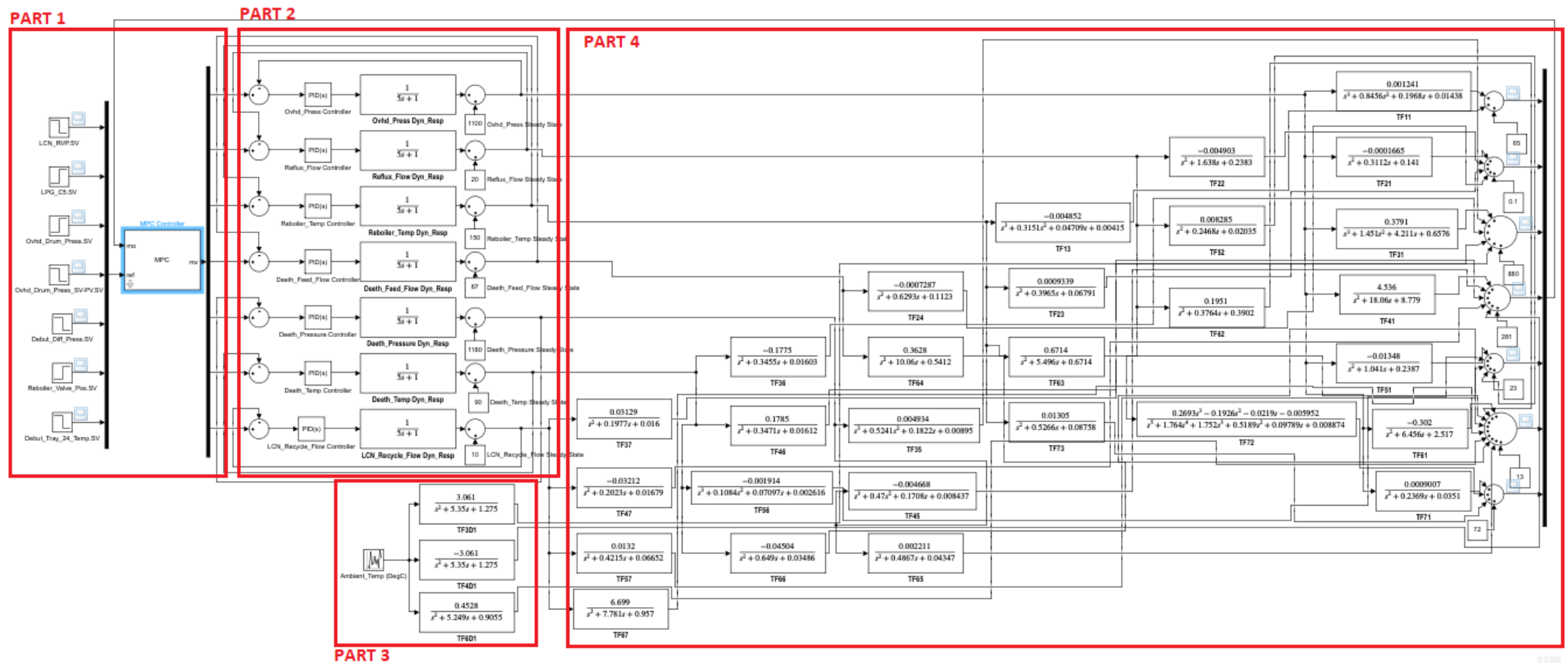


Figure 6.4: Seventh order step response prediction model of the debutanizer distillation process configured in Simulink



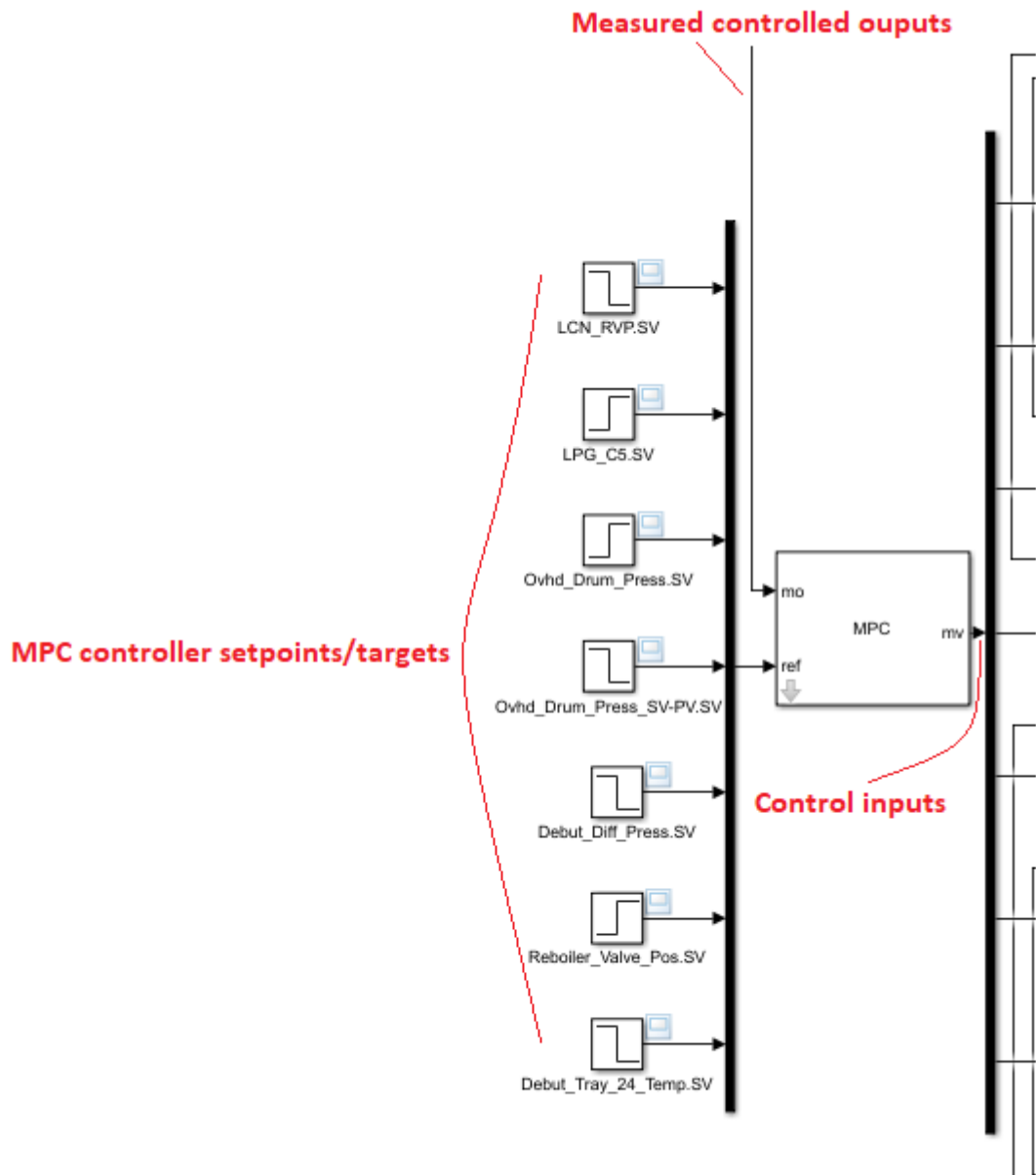
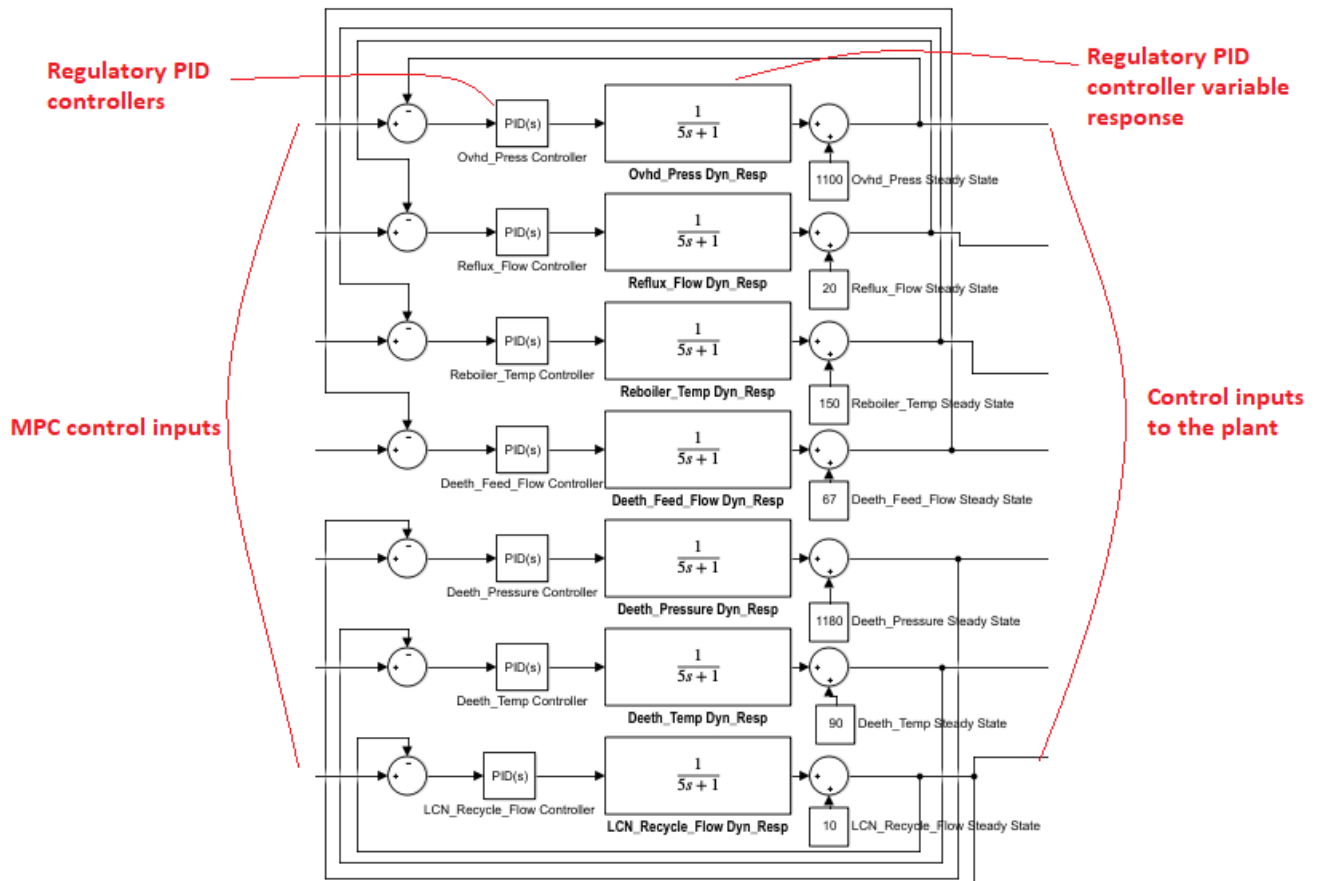


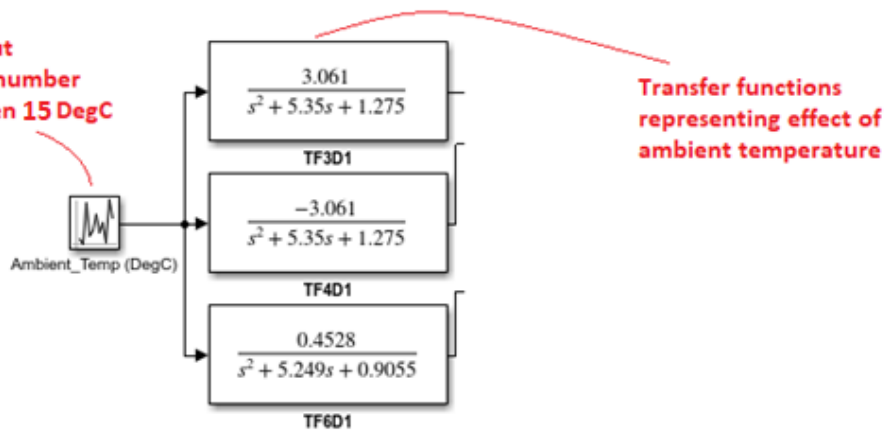
Figure 6.5: Simulink model Part 1 - MPC controller



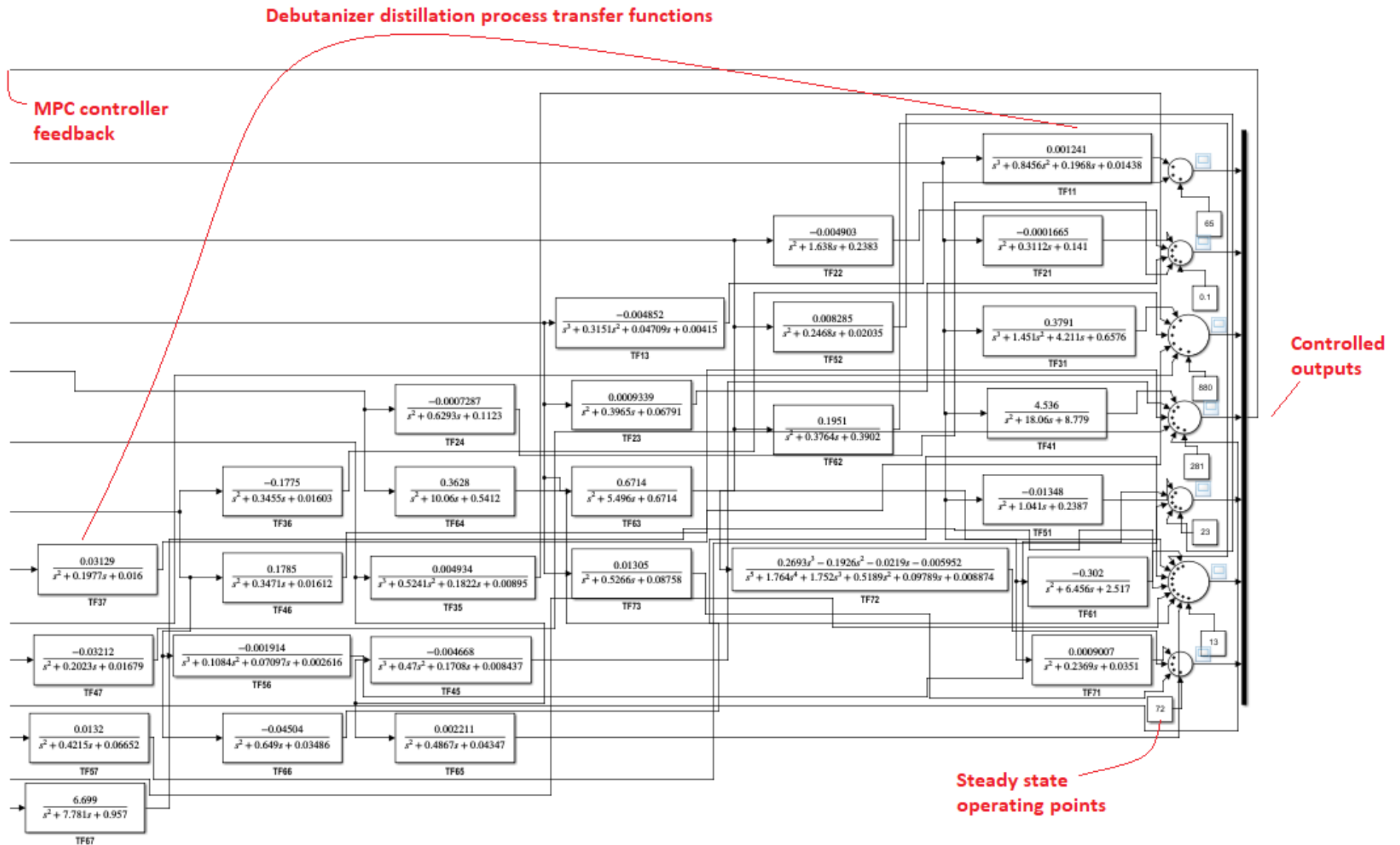
**Figure 6.6: Simulink model Part 2 - DCS regulatory PID controllers**

The PID controller gain settings for the regulatory PID controllers are obtained using the MATLAB/Simulink PID Tuner and are identical for all the controllers since all the lower level regulatory PID controller dynamics are assumed to be ideally represented by a first-order plus dead time (FOPTD) transfer function approximation. The PID controller gains for the DCS controllers in model are set at  $K_p = 5.47$ ,  $\tau_I = 2.57$  and  $\tau_D = -0.84$  where  $K_p$  is the proportional gain,  $\tau_I$  is the integral gain, and  $\tau_D$  is the derivative gain with a Filter Coefficient,  $N = 3.19$ . The PID controllers are tuned to exhibit good setpoint tracking without steady-state error.

**Ambient temperature input represented by a random number signal with a range between 15 DegC to 38 DegC**



**Figure 6.7: Simulink model Part 3 - Ambient temperature disturbance**



**Figure 6.8: Simulink model Part 4 - debutanizer distillation process transfer functions**

### Step 3: Open MPC Designer App

Double click on the MPC controller to open the Block Parameters Window. Click on Design to Open the MPC Designer App.

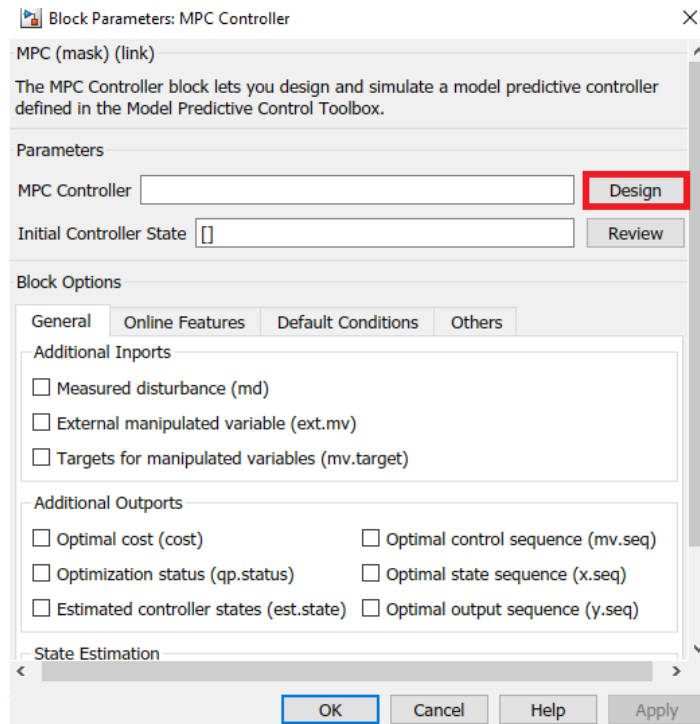


Figure 6.9: MPC Controller Block Parameters

### Step 4: Specify MPC Structure

Click on MPC Structure.

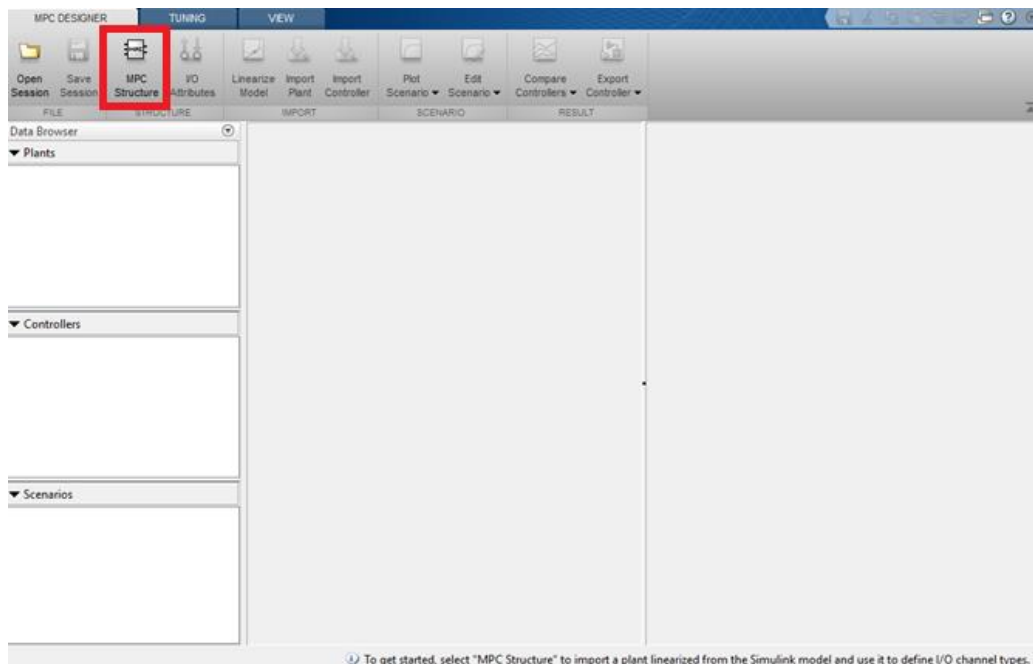
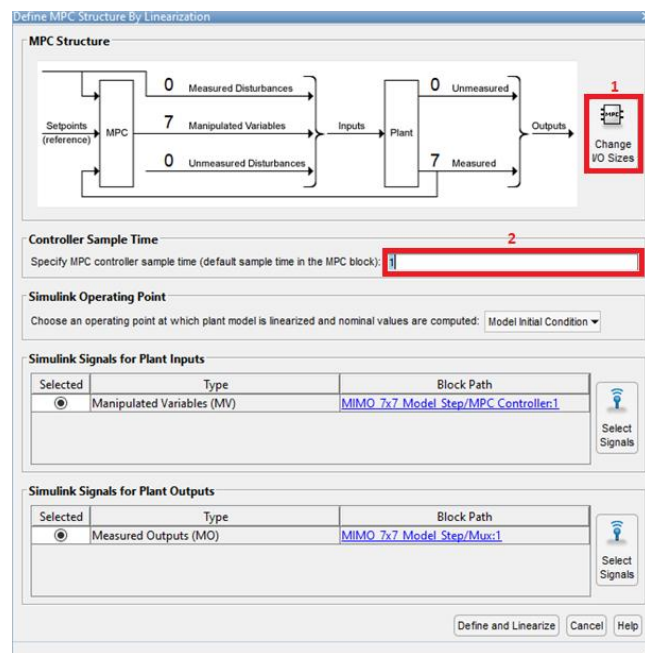


Figure 6.10: MPC Designer App

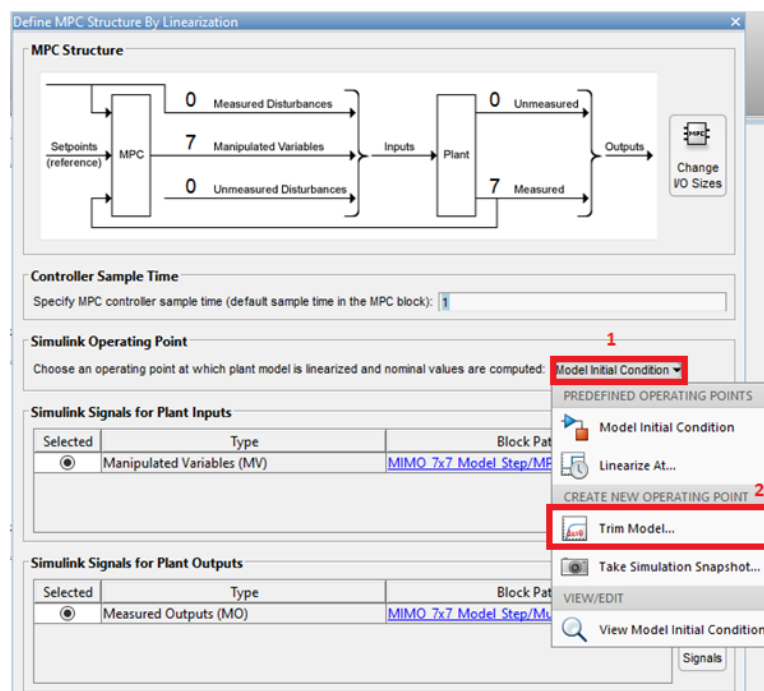
Click on Change I/O Sizes to specify the number of inputs and outputs. The sample time specified is 1 second.



**Figure 6.11: MPC Controller Structure**

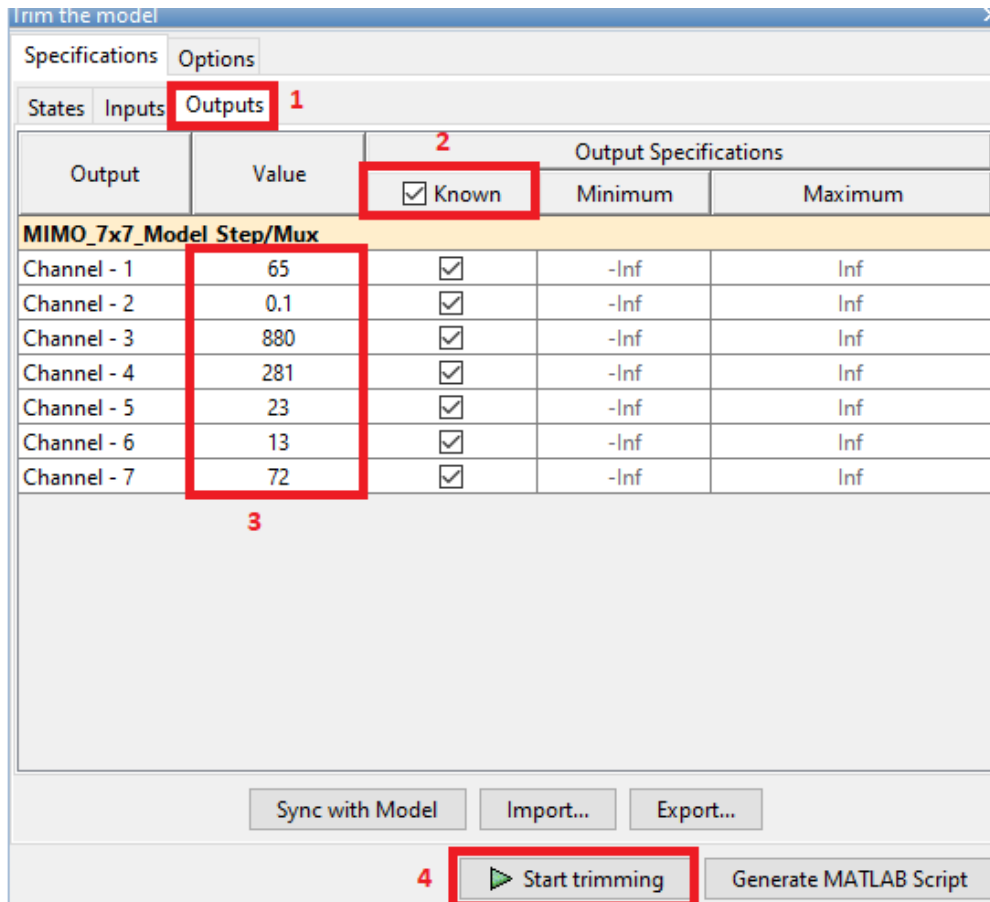
**Step 5: Define steady state operating point**

Create a new operating point by selecting the Model Initial Condition drop-down menu and click on Trim Model.



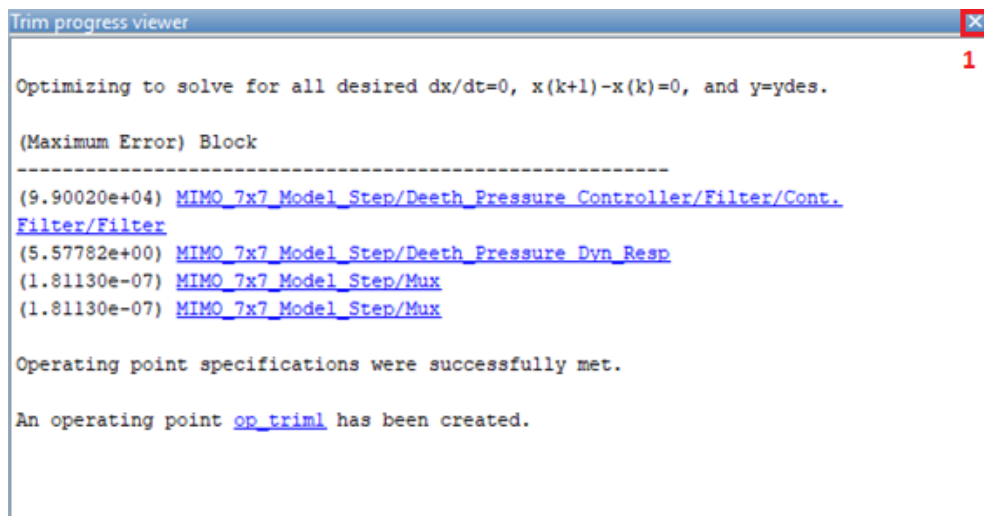
**Figure 6.12: Trim Model**

Specify the nominal controlled output values under the Outputs tab in the Trim the Model Window. The nominal values are specified based on the operating point of the debutanizer distillation process. Click on Start trimming (4) to create a new operating point.



**Figure 6.13: Operating Point Specification**

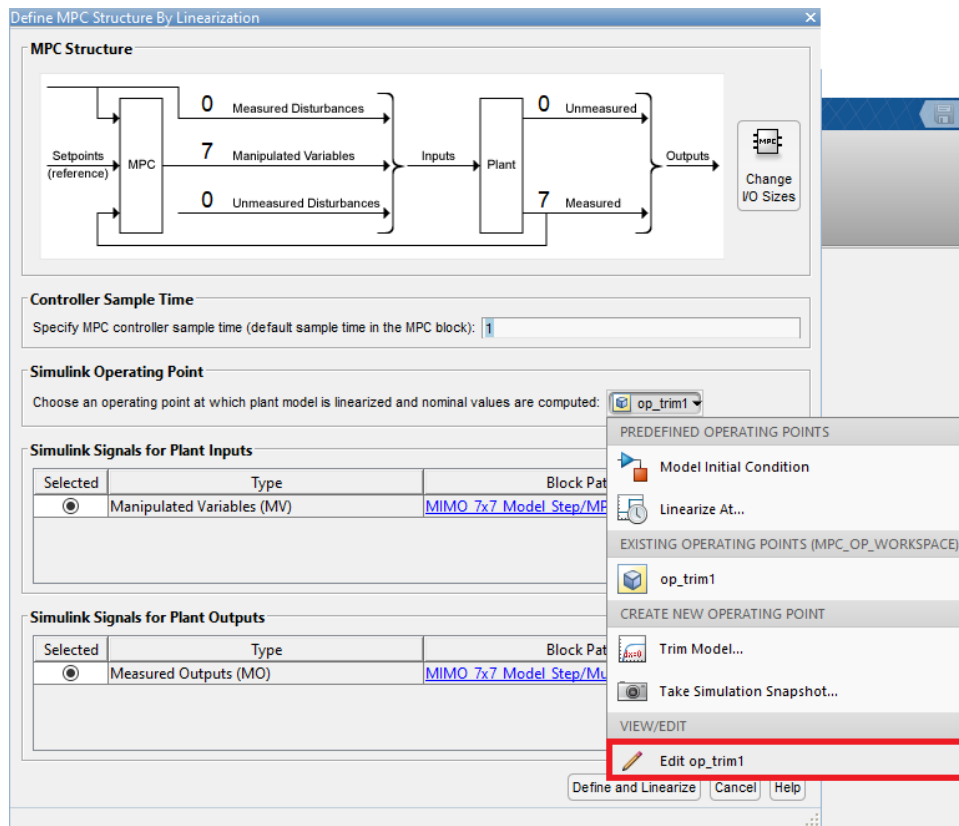
Once the new operating point has been successfully created, close the window.



**Figure 6.14: Trim Progress Viewer**

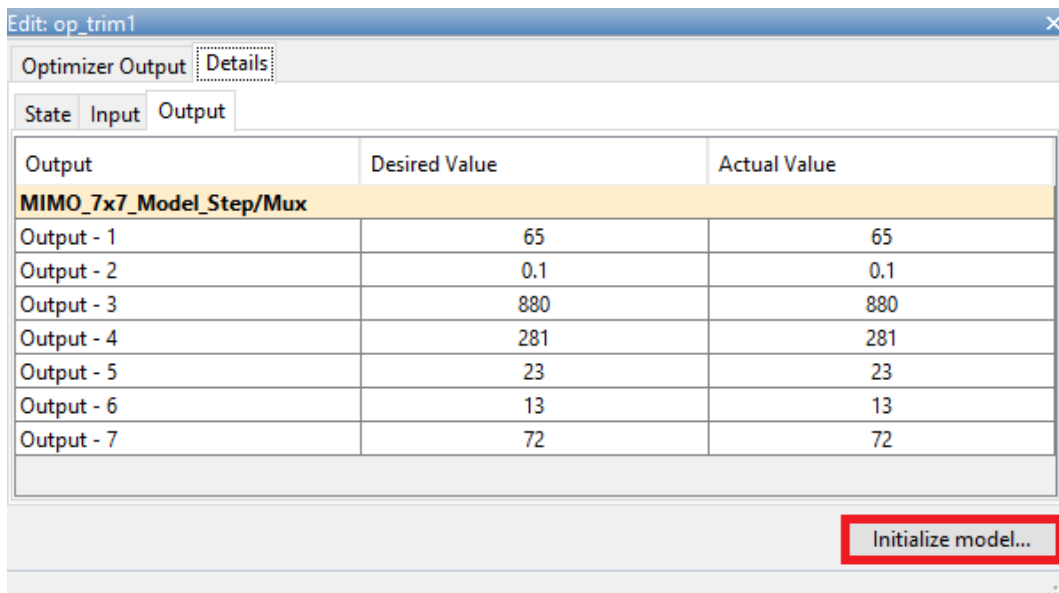
## Step 6: Initialize model around new operating point

Once the model trimming is completed, the operating point created is reviewed by selecting View/Edit Operating point from the Model Initial Condition from the MPC Structure Window.



**Figure 6.15: View/Edit Operating Point**

Click on Initialize model, save the operating point in the Workspace, and close the window.



**Figure 6.16: Initialize Model**

## Step 7: Define and Linearize Model

Linearize the model by clicking on Define and Linearize.

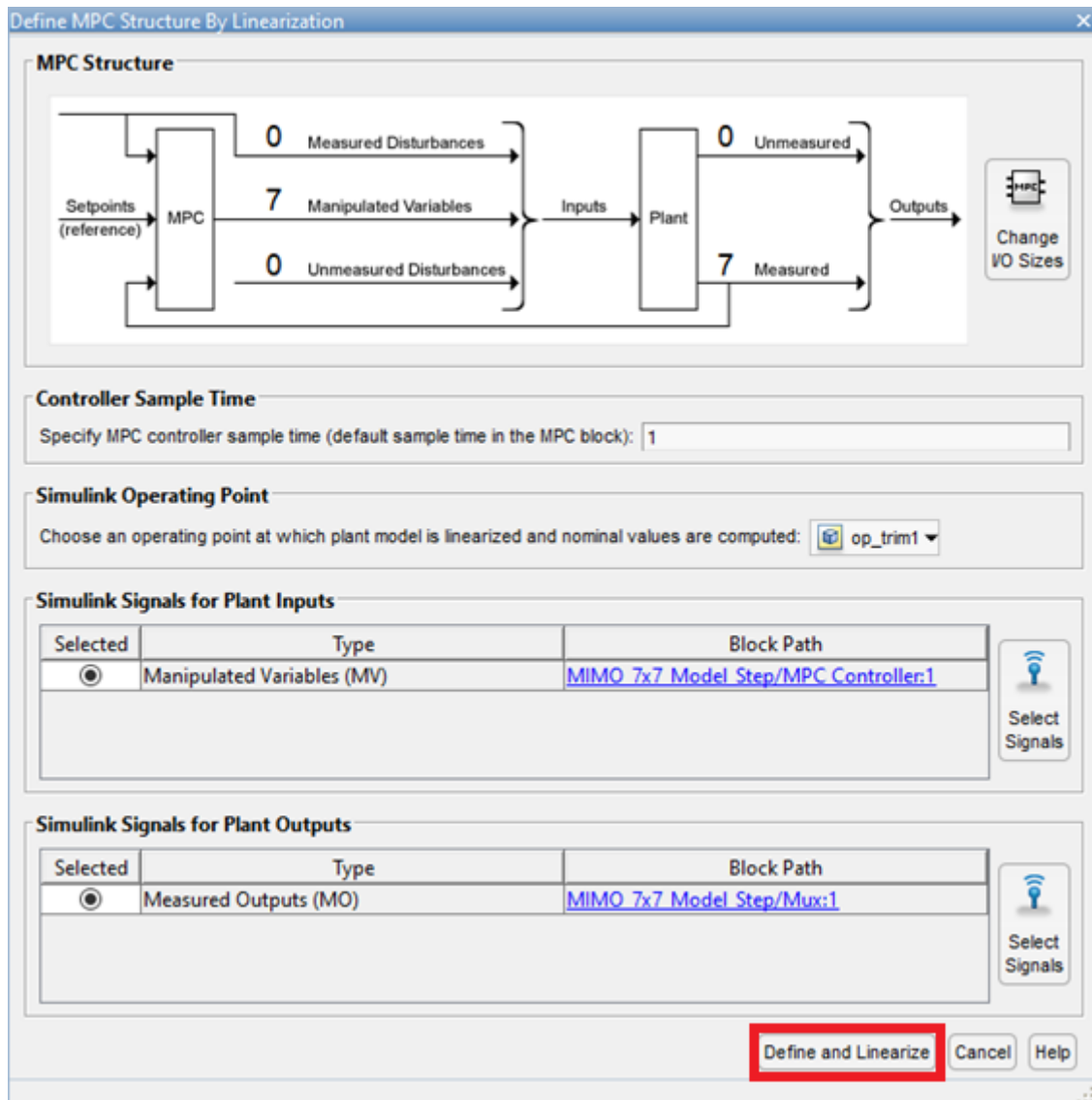


Figure 6.17: Define and Linearize Model

## Step 8: Specify the Input and Output Attributes

In the MPC Designer main window, click on I/O Attributes.



Figure 6.18: I/O Attributes



Specify the control input and controlled output tag names, units, nominal values, and scale factors as per Tables 6.2 and 6.3.

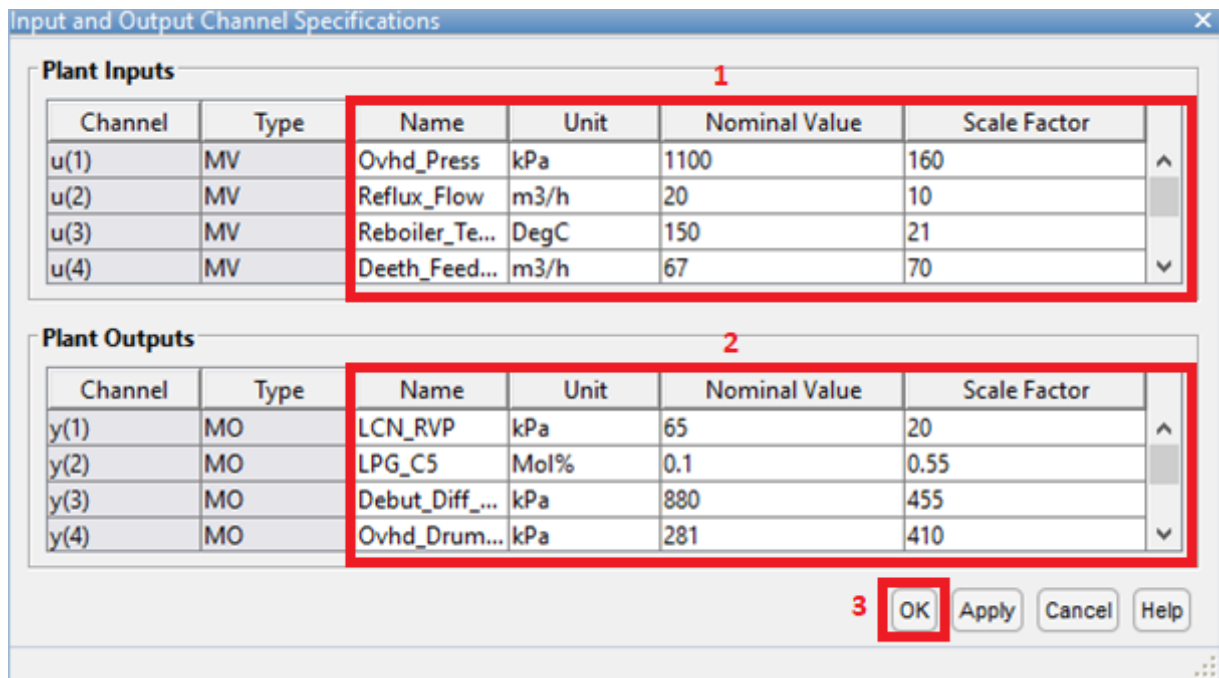


Figure 6.19: Input and Output Attributes Settings

**Step 9: Specify the MPC prediction horizon, and control horizon**

In the MPC Designer main window, select the Tuning tab and specify the prediction horizon, and control horizon as per Table 6.4.



Figure 6.20: Prediction horizon, and control horizon

**Step 10: Specify Constraints**

Under the Tuning tab, click on Constraints.

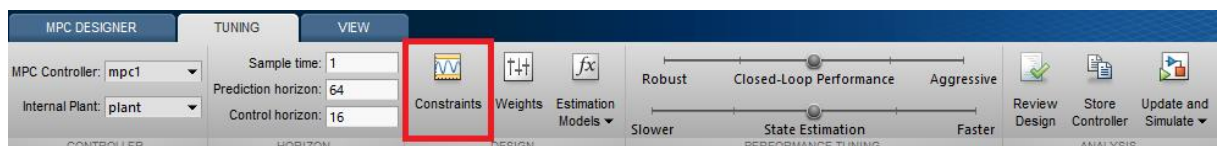
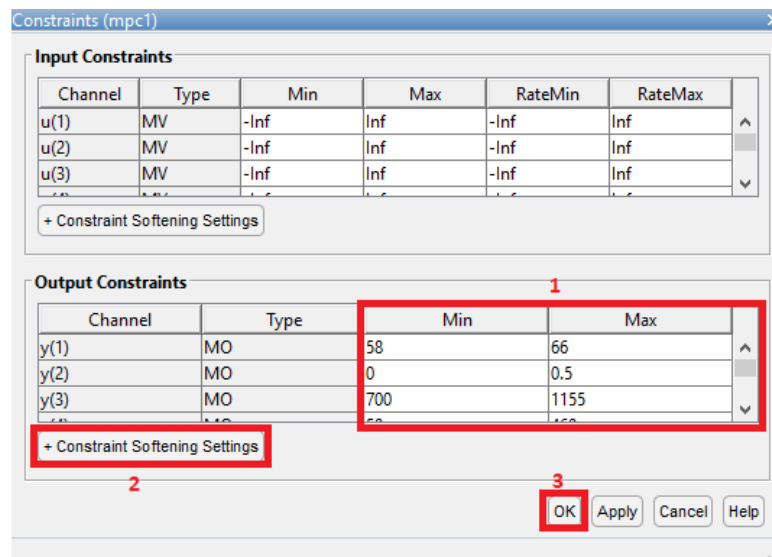


Figure 6.21: Constraints

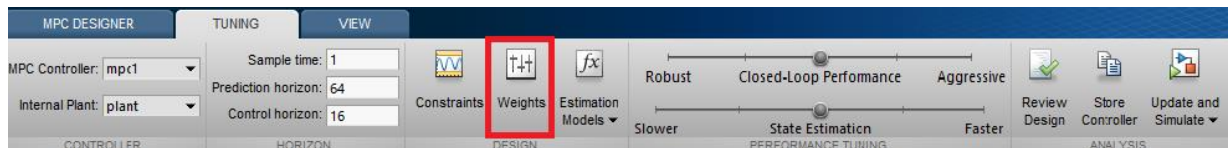
Specify the control input and controlled output constraint settings as per Table 6.5 and constraint softening factors as per Table 6.6.



**Figure 6.22: Constraints Settings**

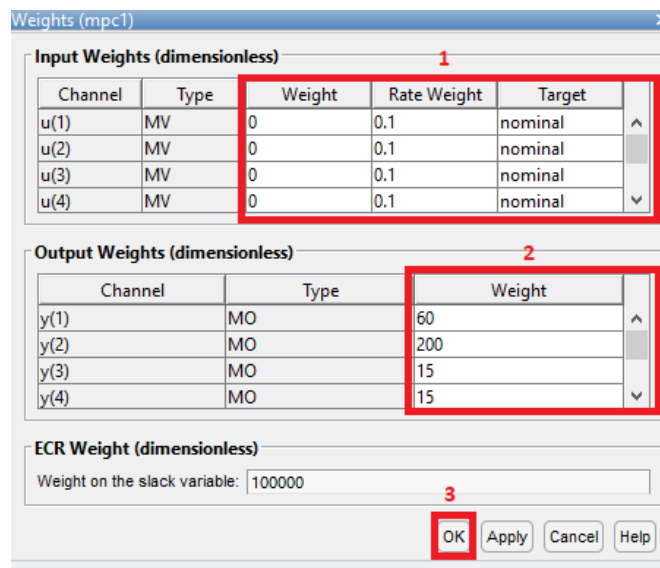
### Step 11: Specify the Tracking and Increment Suppression Weights

Under the Tuning tab, click on Weights.



**Figure 6.23: Tuning Weights**

Specify the tracking and increment suppression weights for the controlled outputs and control inputs as per Tables 6.7 and 6.8.



**Figure 6.24: Tracking and Increment Suppression Weights**

## Step 12: Closed-loop Performance Tuning

Under the Tuning tab, set the closed-loop performance tuning slider to Robust to ensure smooth control inputs and lower percentage overshoot of the controlled outputs.

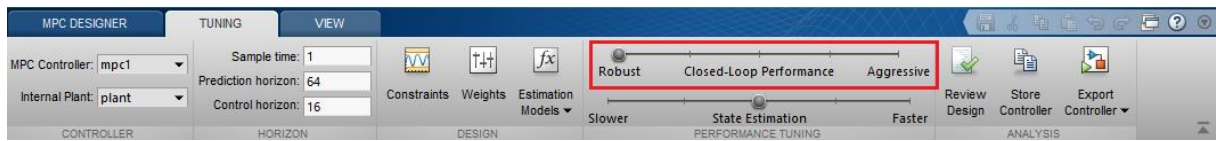


Figure 6.25: Closed-loop Performance Tuning

## Step 13: Review Design

Under the Tuning tab, click on Review Design. The controller design is reviewed making use of the Review Design feature of the MPC Designer App, which reviews errors in the specified design including analysis of the run-time stability and numerical values of the tuning weights (Bemporad et al., 2015).

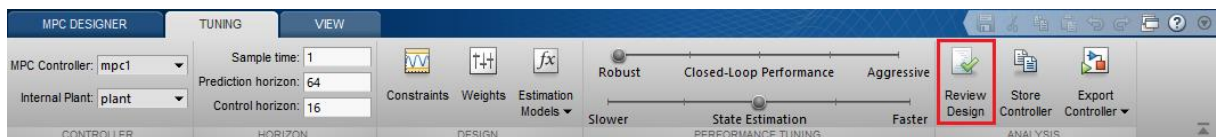


Figure 6.26: Review MPC Design

## Step 14: Export Controller

The last step of the procedure is to Export the designed controller into the Simulink model and update the MPC block with the configured controller settings and simulate the model. Under the Tuning tab, open the Export Controller drop down menu.

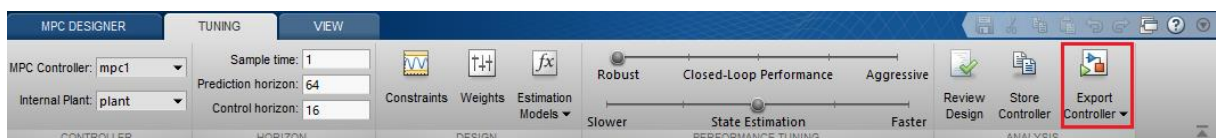


Figure 6.27: Update and Simulate drop down menu

Under the Export Controller drop down menu, select Update Block and Run Simulation.

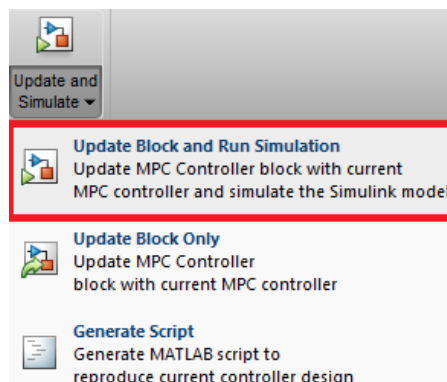


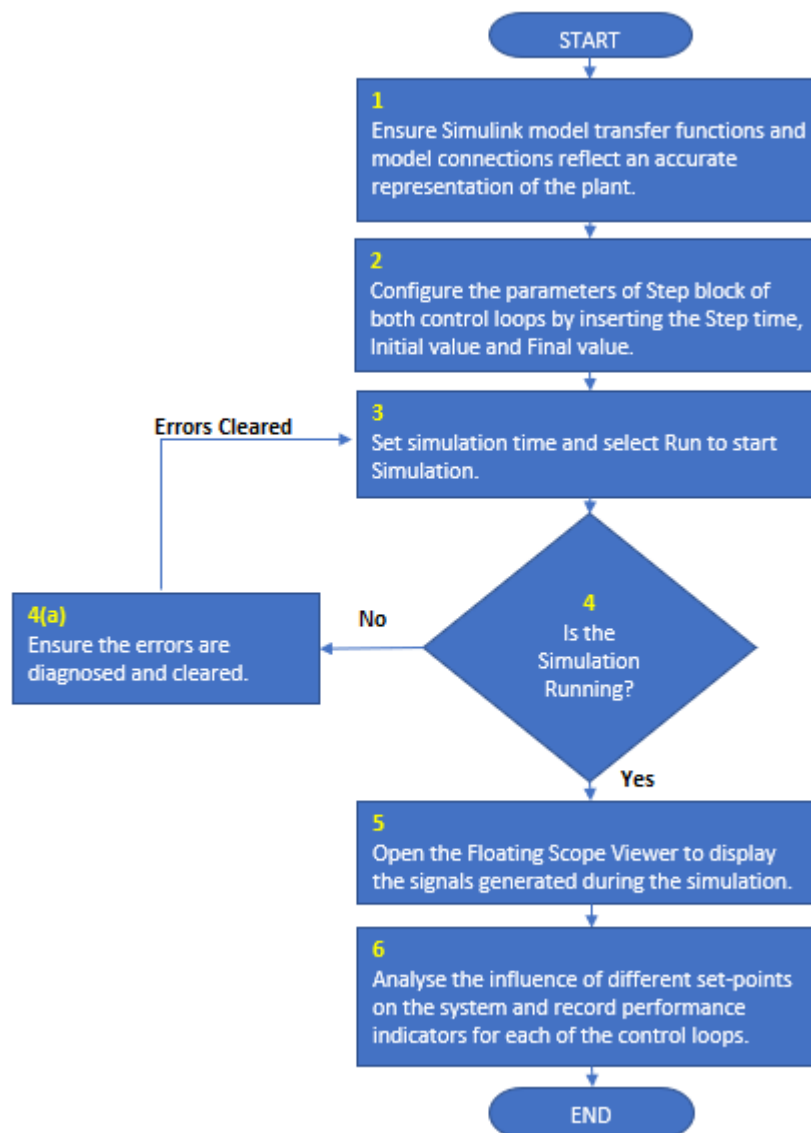
Figure 6.28: Update Block and Run Simulation

The MPC controller configuration procedure is complete. It is advisable to save the session as a MATLAB file (.mat) before closing the MPC Designer App for future reference. The controller is configured with the design parameters selected in the previous sections. The controller can be simulated in closed-loop in the Simulink model of the debutanizer distillation process. The next section presents the simulation case studies carried out in Simulink to investigate the effectiveness of the tuning parameters configured in the controller.

#### **6.4. Simulation case study in Simulink**

The Simulink model of the debutanizer distillation process presented in the previous section is simulated in closed loop with the MPC controller designed using the MPC Toolbox to investigate the effectiveness of the configured tuning parameters for closed loop performance. The system is simulated first without disturbances and followed by simulations with disturbances included at the system outputs. Similar to the simulation study of the previous chapter, the simulation study presented in this section follows a pre-defined simulation plan as outlined by the flow chart shown in Figure 6.29.

The flow chart consists of six steps. The first step is to ensure that the configured Simulink model transfer functions and model connections reflect an accurate representation of the plant and that all typing errors have been identified and removed. The second step is to configure the parameters of Step input block for the control loops by inserting the Step time, Initial value, and Final value parameters. The third step is to appropriately set the simulation time and select Run to start the Simulation. The fourth step is to ensure that the simulation is running without errors and, if errors are present, to ensure the errors are diagnosed and cleared. The fifth step is to open the floating scope viewer to display the signals generated during the simulation. Lastly, the sixth step is to analyse the influence of different set-points on the system and record performance indicators for each of the control loops.



**Figure 6.29: Process flowchart for the MPC controller simulation study**

The flow chart establishes a consistent approach in simulating and observing the performance of the system. The setpoint step changes are entered in the Simulink Step blocks.

#### **6.4.1. Transient behaviour of the seventh order debutanizer distillation process**

The closed loop simulation is carried out in Simulink and is presented in this section. The setpoint cases for the step response tests to investigate the transient behaviour are varied near their steady state ranges as outlined in Table 6.9 below.

**Table 6.9: Case study of set points for the seventh order system**

Case #	Loop Name	Initial Setpoint	Final Setpoint	Step Size
6.9.1	LCN_RVP	65 kPa	63 kPa	-2 kPa
	LPG_C5	0.1 Mol%	0.3 Mol%	+0.2 Mol%
	Ovhd_Drum_Press	880 kPa	1100 kPa	+220 kPa
	Ovhd_Drum_Press_SV-PV	281 kPa	400 kPa	+119 kPa
	Debut_Diff_Press	23 kPa	15 kPa	-8 kPa
	Reboiler_Valve_Pos	13 %	20 %	+7 %
	Debut_Tray_24_Temp	72 DegC	65 DegC	-7 DegC
6.9.2	LCN_RVP	63 kPa	60 kPa	-3 kPa
	LPG_C5	0.3 Mol%	0.5 Mol%	+0.2 Mol%
	Ovhd_Drum_Press	1100 kPa	800 kPa	-300 kPa
	Ovhd_Drum_Press_SV-PV	400 kPa	200 kPa	-200 kPa
	Debut_Diff_Press	15 kPa	11 kPa	-4 kPa
	Reboiler_Valve_Pos	20 %	55 %	+35 %
	Debut_Tray_24_Temp	65 DegC	61 DegC	-4 DegC
6.9.3	LCN_RVP	60 kPa	63 kPa	+3 kPa
	LPG_C5	0.5 Mol%	0.01 Mol%	-0.49 Mol%
	Ovhd_Drum_Press	800 kPa	700 kPa	-100 kPa
	Ovhd_Drum_Press_SV-PV	200 kPa	80 kPa	-120 kPa
	Debut_Diff_Press	11 kPa	25 kPa	+14 kPa
	Reboiler_Valve_Pos	55 %	30 %	-25 %
	Debut_Tray_24_Temp	61 DegC	75 DegC	+14 DegC
6.9.4	LCN_RVP	63 kPa	66 kPa	+3 kPa
	LPG_C5	0.01 Mol%	0.41 Mol%	+0.4 Mol%
	Ovhd_Drum_Press	700 kPa	820 kPa	+120 kPa
	Ovhd_Drum_Press_SV-PV	80 kPa	55 kPa	-25 kPa
	Debut_Diff_Press	25 kPa	29 kPa	+4 kPa
	Reboiler_Valve_Pos	30 %	10 %	-20 %
	Debut_Tray_24_Temp	75 DegC	79 DegC	+4 DegC
6.9.5	LCN_RVP	66 kPa	65 kPa	-1 kPa
	LPG_C5	0.41 Mol%	0.1 Mol%	-0.31 Mol%
	Ovhd_Drum_Press	820 kPa	880 kPa	+60 kPa
	Ovhd_Drum_Press_SV-PV	55 kPa	281 kPa	+226 kPa
	Debut_Diff_Press	29 kPa	23 kPa	-6 kPa
	Reboiler_Valve_Pos	10 %	13 %	+3 %
	Debut_Tray_24_Temp	79 DegC	72 DegC	-7 DegC

The simulation results showing the closed loop transient behaviour are presented in the Figures 6.30 – 6.34 below.

Figure 6.30 shows the dynamic response to a -2 kPa step change in the LCN RVP setpoint; a +0.2 Mol% step change in the LPG C5 Concentration setpoint; a +220 kPa step change in the Overhead Drum Pressure setpoint; a +119 kPa step change in the Overhead Drum Pressure SV-PV Gap setpoint; a -8 kPa step change in the Debutanizer Differential Pressure setpoint; a +7 % step change in the Debutanizer Reboiler Valve Position setpoint and a -7 DegC step change in the Tray 24 Temperature setpoint.

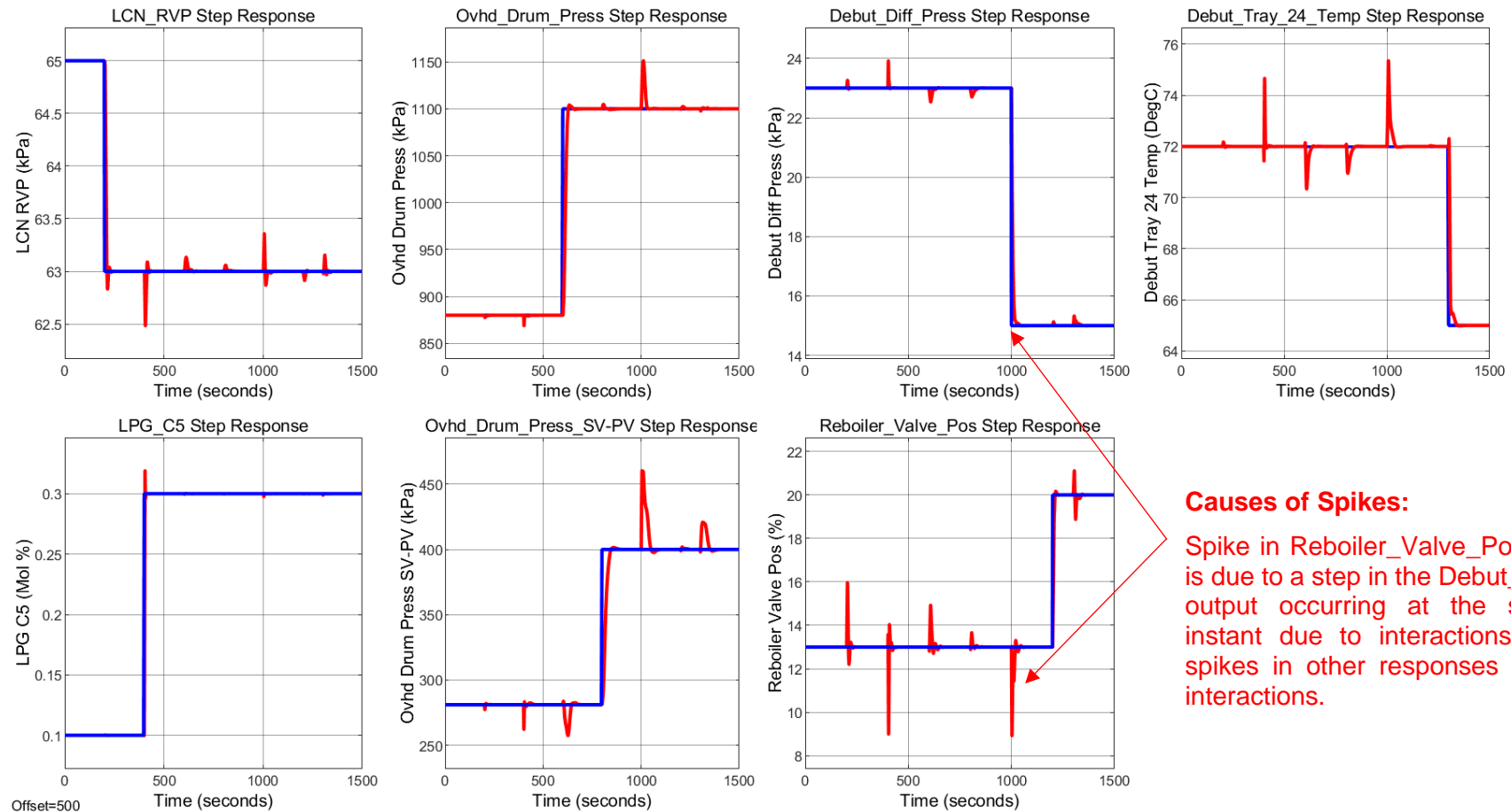


Figure 6.30: Case #6.9.1 – Dynamic step response

Figure 6.31 shows the dynamic response to a -3 kPa step change in the LCN RVP setpoint; a +0.2 Mol% step change in the LPG C5 Concentration setpoint; a -300 kPa step change in the Overhead Drum Pressure setpoint; a -200 kPa step change in the Overhead Drum Pressure SV-PV Gap setpoint; a -4 kPa step change in the Debutanizer Differential Pressure setpoint; a +35 % step change in the Debutanizer Reboiler Valve Position setpoint and a -4 DegC step change in the Tray 24 Temperature setpoint.

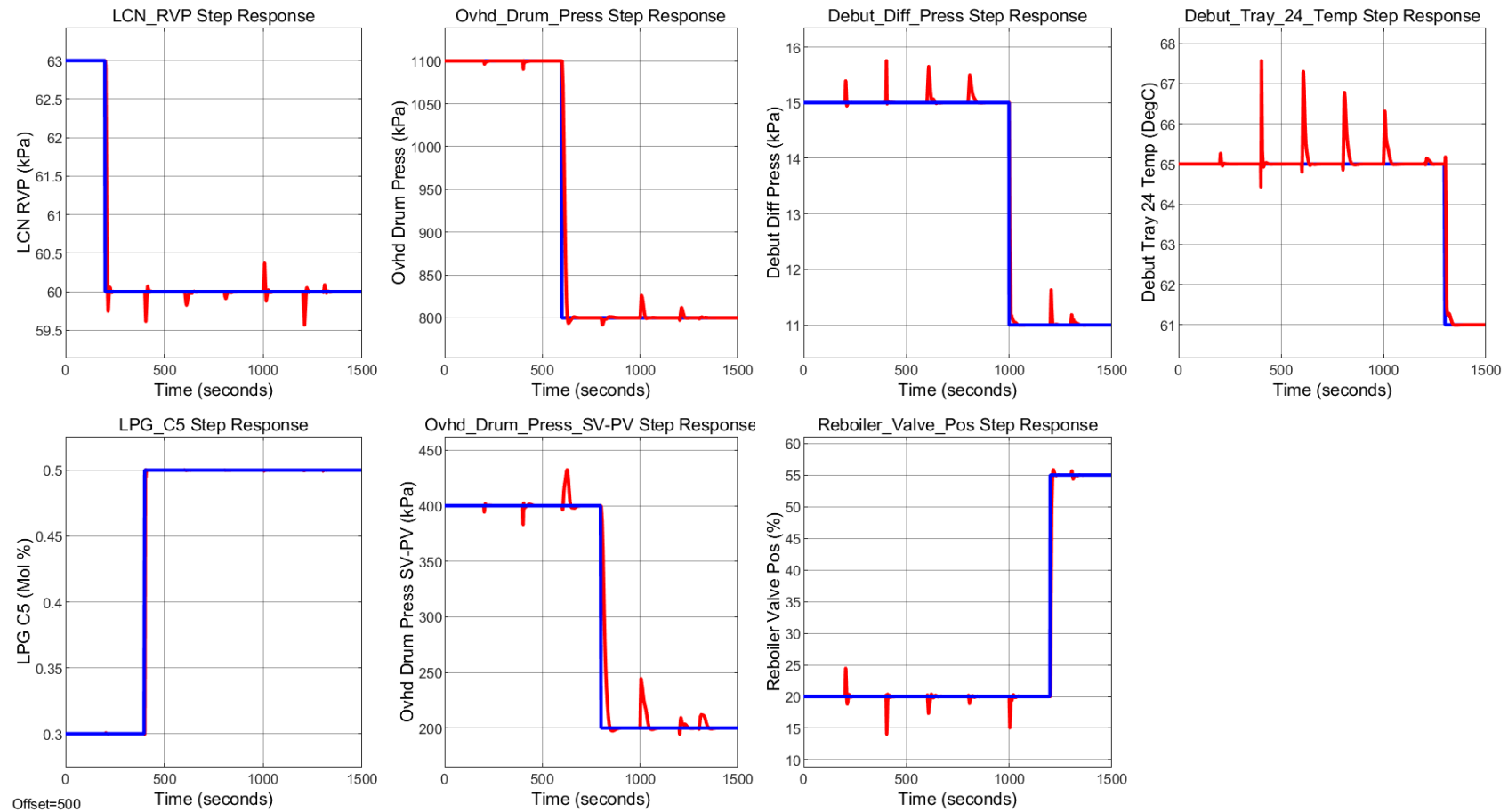


Figure 6.31: Case #6.9.2 – Dynamic step response



Figure 6.32 shows the dynamic response to a +3 kPa step change in the LCN RVP setpoint; a -0.49 Mol% step change in the LPG C5 Concentration setpoint; a -100 kPa step change in the Overhead Drum Pressure setpoint; a -120 kPa step change in the Overhead Drum Pressure SV-PV Gap setpoint; a +14 kPa step change in the Debutanizer Differential Pressure setpoint; a -25 % step change in the Debutanizer Reboiler Valve Position setpoint and a +14 DegC step change in the Tray 24 Temperature setpoint.

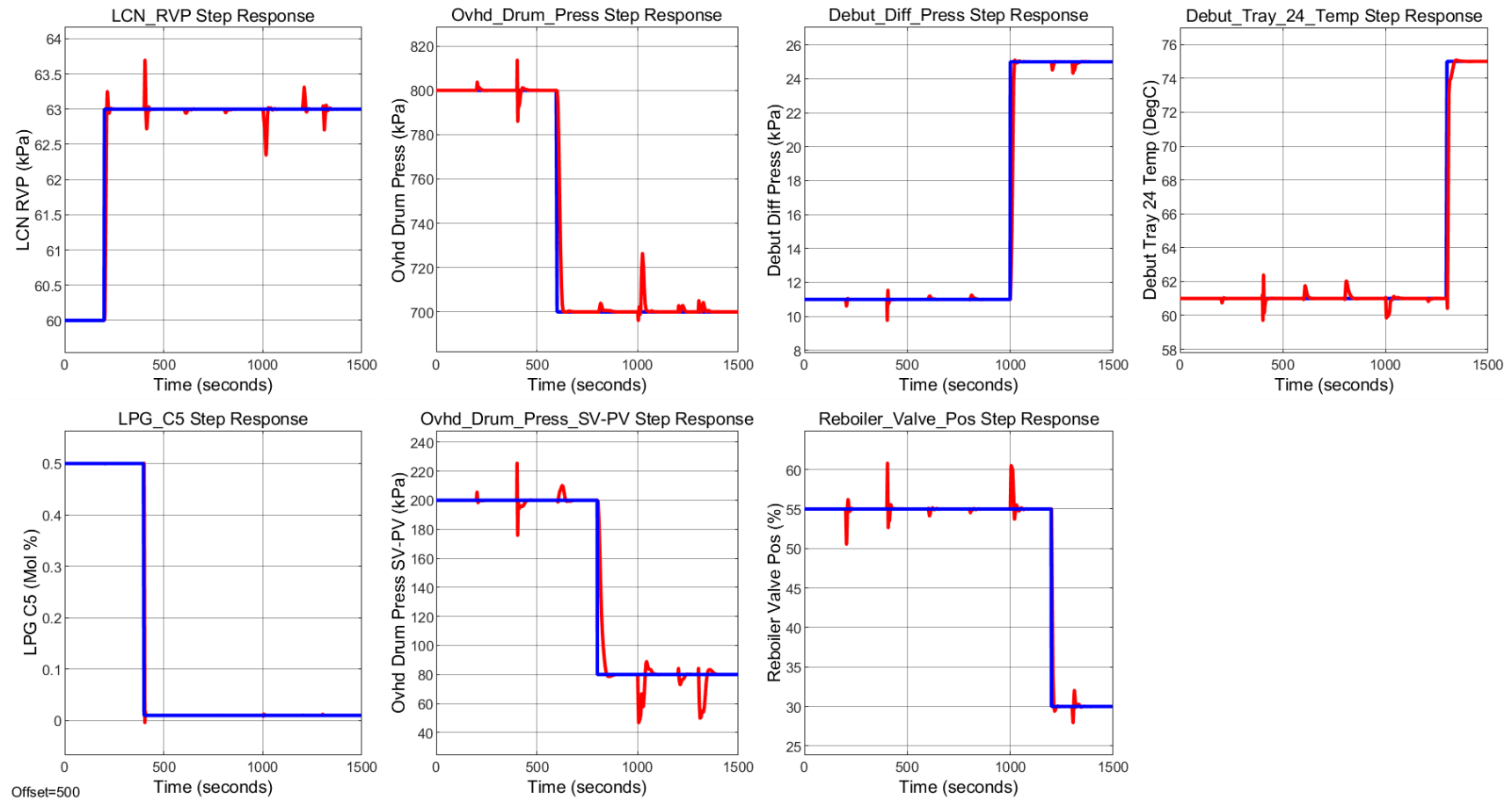


Figure 6.32: Case #6.9.3 – Dynamic step response

Figure 6.33 shows the dynamic response to a +3 kPa step change in the LCN RVP setpoint; a +0.4 Mol% step change in the LPG C5 Concentration setpoint; a +120 kPa step change in the Overhead Drum Pressure setpoint; a -25 kPa step change in the Overhead Drum Pressure SV-PV Gap setpoint; a +4 kPa step change in the Debutanizer Differential Pressure setpoint; a -20 % step change in the Debutanizer Reboiler Valve Position setpoint and a +4 DegC step change in the Tray 24 Temperature setpoint.

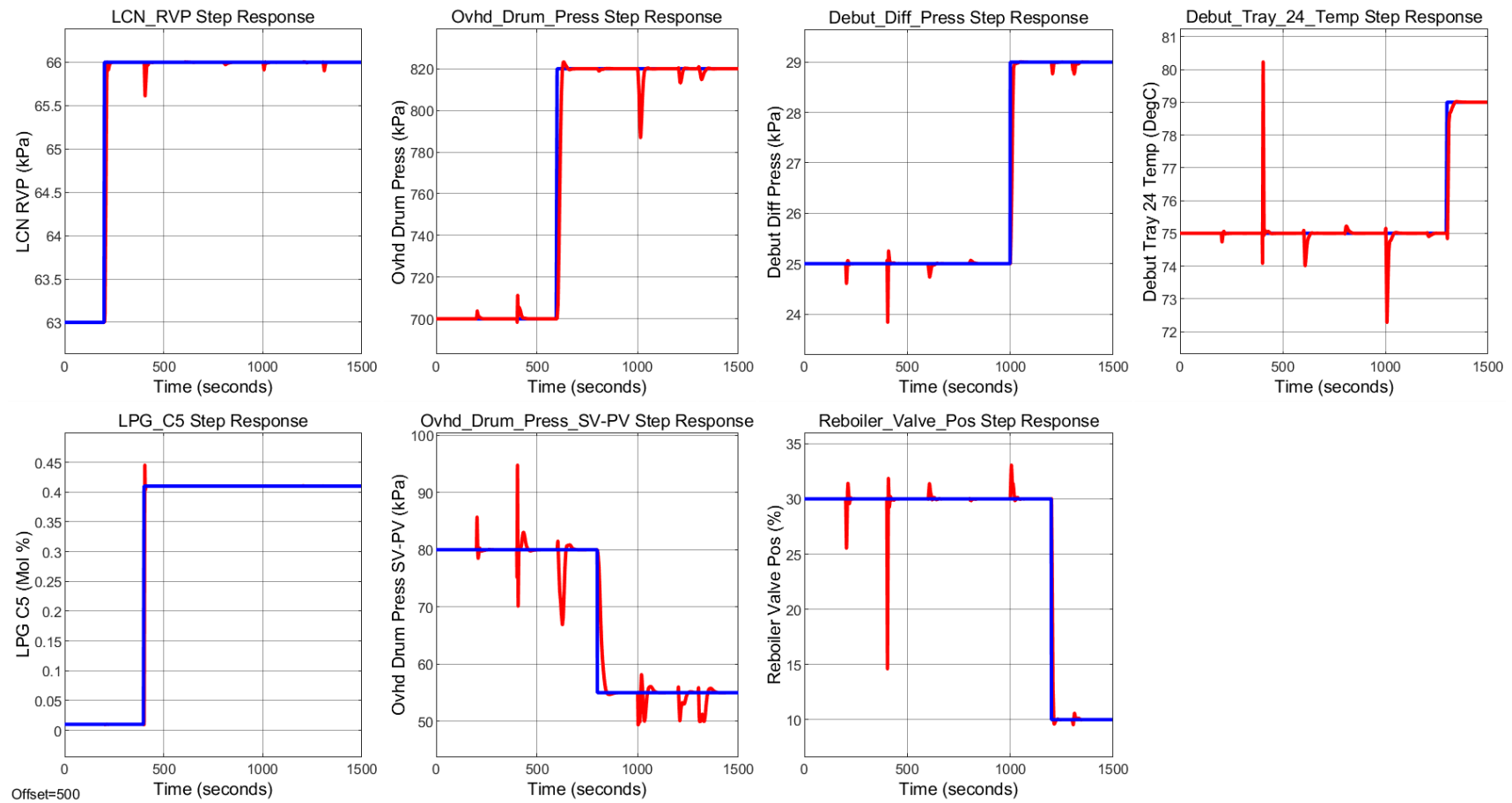


Figure 6.33: Case #6.9.4 – Dynamic step response

Figure 6.34 shows the dynamic response to a -1 kPa step change in the LCN RVP setpoint; a -0.31 Mol% step change in the LPG C5 Concentration setpoint; a +60 kPa step change in the Overhead Drum Pressure setpoint; a +226 kPa step change in the Overhead Drum Pressure SV-PV Gap setpoint; a -6 kPa step change in the Debutanizer Differential Pressure setpoint; a +3 % step change in the Debutanizer Reboiler Valve Position setpoint and a -7 DegC step change in the Tray 24 Temperature setpoint.

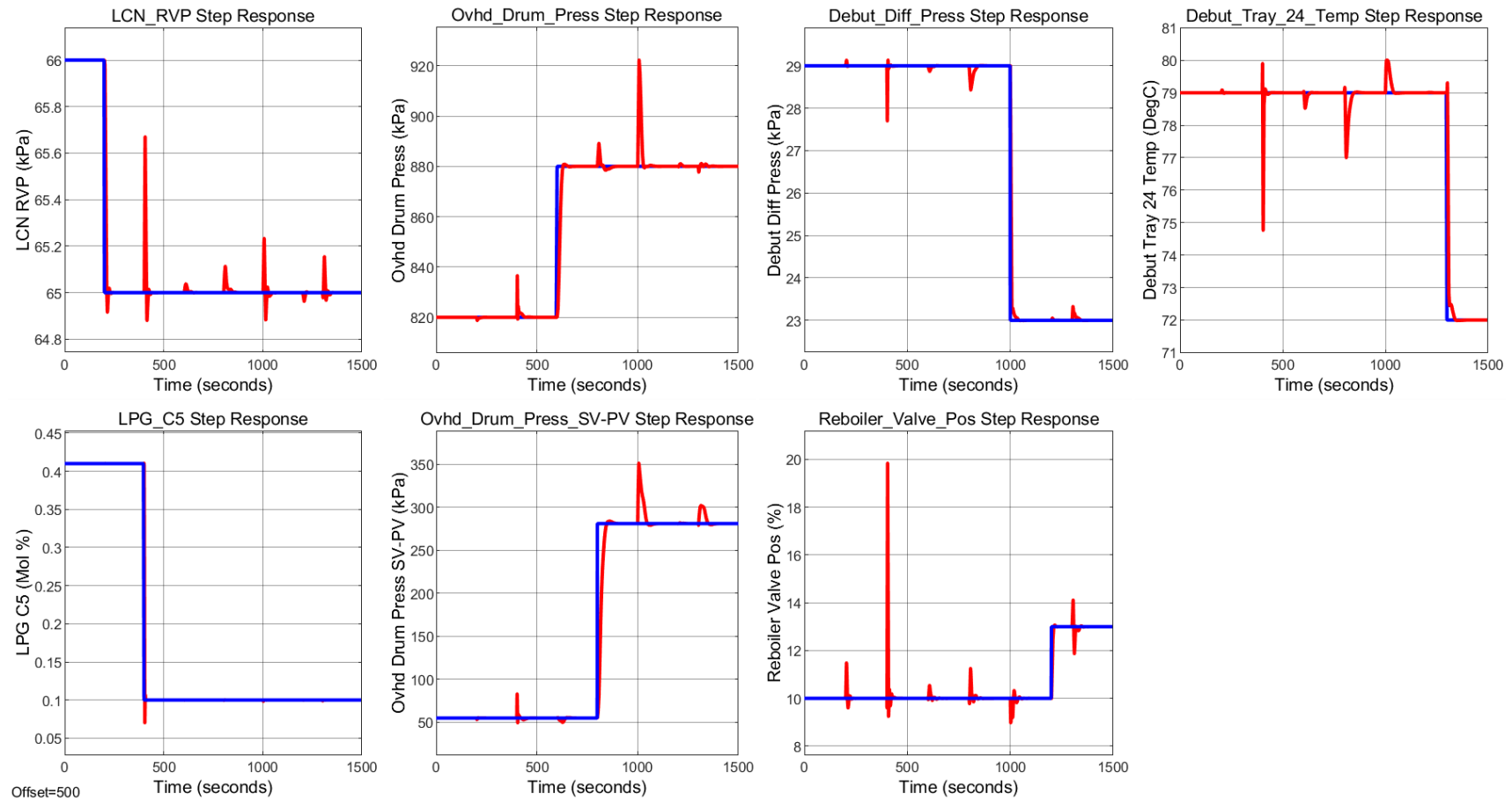


Figure 6.34: Case #6.9.5 – Dynamic step response

In section 6.4.3, a detailed discussion on the observed simulation results is provided. The next section presents the simulation case studies carried out in Simulink to investigate the influence of unmeasured output disturbances on the MPC controller performance.

#### 6.4.2. Transient behaviour of the seventh order debutanizer distillation process under the influence of unmeasured disturbances

The system is further simulated with unmeasured disturbances added to the controlled outputs to investigate the influence of disturbances on the performance of the MPC controller. The process outputs are influenced by ambient temperature as well as white noise as unmeasured disturbances. While white noise influences all the controlled outputs, the ambient temperature is modelled as influencing only the Overhead Drum Pressure (kPa), the Overhead Drum Pressure SV-PV Gap (kPa) and the Debutanizer Reboiler Valve Position (%) controlled outputs. This is in accordance with the original model of the debutanizer distillation process being studied in this research. For this research, the ambient temperature is represented by a Simulink Uniform Random Number block which outputs a uniformly distributed random signal configured with a range between 15 DegC to 38 DegC with an average of 23 DegC. White noise is represented by a Simulink Band-Limited White Noise block which generates normally distributed random numbers. The cases for the step response tests to investigate the influence of unmeasured disturbances on the system transient behaviour are presented in Table 6.10.

**Table 6.10: Simulation case study to investigate the influence of unmeasured disturbances**

Case #	Loop Name	Initial Setpoint	Final Setpoint	Step Size	White Noise
6.11.1	LCN_RVP	65 kPa	63 kPa	-2 kPa	±1E-4 kPa
	LPG_C5	0.1 Mol%	0.3 Mol%	+0.2 Mol%	±1E-5 Mol%
	Ovhd_Drum_Press	880 kPa	1100 kPa	+220 kPa	±1E-2 kPa
	Ovhd_Drum_Press_SV-PV	281 kPa	400 kPa	+119 kPa	±1E-2 kPa
	Debut_Diff_Press	23 kPa	15 kPa	-8 kPa	±1E-3 kPa
	Reboiler_Valve_Pos	13 %	20 %	+7 %	±1E-4 %
	Debut_Tray_24_Temp	72 DegC	65 DegC	-7 DegC	±1E-4 DegC
6.11.2	LCN_RVP	63 kPa	60 kPa	-3 kPa	±1E-4 kPa
	LPG_C5	0.3 Mol%	0.5 Mol%	+0.2 Mol%	±1E-5 Mol%
	Ovhd_Drum_Press	1100 kPa	800 kPa	-300 kPa	±1E-2 kPa
	Ovhd_Drum_Press_SV-PV	400 kPa	200 kPa	-200 kPa	±1E-2 kPa
	Debut_Diff_Press	15 kPa	11 kPa	-4 kPa	±1E-3 kPa
	Reboiler_Valve_Pos	20 %	55 %	+35 %	±1E-4 %
	Debut_Tray_24_Temp	65 DegC	61 DegC	-4 DegC	±1E-4 DegC
6.11.3	LCN_RVP	60 kPa	63 kPa	+3 kPa	±1E-4 kPa
	LPG_C5	0.5 Mol%	0.01 Mol%	-0.49 Mol%	±1E-5 Mol%
	Ovhd_Drum_Press	800 kPa	700 kPa	-100 kPa	±1E-2 kPa
	Ovhd_Drum_Press_SV-PV	200 kPa	80 kPa	-120 kPa	±1E-2 kPa
	Debut_Diff_Press	11 kPa	25 kPa	+14 kPa	±1E-3 kPa
	Reboiler_Valve_Pos	55 %	30 %	-25 %	±1E-4 %
	Debut_Tray_24_Temp	61 DegC	75 DegC	+14 DegC	±1E-4 DegC
6.11.4	LCN_RVP	63 kPa	66 kPa	+3 kPa	±1E-4 kPa
	LPG_C5	0.01 Mol%	0.41 Mol%	+0.4 Mol%	±1E-5 Mol%
	Ovhd_Drum_Press	700 kPa	820 kPa	+120 kPa	±1E-2 kPa
	Ovhd_Drum_Press_SV-PV	80 kPa	55 kPa	-25 kPa	±1E-2 kPa
	Debut_Diff_Press	25 kPa	29 kPa	+4 kPa	±1E-3 kPa
	Reboiler_Valve_Pos	30 %	10 %	-20 %	±1E-4 %

Case #	Loop Name	Initial Setpoint	Final Setpoint	Step Size	White Noise
	Debut_Tray_24_Temp	75 DegC	79 DegC	+4 DegC	±1E-4 DegC
6.11.5	LCN_RVP	66 kPa	65 kPa	-1 kPa	±1E-4 kPa
	LPG_C5	0.41 Mol%	0.1 Mol%	-0.31 Mol%	±1E-5 Mol%
	Ovhd_Drum_Press	820 kPa	880 kPa	+60 kPa	±1E-2 kPa
	Ovhd_Drum_Press_SV-PV	55 kPa	281 kPa	+226 kPa	±1E-2 kPa
	Debut_Diff_Press	29 kPa	23 kPa	-6 kPa	±1E-3 kPa
	Reboiler_Valve_Pos	10 %	13 %	+3 %	±1E-4 %
	Debut_Tray_24_Temp	79 DegC	72 DegC	-7 DegC	±1E-4 DegC

The simulation results showing the closed loop transient behaviour under the influence of unmeasured disturbances are presented in the Figures 6.35 – 6.39 below.

Figure 6.35 shows the dynamic response to a -2 kPa step change in the LCN RVP setpoint; a +0.2 Mol% step change in the LPG C5 Concentration setpoint; a +220 kPa step change in the Overhead Drum Pressure setpoint; a +119 kPa step change in the Overhead Drum Pressure SV-PV Gap setpoint; a -8 kPa step change in the Debutanizer Differential Pressure setpoint; a +7 % step change in the Debutanizer Reboiler Valve Position setpoint and a -7 DegC step change in the Tray 24 Temperature setpoint.

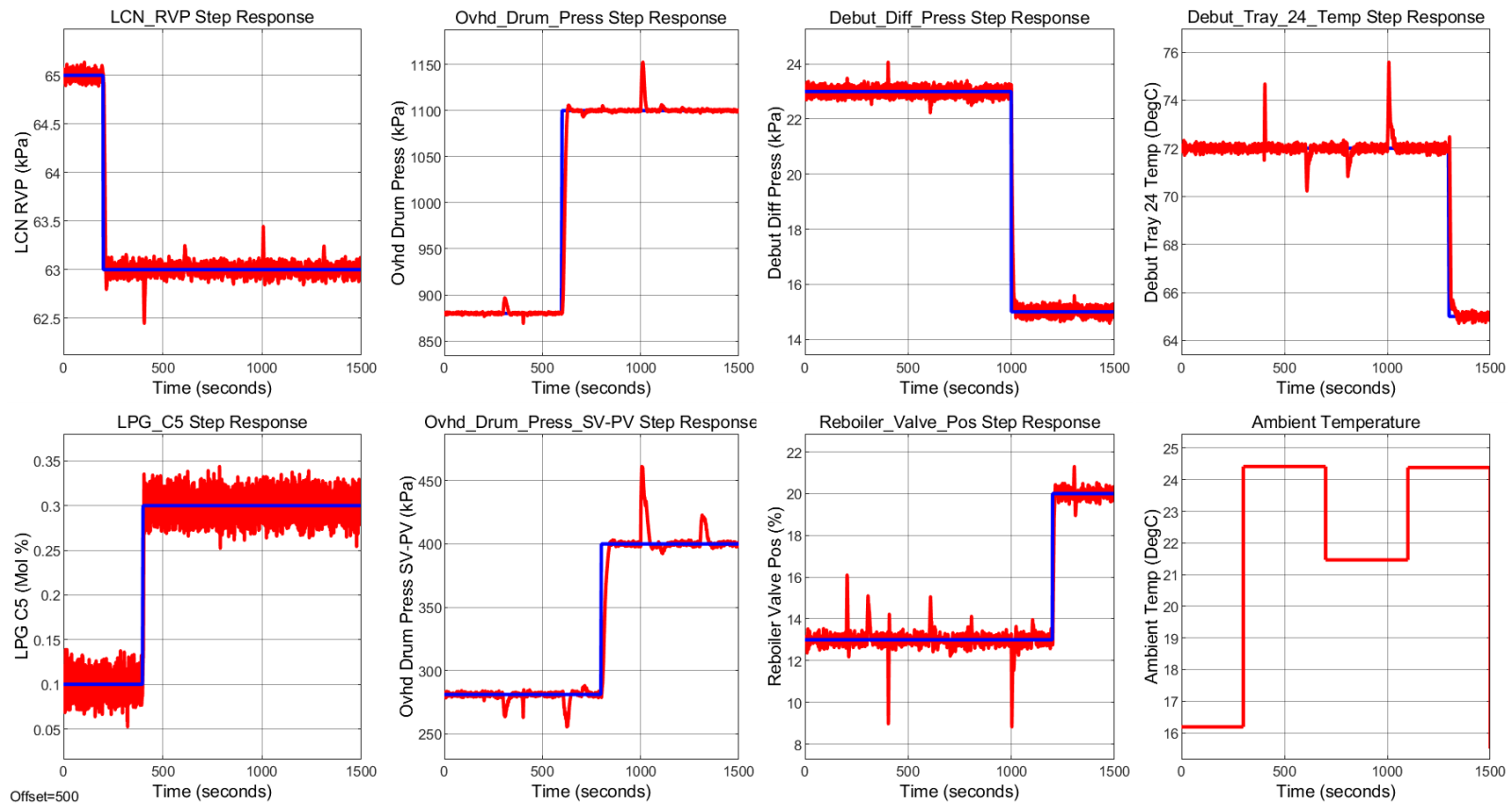


Figure 6.35: Disturbance Case #6.11.1 – Dynamic step response

Figure 6.36 shows the dynamic response to a -3 kPa step change in the LCN RVP setpoint; a +0.2 Mol% step change in the LPG C5 Concentration setpoint; a -300 kPa step change in the Overhead Drum Pressure setpoint; a -200 kPa step change in the Overhead Drum Pressure SV-PV Gap setpoint; a -4 kPa step change in the Debutanizer Differential Pressure setpoint; a +35 % step change in the Debutanizer Reboiler Valve Position setpoint and a -4 DegC step change in the Tray 24 Temperature setpoint.

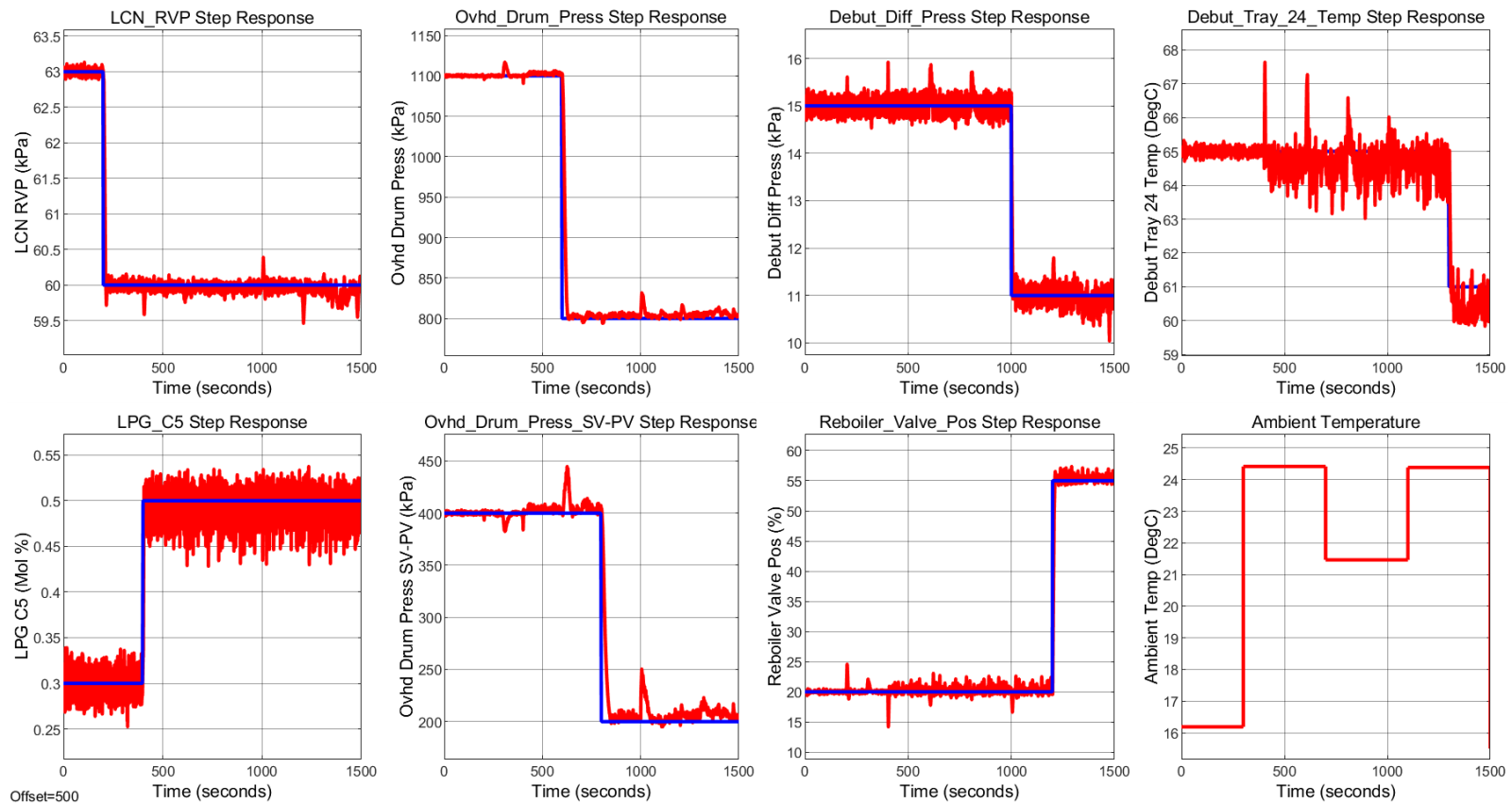


Figure 6.36: Disturbance Case #6.11.2 – Dynamic step response

Figure 6.37 shows the dynamic response to a +3 kPa step change in the LCN RVP setpoint; a -0.49 Mol% step change in the LPG C5 Concentration setpoint; a -100 kPa step change in the Overhead Drum Pressure setpoint; a -120 kPa step change in the Overhead Drum Pressure SV-PV Gap setpoint; a +14 kPa step change in the Debutanizer Differential Pressure setpoint; a -25 % step change in the Debutanizer Reboiler Valve Position setpoint and a +14 DegC step change in the Tray 24 Temperature setpoint.

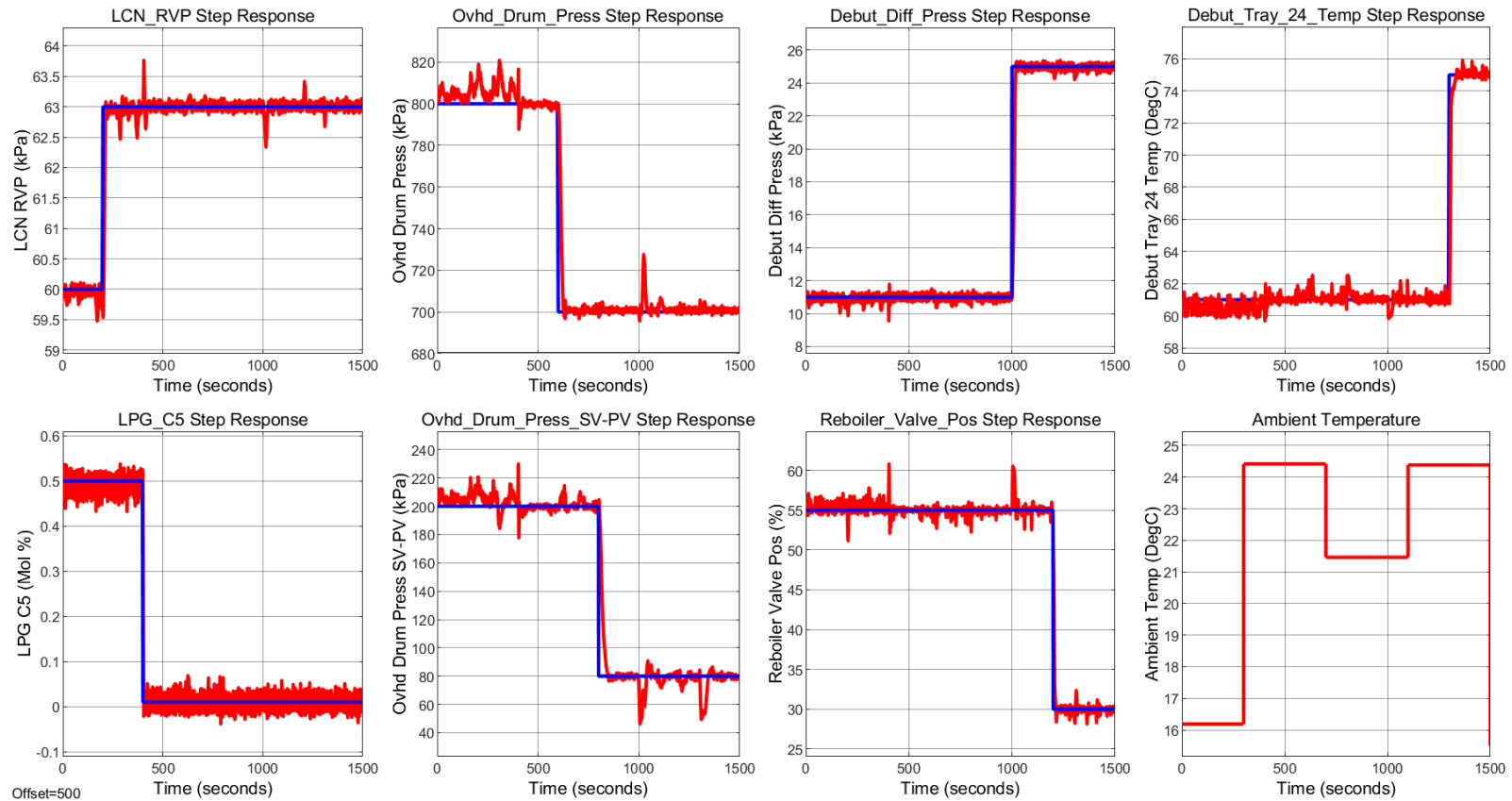


Figure 6.37: Disturbance Case #6.11.3 – Dynamic step response



Figure 6.38 shows the dynamic response to a +3 kPa step change in the LCN RVP setpoint; a +0.4 Mol% step change in the LPG C5 Concentration setpoint; a +120 kPa step change in the Overhead Drum Pressure setpoint; a -25 kPa step change in the Overhead Drum Pressure SV-PV Gap setpoint; a +4 kPa step change in the Debutanizer Differential Pressure setpoint; a -20 % step change in the Debutanizer Reboiler Valve Position setpoint and a +4 DegC step change in the Tray 24 Temperature setpoint.

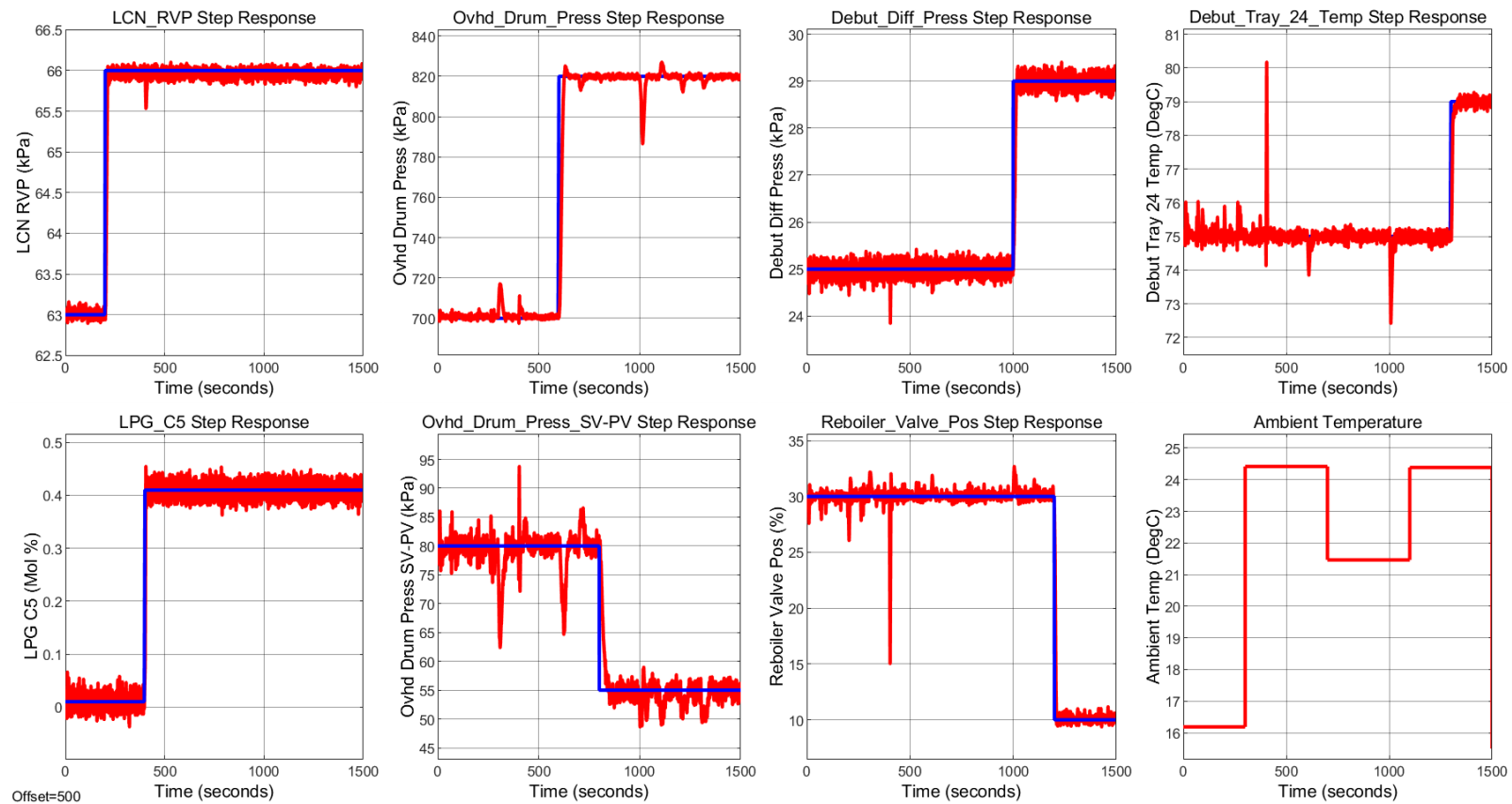


Figure 6.38: Disturbance Case #6.11.4 – Dynamic step response

Figure 6.39 shows the dynamic response to a -1 kPa step change in the LCN RVP setpoint; a -0.31 Mol% step change in the LPG C5 Concentration setpoint; a +60 kPa step change in the Overhead Drum Pressure setpoint; a +226 kPa step change in the Overhead Drum Pressure SV-PV Gap setpoint; a -6 kPa step change in the Debutanizer Differential Pressure setpoint; a +3 % step change in the Debutanizer Reboiler Valve Position setpoint and a -7 DegC step change in the Tray 24 Temperature setpoint.

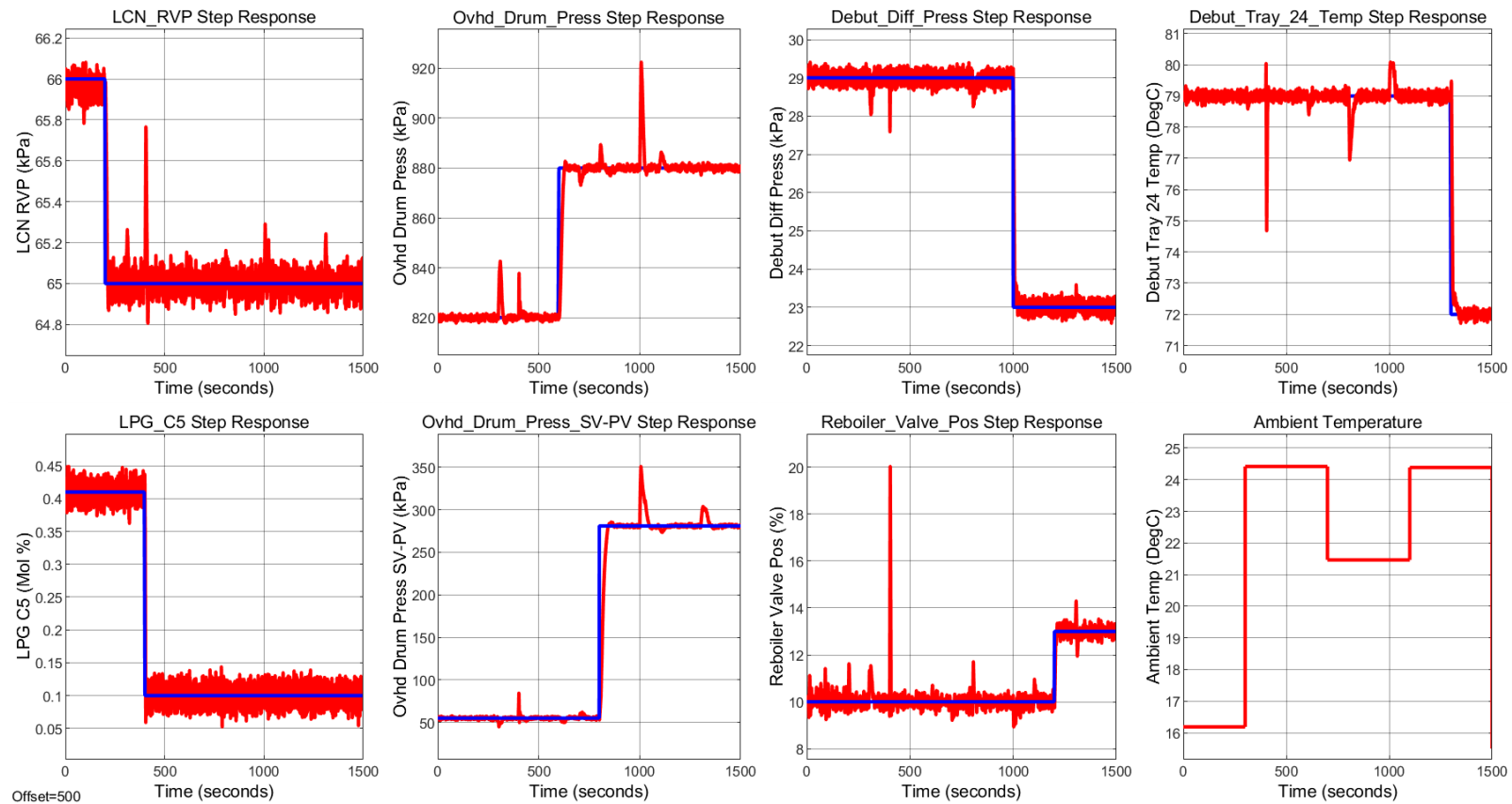


Figure 6.39: Disturbance Case #6.11.5 – Dynamic step response

In the next sub-section, a detailed discussion on the observed simulation results with and without disturbances is provided.

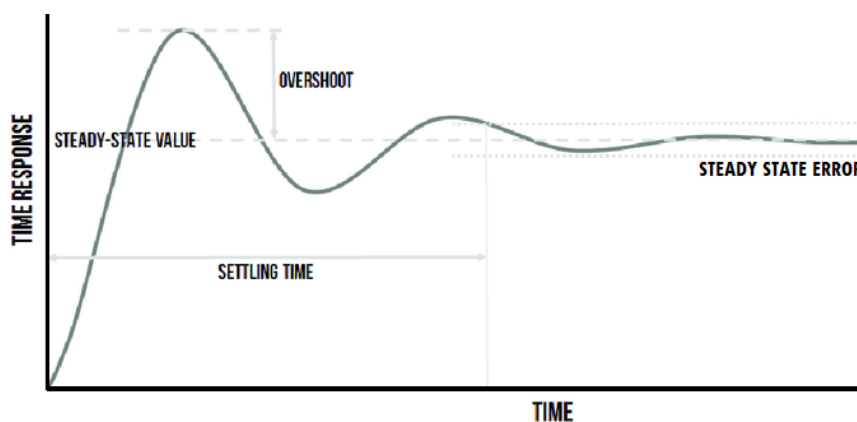
### 6.4.3. Discussion of the results

This sub-section presents a discussion of the observed results from the performed Simulink simulation case studies. The performance metrics are first discussed, and they are the percentage overshoot (%), the settling time (seconds) and the absolute steady state error. The discussion proceeds to further describe the effectiveness of the designed MPC controller in meeting the objectives of eliminating process interactions, achieving satisfactory setpoint tracking and disturbance rejection.

As previously noted in Chapter 5, it is desirable to have a well-designed and well-tuned controller that is able to keep all the controlled outputs at their target setpoints at all times with dynamic behaviour that exhibits short settling time, near zero percent overshoot and zero steady state error. A percentage overshoot metric on time domain step response curves describes a maximum peak value reached by the output response relative to the steady state setpoint and it is representative of the relative stability of the system while the settling time represents the largest time constant of the system and can be defined as the time it takes for the output response to reach and remain within a small range about the target steady state setpoint (Ogata, 2010). The equation for calculating the maximum time domain step response maximum percent overshoot is given by Equation 6.2 (Ogata, 2010):

$$\text{Maximum percent overshoot} = \frac{\text{Peak Output} - \text{Steady State Setpoint}}{\text{Steady State Setpoint}} \times 100\% \quad (6.3)$$

A graphical representation of the time-domain step response performance metrics is given by Figure 6.40 showing the steady state value, the overshoot, the settling time, and the steady state error.



**Figure 6.40:** Step response performance metrics adapted from (Nowakova and Pokorny, 2020)

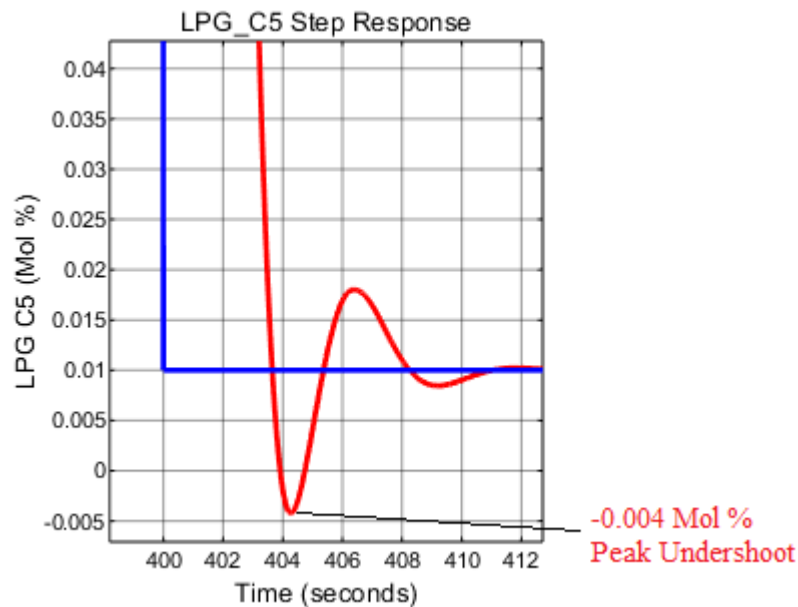
The step response curves of the seventh order debutanizer distillation process simulated in the preceding sub-subsection are analysed and their performance metrics recorded as part of the simulation study and a summary of the observed results for all the simulation cases without disturbances is given in Table 6.11.

**Table 6.11: Analysis of the performance metrics for each of the setpoint variations**

Loop Name	Initial Setpoint	Final Setpoint	Step Size	Percent Overshoot	Settling Time	Steady State Error	Figure Reference
LCN_RVP	65 kPa	63 kPa	-2 kPa	-0.27%	35.6 s	0 kPa	Figure 6.30
LPG_C5	0.1 Mol%	0.3 Mol%	+0.2 Mol%	6.30%	16.23 s	0 Mol%	
Ovhd_Drum_Press	880 kPa	1100 kPa	+220 kPa	0.36%	70.77 s	0 kPa	
Ovhd_Drum_Press_SV-PV	281 kPa	400 kPa	+119 kPa	0.38%	101.05 s	0 kPa	
Debut_Diff_Press	23 kPa	15 kPa	-8 kPa	-0.07%	90.82 s	0 kPa	
Reboiler_Valve_Pos	13 %	55 %	+42 %	0.85%	33.95 s	0 %	
Debut_Tray_24_Temp	72 DegC	65 DegC	-7 DegC	-0.02%	85.144 s	0 DegC	
LCN_RVP	63 kPa	60 kPa	-3 kPa	-0.42%	40 s	0 kPa	Figure 6.31
LPG_C5	0.3 Mol%	0.5 Mol%	+0.2 Mol%	0.08%	12.44 s	0 Mol%	
Ovhd_Drum_Press	1100 kPa	800 kPa	-300 kPa	-13.37%	89.189 s	0 kPa	
Ovhd_Drum_Press_SV-PV	400 kPa	200 kPa	-200 kPa	-1.25%	103.087 s	0 kPa	
Debut_Diff_Press	15 kPa	11 kPa	-4 kPa	0.00%	43.498 s	0 kPa	
Reboiler_Valve_Pos	20 %	55 %	+35 %	1.55%	51.955 s	0 %	
Debut_Tray_24_Temp	65 DegC	61 DegC	-4 DegC	0.00%	78 s	0 DegC	
LCN_RVP	60 kPa	63 kPa	+3 kPa	0.40%	36.602 s	0 kPa	Figure 6.32
LPG_C5	0.5 Mol%	0.01 Mol%	-0.49 Mol%	-140%	54.615 s	0 Mol%	
Ovhd_Drum_Press	800 kPa	700 kPa	-100 kPa	0.00%	88.47 s	0 kPa	
Ovhd_Drum_Press_SV-PV	200 kPa	80 kPa	-120 kPa	-1.66%	135.145 s	0 kPa	
Debut_Diff_Press	11 kPa	25 kPa	+14 kPa	0.40%	74.063 s	0 kPa	
Reboiler_Valve_Pos	55 %	30 %	-25 %	-2.07%	57.072 s	0 %	
Debut_Tray_24_Temp	61 DegC	75 DegC	+14 DegC	0.11%	89.944 s	0 DegC	
LCN_RVP	63 kPa	66 kPa	+3 kPa	0.00%	28.267 s	0 kPa	Figure 6.33
LPG_C5	0.01 Mol%	0.41 Mol%	+0.4 Mol%	8.61%	15.068 s	0 Mol%	
Ovhd_Drum_Press	700 kPa	820 kPa	+120 kPa	2.83%	87.405 s	0 kPa	
Ovhd_Drum_Press_SV-PV	80 kPa	55 kPa	-25 kPa	-0.53%	101.054 s	0 kPa	
Debut_Diff_Press	25 kPa	29 kPa	+4 kPa	0.00%	40.729 s	0 kPa	
Reboiler_Valve_Pos	30 %	10 %	-20 %	-4.05%	54.218 s	0 %	
Debut_Tray_24_Temp	75 DegC	79 DegC	+4 DegC	0.03%	76.059 s	0 DegC	
LCN_RVP	66 kPa	65 kPa	-1 kPa	-0.12%	27.984 s	0 kPa	Figure 6.34
LPG_C5	0.41 Mol%	0.1 Mol%	-0.31 Mol%	-29.82%	18.033 s	0 Mol%	
Ovhd_Drum_Press	820 kPa	880 kPa	+60 kPa	0.11%	85.321 s	0 kPa	
Ovhd_Drum_Press_SV-PV	55 kPa	281 kPa	+226 kPa	1.00%	102.29 s	0 kPa	
Debut_Diff_Press	29 kPa	23 kPa	-6 kPa	0.00%	48.243 s	0 kPa	
Reboiler_Valve_Pos	10 %	13 %	+3 %	0.54%	24.324 s	0 %	
Debut_Tray_24_Temp	79 DegC	72 DegC	-7 DegC	0.00%	40.854 s	0 DegC	

All of the output responses are observed to settle in under two minutes of the simulation time on average. This is considered satisfactory from the perspective of an industrial chemical process control problem. The response times of industrial chemical processes are slow relative

to system response times of robotic systems or the aerospace industry where faster response times are desired (Bemporad et al., 2015). The percent overshoot or undershoot of the output responses are observed to be with acceptable limits of less than 10 - 15% with the exception of the LPG C5 Concentration (Mol %) where an undershoots of a value of -29.82% and -140% are observed. Figure 6.41 provides an enlarged view of the response shown in Figure 6.32 where the undershoot of -140% is observed in the LPG C5 Concentration (Mol %) output response.

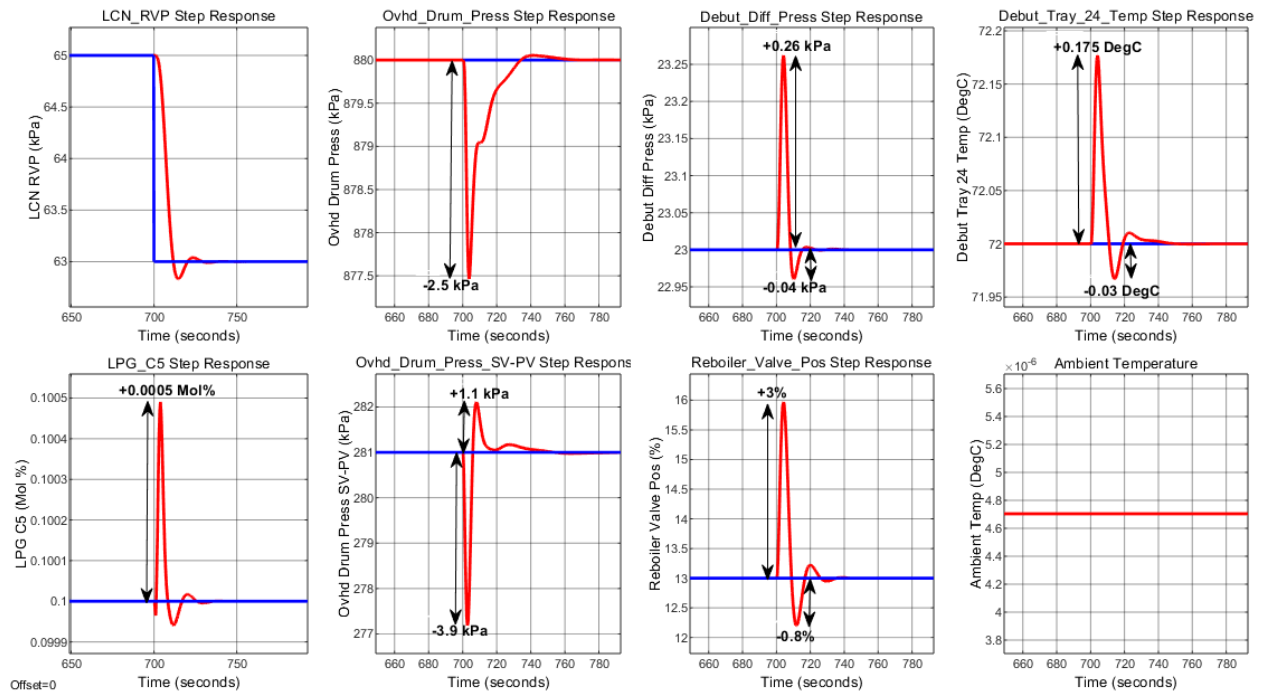


**Figure 6.41: LPG C5 Concentration (Mol %) exhibiting a -140% undershoot during a - 0.49 Mol % step change**

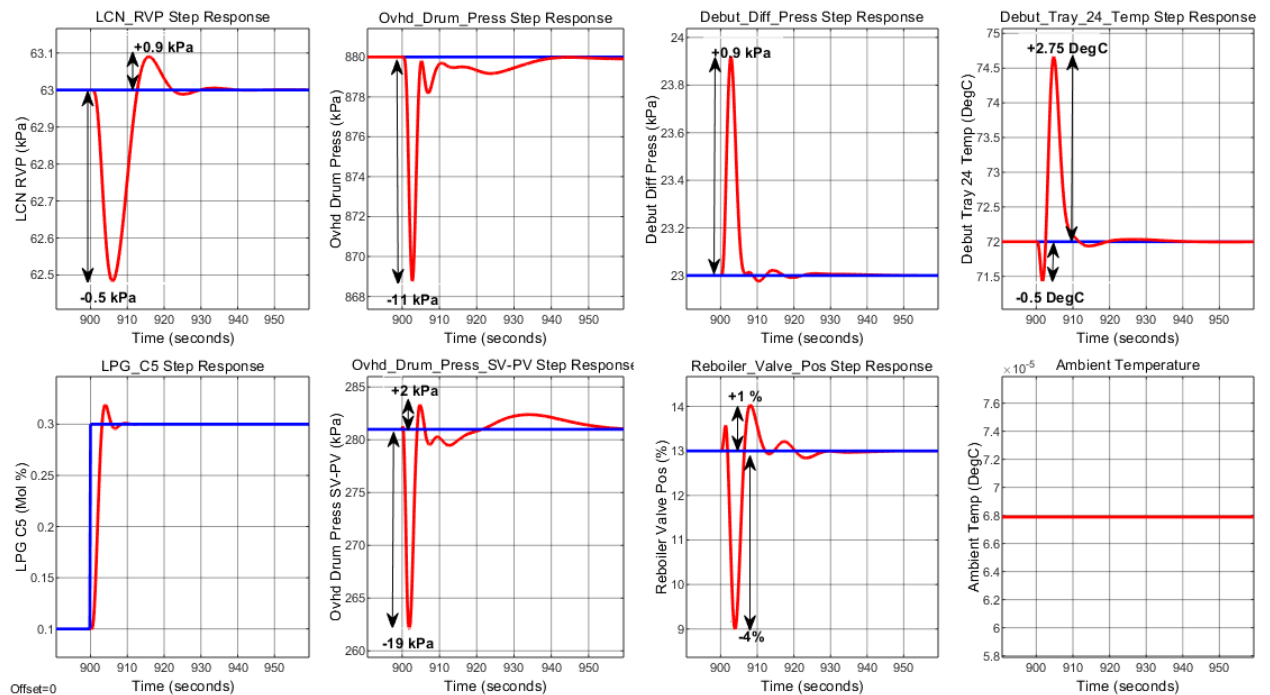
The cause for the undershoot can be attributed to the controller tuning where the LPG C5 Concentration (Mol %) is assigned the largest output reference tracking weight of 27.0671 as given in Table 6.7. This results in the controller being more aggressive in response to setpoint error in the LPG C5 Concentration (Mol %) output. As outlined by Ogata (2010), a faster controller transient response is often at the expense of a larger percent overshoot. However, in cases where a longer transient response time is tolerable, the percent overshoot can be reduced leading to an overdamped output response. It is desirable to have a relatively fast transient response time for the LPG C5 Concentration (Mol %) in order to meet LPG product specifications. Therefore, the observed simulation results are indicative of a controller that is well designed and well-tuned.

The designed MPC controller is observed to not completely eliminate the effect of process coupling. The coupling effect of the debutanizer distillation process is observed in the interactions that other process variables experience during set point step changes of other variables. The observed interactions appear as “spikes” in the controlled variable responses. The spikes observed occur as the other controlled outputs are changed and are due to process

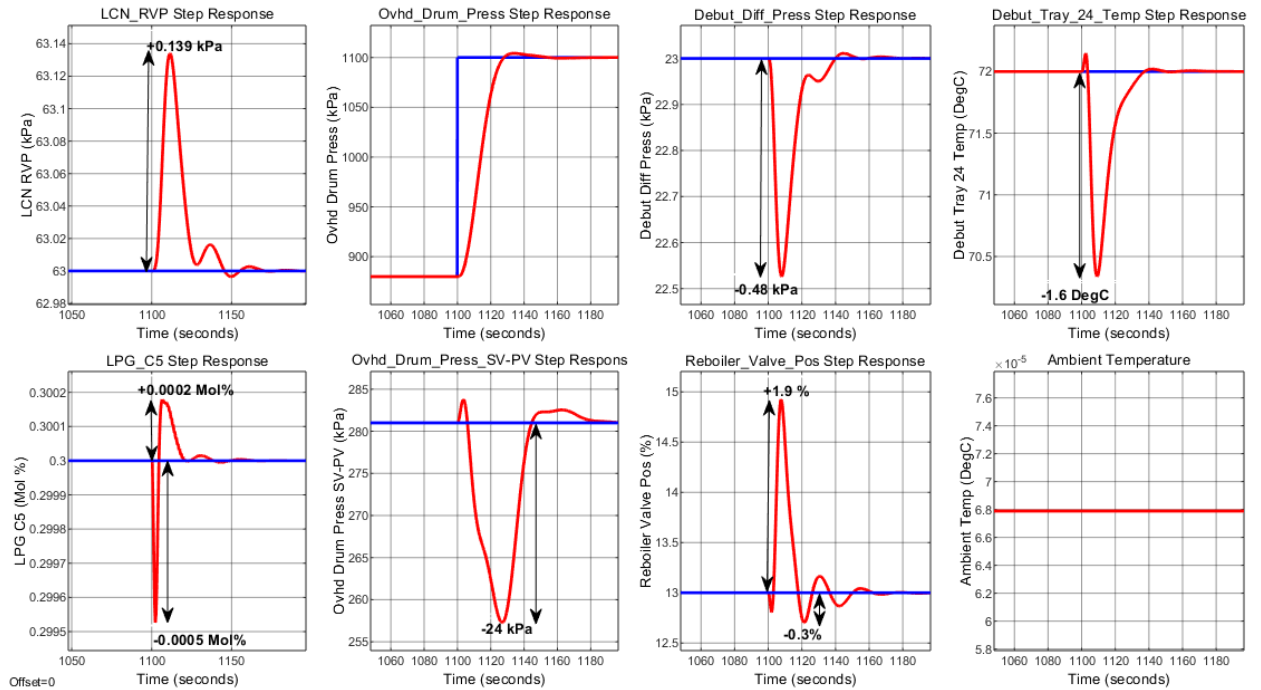
interactions. Figures 6.42 – 6.48 show the response of all the controlled outputs as the setpoints of each output is individually and independently varied.



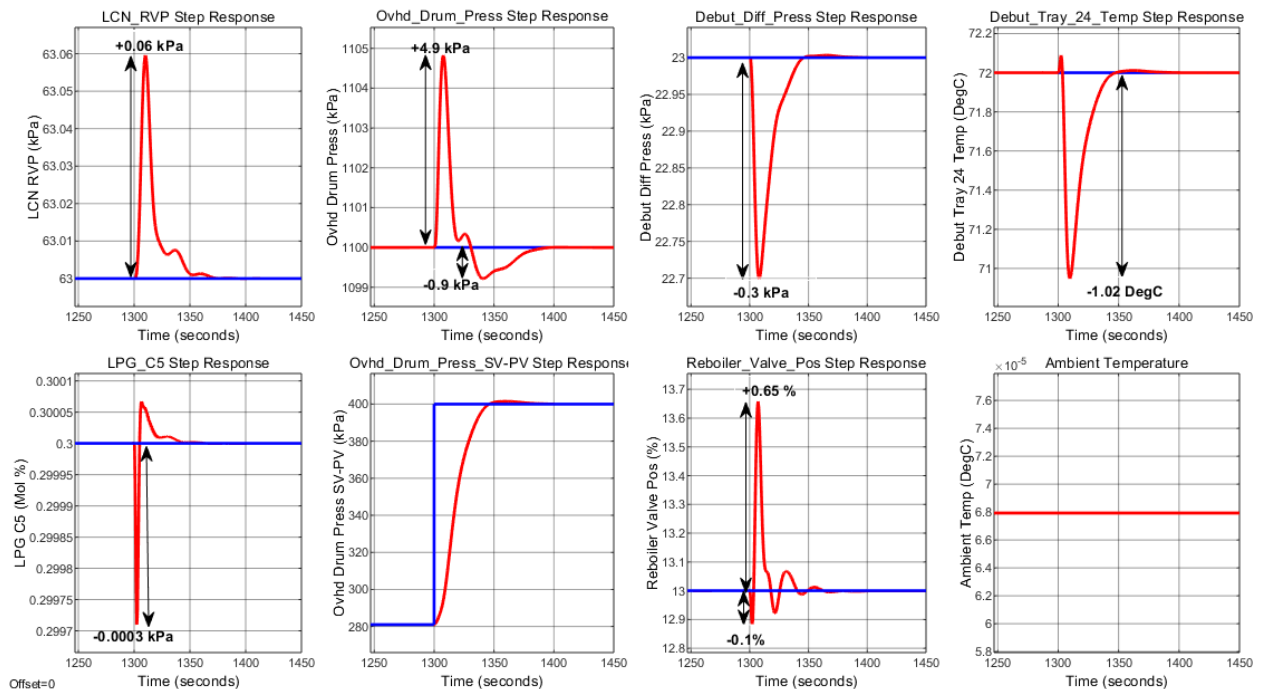
**Figure 6.42:** Spikes due to interactions on the rest of the controlled outputs at time 200 seconds due to an influence of a -2 kPa step change in the LCN RVP setpoint with all the other setpoints kept constant



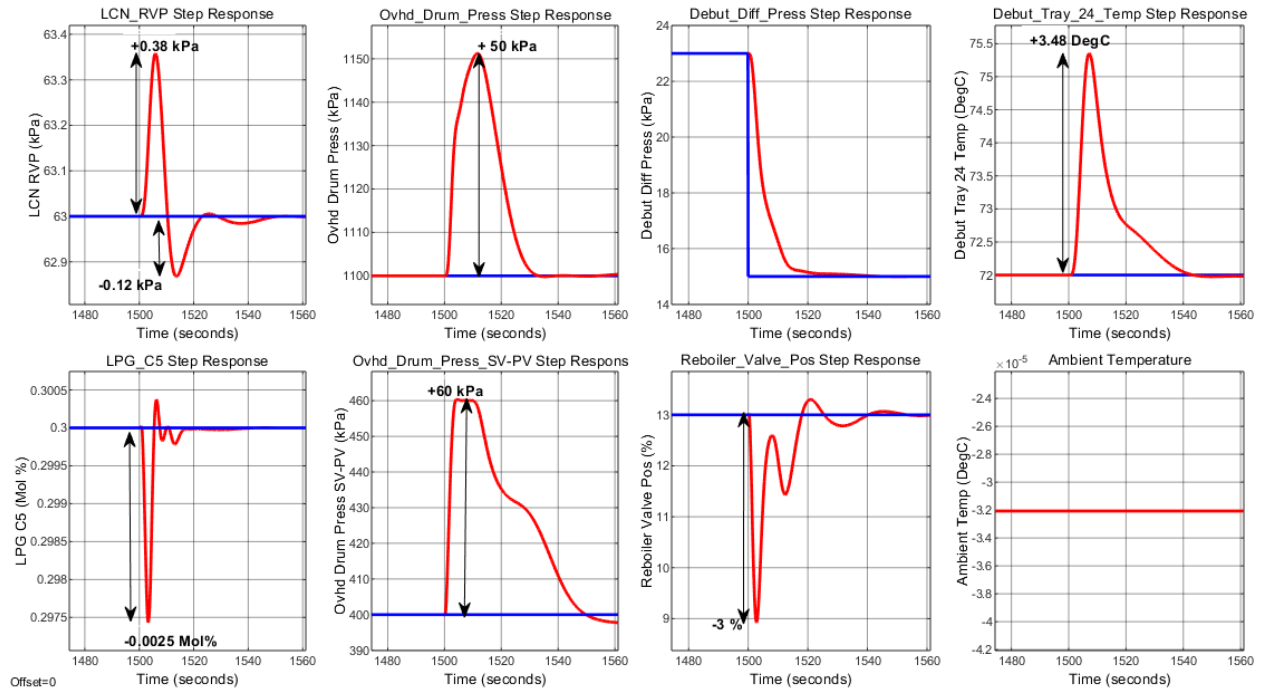
**Figure 6.43:** Spikes due to interactions on the rest of the controlled outputs at time 900 seconds due to an influence of a +0.2 Mol% step change in the LPG C5 Concentration setpoint with all the other setpoints kept constant



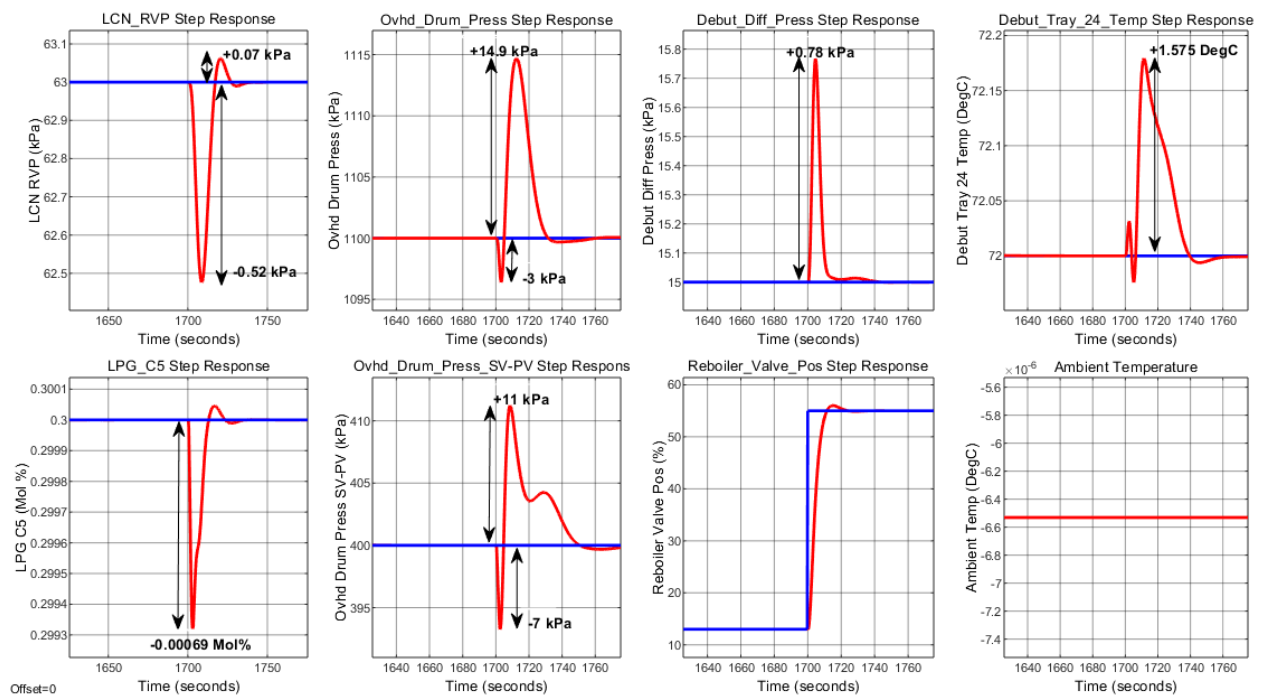
**Figure 6.44:** Spikes due to interactions on the rest of the controlled outputs at time 1100 seconds due to an influence of a +220 kPa step change in the Overhead Drum Pressure setpoint with all the other setpoints kept constant



**Figure 6.45:** Spikes due to interactions on the rest of the controlled outputs at time 1300 seconds due to an influence of a +119 kPa step change in the Overhead Drum Pressure SV-PV Gap setpoint with all the other setpoints kept constant

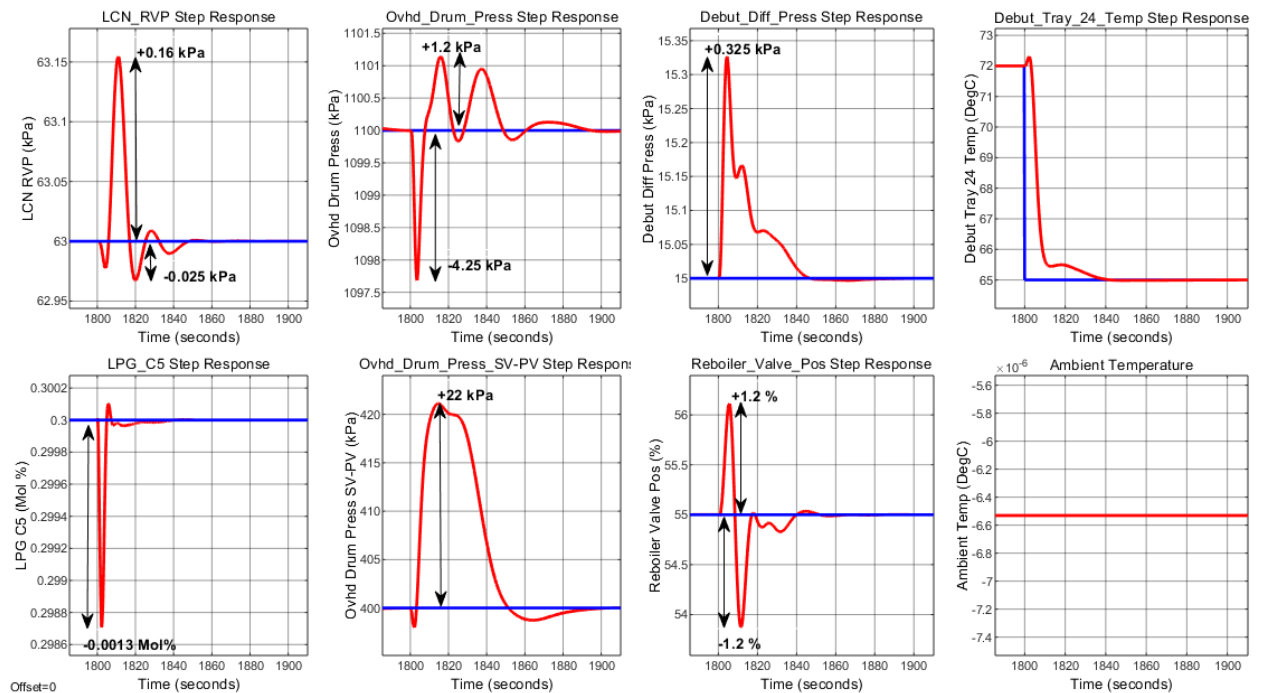


**Figure 6.46:** Spikes due to interactions on the rest of the controlled outputs at time 1500 seconds due to an influence of a -8 kPa step change in the Debutanizer Differential Pressure setpoint with all the other setpoints kept constant



**Figure 6.47:** Spikes due to interactions on the rest of the controlled outputs at time 1500 seconds due to an influence of a +42% step change in the Debutanizer Reboiler Valve Position setpoint with all the other setpoints kept constant





**Figure 6.48: Spikes due to interactions on the rest of the controlled outputs at time 1800 seconds due to an influence of a -7 DegC step change in the Tray 24 Temperature setpoint with all the other setpoints kept constant**

Since the debutanizer distillation process is coupled and multivariable in its structure, without the use of decoupling compensators, the process variable interactions are inevitable where a single process variable's dynamic behaviour influences other process variables. The designed controller, however, still manages to correct the deviations and maintain all the controlled outputs at their desired setpoints exhibiting satisfactory set point tracking and closed loop control performance. As can be observed in Figures 6.42 – 6.48, the peak amplitudes of the “spikes” are relatively small compared to their steady state. Furthermore, the observed “spikes” have a short time duration due to the controller's ability to return the outputs to their setpoints. Apart from the influence of interactions described above, the controlled variable responses exhibit zero overshoot, have short settling times, and show zero steady state error.

Finally, the effects of unmeasured disturbances on the outputs are investigated, and it is noted that disturbances are effectively rejected and only introduce noise to the outputs while the controller continues to maintain setpoint tracking. Similar to the results obtained in the simulation case study of the second order debutanizer distillation process, the observed control loop responses demonstrate good controller performance for low noise amplitude disturbances and as the disturbance amplitude increases, the controller continues to track the setpoint satisfactorily, however, with increased output variability. Furthermore, larger noise amplitude disturbances can cause the outputs to violate their constraints when the system is operated near its constraints.

The next section presents the concluding remarks for this chapter and a brief introduction of the following chapter.

## **6.5. Conclusion**

This chapter focused on the development of a model predictive control system using the MATLAB/Simulink Model Predictive Control Toolbox and testing the designed controller in an industrial seventh order debutanizer distillation process model. The process of developing and configuring the MPC controller including the controller structure, the selection of the controller parameters such as scale factors, prediction horizon, the control horizon, sampling time, input and output constraints, constraint softening factors, reference tracking and increment suppression weights are presented. A step-by-step procedure that is followed for this research is presented and a closed-loop simulation case study is carried out to investigate the suitability of the designed controller. It is observed and concluded from the closed-loop simulation case study results that the designed controller maintains all the controlled outputs at their desired setpoints satisfactorily. The transient response analysis reveals some shortcomings of the controller in eliminating interactions brought about by coupling. However, the controller is able to return the controlled outputs to their setpoints in a relatively short period of time following disturbances, demonstrating good setpoint tracking and controller tuning. Furthermore, the effects of unmeasured disturbances on inputs and outputs are investigated, and it is noted that small disturbance magnitudes tend to introduce noise to the controlled output signals whereas large disturbance magnitudes causes the controller to violate the set minimum and maximum constraint limits, especially when the controlled outputs are operated near their constraint limits. However, it can be concluded from the observed results that the controller is still able to maintain good setpoint tracking in the presence of disturbances thereby demonstrating controller robustness.

The results of this chapter and Chapter 5 are obtained within the simulation environment of MATLAB/Simulink. However, the next chapter covers the implementation of the second order debutanizer distillation process model in the LabVIEW real-time simulation environment and the decentralized PID controllers in the Beckhoff's TwinCAT 3.1 real-time software environment with the system configured in closed-loop in a Hardware-in-the-Loop (HiL) testbed. Furthermore, the seventh order debutanizer distillation process model and the MPC controller are implemented in the real-time simulation environment.

## **CHAPTER SEVEN: REAL-TIME IMPLEMENTATION**

### **7.1. Introduction**

This chapter presents the practical implementation of the simulation models developed in the MATLAB/Simulink software environment which are presented in Chapters 5 and 6. The decentralized proportional-integral-derivative (PID) controllers presented in Chapter 5 are programmed in Simulink and transformed into TwinCAT 3 separately from the model of the second order debutanizer distillation process which is programmed in the LabVIEW environment to form a Hardware-in-the-Loop testbed. On the other hand, the centralized model predictive controller (MPC) presented in Chapter 6 is programmed in Simulink in closed-loop with the seventh order distillation process model and the system is transformed into TwinCAT 3. This chapter describes in detail the model transformation technique used to transform the Simulink models into TwinCAT 3 and outlines the development of the Hardware-in-the-Loop testbed for the second order system including both software and hardware architectures. The work by (Grega, 1999) describes the Hardware-in-the-Loop methodology and provides an overview of what is involved in setting up a Hardware-in-the-Loop experiment with emphasis on its resourcefulness in enabling students to carry out lab scale experiments. Hardware-in-the-Loop configurations are essential in facilitating learning for process control students in academic institutions to aid their understanding of theoretical concepts, and as a result, the work developed in this research aids in achieving this important objective.

This remainder of the chapter is outlined as follows; section 7.2 presents an overview of the MATLAB/Simulink environment and the Simulink models developed as part of this research for both the second order and seventh order systems. Section 7.3 provides an overview of the TwinCAT environment, and the model transformation technique used to transform the Simulink models into TwinCAT 3. In section 7.4, a description of the software development required in the LabVIEW environment for the second order debutanizer distillation process model is provided. Section 7.5 presents the Hardware-in-the-Loop configuration as well as the necessary physical connections to achieve a closed-loop system architecture. Sections 7.6 and 7.7 present the real-time simulation case studies for the second order and seventh order systems, respectively, with performance analysis and discussion of the observed results for both systems. Lastly, section 7.8 provides concluding remarks for this chapter.

### **7.2. MATLAB/Simulink**

MATLAB is both a software development environment and a matrix based computational language used predominantly in the engineering and scientific community for developing mathematical algorithms, developing system models, and analysing data (Mathworks, 1994). Simulink is a MATLAB-integrated graphical model development environment for modelling, simulating, and analysing dynamic systems (Reedy and Lunzman, 2010). As part of the practical implementation component of this research, the Simulink environment is used to

develop mathematical models of the debutanizer distillation process and for designing the decentralized PID controllers and the centralized MPC controller.

A signal scaling algorithm for the decentralized PID controller inputs and outputs is necessary to create a Hardware-in-the-Loop testbed for the second order system and forms part of the Simulink model of the decentralized PID controllers. The following sub-section describes the signal scaling algorithm followed by a description of the Simulink models for the decentralized PID controllers and centralized MPC control system.

### 7.2.1. Scaling of decentralized PID controller input and output signals

In the TwinCAT 3 environment, signal information is by default represented as 16-bit signed integers meaning the input and output signals within TwinCAT 3 are by default ranged from -32768 to 32767. To enable physical integration and transfer of information via the inputs and outputs of the two hardware platforms where the process model and the PID controllers are executed, it is necessary to implement signal scaling with software for all the signals transferred between the two systems. The range of the signals in TwinCAT 3 must be converted from 16-bit signed integer raw values to engineering units using Equation 7.1 while Equation 7.2 is used to convert back from engineering units to 16-bit signed integer raw values.

$$\text{Eng\_Out} = (\text{Raw\_In} - \text{Min\_Raw}) \times \frac{(\text{Max\_Eng} - \text{Min\_Eng})}{(\text{Max\_Raw} - \text{Min\_Raw})} + \text{Min\_Eng} \quad (7.1)$$

$$\text{Raw\_Out} = (\text{Eng\_In} - \text{Min\_Eng}) \times \frac{(\text{Max\_Raw} - \text{Min\_Raw})}{(\text{Max\_Eng} - \text{Min\_Eng})} + \text{Min\_Raw} \quad (7.2)$$

Where **Raw\_Out** is the desired output raw value, **Eng\_Out** is the desired engineering unit output value, **Max\_Raw** is the upper range value of the raw value, **Min\_Raw** is the lower range value of the raw value, **Eng\_In** is the incoming signal to be scaled in engineering units, **Min\_Eng** is the lower range value in engineering units and **Max\_Eng** is upper range value in engineering units. Since the second PID controller model is controlling the debutanizer process model located in a different platform, the inputs and outputs of the Simulink model must be modified to account for the scaling discussed above using Equations 7.1 and 7.2 as depicted in Tables 7.1 and 7.2, respectively.

**Table 7.1: Simulink model input scaling**

Variable	Simulink model inputs	
	Raw_In	Eng_Out
LCN RVP	0 to 32767	0 to 100 kPa
LPG C5 Concentration	0 to 32767	0 to 2 Mol %

**Table 7.2: Model output scaling**

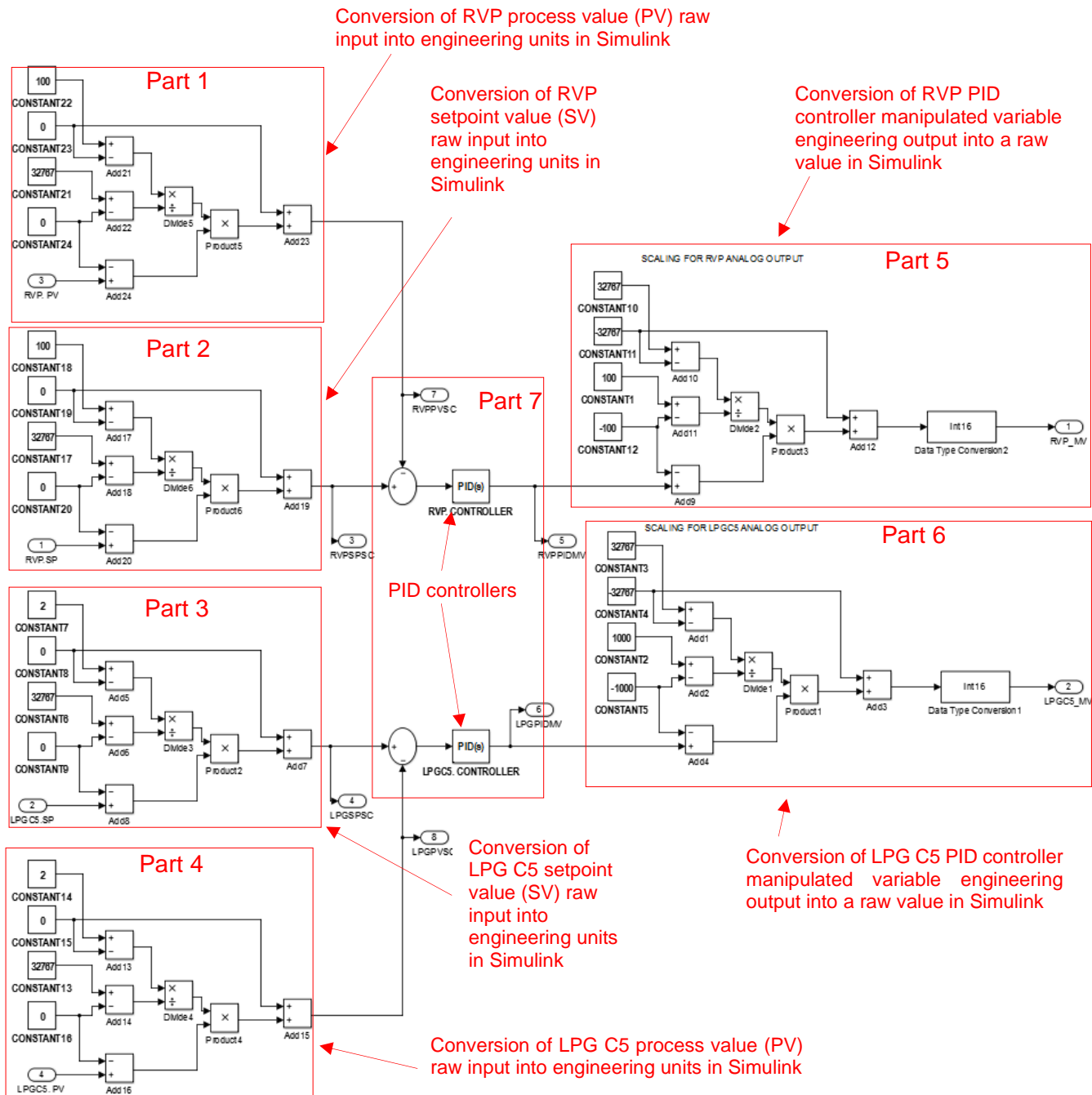
Variable	Simulink model outputs	
	Eng_In	Raw_Out
PID controller Manipulated Variable (MV) 1	-100 to 100	-32767 to 32767
PID controller Manipulated Variable (MV) 2	-1000 to 1000	-32767 to 32767

Where the LCN RVP is the Light Cracked Naphtha Reid Vapour Pressure and the LPG C5 is the Liquefied Petroleum Gas C<sub>5</sub> concentration, both of which are the controlled variables. And where PID controller Manipulated Variable (MV) 1 and 2 are the manipulated variables of the two decentralized PID controllers, respectively.

This sub-section described the signal scaling algorithm used to integrate the decentralized controllers with the process model. The following sub-section presents the Simulink model of the decentralized PID controllers which includes the signal scaling algorithm described above.

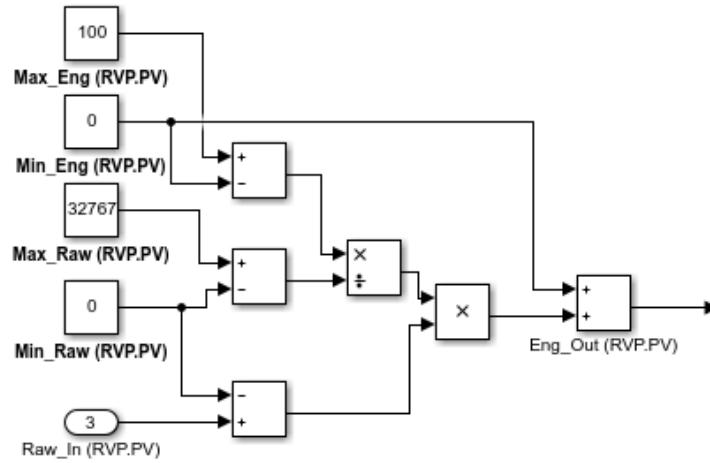
### 7.2.2. Simulink model of the second order decentralized PID controllers

In Chapter 5, controller design of decentralized PID controllers for the second order debutanizer distillation process model is performed including closed-loop simulations in the Simulink environment. In this chapter, the decentralized PID controllers are separated from the plant to form a Hardware-in-the-Loop testbed where the process model is programmed in the LabVIEW environment. To form a Hardware-in-the-Loop testbed it is necessary to programme the decentralized PID controllers in Simulink in order to be transformed into TwinCAT 3 for execution in a real-time target while controlling the plant model that is programmed in the LabVIEW environment. Shown in Figure 7.1 is the separated model of the decentralized PID controllers together with the input and output scaling algorithm programmed in Simulink.

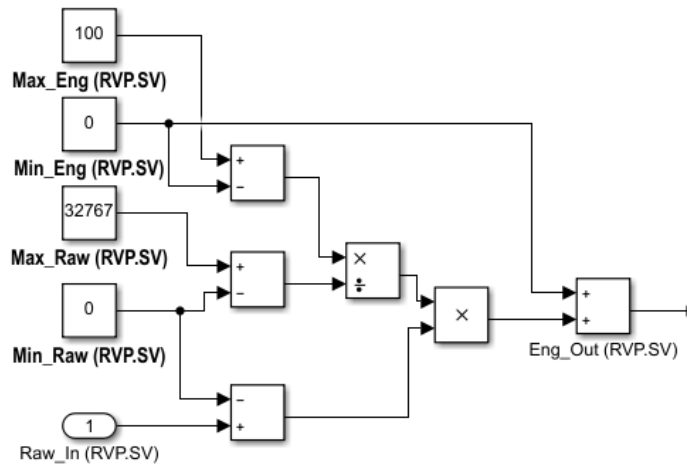


**Figure 7.1: Simulink second order PID controller model**

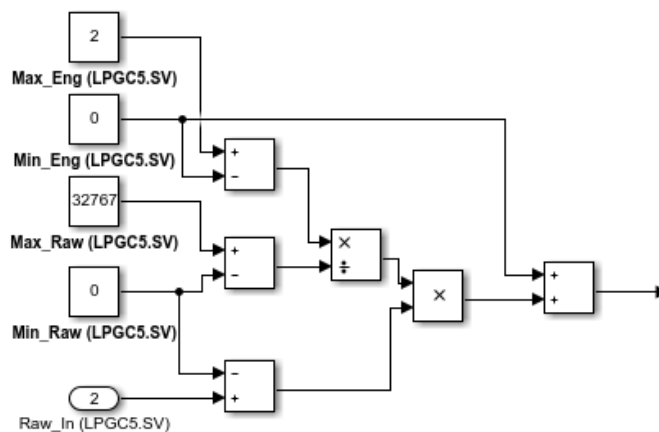
The Simulink model can be broken down into seven parts. The first part, (Part 1), is the programmed scaling equation given by Equation 7.1 to convert the RVP process value (PV) raw input into engineering units. Part 2 is to convert the RVP setpoint value (SV) raw input into engineering units, part 3 converts the LPG C5 setpoint value (SV) raw input into engineering units and part 4 converts the LPG C5 process value (PV) raw input into engineering units. Part 5 is the programmed scaling equation given by Equation 7.2 to convert the of RVP PID controller manipulated variable engineering output into a raw value and part 6 converts the LPG C5 PID controller manipulated variable engineering output into a raw value. Lastly, part 7 shows the decentralized PID controllers that are designed using the IMC method as described in Chapter 5. Parts 1 – 6 of Figure 7.1 are further shown in Figures 7.2 – 7.7 below for clarity of the model details.



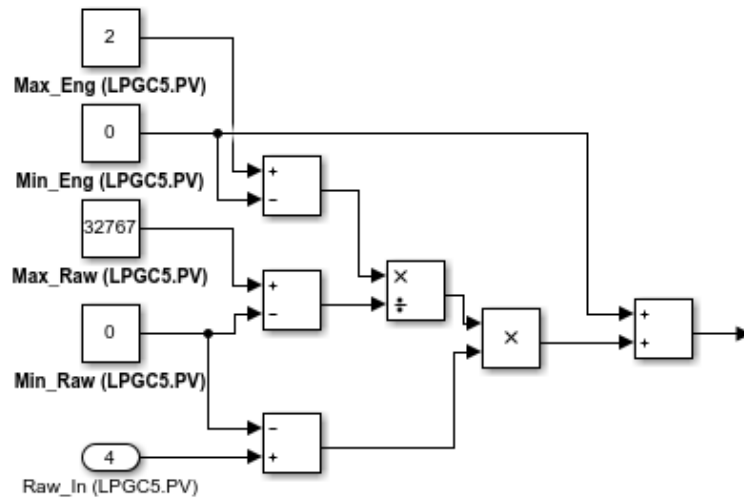
**Figure 7.2: Conversion of RVP process value raw input into engineering units in Simulink**



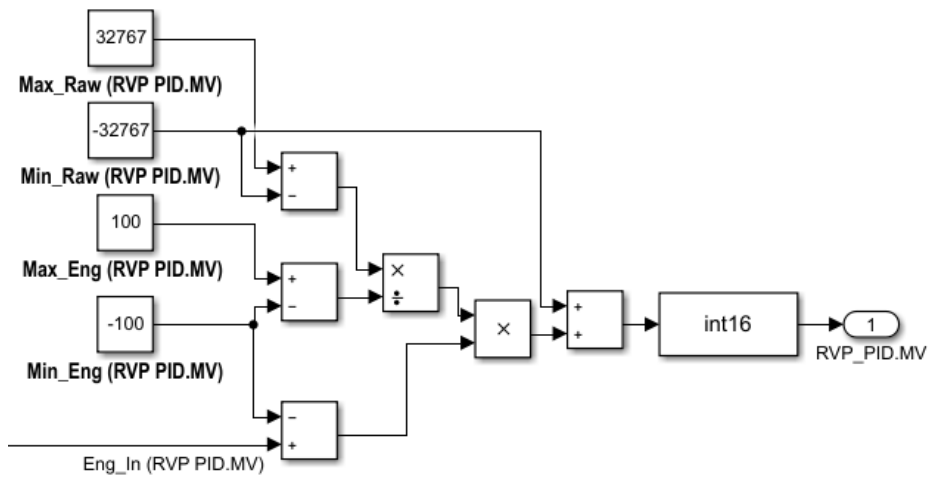
**Figure 7.3: Conversion of RVP setpoint value raw input into engineering units in Simulink**



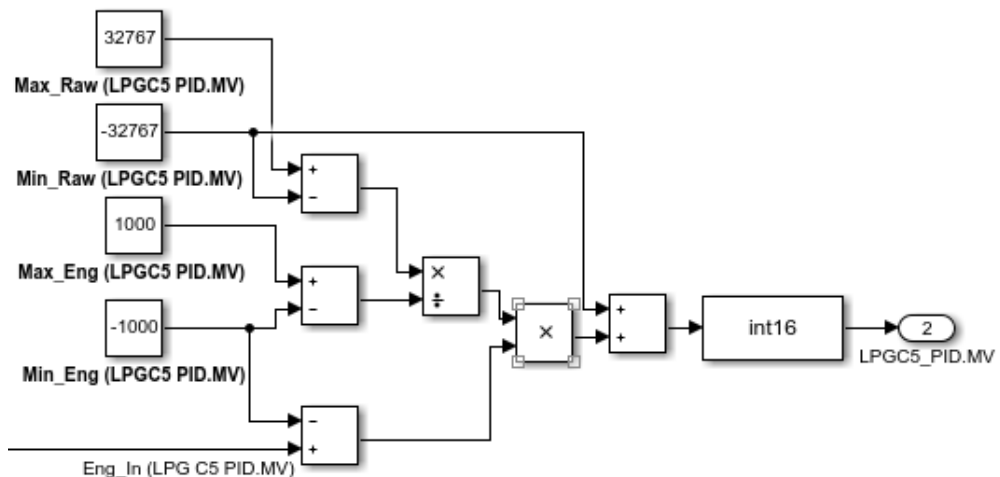
**Figure 7.4: Conversion of LPG C5 setpoint value raw input into engineering units in Simulink**



**Figure 7.5:** Conversion of LPG C5 process value raw input into engineering units in Simulink



**Figure 7.6:** Conversion of RVP PID controller manipulated variable engineering output into raw value in Simulink



**Figure 7.7:** Conversion of LPG C5 PID controller manipulated variable engineering output into raw value in Simulink



This sub-section presented the Simulink model of the decentralized PID controllers. The Simulink model is configured with a scaling algorithm for use in a Hardware-in-the-Loop configuration controlling the second order debutanizer distillation process model programmed in the LabVIEW environment. The next sub-section presents the Simulink model of the seventh order system.

### **7.2.3. Seventh order Simulink model**

In Chapter 6, a closed-loop control system comprised of the seventh order debutanizer distillation process model under the control of a model predictive controller is presented. The controller is designed using the Simulink Model Predictive Control Toolbox and the system is simulated in closed-loop in the Simulink environment. The seventh order model of the debutanizer distillation process configured in Simulink is given in Figure 7.8. As previously described in Chapter 6, the model can be broken down into four parts: Part 1) the MPC controller, Part 2) the DCS regulatory PID controllers, Part 3) the ambient temperature disturbance and, Part 4) the debutanizer distillation process transfer functions. The complete Simulink model is given in Figure 7.8 and the expanded four parts are further given in Figures 7.9 – 7.12 for clarity of the model details.

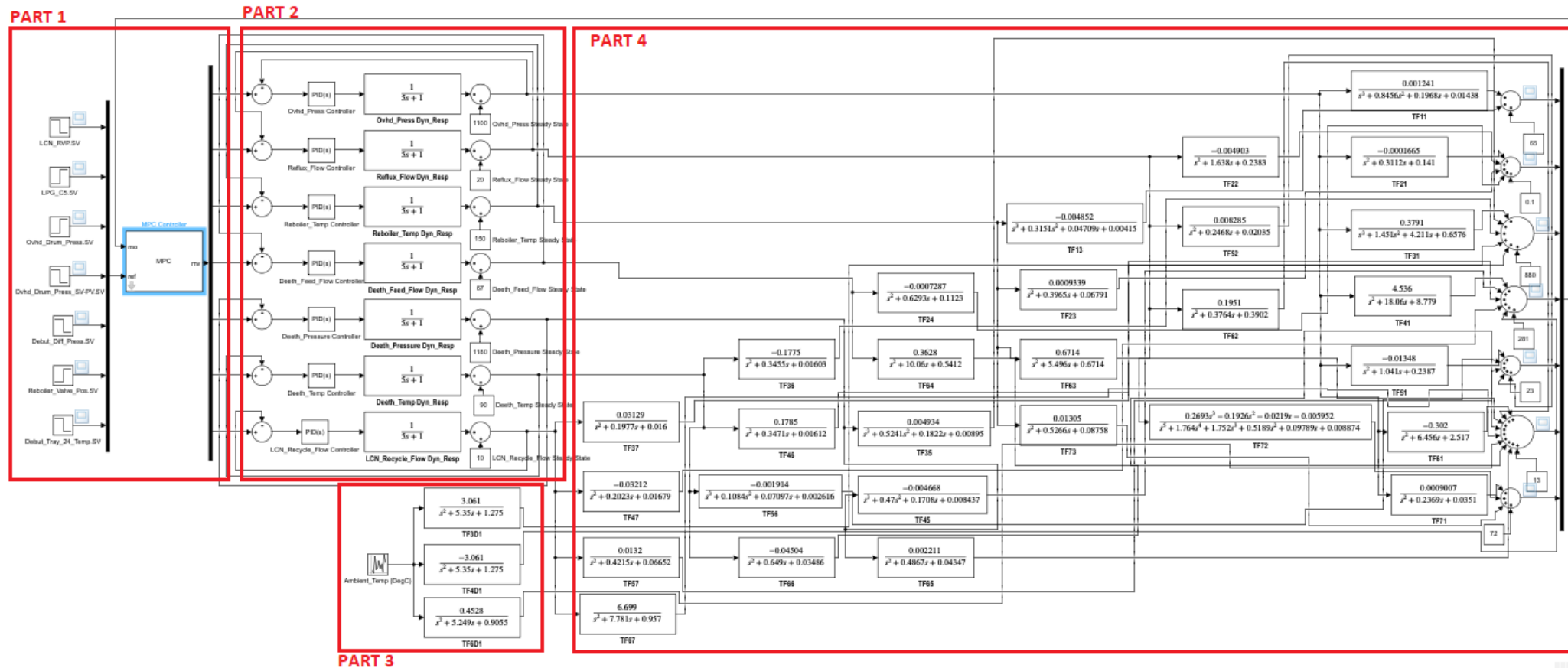


Figure 7.8: Seventh order step response prediction model of the debutanizer distillation process configured in Simulink

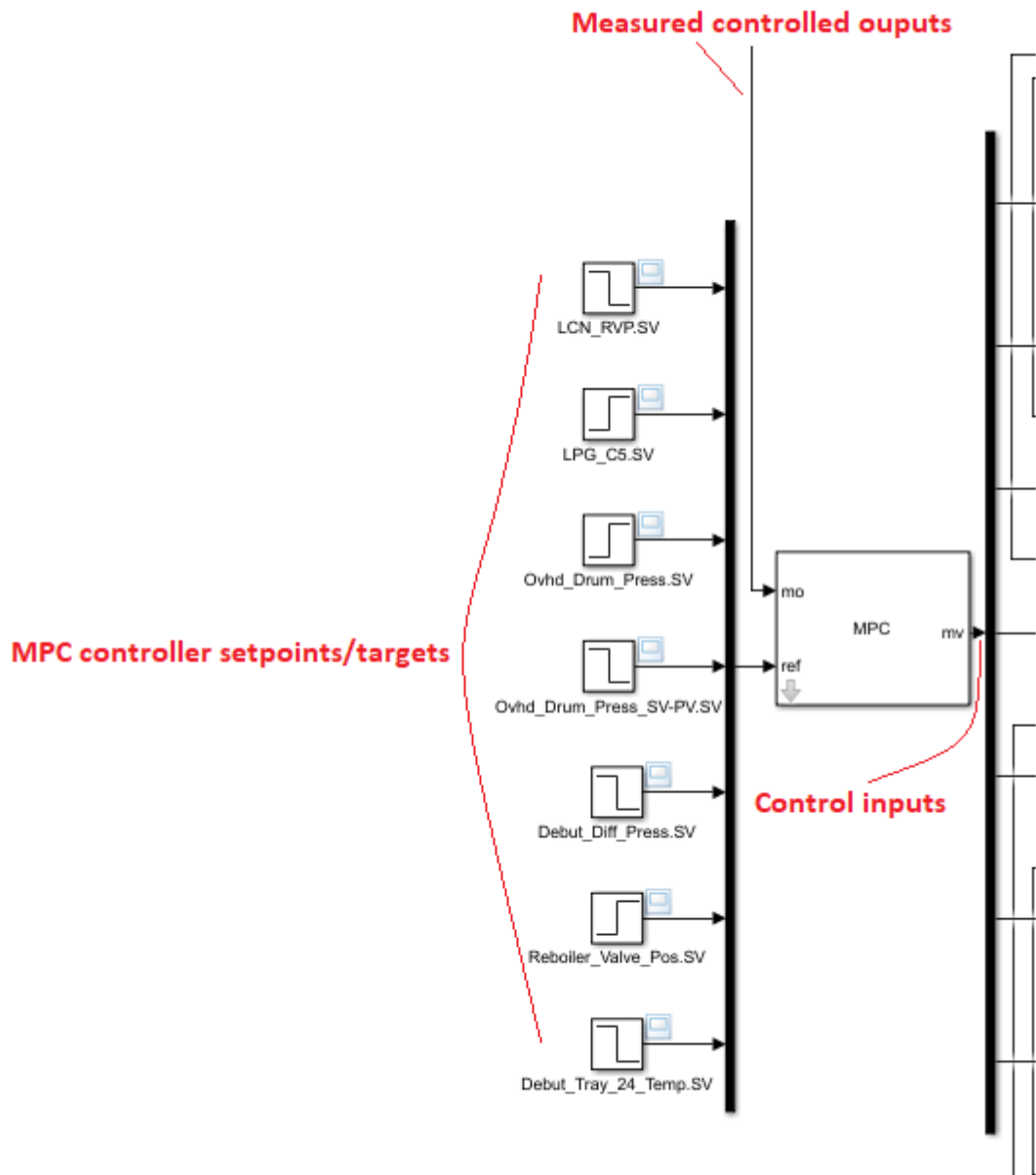
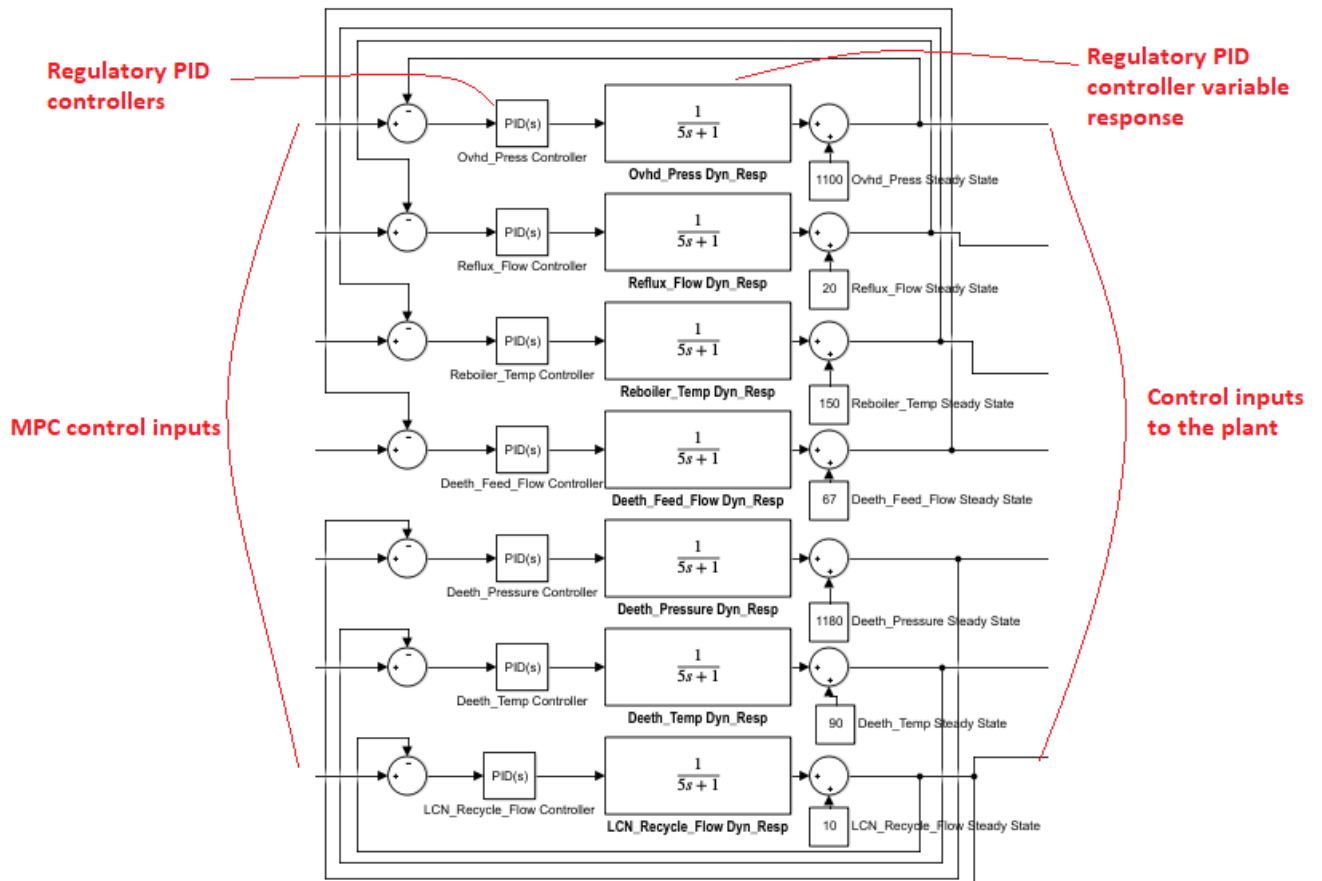
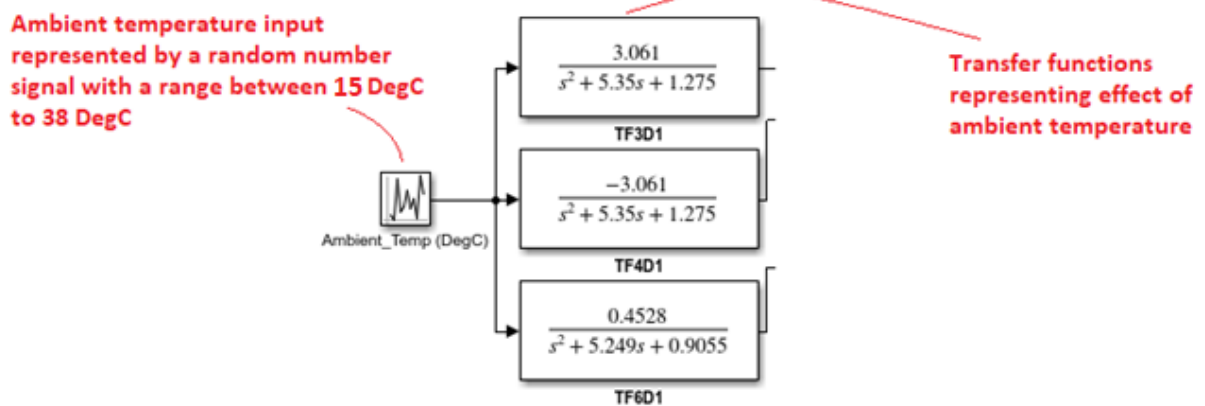


Figure 7.9: Simulink model Part 1 - MPC controller



**Figure 7.10: Simulink model Part 2 - DCS regulatory PID controllers**

The PID controller gain settings for the regulatory PID controllers are obtained using the Simulink PID Tuner and are identical for all the controllers since all the lower level regulatory PID controller dynamics are assumed to be ideally represented by a first-order plus dead time (FOPDT) transfer function approximation. The PID controller gains for the DCS controllers in model are set at  $K_p = 5.47$ ,  $\tau_I = 2.57$  and  $\tau_D = -0.84$  where  $K_p$  is the proportional gain,  $\tau_I$  is the integral gain, and  $\tau_D$  is the derivative gain with a Filter Coefficient,  $N = 3.19$ . The PID controllers exhibit good setpoint tracking without steady-state error.



**Figure 7.11: Simulink model Part 3 - Ambient temperature disturbance**

Debutanizer distillation process transfer functions

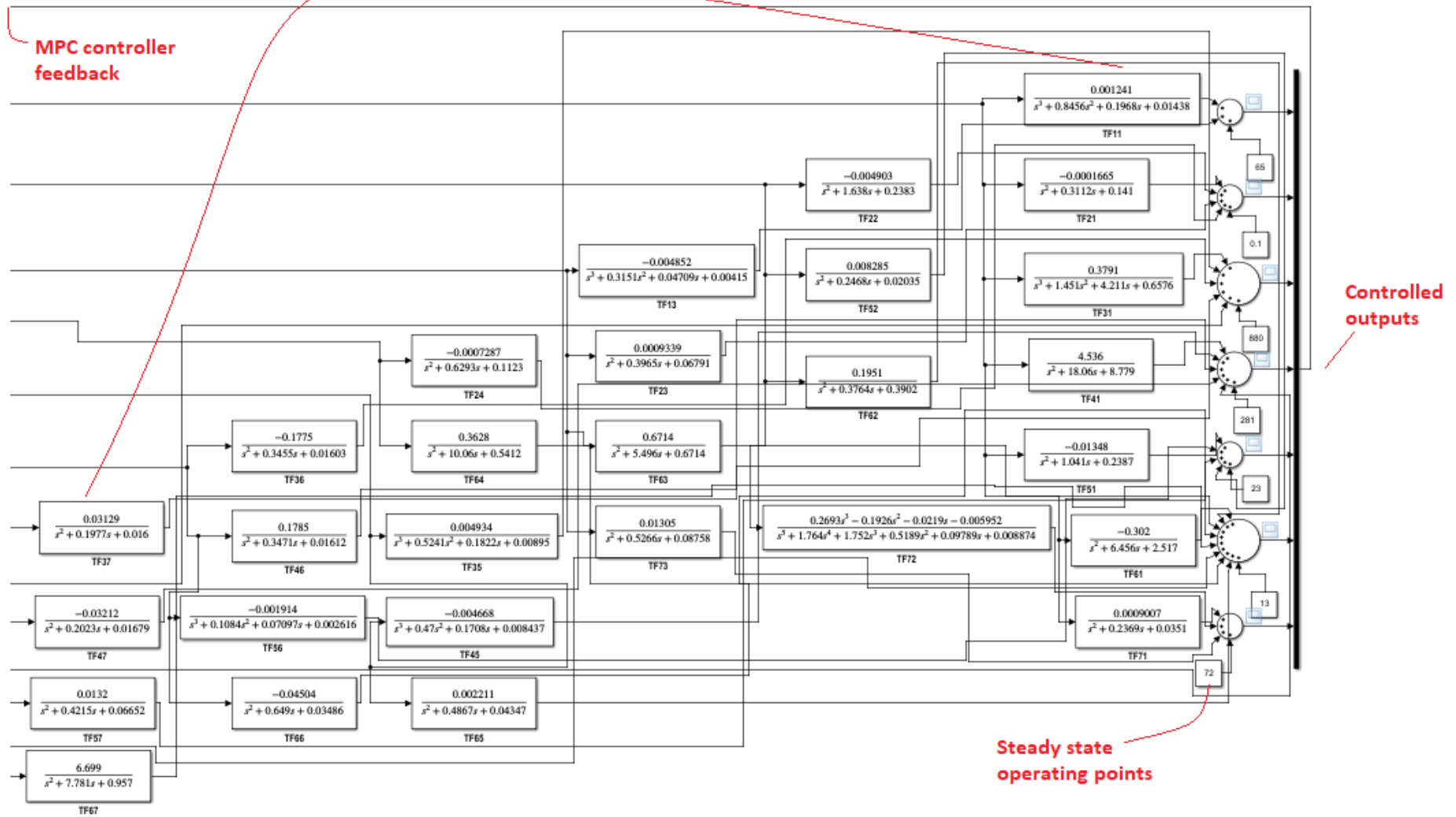
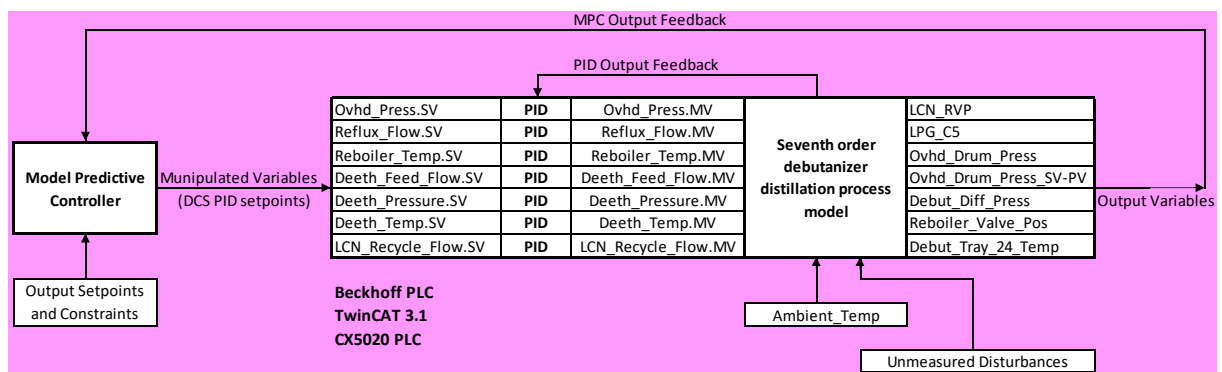


Figure 7.12: Simulink model Part 4 - debutanizer distillation process transfer functions

It is the objective of this chapter to have the Simulink model described above simulated in the TwinCAT 3 real-time environment. While the second order debutanizer distillation process model is implemented in a Hardware-in-the-Loop testbed, the seventh order model is not. Attempts to implement the seventh order model in a Hardware-in-the-Loop testbed as part of this research are temporarily prohibited by the unavailability of hardware in the form of sufficient number of input and output modules to enable the transfer of signal information between the two platforms, namely, LabVIEW and TwinCAT 3. Therefore, the implementation of the seventh order debutanizer distillation process model in a Hardware-in-the-Loop testbed is deferred for future work. The scope of implementation for the seventh order model is the transformation of the Simulink model presented in Chapter 6 into the TwinCAT 3 environment followed by closed-loop simulations.

Therefore, for the seventh order model, the MPC controller and the debutanizer process model developed in the Simulink environment are both transformed into the TwinCAT 3 environment and executed in real-time in a Beckhoff programmable logic controller (PLC) target without external interfaces as illustrated in Figure 7.13. The models are transformed from Simulink into TwinCAT 3 using the procedure described in the next section.



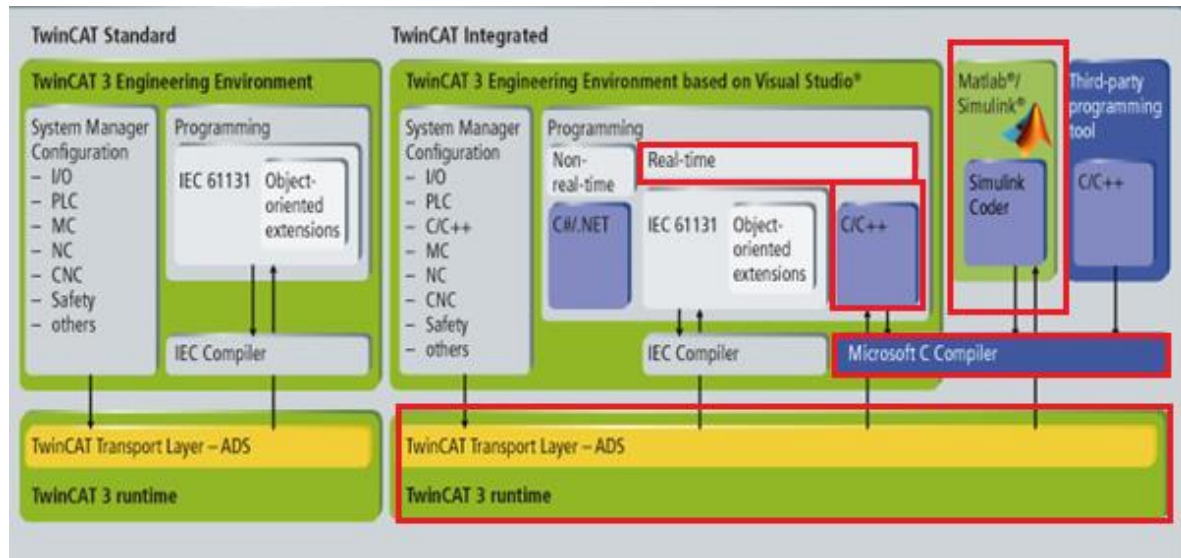
**Figure 7.13: Overview of the hardware and software architecture for the seventh order debutanizer closed loop control system**

This section presented the scaling algorithm and the models of both the decentralized PID controllers and the seventh order system which are programmed in the Simulink environment. It is the objective of this chapter to transform the developed Simulink models into the TwinCAT 3 environment followed by closed-loop simulations in real-time. The following section presents an overview of the Simulink environment and a detailed description of the model transformation technique used to transform the Simulink models presented in this section into TwinCAT 3.

### 7.3. TwinCAT

The Windows Control and Automation Technology (or simply TwinCAT) is an engineering development environment from Beckhoff Automation’s core control system (Beckhoff Automation, 2020a). Beckhoff specialises in personal computer (PC) based control technology

with a product range that includes, but is not limited to, industrial PCs, input/output (I/O) modules, fieldbus components and drive technology. The TwinCAT eXtended Automation Engineering (XAE) environment allows for models developed in Simulink to be deployed onto a Beckhoff real-time target. The overall philosophy of the TwinCAT eXtended Automation Engineering (XAE) environment that allows for this kind of project deployment is illustrated in Figure 7.14 below.



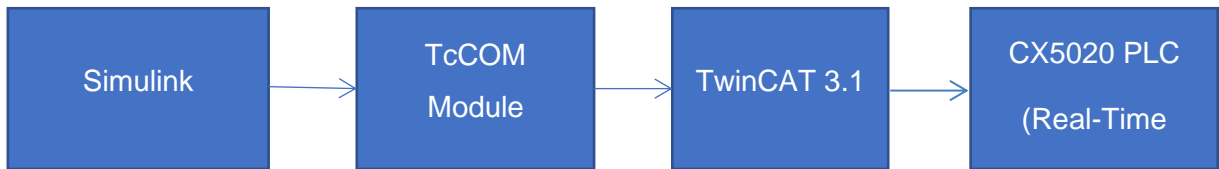
**Figure 7.14: TwinCAT 3 eXtended Automation Engineering (XAE) Philosophy** (Beckhoff Automation, 2020a)

The model transformation technique can be described as follows; a model is developed in Simulink and the Simulink code generator is used with a Visual Studio compiler to generate C/C++ code from the Simulink models. The C/C++ code is then transformed into TwinCAT Object Models (TcCOMs) with the use of the TE1400 TwinCAT Target for Simulink software module. The TwinCAT Object Models are then instantiated in the Beckhoff TwinCAT 3 development environment and executed in real-time, thus enabling end-users to design and implement Simulink models onto Beckhoff PLC targets (Beckhoff Automation, 2021).

Therefore, TwinCAT 3 is used in this research to execute the developed Simulink models in real-time using the above-mentioned transformation technique. The following sub-section provides a detailed description of the model transformation procedure.

### 7.3.1. Simulink to Beckhoff TwinCAT 3 model transformation procedure

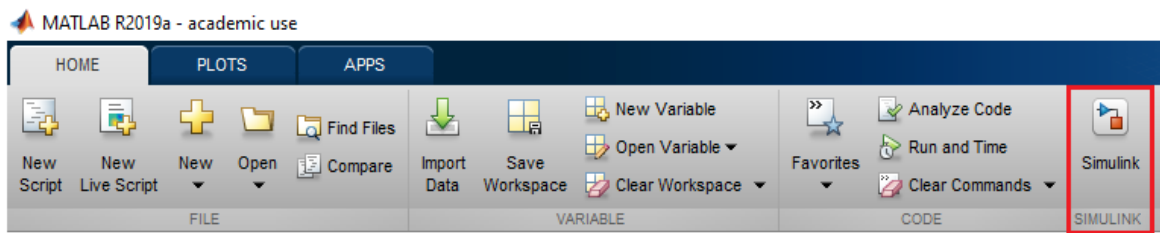
To illustrate the procedure, the Simulink model of the decentralized PID controllers is used; however, it is worth noting that the same procedure is applicable for the seventh closed loop model. The overall process flow diagram of the procedure is illustrated in Figure 7.15.



**Figure 7.15: Flow diagram of the model transformation from Simulink to TwinCAT 3**

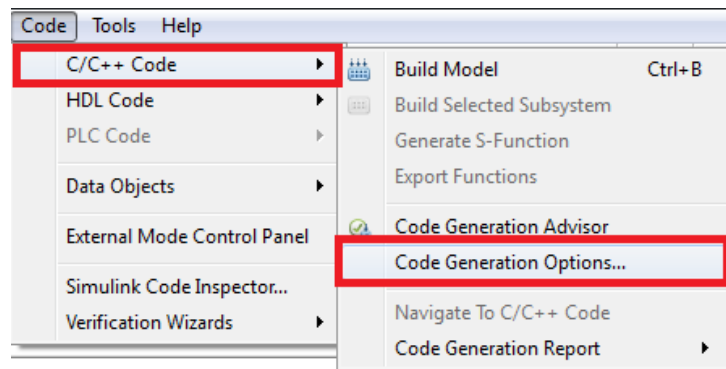
The procedure begins in the Simulink environment where the model is converted into TcCOM modules which are then imported into TwinCAT 3 and deployed to the Beckhoff PLC for real-time execution.

**Step 1.** Start MATLAB and open the Simulink model with the decentralized PID controllers.



**Figure 7.16: Open Simulink**

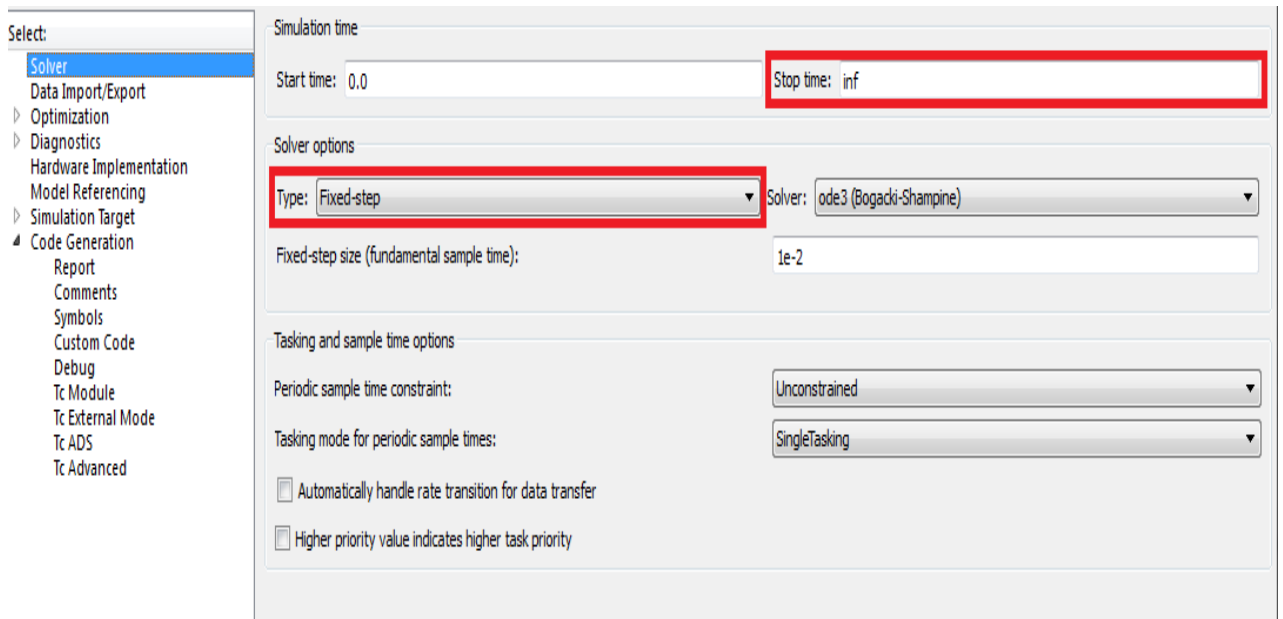
**Step 2.** Navigate the task bar and open the Code Generation Options



**Figure 7.17: Code Generation Options in Simulink**

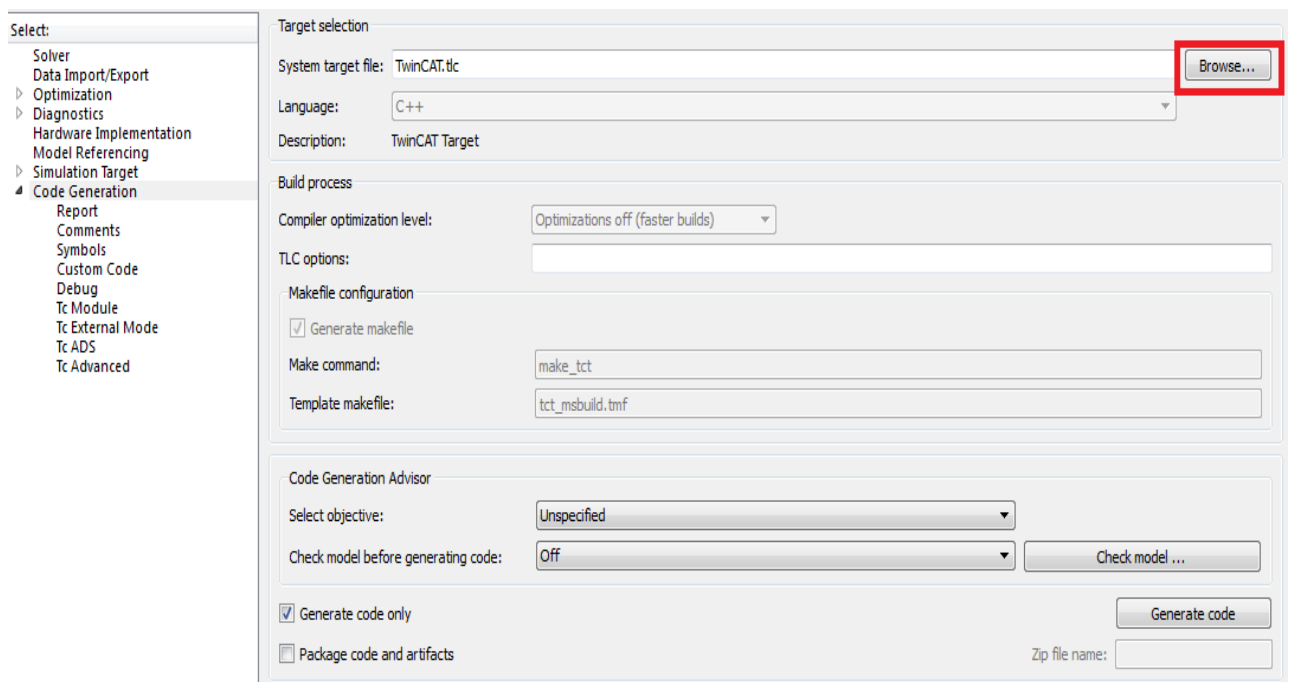


**Step 3.** Select a Fixed-step solver type and change the simulation stop time to infinity (**inf**). The reason for changing the simulation time to infinity is to enable an endless real-time execution of the program in the TwinCAT environment.



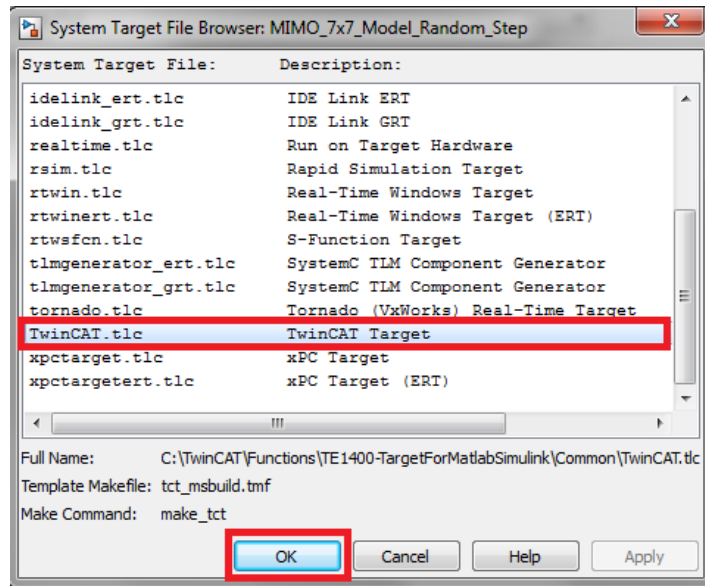
**Figure 7.18: Simulink Solver**

**Step 4.** Select Code Generation and click on Browse to select the system target file.

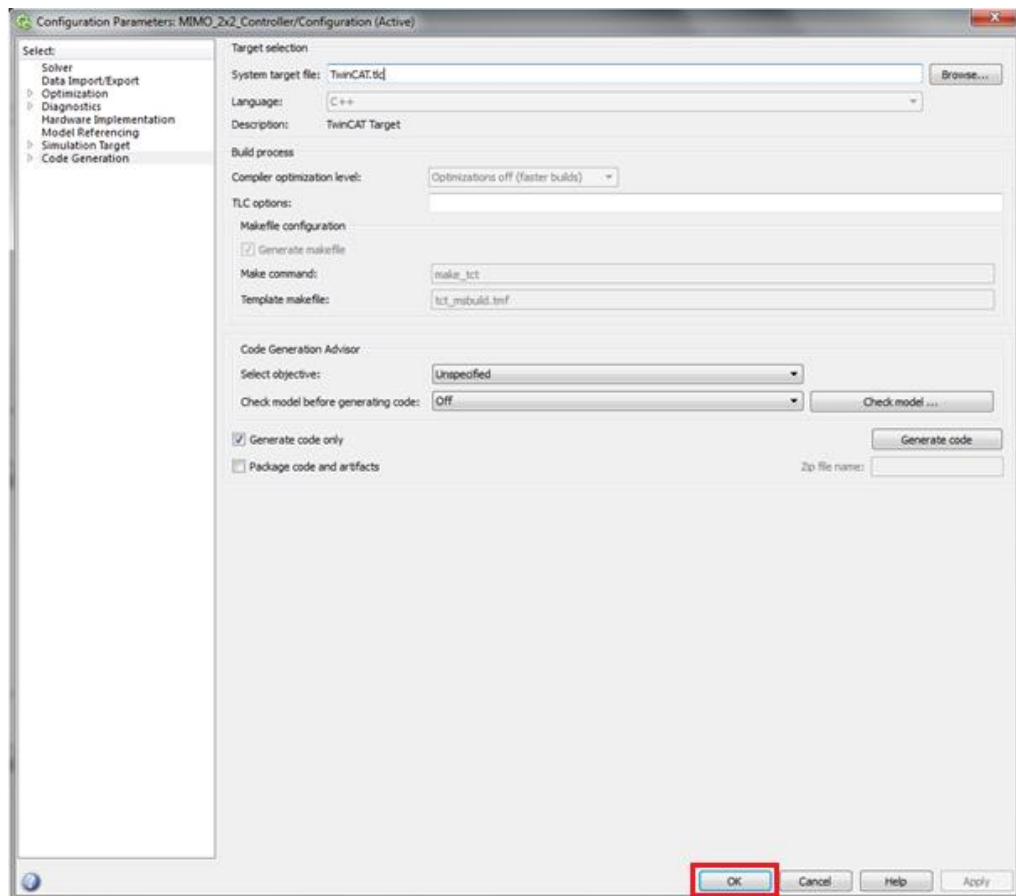


**Figure 7.19: Target file selection**

**Step 5.** Choose the TwinCAT.tlc target file from the System Target File Browser list and click OK and complete the Code Generation Options setup by clicking on apply and OK.

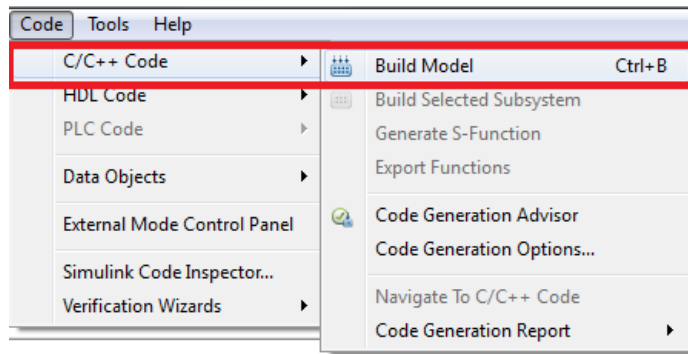


**Figure 7.20: System Target File Browser**



**Figure 7.21: Code Generation Options Complete**

**Step 6.** Navigate the task bar and select Build Model to begin the code generation process and development of the TwinCAT Object Models.



**Figure 7.22: Build Model in Simulink**

**Step 7.** Build progress and report is shown in the MATLAB Command Window

```

### Starting build procedure for model: MIMO_2x2_Controller
### Generating code into build folder: C:\Users\Tzoneva\Desktop\AndisiweMbadamana\MIMO_2x2_Controller_tct
### Invoking Target Language Compiler on MIMO_2x2_Controller.rtw
### Using System Target File: C:\TwinCAT\Functions\TE1400-TargetForMatlabSimulink\Common\TwinCAT.tlc
#####
### TwinCAT Target was started for "MIMO_2x2_Controller"
### MATLAB R2013a (win64)
### TwinCAT 3.1.4010
### TE1400 1.1.1105
#####');
  
```

**Figure 7.23: Starting build procedure**

```

Build succeeded.
    0 Warning(s)
    0 Error(s)

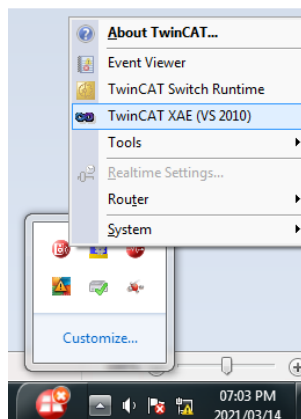
Time Elapsed 00:00:03.80
### Now you can instantiate the generated module in TwinCAT3 on the target platform(s) "TwinCAT RT (x86)".
### Publish procedure completed successfully for TwinCAT RT (x86)

### Used time for code generation and build (HH:MM:SS): 00:00:08

### Generating code generation report #####
  
```

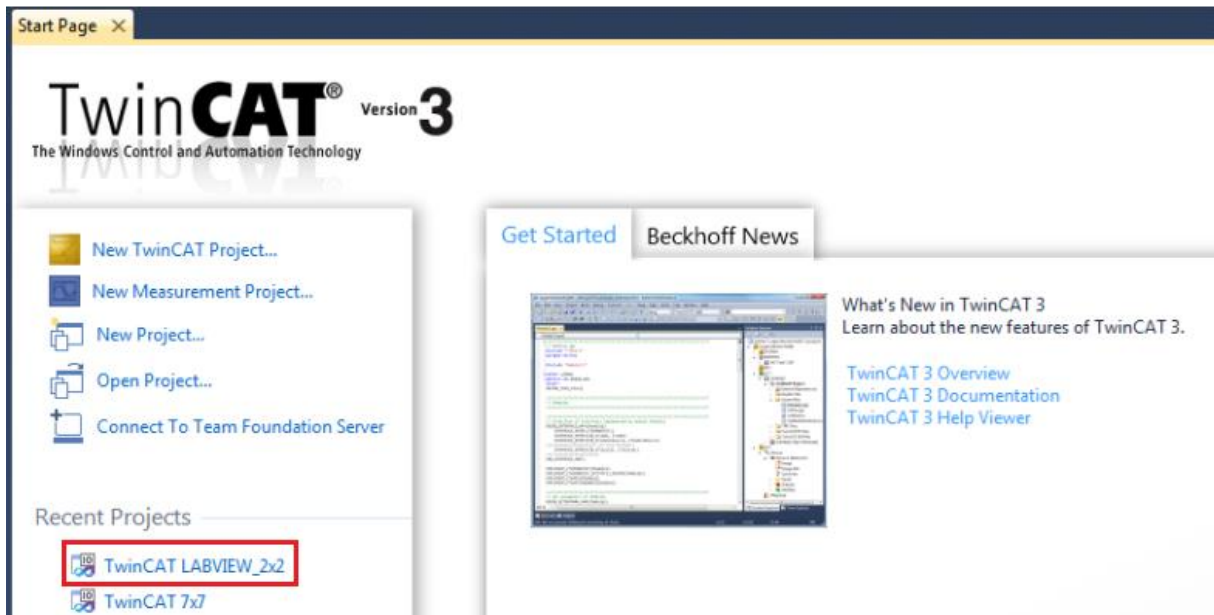
**Figure 7.24: Build successful**

**Step 8.** Open TwinCAT 3 from the Engineering PC.



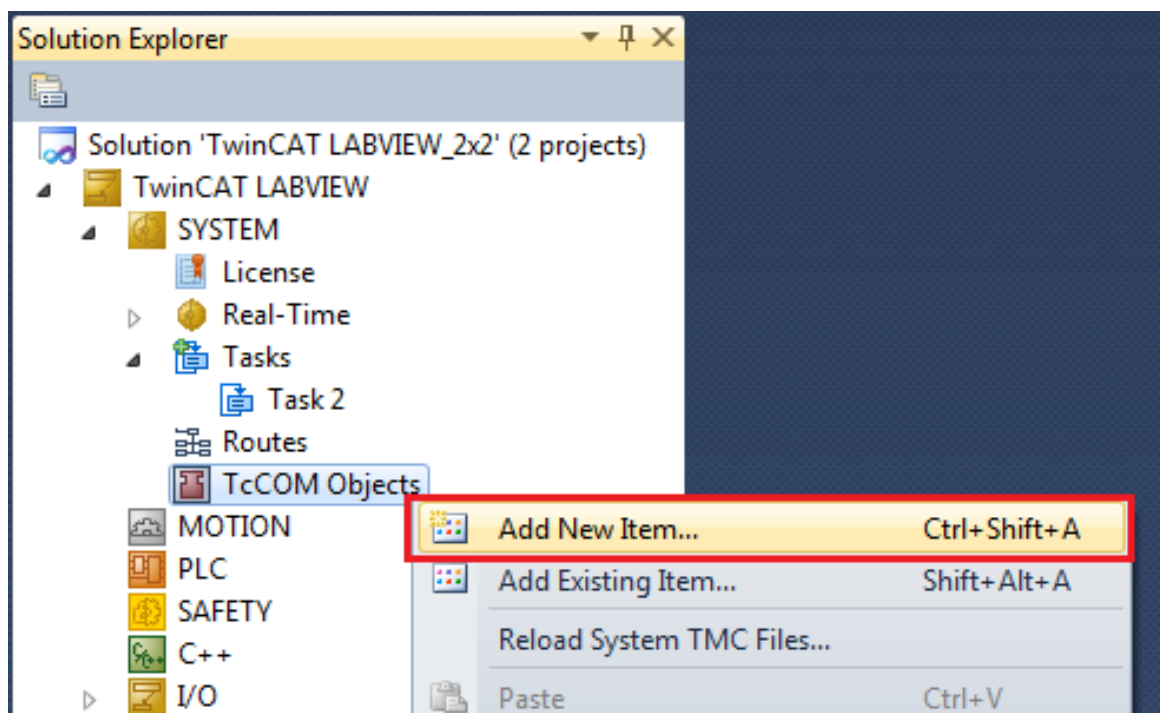
**Figure 7.25: Start TwinCAT**

**Step 9.** Open or Create New TwinCAT 3 Project



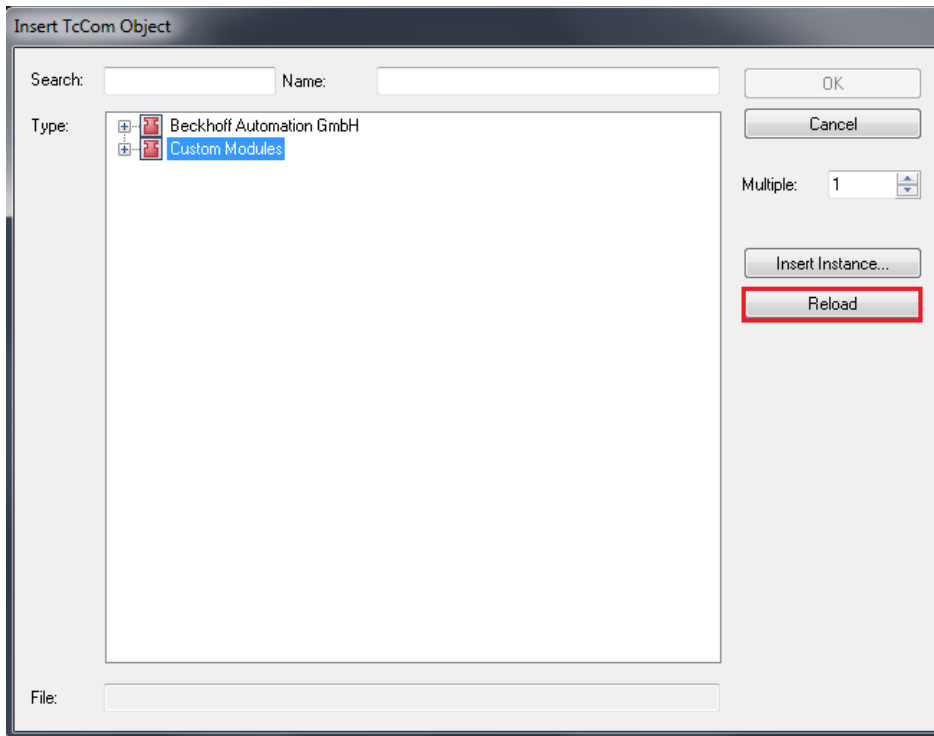
**Figure 7.26:** Open or Create new TwinCAT project

**Step 10.** Right click on TcCOM Objects in the Solutions Explorer and select Add New Item



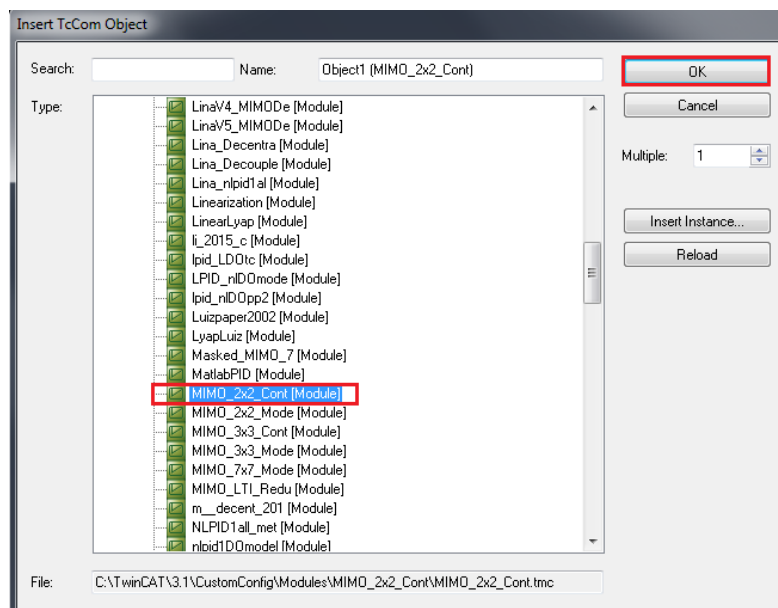
**Figure 7.27:** Adding new TcCOM Objects

**Step 11.** Select Reload and expand the Custom Modules menu.



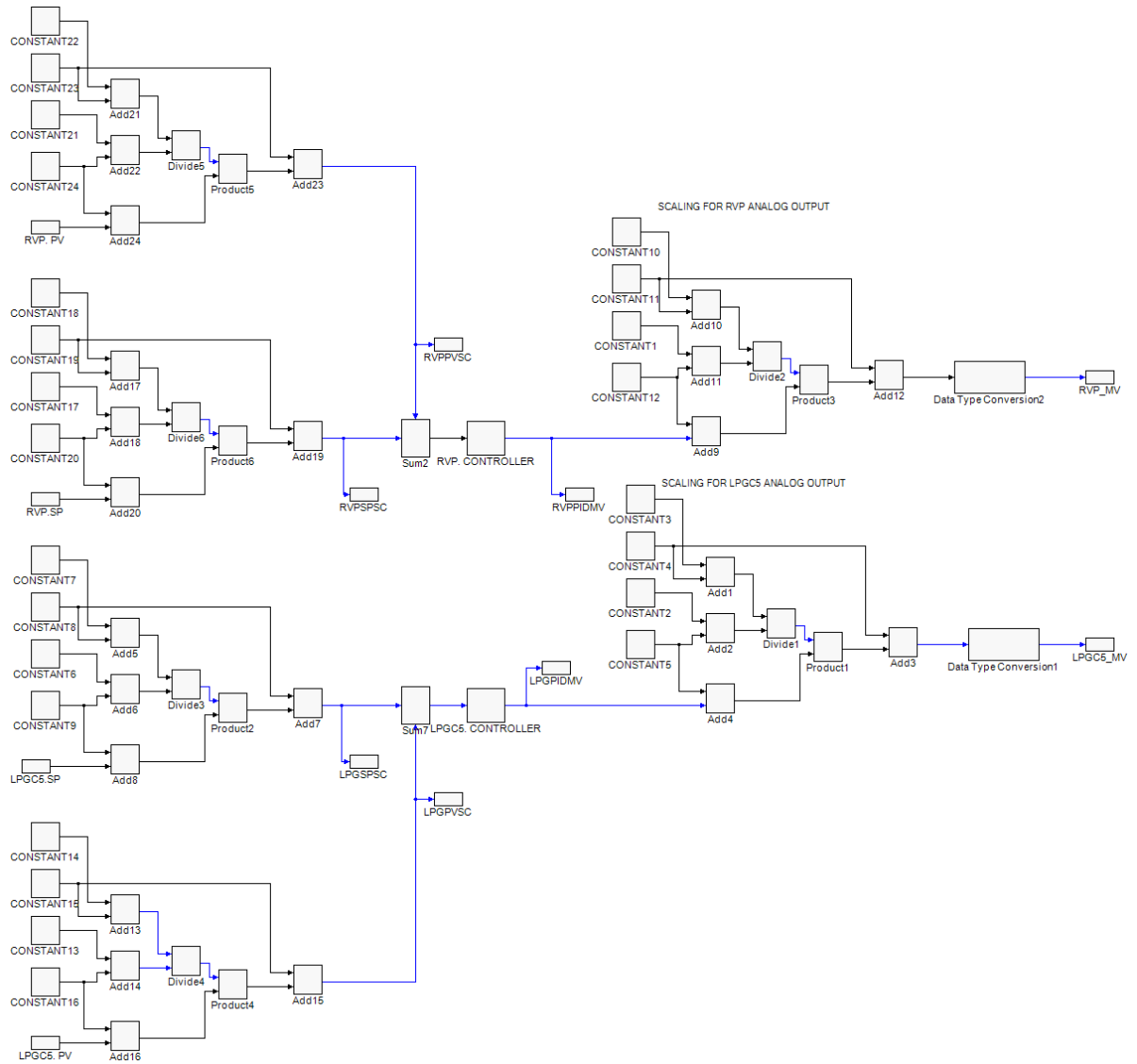
**Figure 7.28:** Expand custom modules

**Step 12.** Select the TcCOM module with the same name as the Simulink model. Click OK.



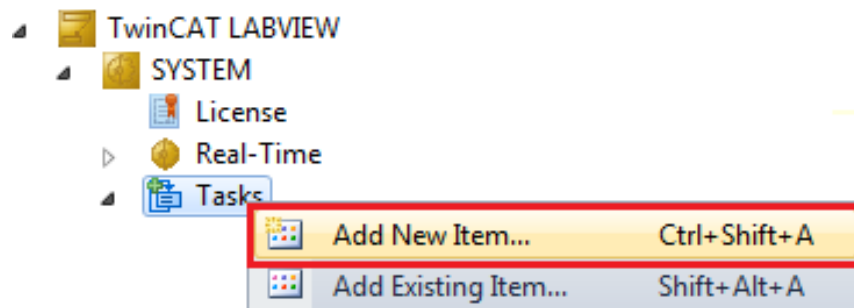
**Figure 7.29:** Inserting Simulink model TcCOM module

**Step 13.** Review Block Diagram of the Uploaded TcCOM Module.



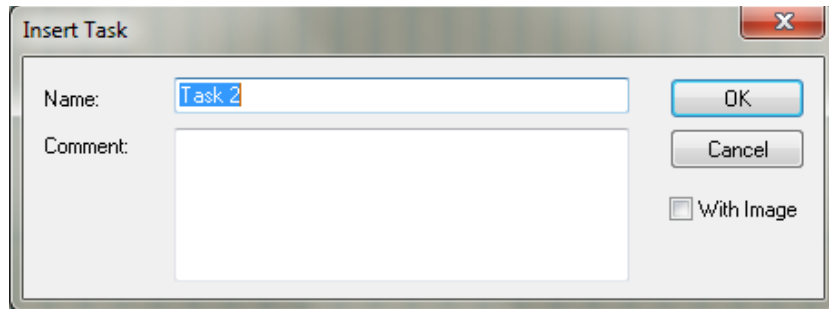
**Figure 7.30:** Simulink model block diagram in TwinCAT

**Step 14.** Right Click on Tasks and Click on Add New Item to create a new task.



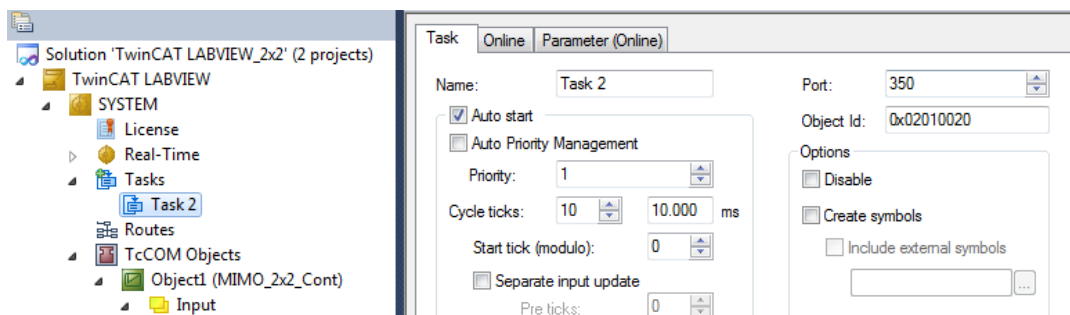
**Figure 7.31:** Creating an execution Task

**Step 15.** Rename Task and Click OK.



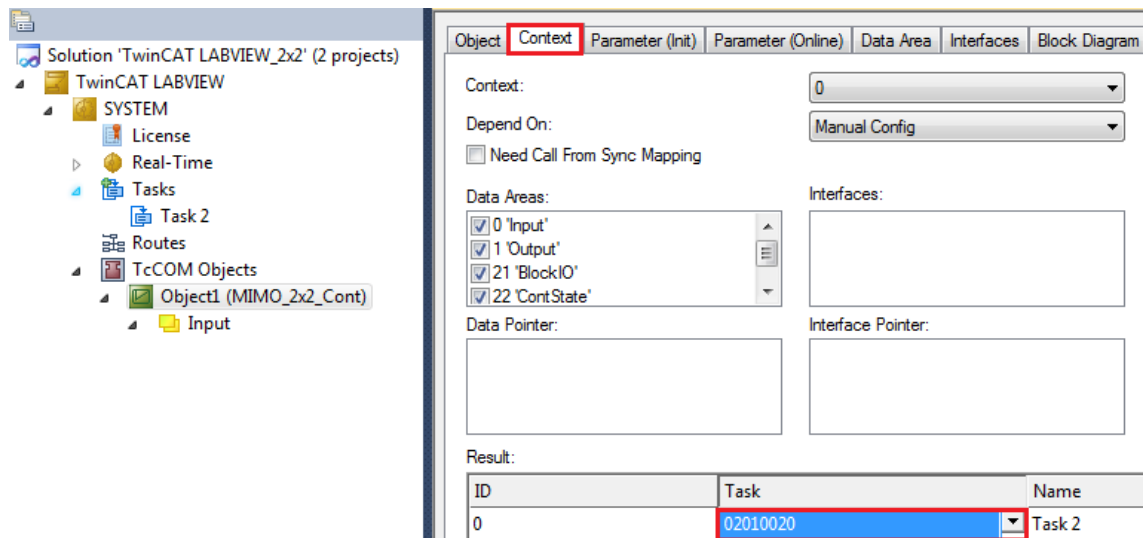
**Figure 7.32: Rename Task**

**Step 16.** Confirm Task has been successfully created. It is not necessary to modify any of the Default parameters.



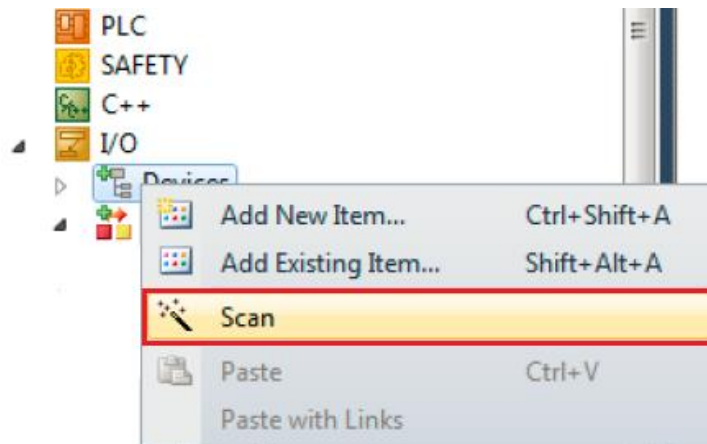
**Figure 7.33: Task has been successfully created**

**Step 17.** Link the Task to the TcCOM object for real-time execution. Click on the TcCOM module, assign the Task under the Context menu.



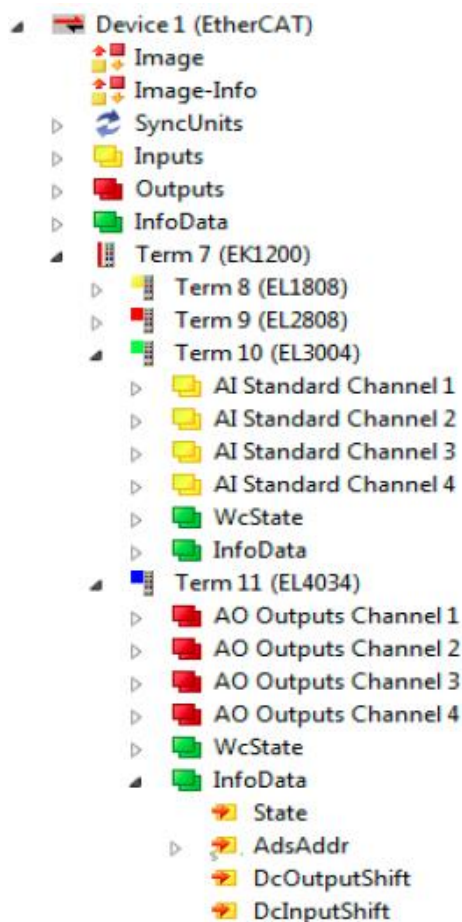
**Figure 7.34: Linking the TcCOM object to the execution Task**

**Step 18.** Ensure the PLC is connected to the Engineering PC and communication has been established. To load the PLC modules, expand the I/O menu and Right Click on Device and select scan.



**Figure 7.35:** Scanning for PLC I/O hardware

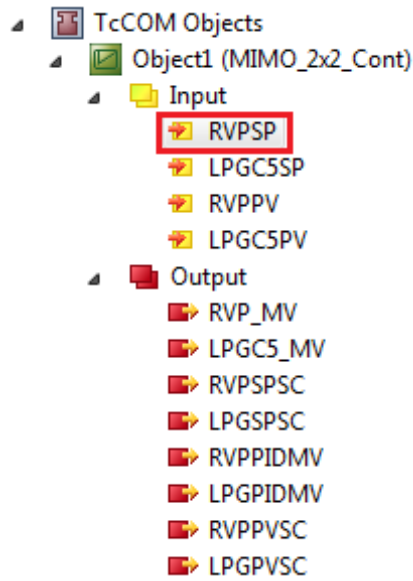
**Step 19.** Confirm all the PLC I/O modules have been successfully loaded.



**Figure 7.36:** PLC I/O modules have been successfully loaded

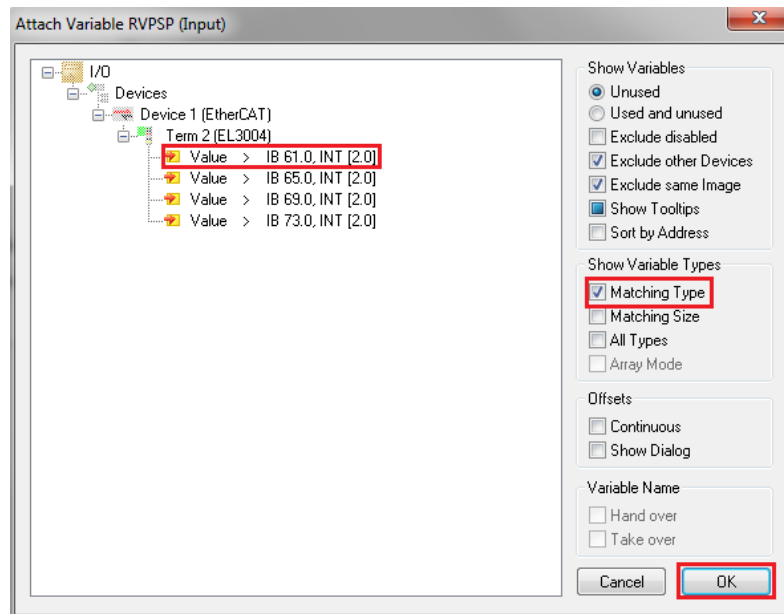


**Step 20.** To Link the model block diagram inputs and outputs to the corresponding PLC inputs and outputs, expand the TcCOM module object and Double Click on the inputs and outputs individually.



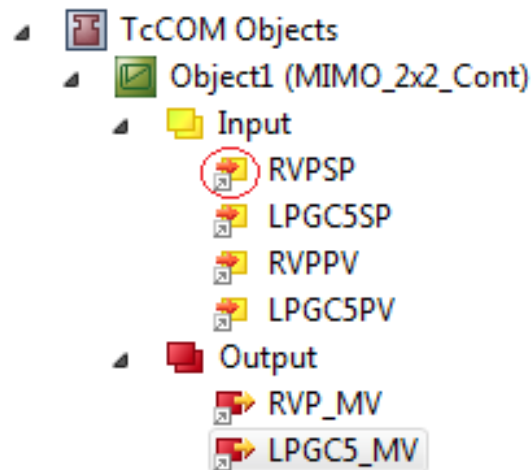
**Figure 7.37: Opening PLC I/O points**

**Step 21.** Check Matching Type and Select the correct PLC I/O and Click OK.



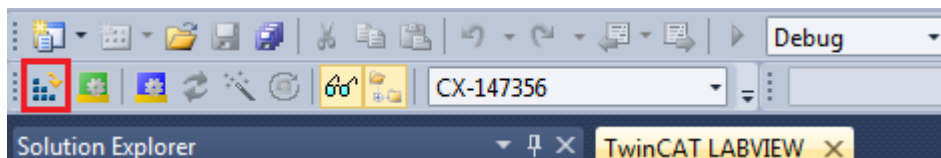
**Figure 7.38: Linking the PLC I/O to the model I/O**

**Step 22.** Repeat **Steps 20** and **21** to Link all inputs and outputs. All linked I/O are indicated with a white upward pointing arrow.



**Figure 7.39: PLC I/O have been successfully linked**

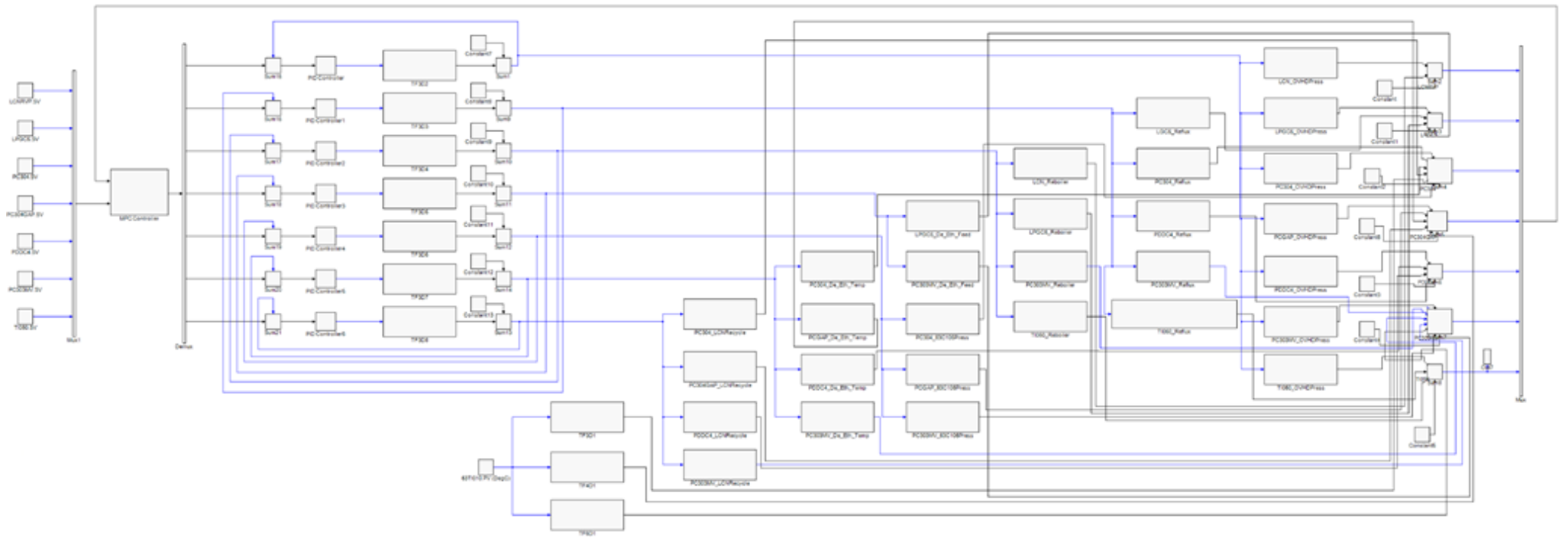
**Step 23.** The procedure is complete. Click on the Activate Configuration icon and place the PLC in Run mode.



**Figure 7.40: Activate Configuration**

The completion of **Step 23** means the Simulink models have been successfully imported into TwinCAT 3 and have been downloaded to the Beckhoff PLC by following the above-mentioned procedure. There are no changes required to any parts of the Simulink models to execute in the TwinCAT 3 environment. All the steps of the procedure, except for **Steps 20-22**, are applicable to both the decentralized PID controllers and seventh order system models. **Steps 20-22** are only applicable to the decentralized PID controller model since it is executed in a Hardware-in-the-Loop configuration where it is necessary for its inputs and outputs to be linked to the real-time target physical inputs and outputs. Following the above procedure for the seventh order system yields the transformed TwinCAT 3 model for the seventh order system shown in block diagram form in Figure 7.41. It is worth noting that the model illustrated in Figure 7.41 is a transformed TwinCAT 3 version of the Simulink model given in Figure 7.8 following the procedure described above.

This section presented an overview of the TwinCAT environment followed by a detailed step-by-step procedure of the model transformation technique. In the following section the programming of the second order debutanizer distillation process model in the LabVIEW environment is presented.



**Figure 7.41:** Simulink model of the seventh order debutanizer distillation process

## 7.4. LabVIEW

The LabVIEW (Laboratory Virtual Instrument Engineering Workbench) environment is a graphical programming software and real-time simulation environment developed by National Instruments (NI) that makes use of icons and virtual instruments (VIs) to represent physical systems (Travis and Kring, 2007). In this chapter, LabVIEW is utilized to program the second order debutanizer distillation process model for execution in a real-time target.

To implement the second order debutanizer distillation process model in LabVIEW for execution in real-time, the transfer function model equations characterizing the systems' dynamic response are programmed into LabVIEW. As described in Chapter 5, the model of the second order debutanizer distillation process is given by Equation 7.3 with the dynamic decouplers used to compensate for the process interactions given in Equations 7.4 and 7.5.

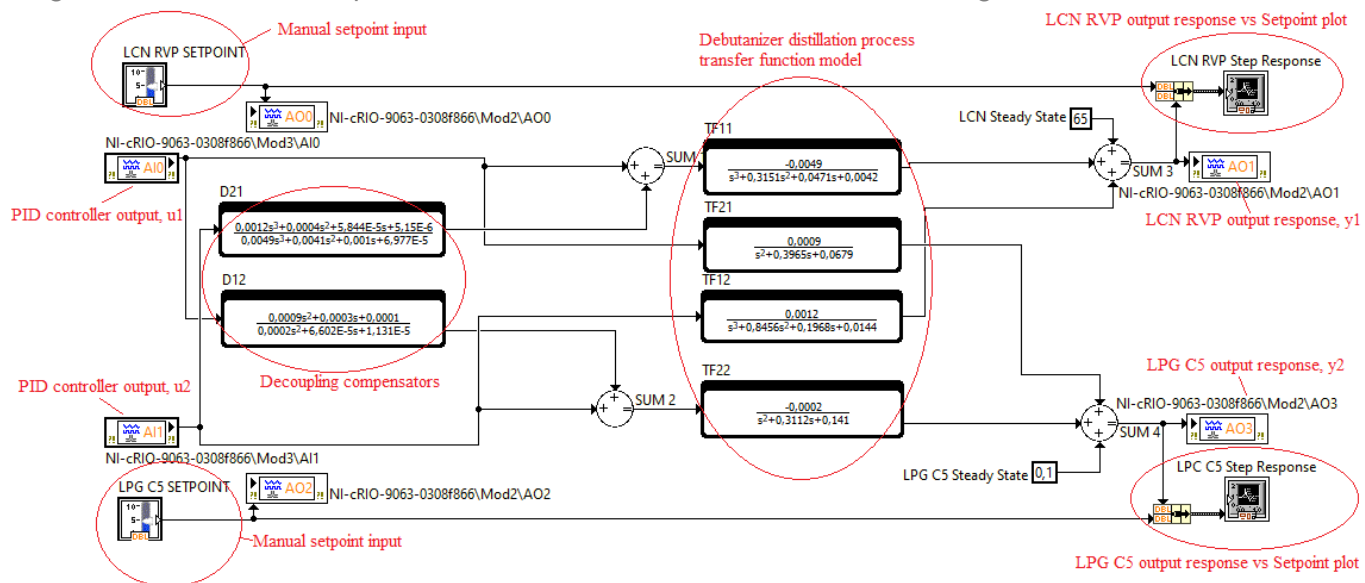
$$\begin{bmatrix} Y_1(s) \\ Y_2(s) \end{bmatrix} = TF(s)U(s) = \begin{bmatrix} TF(s)_{11} & TF(s)_{12} \\ TF(s)_{21} & TF(s)_{22} \end{bmatrix} \begin{bmatrix} U_1(s) \\ U_2(s) \end{bmatrix} = \dots$$

$$\begin{bmatrix} \frac{-0.004852}{s^3 + 0.3151s^2 + 0.04709s + 0.00415} & \frac{0.001241}{s^3 + 0.8456s^2 + 0.1968s + 0.01438} \\ \frac{0.0009339}{s^2 + 0.3965s + 0.06791} & \frac{-0.0001665}{s^2 + 0.3112s + 0.141} \end{bmatrix} \begin{bmatrix} U_1(s) \\ U_2(s) \end{bmatrix} \quad (7.3)$$

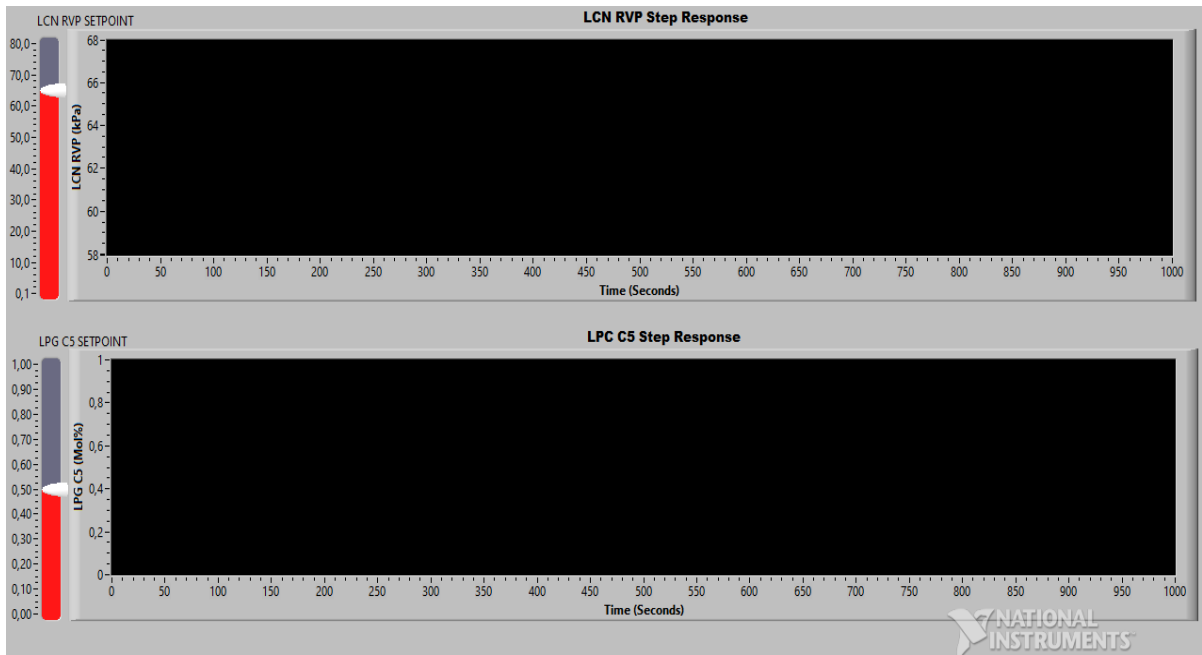
$$D_{12}(s) = \frac{0.0009339s^2 + 0.0002906s + 0.0001317}{0.0001665s^2 + 6.602e-05s + 1.131e-05} \quad (7.1)$$

$$D_{21}(s) = \frac{0.001241s^3 + 0.000391s^2 + 5.844e-05s + 5.15e-06}{0.004852s^3 + 0.004103s^2 + 0.0009549s + 6.977e-05} \quad (7.2)$$

The second order model is identical to the Simulink model described in Chapter 5 with the exception that the decentralized controllers are excluded from the model. Therefore, the decoupled second order debutanizer distillation process programmed in LabVIEW is shown in Figure 7.42 and the front panel, utilized as a user interface, is shown in Figure 7.43.



**Figure 7.42: Block diagram of the second order debutanizer distillation process model in LabVIEW**



**Figure 7.43: Front panel of the second order debutanizer distillation process model in LabVIEW**

The objects used in the programming of the block diagram in LabVIEW are described in Table 7.3. The first column of Table 7.3 provides a description for each the objects while the second column provides the object symbols.

**Table 7.3: LabVIEW block diagram object descriptions**

Object description	Object Symbol
A numerical control object used to enter or display numeric data (National Instruments, 2018a).	
A pointer slide used to display numeric data in a vertical or horizontal slide with a customizable scale and a pointer that helps the user to see the exact value (National Instruments, 2018a).	
Representation of a shared variable on the block diagram. The shared variable node is used to interface with the real-time execution hardware target (National Instruments, 2018b).	
A summing function used to add and/or subtract the input signals (National Instruments, 2018c).	
A waveform chart used for displaying one or more plots of data acquired at a constant rate (National Instruments, 2018d).	
A pulse train signal generator whose value switches between zero and a specified amplitude (National Instruments, 2018e).	
A transfer function block used to implement a system model in transfer function form. The system model is defined by specifying the Numerator and Denominator of the transfer function equation (National Instruments, 2018f).	
A bundle used to assemble a cluster from individual elements (National Instruments, 2018g).	

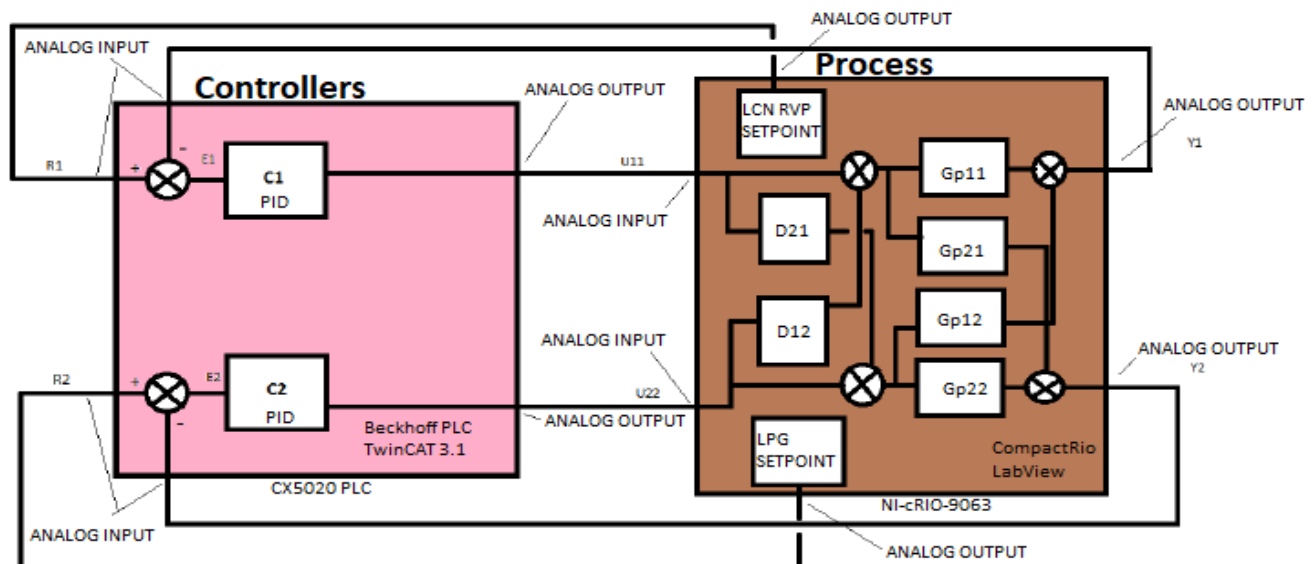
The model is compiled and deployed to the real-time target by clicking the RUN icon. In the absence of errors, the configuration is loaded to the real-time target and in execution.

This section presented an overview of the LabVIEW environment and the description of the programmed second order debutanizer distillation process model transfer functions in the

LabVIEW environment. The following section provides an overview of the Hardware-in-the-Loop architecture configured for the implementation of the second order system of this research.

### 7.5. Hardware-in-the-Loop (HiL) configuration for the second order system simulation

In this section, the hardware and software architecture used in the implementation of the Hardware-in-the-Loop (HiL) configuration is outlined. The second order debutanizer distillation process model is programmed in the LabVIEW real-time simulation environment while the decentralized PID controllers are transformed from Simulink into Beckhoff's TwinCAT 3 real-time simulation environment. The overall closed-loop second order system is configured in a Hardware-in-the-Loop testbed. The physical hardware architecture necessary to achieve a Hardware-in-the-Loop (HiL) simulation testbed is illustrated in the block diagram shown in Figure 7.44.



**Figure 7.44: Overview of the hardware and software architecture for the second order debutanizer closed loop control system**

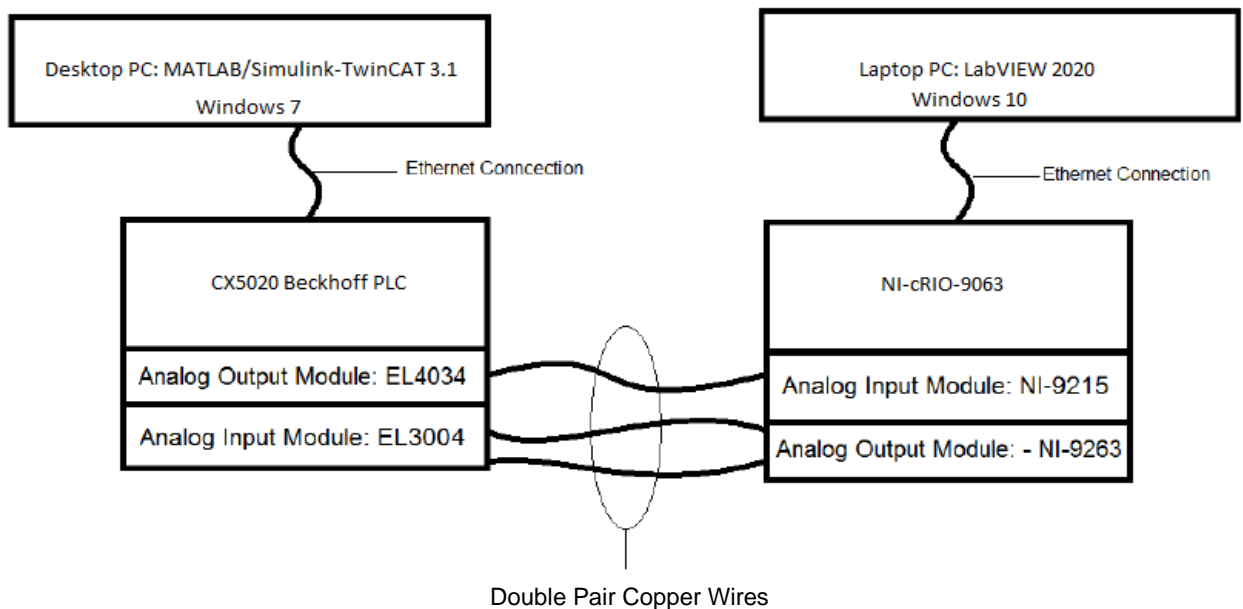
The two hardware platforms used in this research are the Beckhoff CX5020 PLC and the National Instruments CompactRIO NI-cRIO-9063. The Beckhoff PLC is the controller hardware where the decentralized PID controllers are executed whereas the CompactRIO is the virtual plant environment where the model of the second order debutanizer distillation process model is executed. The hardware specifications of the Beckhoff PLC and CompactRIO are provided in **Appendix C**. The Beckhoff PLC and the CompactRIO are physically hardwired together to form a Hardware-in-the-Loop testbed. The PID controllers are connected to the process model in LabVIEW with hardwiring between the Beckhoff PLC and the CompactRIO input and output (I/O) modules. The analog inputs of the CompactRIO are the PID controller outputs which are the analog outputs of the Beckhoff PLC. Similarly, the analog inputs of the Beckhoff PLC are

the outputs of the process model and their target setpoints which are analog outputs of CompactRIO, as illustrated in Figure 7.44. A summary of the system hardware and software components used in the configuration of the Hardware-in-the-Loop architecture are listed in Table 7.4.

**Table 7.4: Summary of the system hardware and software components**

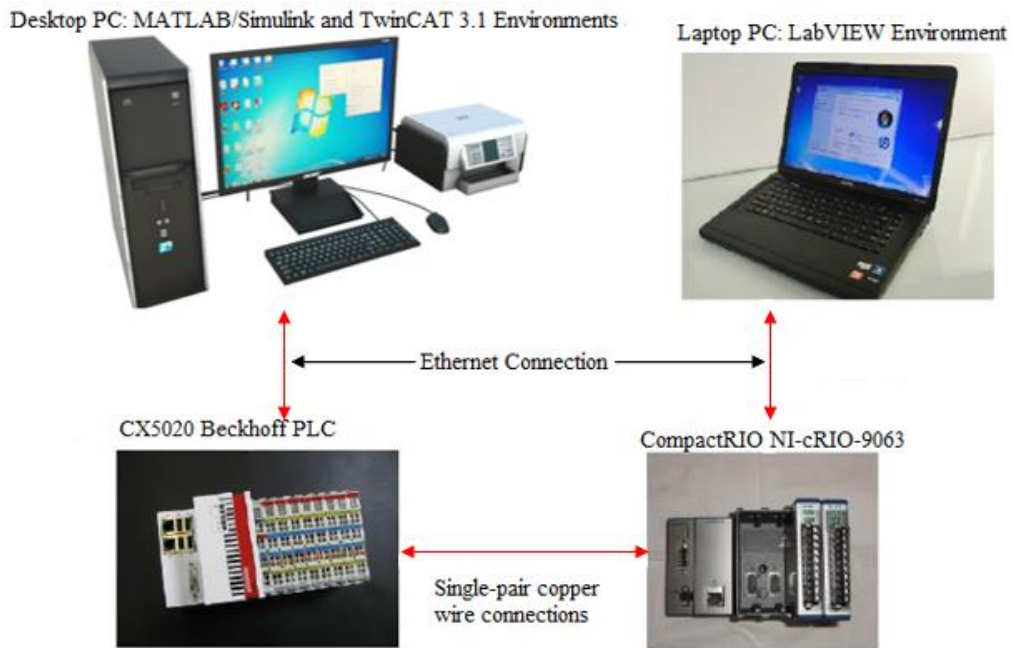
PID controllers		Second order debutanizer distillation process	
Desktop PC with Windows 7		Laptop PC with Windows 10	
MATLAB/Simulink - TwinCAT 3		LabVIEW 2020	
Beckhoff PLC CX5020		NI-cRIO-9063	
EL3004 Analog Input	EL4034 Analog Output	NI 9215 Analog Input	NI 9263 Analog Output

Figure 7.45 illustrates the system architecture and physical connections. The desktop personal computer (PC) where the MATLAB/Simulink environments are installed is connected to the Beckhoff PLC via an Ethernet local area network (LAN) cable connection. The Beckhoff PLC is comprised of two input and output modules which are connected to the CompactRIO input and output modules via copper cable connections. The laptop personal computer (PC) where the LabVIEW software environment is installed is connected to the CompactRIO via an Ethernet local area network (LAN) cable connection. The power supplies are omitted to simplify the diagram shown in Figure 7.45 and improve clarity. However, it is worth noting that the Beckhoff PLC is supplied with a 24 V DC power supply whereas the CompactRIO is supplied with a wall socket 230 V AC and 50 Hz power.



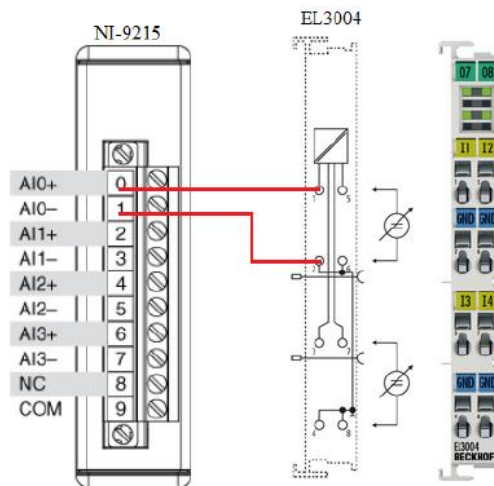
**Figure 7.45: Connections between systems in the Beckhoff PLC and the CompactRIO**

A high-level overview diagram showing the signal information flow between the interconnected physical systems is shown in Figure 7.46. The required physical connections are not complex thus making the system easily configurable.



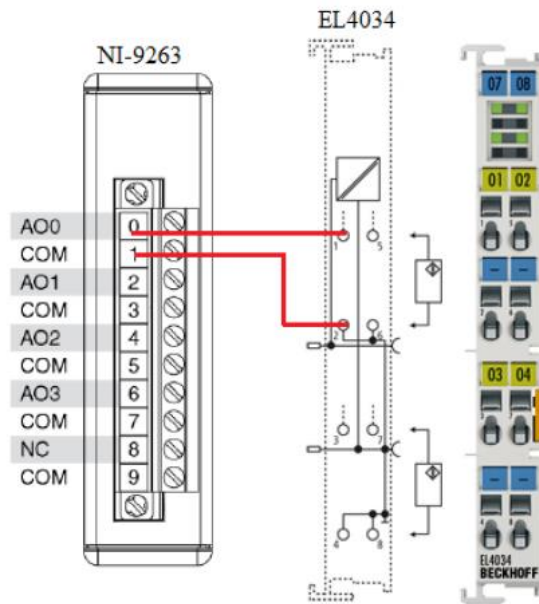
**Figure 7.46: Signal information flow between the interconnected physical systems**

The wiring diagrams utilized for making physical connections between the Beckhoff PLC and CompactRIO input and output modules are shown in Figures 7.47 and 7.48. The connections are made with both power supplies disconnected to minimize the risk of creating short-circuit connections leading to potential irreversible damage to the modules. It is worth noting that the PLC modules utilize spring-loaded terminals whereas the CompactRIO modules are screwed-type connection terminals.



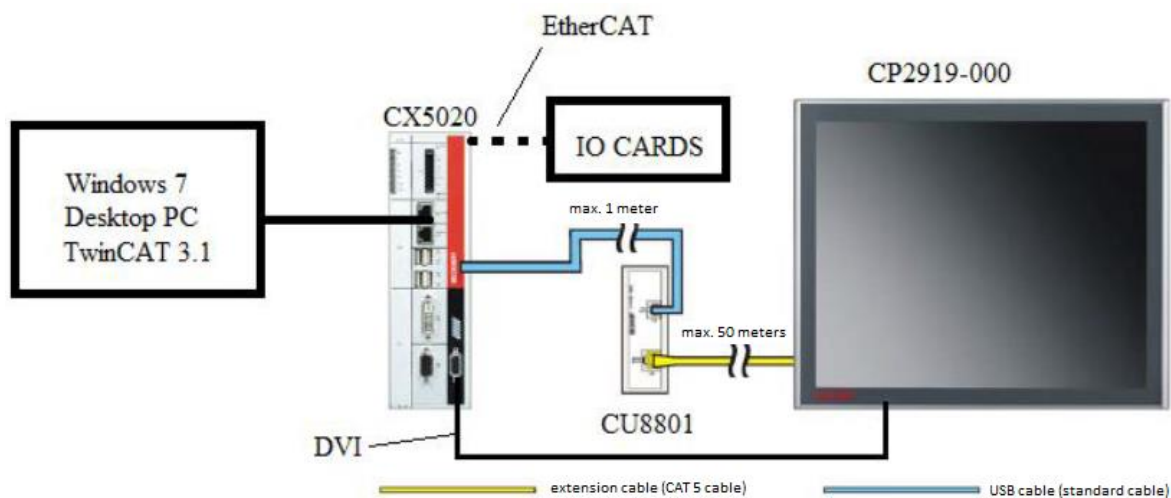
**Figure 7.47: NI-9215 and EL3004 typical wiring diagram**





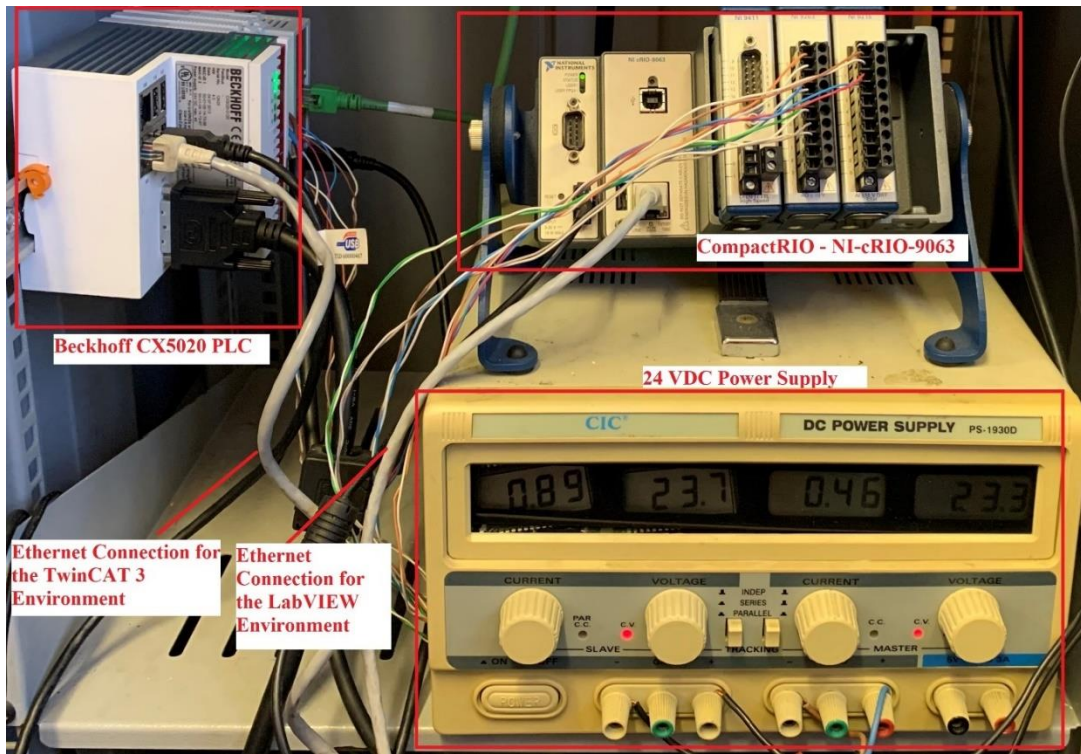
**Figure 7.48: NI-9263 and EL4034 typical wiring diagram**

The Beckhoff PLC is further connected to a Beckhoff multi-touch control panel with a digital visual interface (DVI) and universal serial bus (USB) extended interface. The control panel is typically used when the Beckhoff PLC is configured for remote panel operation. However, for the purposes of this research the control panel is not utilized other than for displaying errors originating from the Beckhoff PLC during system development. Shown in Figure 7.49 below is the connection of the multi-touch control panel to the Beckhoff PLC.



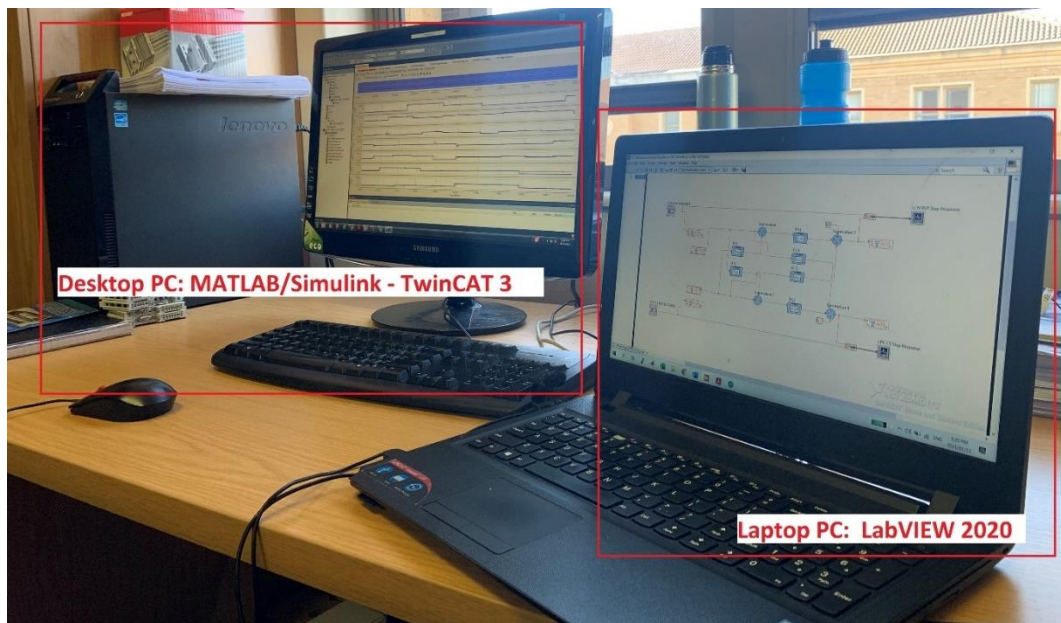
**Figure 7.49: Connection of the CP2919 multi-touch control panel to the Beckhoff PLC**

The purpose of the CU8801 universal serial bus (USB) extender interface is to extend the allowable length of a standard USB connection from 5 meters up to a maximum of 50 meters (Beckhoff Automation, 2020b). The physical system connected in a Hardware-in-the-Loop configuration for this research is given in Figure 7.50 where the 24 V DC power supply, the CompactRIO, the Beckhoff PLC and the two LAN Ethernet connections linked to the PC's are shown.



**Figure 7.50:** Physical system connected in a Hardware-in-the-Loop configuration

The two PCs used in this research are shown in Figure 7.51. The desktop PC is where the MATLAB/Simulink environments are installed, and the laptop PC is where the LabVIEW software environment is installed.

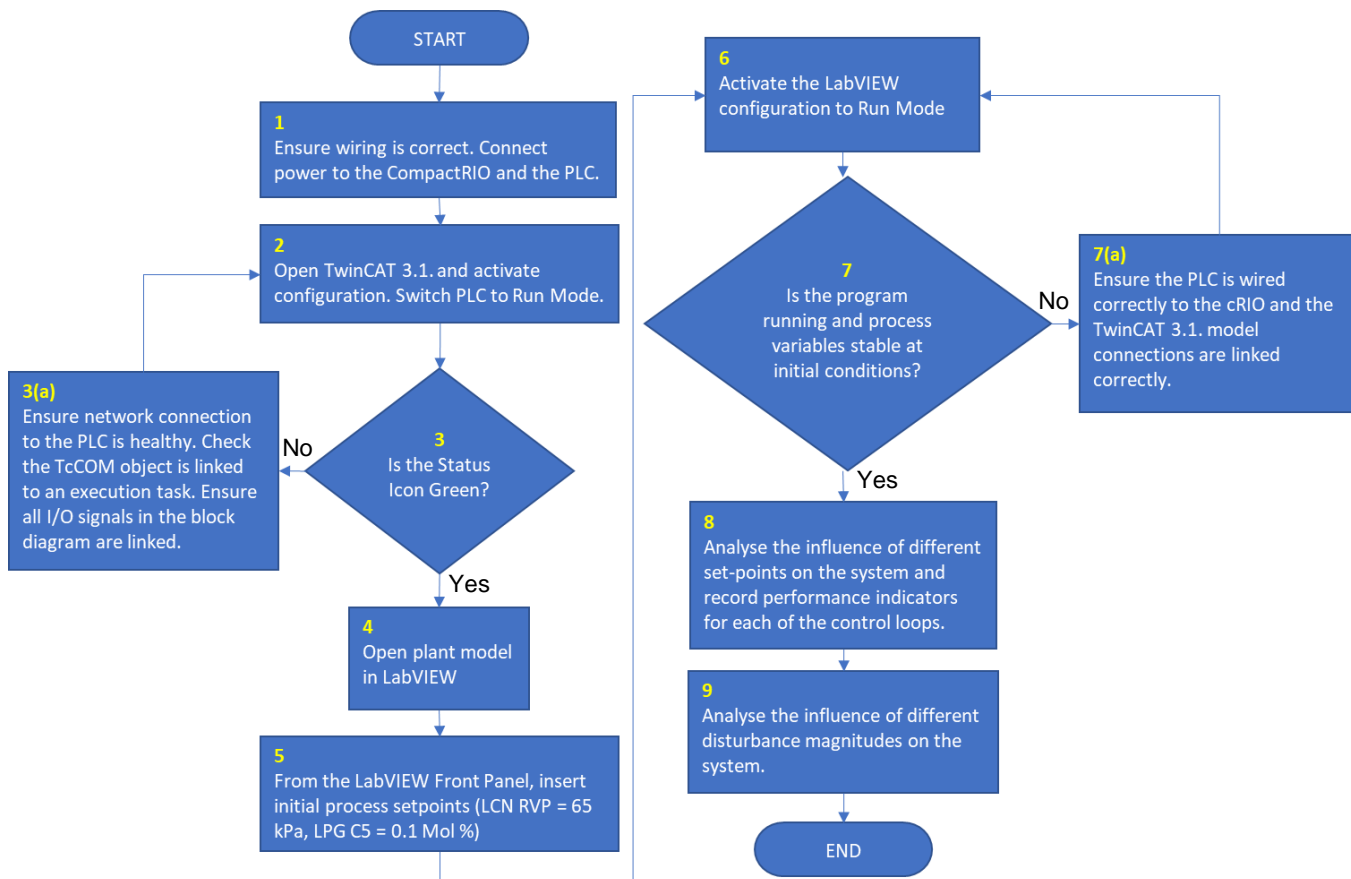


**Figure 7.51:** Personal computers where the development environments are installed

In this section, the hardware and software architecture used in the configuration of the Hardware-in-the-Loop (HiL) configuration is outlined. In the following section, the real-time simulation of the second order debutanizer distillation process is presented.

## 7.6. Real-time simulation of the second order debutanizer distillation process model

In this section, the real-time Hardware-in-the-Loop (HiL) simulation of the second order debutanizer distillation process is presented. The simulation study follows a pre-defined simulation plan as outlined by the simulation flow chart in Figure 7.52. The flow chart consists of nine steps. The flow chart outlines a continuation from the development of the system from the previous sections and establishes a consistent approach in simulating and observing the performance of the system.



**Figure 7.52: Flowchart for the second order system Hardware-in-the-Loop real-time simulation**

The first step is to ensure that the interface wiring connections are correct and connect power supplies to the CompactRIO and the Beckhoff PLC. The second step is to open TwinCAT, activate the configuration and place the Beckhoff PLC in Run mode. When the Beckhoff PLC is in Run mode, the Status Icon in TwinCAT turns Green. If the Status Icon is not Green, it means the PLC is not in Run mode. As part of the third step, investigate the cause, resolve, and attempt to activate the configuration. Possible causes could be network connectivity or that there are some inputs and outputs that are not linked properly. The fourth step is to open the process model in the LabVIEW environment. The fifth step is to configure the initial setpoints in the LabVIEW front panel using the Slider numerical control object. Once the initial

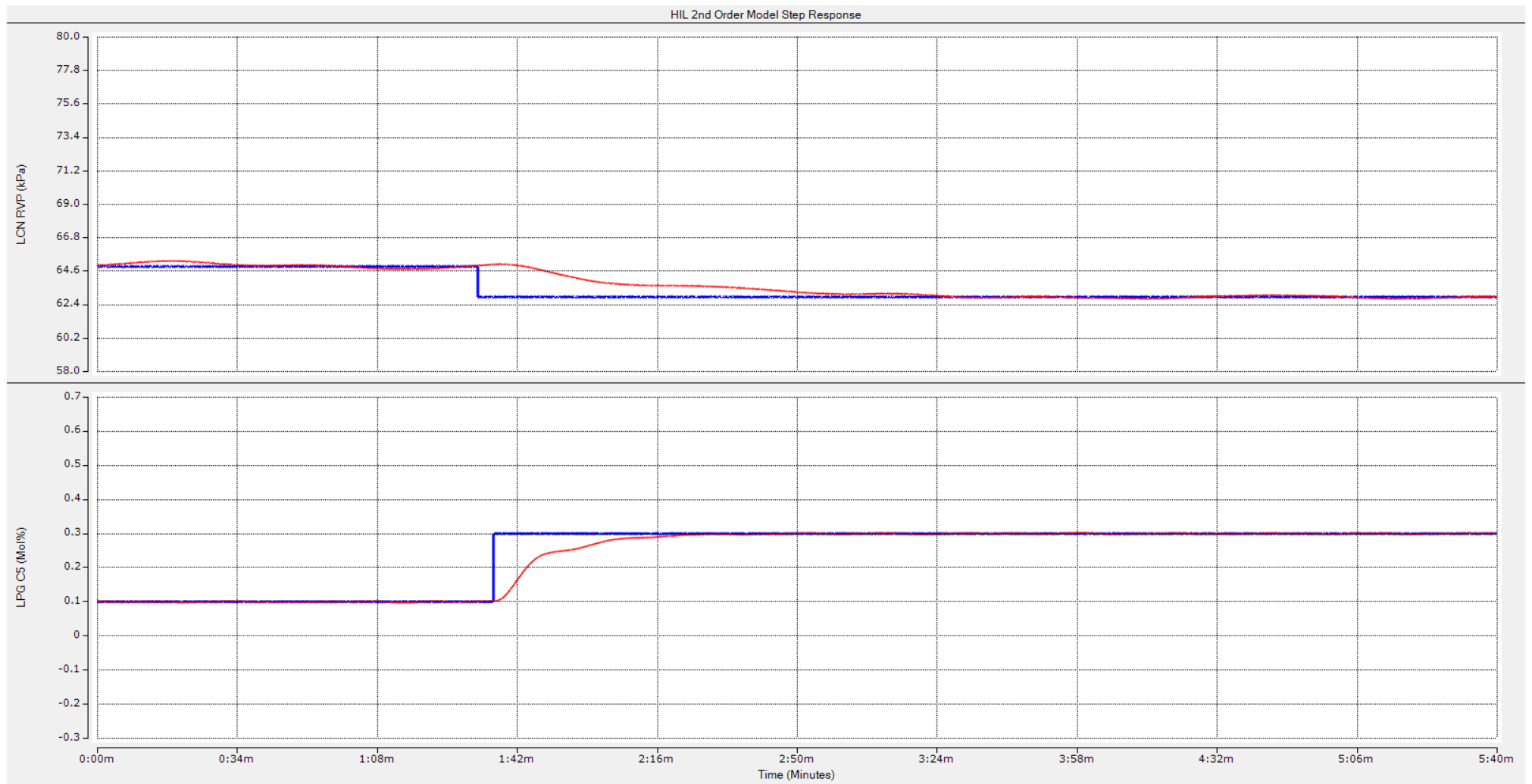
setpoints are entered into the front panel, activate the LabVIEW configuration to Run mode as part of the sixth step.

The completion of the sixth step results in both the CompactRIO and the Beckhoff PLC being in execution model and exchanging signal information. Step seven is to confirm that the controlled variables are stable at their initial target setpoints and resolve any possible issues that may be preventing the program from executing. The eighth step is to analyse the influence of different set-points on the system and record performance indicators for each of the control loops. The ninth and final step is to analyse the influence of different disturbance magnitudes on the system and record performance indicators for each of the control loops. The results obtained from the system are recorded in TwinCAT 3 Scope Viewer.

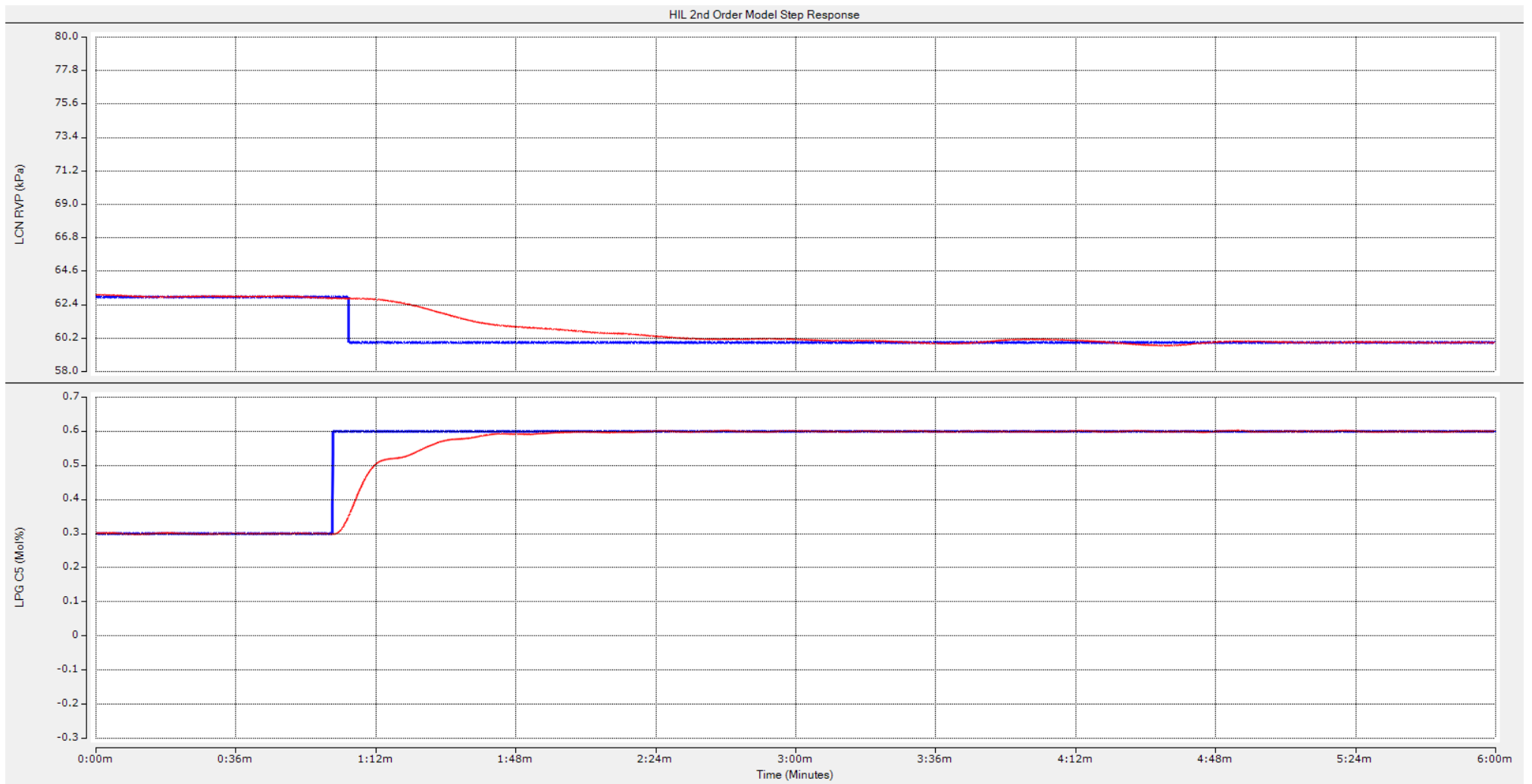
The setpoint step changes are entered in LabVIEW, and the results are recorded in TwinCAT 3 Scope View. The controlled variables are considered linear within the specified range. Table 7.5 below shows the limited range of set points that the system is subjected to. Setpoints outside the specified range could cause the system to be unstable. The LCN\_RVP loop is varied near its steady state range of 60 kPa to 73 kPa. Similarly, the LPG\_C5 set point is varied near its steady state range of 0.01 Mol % to 0.6 Mol %. The step responses for the two decentralized loops are presented in the Figures 7.53 – 7.57. The figures are presented in landscape format to improve clarify of the text contained in the step response charts.

**Table 7.5: Case study of set points for the second order system**

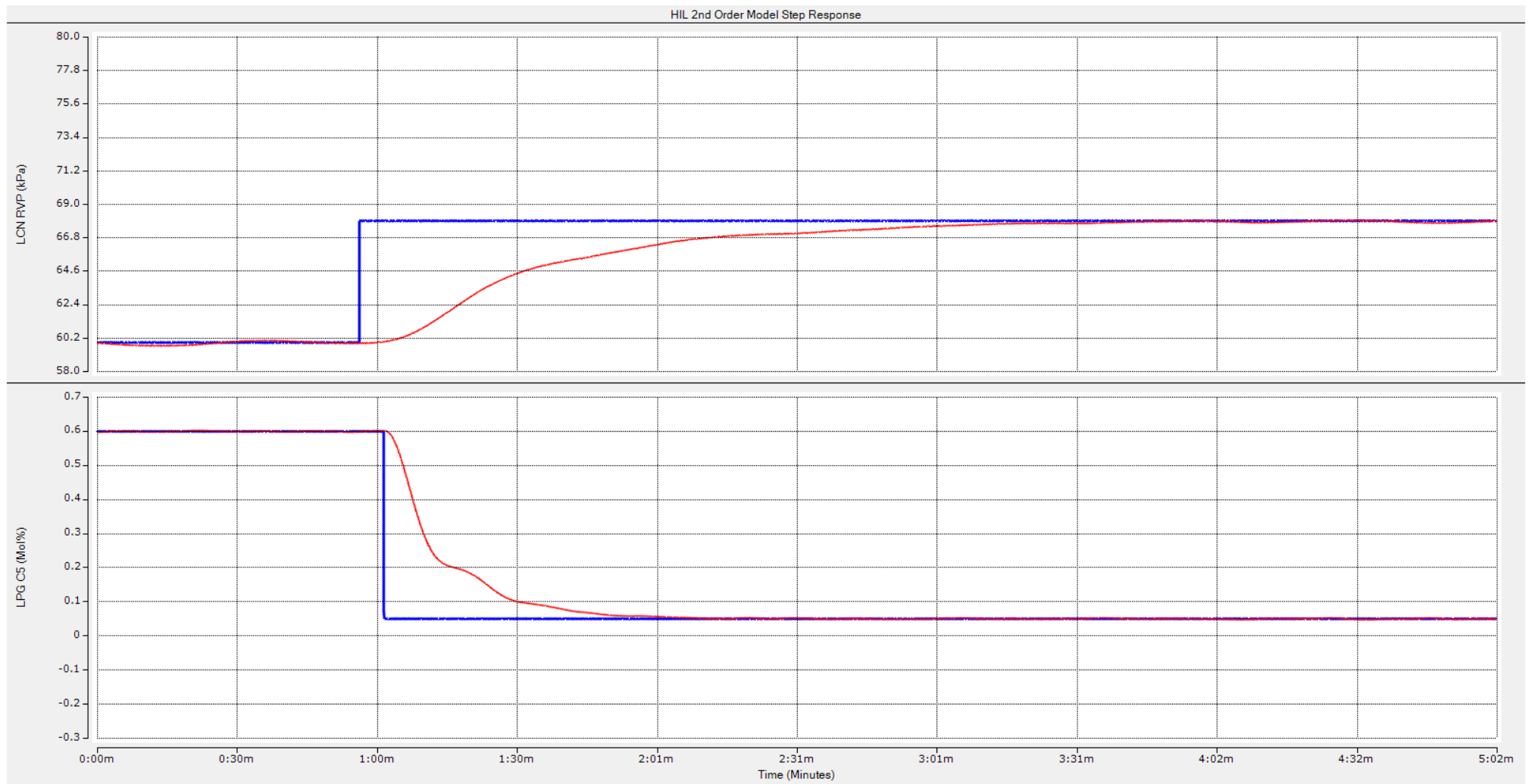
Case #	Loop Name	Initial Setpoint	Final Setpoint	Step Size
7.5.1	LCN_RVP	65 kPa	63 kPa	-2 kPa
	LPG_C5	0.1 Mol%	0.3 Mol%	+0.2 Mol%
7.5.2	LCN_RVP	63 kPa	60 kPa	-3 kPa
	LPG_C5	0.3 Mol%	0.6 Mol%	+0.3 Mol%
7.5.3	LCN_RVP	60 kPa	68 kPa	+8 kPa
	LPG_C5	0.6 Mol%	0.05 Mol%	-0.55 Mol%
7.5.4	LCN_RVP	68 kPa	73 kPa	+5 kPa
	LPG_C5	0.05 Mol%	0.01 Mol%	-0.04 Mol%
7.5.5	LCN_RVP	73 kPa	65.5 kPa	-7.5 kPa
	LPG_C5	0.01 Mol%	0.15 Mol%	+0.14 Mol%



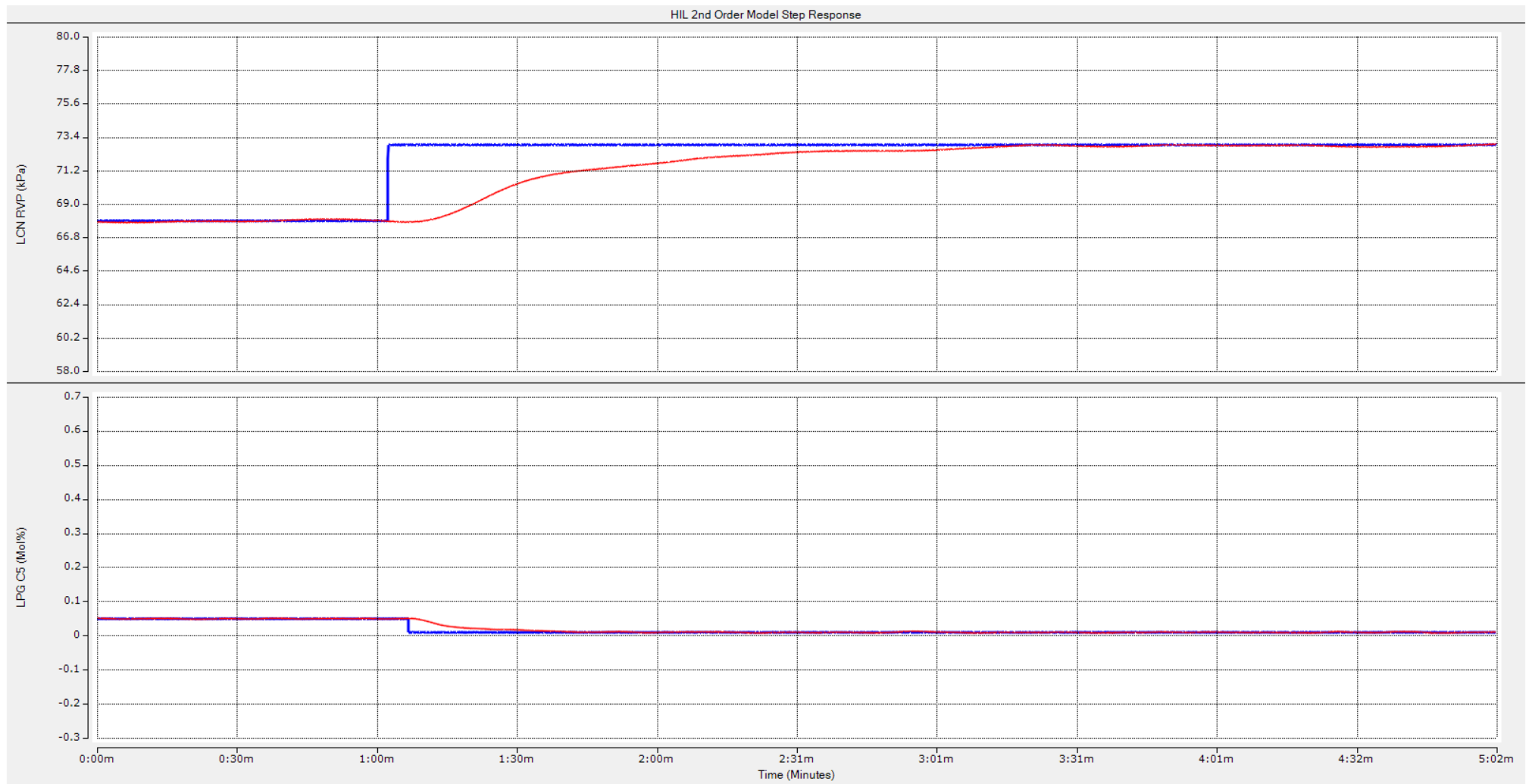
**Figure 7.53:** Case #7.5.1 – LCN RVP dynamic response to a -2 kPa setpoint step change from 65 kPa to 63 kPa and LPG C5 concentration dynamic response to a +0.2 Mol% setpoint step change from 0.1 Mol% to 0.3 Mol% steady state



**Figure 7.54:** Case #7.5.2 – LCN\_RVP dynamic response to a -3 kPa setpoint step change from 63 kPa to 60 kPa steady state and LPG\_C5 concentration dynamic response to a +0.3 Mol% setpoint step change from 0.3 Mol% to 0.6 Mol % steady state

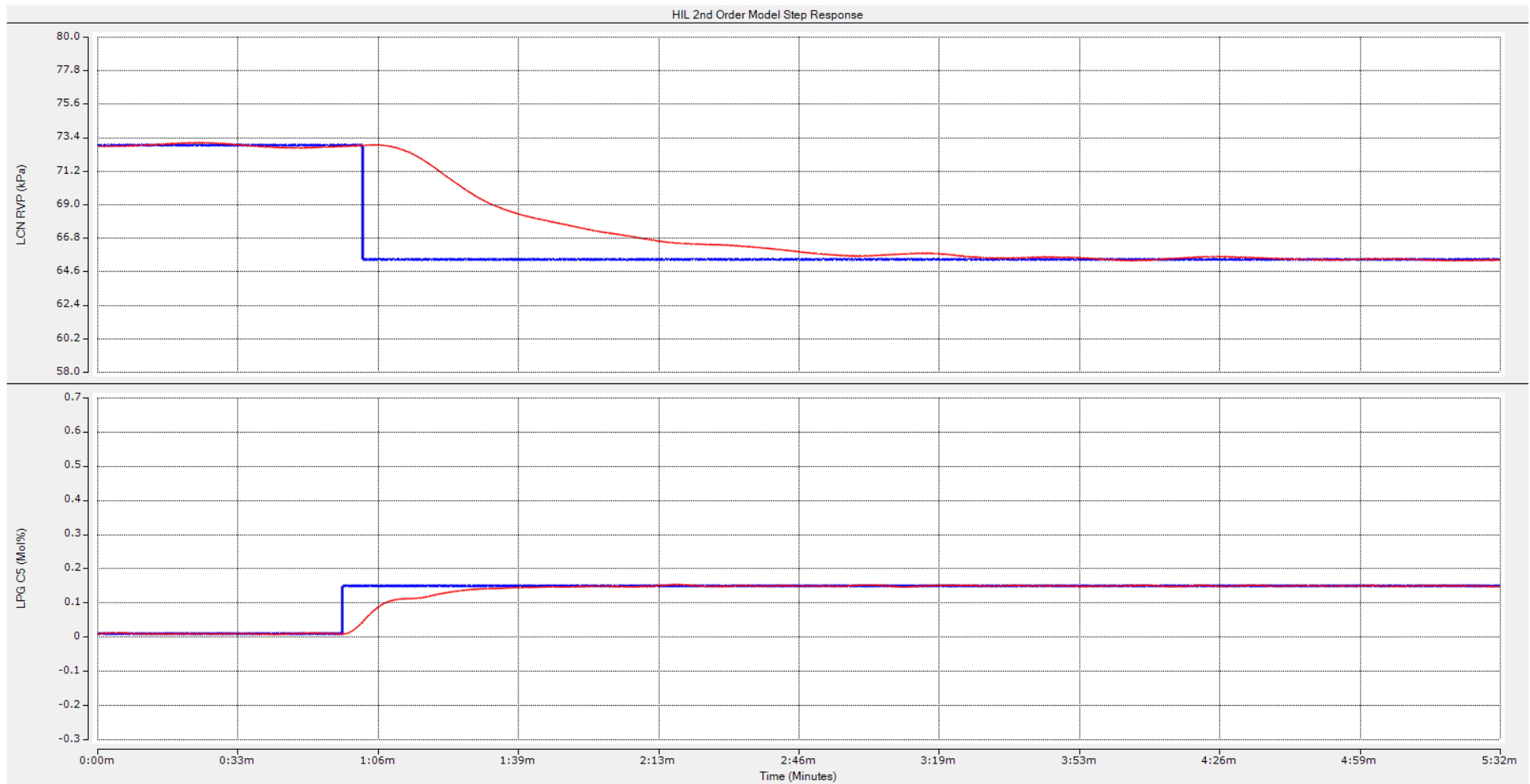


**Figure 7.55:** Case #7.5.3 – LCN\_RVP dynamic response to a +8 kPa setpoint step change from 60 kPa to 68 kPa steady state and LPG\_C5 concentration dynamic response to a -0.55 Mol% setpoint step change from 0.6 Mol % to 0.05 Mol % steady state



**Figure 7.56: Case #7.5.4 – LCN\_RVP dynamic response to a +5 kPa setpoint step change from 68 kPa to 73 kPa steady state and LPG\_C5 concentration dynamic response to a -0.04 Mol% setpoint step change from 0.05 Mol % to 0.01 Mol % steady state**





**Figure 7.57: Case #7.5.5 – LCN\_RVP dynamic response to a -7.5 kPa setpoint step change from 73 kPa to 65.5 kPa steady state and LPG\_C5 concentration dynamic response to a +0.14 Mol% setpoint step change from 0.01 Mol % to 0.15 Mol % steady state**

The above step response tests are conducted following Table 7.5 without introducing disturbances on the inputs and outputs of the process model. To investigate the effect of disturbances on the controller performance, disturbances are added to the process model. Random noise signal generators with bounded amplitudes are used to simulate output disturbances to investigate the effect of sensor measurement noise on controller performance. On the other hand, pulse signals with varying frequencies and amplitudes are used to simulate input disturbances to investigate the effect of unmeasured process disturbances on controller performance. The pulse and noise signal parameters are configured as shown in Tables 7.6 and 7.7.

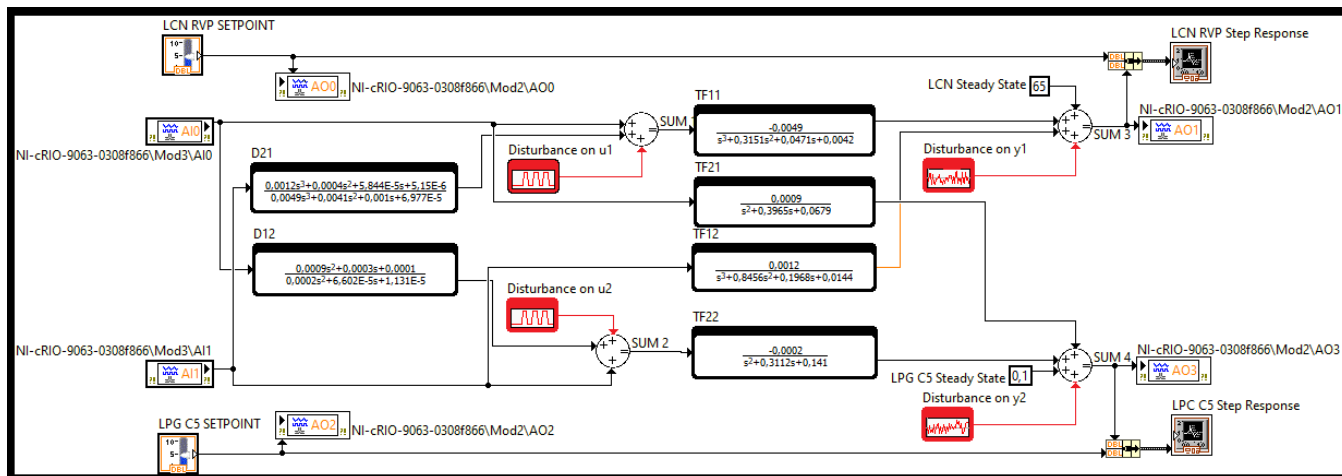
**Table 7.6: Pulse Generator Input Disturbance Parameters**

Input	Start time	Amplitudes	Offset	Duty cycle	Period
u1	0 seconds	1; 2; 3	0	50%	500 seconds
u2	0 seconds	10; 20; 30	0	50%	500 seconds

**Table 7.7: Random Noise Generator Output Disturbance Parameters**

Input	Signal type	Amplitudes	Offset	Frequency	Phase
y1	Random	0.01; 0.1; 1	0	Ignored	0 degrees
y2	Random	0.001; 0.01; 0.1	0	Ignored	0 degrees

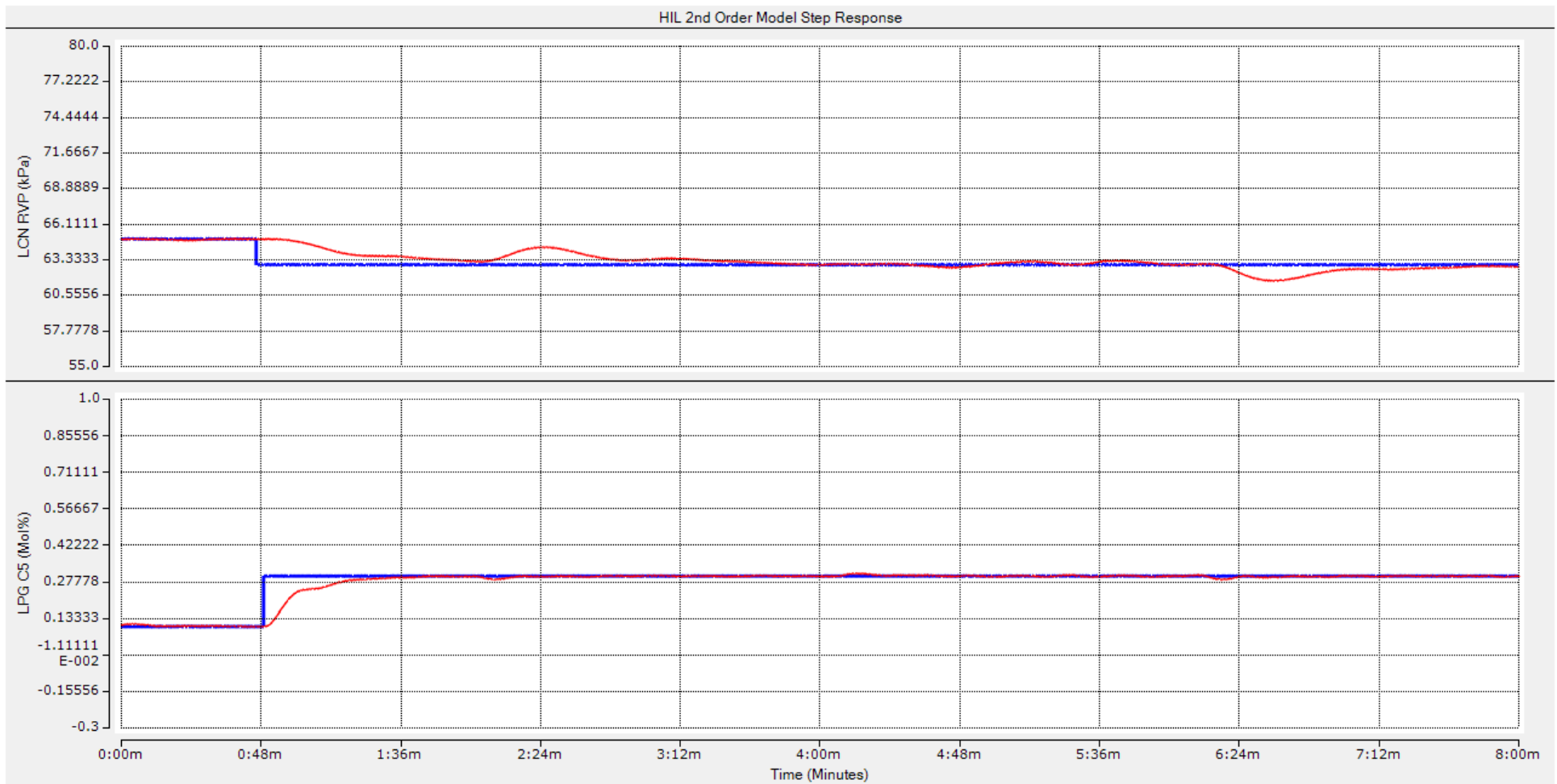
Figure 7.58 shows the LabVIEW block diagram of the process with the presence of disturbances. The case study step tests with the disturbance characteristics are given in Table 7.8 and the responses are given in Figures 7.59 – 7.61.



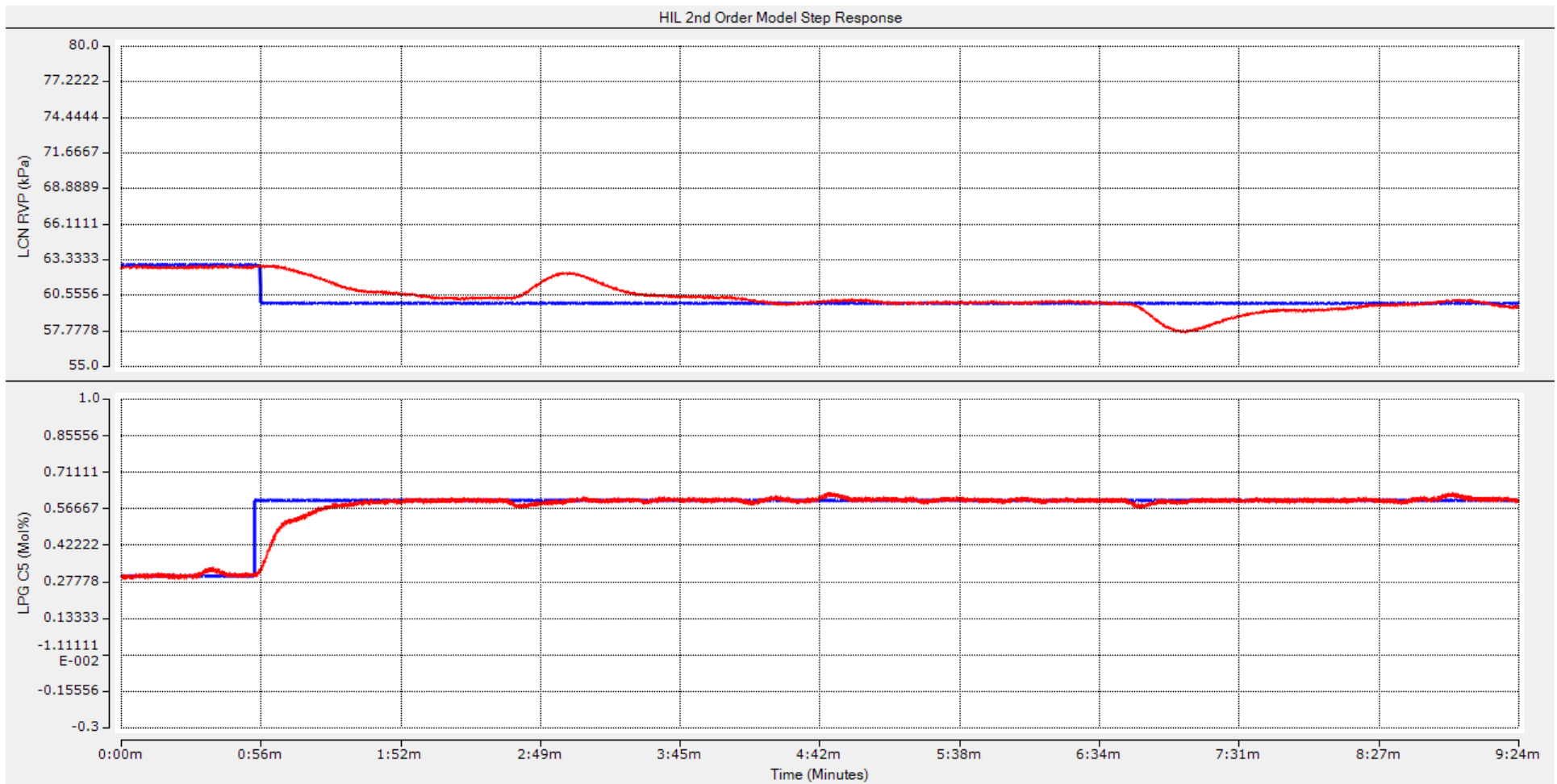
**Figure 7.58: Second order debutanizer process model block diagram with disturbances**

**Table 7.8: Case study of disturbance rejection for the second order system**

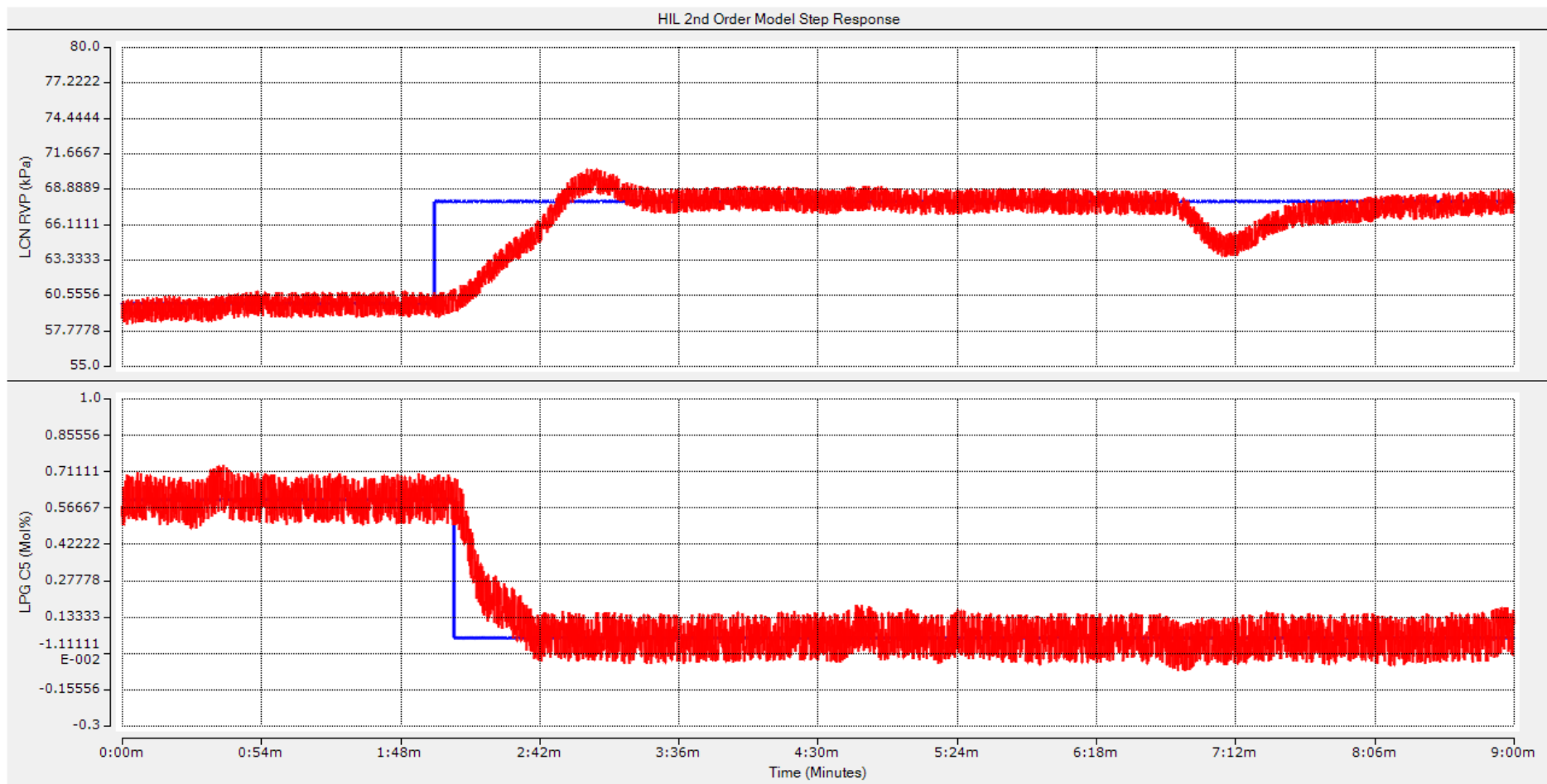
Disturbance Case #	Loop Name	Initial Setpoint	Final Setpoint	Step Size	Input Disturbance Amplitude	Output Noise Disturbance Amplitude
7.6.1	LCN_RVP	65 kPa	63 kPa	-2 kPa	1	0.01
	LPG_C5	0.1 Mol%	0.3 Mol%	+0.2 Mol%	10	0.001
7.6.2	LCN_RVP	63 kPa	60 kPa	-3 kPa	2	0.1
	LPG_C5	0.3 Mol%	0.6 Mol%	+0.3 Mol%	20	0.01
7.6.3	LCN_RVP	60 kPa	68 kPa	+8 kPa	3	1
	LPG_C5	0.6 Mol%	0.05 Mol%	-0.55 Mol%	30	0.1



**Figure 7.59:** Case #7.6.1 – LCN\_RVP dynamic response to a -2 kPa setpoint step change from 65 kPa to 63 kPa steady state with an input disturbance amplitude of 1 and output disturbance amplitude of 0.01 and LPG\_C5 concentration dynamic response to a +0.2 Mol% setpoint step change from 0.1 Mol % to 0.3 Mol % steady state with an input disturbance amplitude of 10 and output disturbance amplitude of 0.001



**Figure 7.60:** Case #7.6.2 – LCN\_RVP dynamic response to a -2 kPa setpoint step change from 65 kPa to 63 kPa steady state with an input disturbance amplitude of 2 and output disturbance amplitude of 0.1 and LPG\_C5 concentration dynamic response to a +0.3 Mol% setpoint step change from 0.3 Mol % to 0.6 Mol % steady state with an input disturbance amplitude of 20 and output disturbance amplitude of 0.01



**Figure 7.61:** Case #7.6.3 – LCN\_RVP dynamic response to a +8 kPa setpoint step change from 60 kPa to 68 kPa steady state with an input disturbance amplitude of 3 and output disturbance amplitude of 1 and LPG\_C5 concentration dynamic response to a -0.55 Mol% setpoint step change from 0.6 Mol % to 0.05 Mol % steady state with an input disturbance amplitude of 30 and output disturbance amplitude of 0.1

This section presented the real-time simulation case study for the second order debutanizer distillation process which is configured in a Hardware-in-the-Loop testbed where the control system is programmed into a Beckhoff PLC, and the process mode is programmed into a CompactRIO. The following sub-section presents the performance analysis and discussion of the results observed as part of the real-time simulation case studies for the second order debutanizer distillation process.

### 7.6.1. Performance analysis and discussion of results for the second order system

The controllers' ability to provide satisfactory setpoint tracking with minimum overshoot, low settling times and nearly zero steady state error is demonstrated. The results of the real-time simulations of the system without disturbances considered is given in Figures 7.53 – 7.57 above and the system performance indicators are outlined in Table 7.9.

**Table 7.9: Analysis of the performance indicators for each of the setpoint variations for the second order system**

Case #	Loop Name	Initial Setpoint	Final Setpoint	Step Size	Percentage of Overshoot	Settling Time	Steady State Error
7.5.1	LCN_RVP	65 kPa	63 kPa	-2 kPa	0%	2m15s	0 kPa
	LPG_C5	0.1 Mol%	0.3 Mol%	+0.2 Mol%	0%	1m20s	0 Mol%
7.5.2	LCN_RVP	63 kPa	60 kPa	-3 kPa	0%	4m	0 kPa
	LPG_C5	0.3 Mol%	0.6 Mol%	+0.3 Mol%	0%	1m30s	0 Mol%
7.5.3	LCN_RVP	60 kPa	68 kPa	+8 kPa	0%	3m	0 kPa
	LPG_C5	0.6 Mol%	0.05 Mol%	-0.55 Mol%	0%	2m30s	0 Mol%
7.5.4	LCN_RVP	68 kPa	73 kPa	+5 kPa	0%	3m	0 kPa
	LPG_C5	0.05 Mol%	0.01 Mol%	-0.04 Mol%	0%	35s	0 Mol%
7.5.5	LCN_RVP	73 kPa	65.5 kPa	-7.5 kPa	0%	4m	0 kPa
	LPG_C5	0.01 Mol%	0.15 Mol%	+0.14 Mol%	0%	1m	0 Mol%

The control loop responses in Figures 7.53 – 7.57 are observed to exhibit zero percent overshoot and steady state error, results which are identical to the Simulink simulation. The LCN Reid Vapour Pressure (kPa) output response is observed to have longer settling times compared to the LPG C5 Concentration (Mol %) output with the longest settling time recorded at 4 minutes in real-time. In the Simulink simulation, the settling time of the LCN Reid Vapour Pressure (kPa) output response is the longest as well recorded to be 1600 seconds (26.7 minutes) in simulation time. Even though the magnitude of the times is different between the real-time and simulation environments, the LCN Reid Vapour Pressure (kPa) still exhibits the longest settling time in both environments. This can be attributed to the PID controller tuning settings which are purposefully selected to prioritize the elimination of overshoot at the expense of the transient time response. In the petrochemical industry, a settling time of 4 minutes is negligible and insignificant.

It is necessary to make remarks about the observed impact of the configuration of signal scaling for the Hardware-in-the-Loop system. The input scaling settings configured in LabVIEW for conditioning the controller signals originating from the Beckhoff PLC are noted to

have a significant impact on the overall performance of the PID controllers. The scaling affects the dynamic response of the output signal, and it is possible to lose control and stability of the system due to improper input scaling settings in LabVIEW. During the Hardware-in-the-Loop real-time simulations, the LCN Reid Vapour Pressure (kPa) control loop response is noted to exhibit a response that can be characterized as being marginally stable i.e., oscillatory. To resolve the oscillations, a heuristic approach of adjusting the scaling factors is taken to arrive at input scaling settings that resulted in satisfactory control loop performance. In practice, however, such a method would not be sufficient to guarantee satisfactory controller performance as industrial final elements have physical limitations. Similar to the Simulink environment, when the effect of disturbances is investigated, the observed responses demonstrate good controller performance for low amplitude disturbances. However, it is noted that as the disturbance amplitude increases, the controller continues to track the setpoint satisfactorily albeit with increased variability.

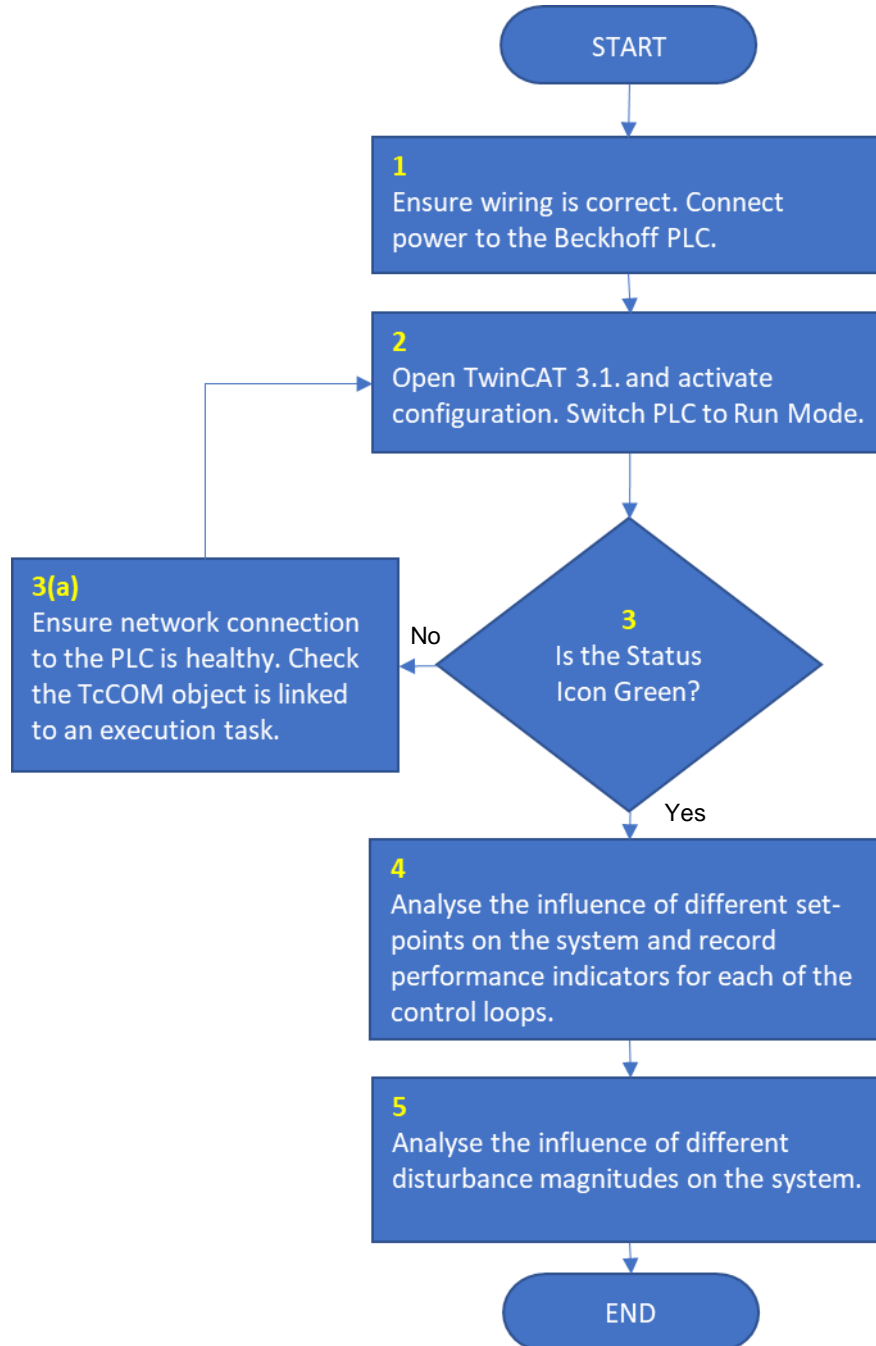
Therefore, it is observed from the simulation study that the designed decentralized PID controllers using the Internal Model Control method achieved good setpoint tracking for the second order debutanizer distillation process and that the dynamic decoupling controllers implemented are effective in eliminating process interactions.

The real-time simulation of the second order debutanizer distillation process together with the performance analysis and discussion of the results observed as part of the real-time simulation case study are presented in this section. The following section presents the real-time simulation of the seventh order debutanizer distillation process together with the performance analysis and discussion of the results observed as part of the real-time simulation case studies.

### **7.7. Real-time simulation of the seventh order Debutanizer distillation process**

This section presents the real-time simulation of the seventh order debutanizer distillation process in the TwinCAT 3 environment. The simulation experiments follow a pre-defined simulation plan as outlined by the flow chart in Figure 7.62. The first step is to ensure that the interface wiring connections are correct and that the power supply is connected to the Beckhoff PLC. The second step is to open TwinCAT, activate the configuration and place the Beckhoff PLC in Run mode. When the Beckhoff PLC is in Run mode, the Status Icon in TwinCAT turns Green. If the Status Icon is not Green, it means the PLC is not in Run mode. As part of the third step, investigate the cause, resolve, and attempt to activate the configuration. Possible causes could be network connectivity or that there are some inputs and outputs that are not linked properly. The setpoints for the model are entered in the Simulink model with step changes occurring at different times apart, thereby automating the setpoint changes. Therefore, in the TwinCAT environment no configuration changes are made. Although it is possible to make manual setpoint changes in TwinCAT, this option is not utilized in this research due to the relatively large number of variables involved.

The fourth step is to analyse the influence of different set-points on the system and record performance indicators for each of the control loops. The fifth and final step is to analyse the influence of different disturbance magnitudes on the system and record performance indicators for each of the control loops. The results obtained from the system are recorded in TwinCAT 3 Scope Viewer.



**Figure 7.62: Flowchart for the seventh order system real-time simulation**

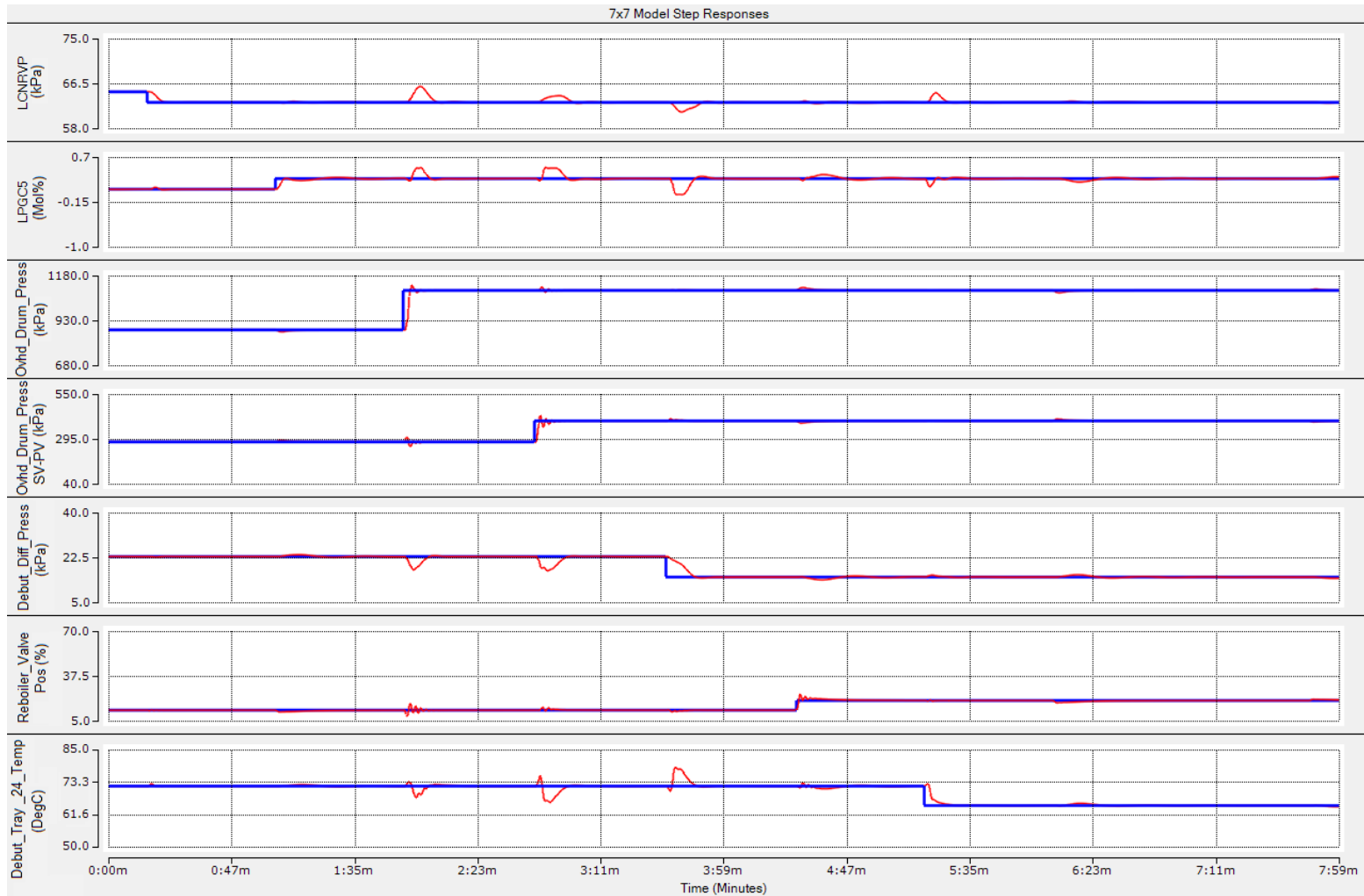
The controlled variables are considered linear within the specified range. Table 7.10 below shows the limited range of setpoints that the system is subjected to. Setpoints outside the specified range could cause the system to be unstable. The step responses for the two



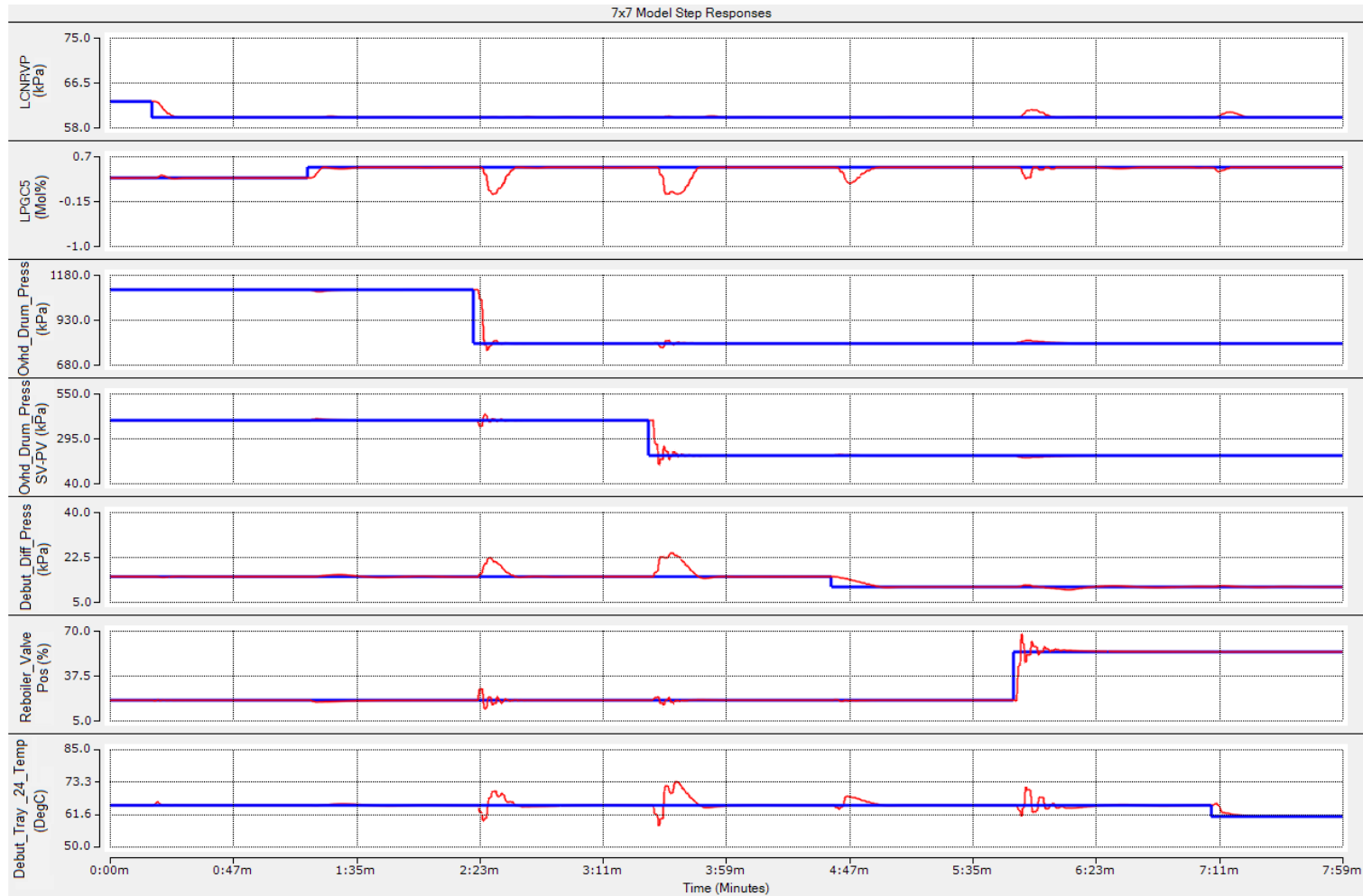
decentralized loops are presented in the Figures 7.63 – 7.67. The figures are presented in landscape format to improve clarify of the text contained in the step response charts.

**Table 7.10: Case study of set points for the seventh order system without disturbances**

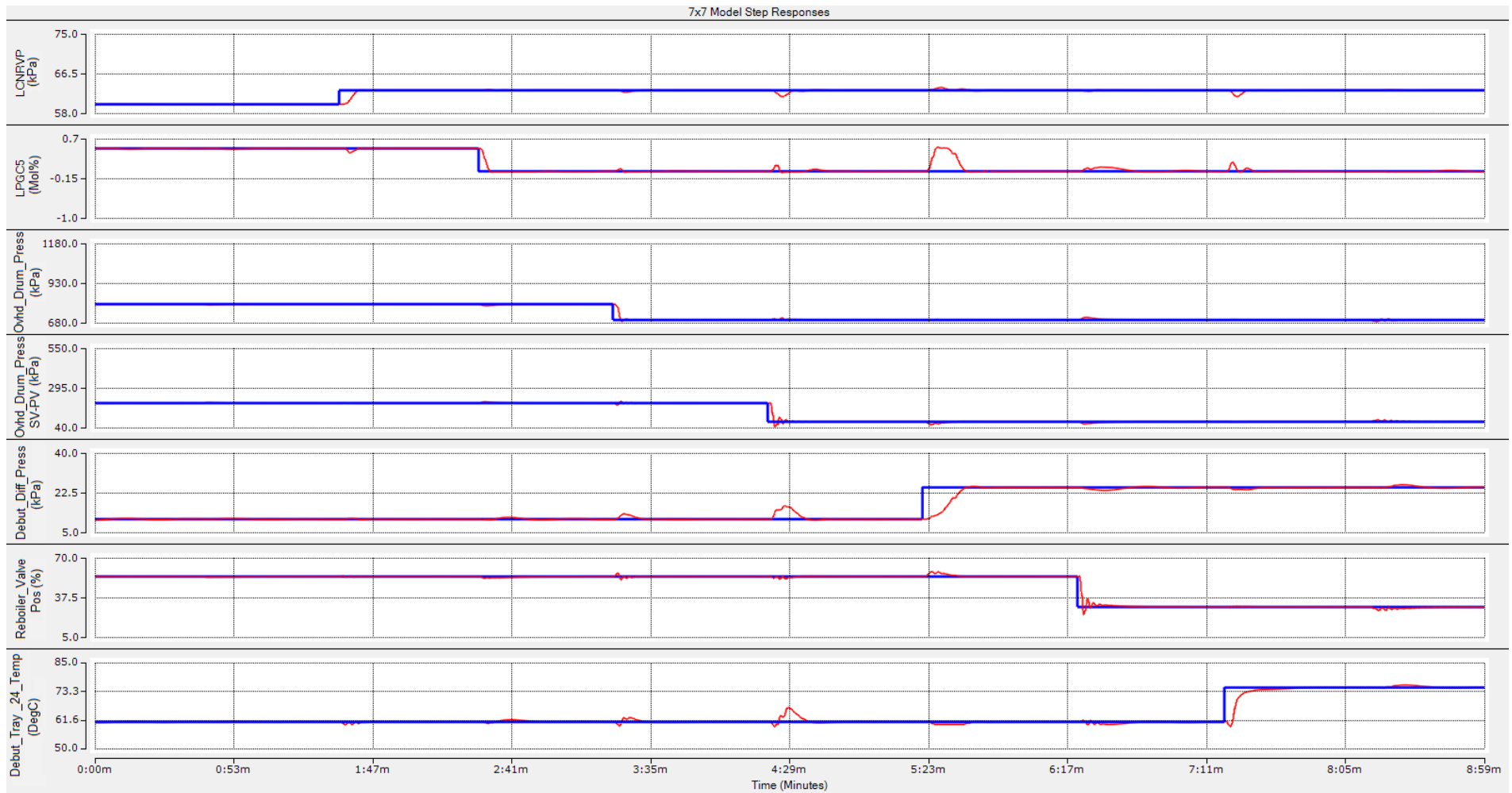
Case #	Loop Name	Initial Setpoint	Final Setpoint	Step Size
7.10.1	LCN_RVP	65 kPa	63 kPa	-2 kPa
	LPG_C5	0.1 Mol%	0.3 Mol%	+0.2 Mol%
	Ovhd_Drum_Press	880 kPa	1100 kPa	+220 kPa
	Ovhd_Drum_Press_SV-PV	281 kPa	400 kPa	+119 kPa
	Debut_Diff_Press	23 kPa	15 kPa	-8 kPa
	Reboiler_Valve_Pos	13 %	20 %	+7 %
	Debut_Tray_24_Temp	72 DegC	65 DegC	-7 DegC
7.10.2	LCN_RVP	63 kPa	60 kPa	-3 kPa
	LPG_C5	0.3 Mol%	0.5 Mol%	+0.2 Mol%
	Ovhd_Drum_Press	1100 kPa	800 kPa	-300 kPa
	Ovhd_Drum_Press_SV-PV	400 kPa	200 kPa	-200 kPa
	Debut_Diff_Press	15 kPa	11 kPa	-4 kPa
	Reboiler_Valve_Pos	20 %	55 %	+35 %
	Debut_Tray_24_Temp	65 DegC	61 DegC	-4 DegC
7.10.3	LCN_RVP	60 kPa	63 kPa	+3 kPa
	LPG_C5	0.5 Mol%	0.01 Mol%	-0.49 Mol%
	Ovhd_Drum_Press	800 kPa	700 kPa	-100 kPa
	Ovhd_Drum_Press_SV-PV	200 kPa	80 kPa	-120 kPa
	Debut_Diff_Press	11 kPa	25 kPa	+14 kPa
	Reboiler_Valve_Pos	55 %	30 %	-25 %
	Debut_Tray_24_Temp	61 DegC	75 DegC	+14 DegC
7.10.4	LCN_RVP	63 kPa	66 kPa	+3 kPa
	LPG_C5	0.01 Mol%	0.41 Mol%	+0.4 Mol%
	Ovhd_Drum_Press	700 kPa	820 kPa	+120 kPa
	Ovhd_Drum_Press_SV-PV	80 kPa	55 kPa	-25 kPa
	Debut_Diff_Press	25 kPa	29 kPa	+4 kPa
	Reboiler_Valve_Pos	30 %	10 %	-20 %
	Debut_Tray_24_Temp	75 DegC	79 DegC	+4 DegC
7.10.5	LCN_RVP	66 kPa	65 kPa	-1 kPa
	LPG_C5	0.41 Mol%	0.1 Mol%	-0.31 Mol%
	Ovhd_Drum_Press	820 kPa	880 kPa	+60 kPa
	Ovhd_Drum_Press_SV-PV	55 kPa	281 kPa	+226 kPa
	Debut_Diff_Press	29 kPa	23 kPa	-6 kPa
	Reboiler_Valve_Pos	10 %	13 %	+3 %
	Debut_Tray_24_Temp	79 DegC	72 DegC	-7 DegC



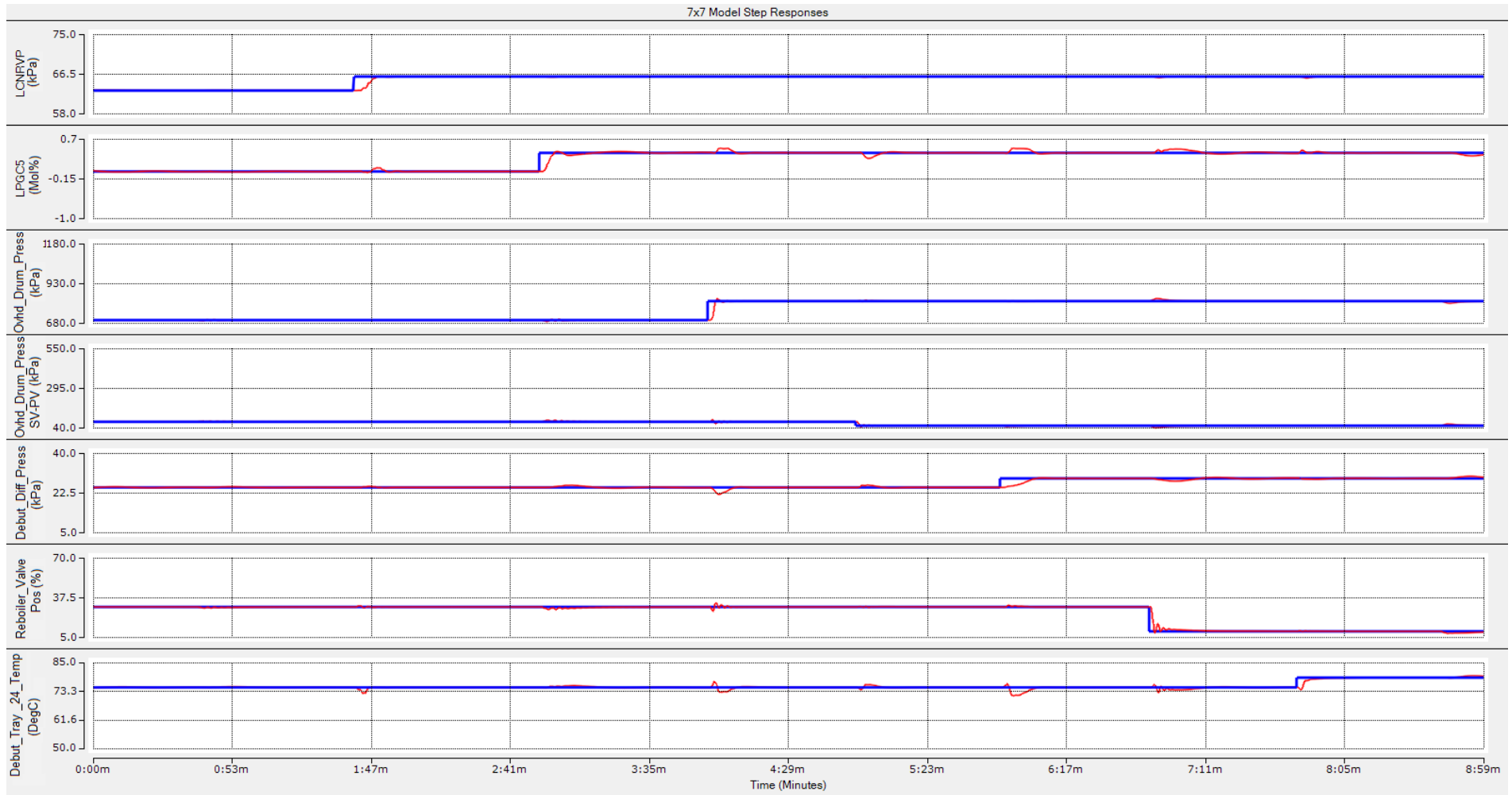
**Figure 7.63: Case #7.10.1 – Dynamic step response to a -2 kPa step change in the LCN RVP setpoint; a +0.2 Mol% step change in the LPG C5 Concentration setpoint; a +220 kPa step change in the Overhead Drum Pressure setpoint; a +119 kPa step change in the Overhead Drum Pressure SV-PV Gap setpoint; a -8 kPa step change in the Debutanizer Differential Pressure setpoint; a +7 % step change in the Debutanizer Reboiler Valve Position setpoint and a -7 DegC step change in the Tray 24 Temperature setpoint**



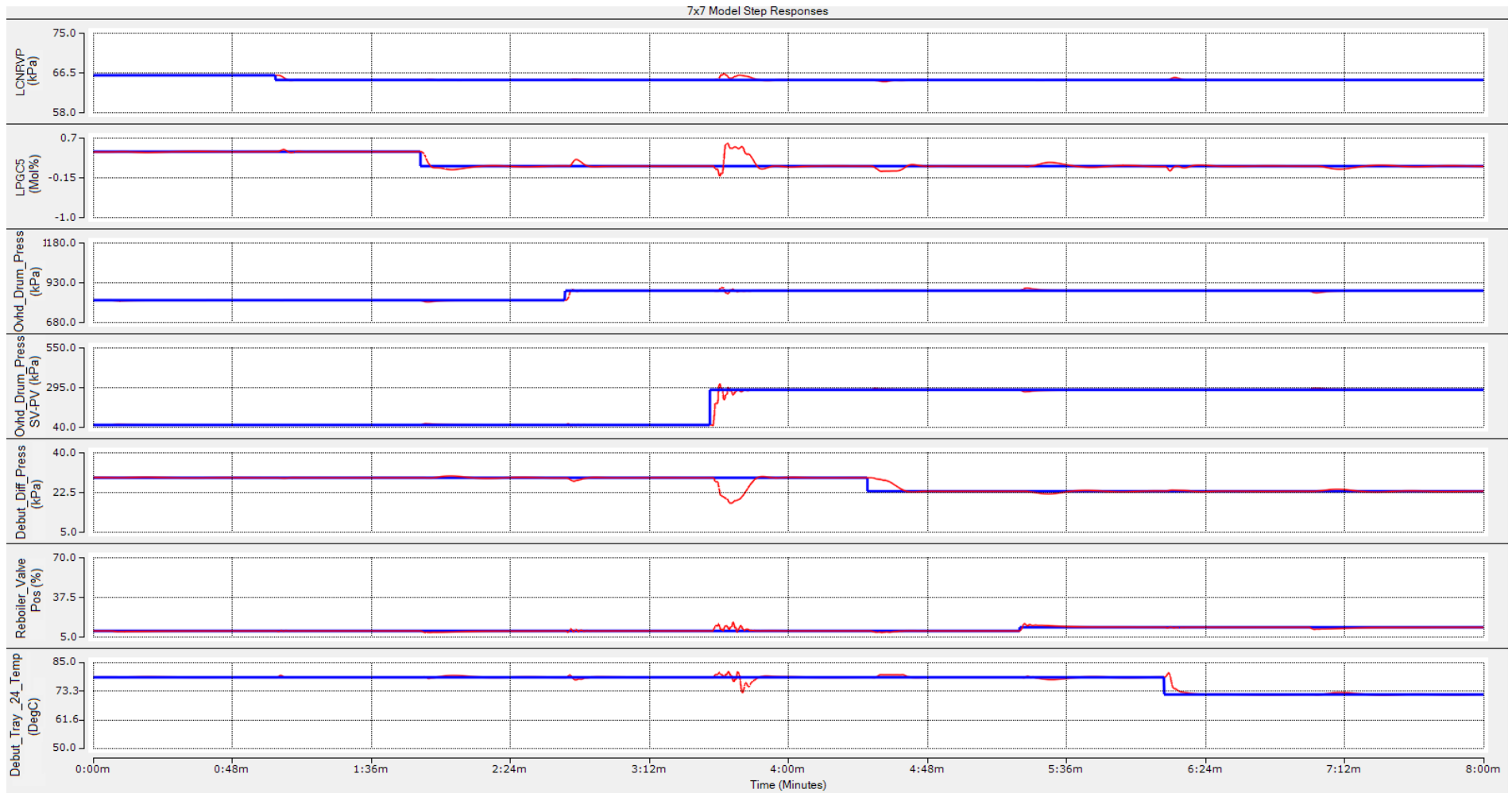
**Figure 7.64:** Case #7.10.2 – Dynamic step response to a -3 kPa step change in the LCN RVP setpoint; a +0.2 Mol% step change in the LPG C5 Concentration setpoint; a -300 kPa step change in the Overhead Drum Pressure setpoint; a -200 kPa step change in the Overhead Drum Pressure SV-PV Gap setpoint; a -4 kPa step change in the Debutanizer Differential Pressure setpoint; a +35 % step change in the Debutanizer Reboiler Valve Position setpoint and a -4 DegC step change in the Tray 24 Temperature setpoint



**Figure 7.65:** Case #7.10.3 – Dynamic step response to a +3 kPa step change in the LCN RVP setpoint; a -0.49 Mol% step change in the LPG C5 Concentration setpoint; a -100 kPa step change in the Overhead Drum Pressure setpoint; a -120 kPa step change in the Overhead Drum Pressure SV-PV Gap setpoint; a +14 kPa step change in the Debutanizer Differential Pressure setpoint; a -25 % step change in the Debutanizer Reboiler Valve Position setpoint and a +14 DegC step change in the Tray 24 Temperature setpoint



**Figure 7.66:** Case #7.10.4 – Dynamic step response to a +3 kPa step change in the LCN RVP setpoint; a +0.4 Mol% step change in the LPG C5 Concentration setpoint; a +120 kPa step change in the Overhead Drum Pressure setpoint; a -25 kPa step change in the Overhead Drum Pressure SV-PV Gap setpoint; a +4 kPa step change in the Debutanizer Differential Pressure setpoint; a -20 % step change in the Debutanizer Reboiler Valve Position setpoint and a +4 DegC step change in the Tray 24 Temperature setpoint

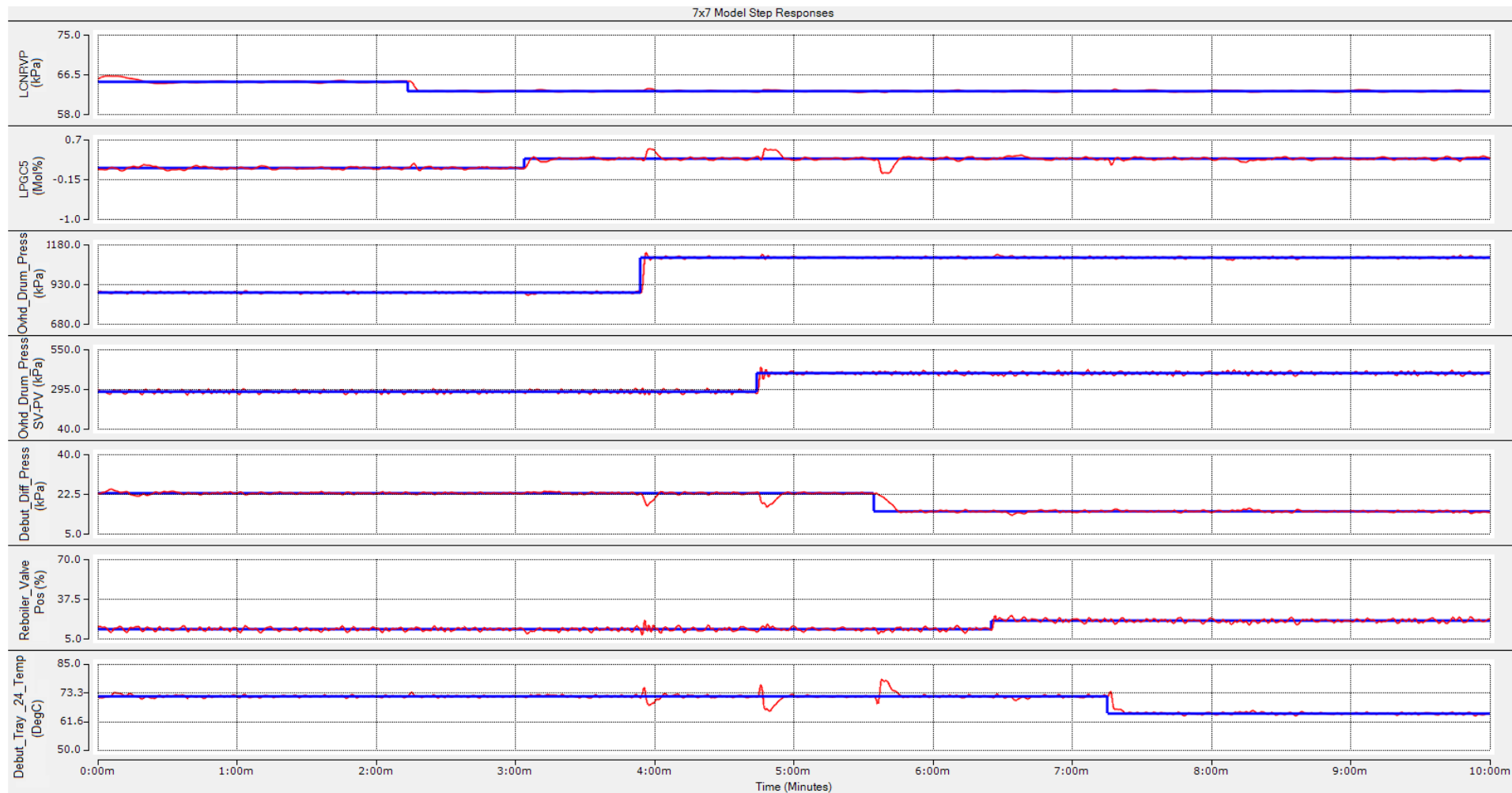


**Figure 7.67:** Case #7.10.5 – Dynamic step response to a -1 kPa step change in the LCN RVP setpoint; a -0.31 Mol% step change in the LPG C5 Concentration setpoint; a +60 kPa step change in the Overhead Drum Pressure setpoint; a +226 kPa step change in the Overhead Drum Pressure SV-PV Gap setpoint; a -6 kPa step change in the Debutanizer Differential Pressure setpoint; a +3 % step change in the Debutanizer Reboiler Valve Position setpoint and a -7 DegC step change in the Tray 24 Temperature setpoint

To investigate the effect of unmeasured noise disturbance on the designed controller, random noise signals with increasing amplitudes are added to the outputs of the system to simulate the effect of increasing sensor measurement noise in real-time as outlined in Table 7.11. Figures 7.68 and 7.69 illustrate the response of the seventh order system under the influence of disturbances. It is discovered immediately that the increase in the magnitude of the noise causes large variations about the setpoint. Similar to the results obtained in the simulation case study conducted in Chapters 5 and 6, the observed control loop responses demonstrate good controller performance for low noise amplitude disturbances and as the disturbance amplitude increases, the controller continues to track the setpoint satisfactorily, however, with increased output variability.

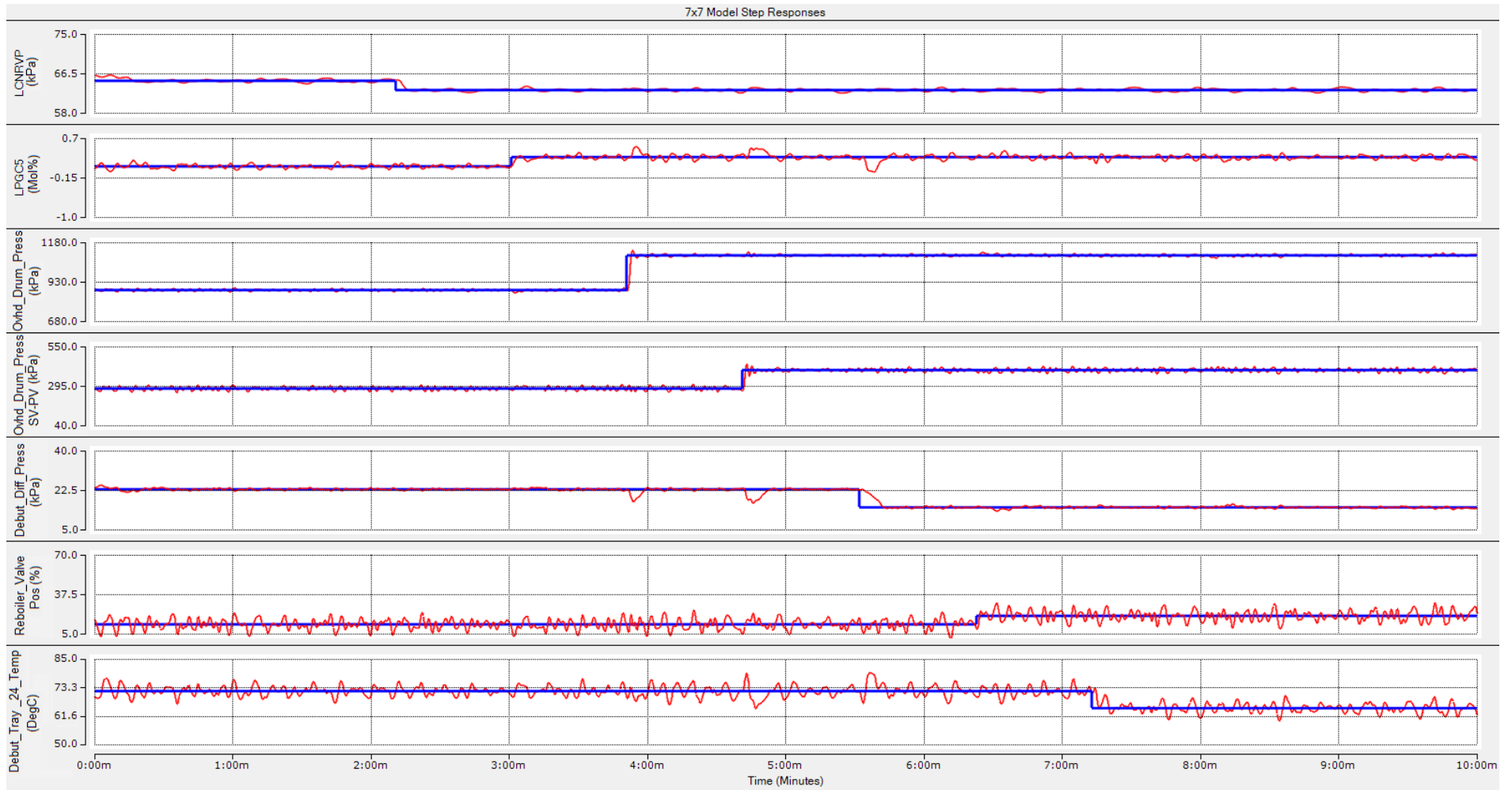
**Table 7.11: Case study of set points for the seventh order system with disturbances**

Case #	Loop Name	Initial Setpoint	Final Setpoint	Step Size	White Noise
7.11.1	LCN_RVP	65 kPa	63 kPa	-2 kPa	1 kPa
	LPG_C5	0.1 Mol%	0.3 Mol%	+0.2 Mol%	0.001 Mol%
	Ovhd_Drum_Press	880 kPa	1100 kPa	+220 kPa	10 kPa
	Ovhd_Drum_Press_SV-PV	281 kPa	400 kPa	+119 kPa	5 kPa
	Debut_Diff_Press	23 kPa	15 kPa	-8 kPa	1 kPa
	Reboiler_Valve_Pos	13 %	20 %	+7 %	2 %
	Debut_Tray_24_Temp	72 DegC	65 DegC	-7 DegC	1 DegC
7.11.2	LCN_RVP	65 kPa	63 kPa	-2 kPa	2 kPa
	LPG_C5	0.1 Mol%	0.3 Mol%	+0.2 Mol%	0.01 Mol%
	Ovhd_Drum_Press	880 kPa	1100 kPa	+220 kPa	25 kPa
	Ovhd_Drum_Press_SV-PV	281 kPa	400 kPa	+119 kPa	10 kPa
	Debut_Diff_Press	23 kPa	15 kPa	-8 kPa	2.5 kPa
	Reboiler_Valve_Pos	13 %	20 %	+7 %	5 %
	Debut_Tray_24_Temp	72 DegC	65 DegC	-7 DegC	2.5 DegC



**Figure 7.68:** Disturbance Case 7.11.1 – Dynamic step response to a -2 kPa step change in the LCN RVP setpoint; a +0.2 Mol% step change in the LPG C5 Concentration setpoint; a +220 kPa step change in the Overhead Drum Pressure setpoint; a +119 kPa step change in the Overhead Drum Pressure SV-PV Gap setpoint; a -8 kPa step change in the Debutanizer Differential Pressure setpoint; a +7 % step change in the Debutanizer Reboiler Valve Position setpoint and a -7 DegC step change in the Tray 24 Temperature setpoint





**Figure 7.69:** Disturbance Case 7.11.2 – Dynamic step response to a -2 kPa step change in the LCN RVP setpoint; a +0.2 Mol% step change in the LPG C5 Concentration setpoint; a +220 kPa step change in the Overhead Drum Pressure setpoint; a +119 kPa step change in the Overhead Drum Pressure SV-PV Gap setpoint; a -8 kPa step change in the Debutanizer Differential Pressure setpoint; a +7 % step change in the Debutanizer Reboiler Valve Position setpoint and a -7 DegC step change in the Tray 24 Temperature setpoint

This section presented the real-time simulation case studies for the seventh order debutanizer distillation process with and without the influence of disturbances. The following section presents the performance analysis and discussion of the results observed as part of the real-time simulation case studies for the seventh order debutanizer distillation process.

### 7.7.1. Performance analysis and discussion of results for the seventh order system

This sub-section presents the performance analysis of the seventh order system simulation results given in Figures 7.63 – 7.67. The system is simulated in real-time in the TwinCAT 3 environment and the performance indicators are outlined in Table 7.12. The settling time metric is omitted from the analysis. Due to the large number of step response outputs displayed, the time axes resolution in the TwinCAT 3 scope viewer presented a challenge in accurately recording the settling times of the individual control. Even though it is not possible to accurately quantify the settling times, it can be observed and reliably concluded that the settling times observed in Figures 7.63 – 7.67 are satisfactory.

**Table 7.12: Analysis of the performance indicators for each of the setpoint variations for the seventh order system**

Case #	Loop Name	Initial Setpoint	Final Setpoint	Step Size	Percentage of Overshoot	Steady State Error
7.9.1	LCN_RVP	65 kPa	63 kPa	-2 kPa	0%	0 kPa
	LPG_C5	0.1 Mol%	0.3 Mol%	+0.2 Mol%	6.66%	0 Mol%
	Ovhd_Drum_Press	880 kPa	1100 kPa	+220 kPa	4.32%	0 kPa
	Ovhd_Drum_Press_SV-PV	281 kPa	400 kPa	+119 kPa	8%	0 kPa
	Debut_Diff_Press	23 kPa	15 kPa	-8 kPa	-3.33%	0 kPa
	Reboiler_Valve_Pos	13 %	20 %	+7 %	22.5%	0 %
7.9.2	Debut_Tray_24_Temp	72 DegC	65 DegC	-7 DegC	0%	0 DegC
	LCN_RVP	63 kPa	60 kPa	-3 kPa	0%	0 kPa
	LPG_C5	0.3 Mol%	0.5 Mol%	+0.2 Mol%	0%	0 Mol%
	Ovhd_Drum_Press	1100 kPa	800 kPa	-300 kPa	-4.38%	0 kPa
	Ovhd_Drum_Press_SV-PV	400 kPa	200 kPa	-200 kPa	-28%	0 kPa
	Debut_Diff_Press	15 kPa	10 kPa	-5 kPa	1%	0 kPa
7.9.3	Reboiler_Valve_Pos	20 %	55 %	+35 %	24.72%	0 %
	Debut_Tray_24_Temp	65 DegC	60 DegC	-5 DegC	0%	0 DegC
	LCN_RVP	60 kPa	73 kPa	+13 kPa	0%	0 kPa
	LPG_C5	0.5 Mol%	0.01 Mol%	-0.49 Mol%	-100%	0.01 Mol%
	Ovhd_Drum_Press	800 kPa	700 kPa	-100 kPa	-1.43%	0 kPa
	Ovhd_Drum_Press_SV-PV	200 kPa	80 kPa	-120 kPa	-40%	0 kPa
7.9.4	Debut_Diff_Press	10 kPa	25 kPa	+15 kPa	1.2%	0 kPa
	Reboiler_Valve_Pos	55 %	30 %	-25 %	-21.66%	0 %
	Debut_Tray_24_Temp	60 DegC	75 DegC	+15 DegC	0%	0 DegC
	LCN_RVP	73 kPa	68 kPa	-5 kPa	0.00%	0 kPa
	LPG_C5	0.01 Mol%	0.41 Mol%	+0.4 Mol%	4.87%	0 Mol%
	Ovhd_Drum_Press	700 kPa	820 kPa	+120 kPa	1.22%	0 kPa
7.9.5	Ovhd_Drum_Press_SV-PV	80 kPa	50 kPa	-30 kPa	-6%	0 kPa
	Debut_Diff_Press	25 kPa	29 kPa	+4 kPa	0.34%	0 kPa
	Reboiler_Valve_Pos	30 %	10 %	-20 %	-10%	0 %
	Debut_Tray_24_Temp	75 DegC	79 DegC	+4 DegC	0%	0 DegC
	LCN_RVP	68 kPa	65 kPa	-3 kPa	0%	0 kPa
	LPG_C5	0.41 Mol%	0.1 Mol%	-0.31 Mol%	-120%	0.01 Mol%
7.9.5	Ovhd_Drum_Press	820 kPa	880 kPa	+60 kPa	1.14%	0 kPa
	Ovhd_Drum_Press_SV-PV	50 kPa	281 kPa	+231 kPa	16.15%	0 kPa
	Debut_Diff_Press	29 kPa	23 kPa	-6 kPa	0.43%	0 kPa

Case #	Loop Name	Initial Setpoint	Final Setpoint	Step Size	Percentage of Overshoot	Steady State Error
	Reboiler_Valve_Pos	10 %	13 %	+3 %	23.85%	0 %
	Debut_Tray_24_Temp	79 DegC	72 DegC	-7 DegC	0%	0 DegC

The analysis of the percentage of overshoot between the Simulink and TwinCAT 3 environments shows the responses are largely similar. An overall average difference of all the recorded percentage of overshoot values amounts to -2.08%. There are outliers in the recorded percentage of overshoot data associated with the LPG C5 Concentration (Mol %) and Debutanizer Reboiler Valve Position (%) output responses. In instances where small amounts of step changes are made to the LPG C5 Concentration (Mol %) output setpoint, it is observed that the response exhibits a significant amount overshoot. This is due to the LPG C5 Concentration (Mol %) output being assigned the largest output reference tracking weight of 27.0671. Similar to the observations made in the Simulink simulation environment, this results in the controller being more aggressive. A large percentage of overshoot is observed in the Reboiler Valve Position (%) output response in the TwinCAT 3 real-time environment which is not as pronounced in the Simulink. An overall average difference of the recorded percentage overshoot values between the two environments amounts to 8.52%, which can be considered significant with a number of possible causes that can be attributed to the observed phenomena. Although controller performance can be further improved with the adjustment of the tuning factors such as an increase in the reference tracking weight of the Reboiler Valve Position (%) output as part of future work, the time it takes the output response to settle is observed to be significantly small. For the purposes of this study, the observed real-time simulation results are indicative of a controller that is well designed and well-tuned. Close inspection of Figures 7.63 – 7.67 shows that the process interactions between the controlled outputs are not completely eliminated. Similar to the Simulink environment, the interactions appear as “spikes” in the output responses occurring as other controlled outputs are changing. In the Simulink simulation results, the observed “spikes” also have a short time duration in the TwinCAT 3 environment due to the controller’s ability to return the outputs to their target steady state setpoints. The designed MPC controller is observed to lack the ability to completely eliminate process interactions without the use of decoupling compensators. A possible solution for that can be considered as part of future work would be to make use of Explicit MPC of the Model Predictive Control Toolbox.

Finally, the effect of unmeasured disturbances is such that good controller performance is observed for low amplitude disturbances. However, as the disturbance amplitude increases, the controller continues to track the setpoint satisfactorily, however, with increased output variability.

The real-time simulation of the seventh order debutanizer distillation process together with the performance analysis and discussion of the results observed as part of the real-time simulation

case study are presented in this section. The following section presents the concluding remarks for this chapter.

## **7.8. Conclusion**

This chapter presented the transitioning of the developed control systems and models from the Simulink simulation environment to the real-time simulation environment. The two models developed as part of this thesis are simulated in real-time. The second order system is simulated in a Hardware-in-the-Loop configuration with the decentralized PID controllers in the TwinCAT 3 environment and the process model of the second order debutanizer distillation process in the LabVIEW environment. On the other hand, the seventh order model is simulated in the TwinCAT 3 environment. The chapter covered the architecture of the hardware and software systems used in the development of the above-mentioned systems, showing the interconnections between the various systems involved. A step-by-step procedure that is followed in the transformation of the Simulink models into the TwinCAT 3 environment is described and illustrated. A description of the software development that is required in the LabVIEW environment for the second order debutanizer distillation process model is presented and the Hardware-in-the-Loop testbed configuration including the physical connections required between the two systems are described. Lastly, the real-time simulation case study results of both systems are presented and discussed.

The following chapter presents the concluding remarks for the thesis, produced research deliverables, developed software, applications of the research, future work and a list of publications emanating from this research.

## **CHAPTER EIGHT: CONCLUSION, THESIS DELIVERABLES, APPLICATIONS AND FUTURE WORK**

### **8.1. Introduction**

The debutanizer distillation process studied in this research is a part of a gas recovery plant of an oil refinery and is used to separate a liquid hydrocarbon mixture into liquified petroleum gas and gasoline. The debutanizer distillation process is coupled and multivariable in nature and coupling occurs when a single process variable's dynamic behaviour influences other process variables giving rise to variable interactions (Seborg et al., 2004). Good process control and operation of debutanizer distillation columns offers significant economic incentives since distillation columns use considerable amounts of energy and are one of the most widely used processes, especially in oil refining facilities. However, distillation columns present process control challenges due to their coupled multivariable structure and often exhibit nonlinear dynamic behaviour (Buckley et al., 1985).

This thesis discusses the development of two control strategies suitable for coupled multivariable processes; decentralized proportional-integral-derivative (PID) control and centralized model predictive control (MPC). The decentralized PID control system is designed using mathematical tools such as the relative gain array (RGA) and the PID controller gain selection is facilitated using the internal model control (IMC) technique. Among the many control technologies available in the market today, the PID controller is the most widely used controller in industry for its simplicity and ease of implementation with relatively low-cost hardware providing satisfactory performance for most control applications encountered in industry (Seborg et al., 2004). The control loop interactions are compensated for by making use of decoupling control techniques.

The model predictive control technique is designed to handle process interactions inherently. Additionally, model predictive control is designed to incorporate constraints on both the manipulated and controlled variables. Model predictive control techniques have been proven to provide enormous economic value and are widely used to achieve increased profitability wherever they have been implemented appropriately (Bullerdiek and Hobbs, 1995), (Masheshri et al., 2000), (Qin and Badgwell, 2003).

Both control strategies, PID and MPC control, developed in this thesis are applied on the dynamic model of the debutanizer distillation process. The work develops a testbed for a real-time implementation of a closed-loop system in a Hardware-in-the-Loop (HiL) configuration. Hardware-in-the-Loop configurations are essential in facilitating learning for process control students in the academic community to aid their understanding of theoretical concepts taught and the work developed in this research furthers such an objective.

This research has answered two main research questions, namely:

- a) Does a centralized multivariable MPC control structure perform better in eliminating process interactions than decoupling compensators do for a decentralized PID control structure?
- b) Does closed-loop control performance significantly differ between a simulation environment and real-time Hardware-in-the-Loop (HiL) testbed?

In the answering of the above two research questions, firstly, the investigations conducted in this thesis reveal that the centralized MPC control structure does not eliminate process interactions better than decoupling compensators with decentralized PID controllers. However, such a conclusion cannot be generalized since design, tuning and development environment of the MPC controller influences the performance of the controller. Furthermore, a direct comparison between the two controller structures is not possible since the MPC controller is a predictive and constraint handling multivariable controller whereas the PID controller is not. Secondly, the simulation results obtained from the MATLAB/Simulink environment and the Hardware-in-the-Loop real-time testbed do not indicate significant differences as demonstrated through a series of simulation case studies conducted. The controller performance and the system dynamic response observed from the two configurations are similar.

This chapter is broken up as follows; Section 8.2 presents the aims and objectives achieved in this research and Section 8.3 provides the outcome of the comprehensive literature review conducted. Section 8.4 presents the thesis deliverables that form part of the outputs of this research with a summary of the main activities undertaken. Section 8.5 presents the list of software developed as part of this thesis. In section 8.6, the applications of the results from this thesis are outlined, the future work that this research could benefit from is presented in Section 8.7 and the list of publications are provided in Section 8.8. Section 8.9 concludes the chapter.

## **8.2. Thesis aim and objectives**

The aim of this research is to develop multivariable controller design methodologies for a debutanizer distillation process model and implement a closed-loop control system in a Hardware-in-the-Loop (HiL) configuration and simulated in real-time.

### **8.2.1. Objectives**

The achieved objectives of this research are broken down into theoretical analysis and real-time practical implementation.

#### **8.2.1.1. Theoretical Analysis**

- a) To review existing literature in the fields of distillation process control, debutanizer column control, multivariable control, model predictive control and its applications on multivariable control systems.

- b) To develop the debutanizer distillation process transfer function model from an industrial empirical model in the MATLAB/Simulink software environment.
- c) To perform a detailed investigation of the mathematical formulation for decoupling compensators for the decentralized PID controller design.
- d) To design controller strategies and analysis methodologies for effective loop pairing and tuning for satisfactory closed-loop performance and perform closed loop simulations to verify the effective elimination of process variable interactions.
- e) To develop a model predictive control system in the MATLAB/Simulink environment and perform simulation studies in closed-loop for set point tracking, constraint handling and disturbance rejection.

#### **8.2.1.2. Real-Time Practical Implementation**

- a) To develop software methods and algorithms in the MATLAB/Simulink, TwinCAT 3.1 and LabVIEW environments to investigate the various models developed.
- b) To perform a transformation of the developed models as portable software modules from the MATLAB/Simulink environment to the Beckhoff TwinCAT 3.1 simulation environment.
- c) To configure a testbed for the real-time implementation of the closed loop system in a Hardware-in-the-Loop (HiL) configuration.
- d) To perform real-time simulation case studies for set point tracking, constraint handling and disturbance rejection for the developed controller design methodologies.

### **8.3. Comprehensive literature review**

A review and analysis of existing literature in the fields of distillation process control, debutanizer column control, multivariable control, model predictive control and its application on multivariable control systems is provided in Chapter 2. Published work is reviewed on the common techniques employed in the above-mentioned fields such as the debutanizer distillation composition control, Relative Gain Array (RGA) interaction measuring method, decoupling control techniques for interaction elimination, Internal Model Control (IMC) tuning strategy, model predictive control and its applications in the petrochemical industry and other industries such as the aviation and power electronics sectors. These topics are reviewed based on the gathered literature, analysed, and compared to develop a thorough understanding of the historical developments and current state-of-the-art for each topic.

The literature review conducted has shown developments and trends on the topics of distillation process control, debutanizer column control, multivariable control and model predictive control and its applications in multivariable control systems. However, the reviewed literature reveals a shortage of research that directly merges industrial practice and academic research. The work performed in this thesis yielded the development of a dynamic transfer

function model of a debutanizer column from step response coefficients exported from an industrial real-life operating plant for study in the MATLAB/Simulink environment commonly used in the academic community. This research provides an opportunity to easily test academically developed control systems on dynamic models of real-life plants. This research presents an opportunity to better understand important design features offered by the internal model control PID design technique that can be useful for industrial practitioners. Furthermore, this research investigates the theoretical background of what has become the standard advanced process control technique in the petrochemical industry today. This enables the study of tuning parameter trade-offs that industrial practitioners often must make in designing model predictive controllers.

#### **8.4. Thesis deliverables**

The development of this thesis produced several deliverables as research outputs which are outlined in the following sub-sections.

##### **8.4.1. Mathematical modelling of the debutanizer distillation process model in the MATLAB/Simulink environment**

The workflow process followed in producing the step response coefficients for the debutanizer distillation process is outlined, starting from the collection of raw process plant data at the start of a project to the development of the mathematical transfer function models. A detailed step-by-step procedure is developed outlining the estimation of transfer function models using the MATLAB System Identification Toolbox. The main steps undertaken are outlined below which include:

- Importing the step response coefficients into the MATLAB environment.
- Creating data objects in MATLAB and loading the data objects in the MATLAB System Identification application.
- Estimating the number of poles and zero required to fit the data and to develop transfer function models in the System Identification application.
- Performing open-loop step response simulations in the MATLAB environment.

##### **8.4.2. Design of the dynamic decoupling and decentralized control for the debutanizer distillation process**

The decentralized controller design methods for a second order model of the debutanizer distillation process are presented. The main tasks performed are as follows:

- The decentralized PID controllers are designed based on the selection of control loop pairings using the Relative Gain Array (RGA) method.
- The PID controller gains are calculated using the Internal Model Control (IMC) method (Garcia and Morari, 1982).



- The loop interactions prevalent in multivariable systems, such as the debutanizer distillation process model studied in this thesis, are compensated for by making use of decoupling control techniques.
- Model reduction techniques are utilized to obtain standard PID controller structures.
- The resulting controllers for each of the models are simulated in the MATLAB/Simulink environment to test the developed algorithms for closed loop performance.

#### **8.4.3. Design of the model predictive control algorithm for the debutanizer distillation process**

The development of a model predictive control algorithm using the Simulink Model Predictive Control Toolbox and testing the designed controller in an industrial seventh order debutanizer distillation process model is performed. A step-by-step procedure followed for the development of a model predictive controller using the Simulink Model Predictive Control application is provided which covers the following main tasks:

- The MPC controller including the controller structure are developed in the Simulink environment.
- The selection of the controller parameters such as scale factors, prediction horizon, the control horizon, sampling time, input and output constraints, constraint softening factors, reference tracking and increment suppression weights are configured in the Simulink MPC application.
- A closed-loop simulation case study is carried out to investigate the suitability of the designed controller.

#### **8.4.4. Development of a transformation procedure for the developed software from the MATLAB/Simulink environment to Beckhoff TwinCAT 3.1 real-time environment for real-time simulation**

The transitioning of the developed control systems and models from the Simulink simulation environment to the real-time simulation environment is presented. A step-by-step procedure that is followed in the transformation of the Simulink models into the TwinCAT 3.1 environment is described and details the following main activities:

- The Simulink model for the second order system inputs and outputs are scaled to ensure transfer of data between the model and an external environment.
- The Simulink models are converted into TcCOM modules using the Simulink code generator and the C/C++ compiler.
- The TcCOM modules imported into TwinCAT 3.1 which are deployed to the Beckhoff PLC for real-time execution.

- The closed-loop and real-time simulations of a seventh order MPC control system are performed in the TwinCAT 3.1 environment for various set points and process disturbances.

#### 8.4.5. Development of a Hardware-in-the-Loop testbed and closed-loop real-time simulation

The second order system is simulated in a Hardware-in-the-Loop configuration with the decentralized PID controllers in TwinCAT 3.1 and the process model of the second order debutanizer distillation process in the LabVIEW software environment. On the other hand, the seventh order model is simulated in the TwinCAT 3.1 environment. The architecture of the hardware and software systems used in the development of the above-mentioned systems, showing the interconnections between the various systems involved is presented with the following main activities performed:

- A description of the software development required in the LabVIEW environment for the second order debutanizer distillation process model is presented.
- The Hardware-in-the-Loop testbed configuration is developed including the architectural layout of the system, the physical wiring and network connections required between the two systems are described.
- The closed-loop and real-time simulation case studies for various set points and process disturbances are performed.

#### 8.5. Developed software

The development of this thesis involved configuration of software and algorithms to investigate and simulate the various models developed as outlined in Table 8.1. The first column of Table 8.1 provides a description of what is contained in the developed software, the second column gives the name and version of the program used to develop the software, the third column presents the file name, and the last column provides a reference of where the program is used in the thesis.

**Table 8.1: Software developed in this thesis**

Program description	Program	File name	Reference
The MATLAB system identification toolbox is used for the purpose of developing the linear time-invariant (LTI) transfer functions from the step response coefficients obtained from the AspenTech's DMC3 Builder software package.	MATLAB R2019a	GCU_Identification.sid	Chapter 4 Figure 4.22
The debutanizer distillation process transfer function models developed in the System Identification Toolbox are manually typed into a MATLAB script file and assigned variable names.	MATLAB R2019a	GCU_Script.m	Appendix A

Program description	Program	File name	Reference
The second order debutanizer distillation process transfer functions are used in the computation of decoupling controllers and the computation of the PID controller gains using the IMC method.	MATLAB R2019a	Debutanizer_Multivariable_Model_2x2_Script_File.m	Appendix B
The Simulink model is a representation the second order debutanizer distillation process transfer functions, decoupling compensators and decentralized PID controllers without consideration of disturbances.	MATLAB R2019a	Decoupled_Second_Order_Model_PID.slx	Chapter 5 Figure 5.3
The Simulink model is a representation of the second order debutanizer distillation process transfer functions and decoupling compensators with disturbances.	MATLAB R2019a	MIMO_7x7_Model_Step.slx	Chapter 6 Figure 6.4
The Simulink model is a representation of the decentralized PID controllers that is transformed into the TwinCAT 3.1 environment and configured in a Hardware-in-the-Loop.	MATLAB R2013a	MIMO_2x2_Controller.slx	Chapter 7 Figure 7.12
The LabVIEW model is a representation of the second order debutanizer distillation process transfer functions and decoupling compensators without disturbances.	LabVIEW 2020	2x2_Debutanizer.vi	Chapter 7 Figure 7.39
The LabVIEW model is a representation of the second order debutanizer distillation process transfer functions and decoupling compensators with disturbances.	LabVIEW 2020	2x2_Debutanizer_Disturbance.vi	Chapter 7 Figure 7.52

## 8.6. Application of the results from this thesis

The application of this research extends to both the industry as well as the academic community.

### 8.6.1. Industrial Application

This can be used to better understand important design features offered by the internal model control PID design technique that can be a useful alternative for industrial practitioners since the PID controller being the most widely used controller in industry. Furthermore, this work can enable the study of tuning parameter trade-offs that industrial practitioners often must make in designing model predictive controllers.

- Tuning of PID controllers with the IMC control strategy and facilitating understanding of trade-offs offered by the various MPC tuning parameters.
- Modelling of industrial plants in the MATLAB/Simulink environment for better understanding of the process dynamics and enable optimization.
- Training of control engineers and technicians to retain critical skills in-house.

### 8.6.2. Academic Application

The developed Hardware-in-the-Loop configurations can be used by process control students in the academic community to aid their understanding of theoretical concepts taught through virtual simulations.

- Teaching undergraduate students industrial control system concepts with practical implementation.
- Enable postgraduate students to carry out future research using Hardware-in-the-Loop testbeds.

### 8.7. Future work

The work developed in this thesis could benefit from further investigations in of the following directions:

- a) A development of a first principles debutanizer distillation process model to improve the accuracy of the modelling.
- b) A review of the debutanizer distillation process model ill-conditioning.
- c) Non-linear controller design techniques.
- d) A review and analysis of the MPC mathematical equations of the MATLAB/Simulink Model Predictive Control Toolbox.
- e) Implementation of the developed control algorithms in a real-life operating process plant to investigate the robustness of the developed algorithms.

### 8.8. Publications

- a) A. Mbadamana, C. Kriger, Y. D. Mfoumboulou. Design of decentralized PID controllers using Internal Model Control for a Binary Distillation Column. Submitted to the Institute of Electrical and Electronic Engineers (IEEE) Transactions on Automatic Control, 2022.
- b) A. Mbadamana, C. Kriger, Y. D. Mfoumboulou. Design of a Centralized MPC Controller using the MATLAB MPC Toolbox for a Debutanizer Distillation Column. **In progress** for submission to the Institute of Electrical and Electronic Engineers (IEEE) Transactions on Automatic Control, 2022.
- c) A. Mbadamana, C. Kriger, Y. D. Mfoumboulou. Design of a Hardware-in-the-Loop (HiL) Testbed for a Binary Distillation Column Model. **In progress** for submission to the Institute of Electrical and Electronic Engineers (IEEE) Transactions on Automatic Control, 2022.

### 8.9. Conclusion

This chapter presents the concluding remarks for the thesis. The thesis aims and objectives achieved by this work are outlined. The outcome of the comprehensive literature review conducted is presented with the contribution made by this work in the knowledge base. The

thesis deliverables produced are provided with a summary of the main activities undertaken in the development of the thesis. A list of the developed software programs with descriptions are provided. Finally, the applications of this research and opportunities for future work are presented. The chapter ends with a list of publications emanating from this research.

## REFERENCES

- Abou-Jeyab, R.A., Gupta, Y.P., Gervais, J.R., Branchi, P.A., Woo, S.S., 2001. *Constrained multivariable control of a distillation column using a simplified model predictive control algorithm*. Journal of Process Control 11, 509–517.
- Adetola, V., Guay, M., 2010. *Integration of real-time optimization and model predictive control*. Journal of Process Control 20, 125–133.
- Allwright, J.C., Papavasiliou, G.C., 1992. *On linear programming and robust model-predictive control using impulse-responses*. Systems and Control Letters 18, 159–164.
- Ansari, R.M., Tadó, M.O., 2000. *Constrained nonlinear multivariable control of a fluid catalytic cracking process*. Journal of Process Control 10, 539–555.
- Ansari, R.M., Tadó, M.O., 1998. *Nonlinear model based multivariable control of a debutanizer*. Journal of Process Control 8, 279–286.
- Beautyman, A.C., 2004. *Assessing Profitability of Real-Time Optimization*. Hydrocarbon processing.
- Beckhoff, 2021. CX5020 | Embedded PC with Intel Atom® processor [WWW Document]. Beckhoff New Automation Technology.
- Beckhoff Automation, 2021. TwinCAT 3 Product Overview.
- Beckhoff Automation, 2020a. *TwinCAT 3*.
- Beckhoff Automation, 2020b. Installation and Operating Instructions for CU8801-0000.
- Bemporad, A., 2006. *Model Predictive Control Design: New Trends and Tools*, in: Proceedings of the 45th IEEE Conference on Decision and Control. IEEE, San Diego.
- Bemporad, A., Morari, M., Ricker, N.L., 2015. Model Predictive Control Toolbox. MathWorks.
- BlUESP, 2018. *APC Modeling - Taining*.
- Bristol, Edgar H., 1966. *On a new measure of interaction for multivariable process control*. IEEE Transactions on Automatic Control 11, 133–134.
- Bristol, Edgar H., 1966. *On a new measure of interaction for multivariable process control*. IEEE Transactions on Automatic Control 11, 133–134.
- Buckley, P.S., Luyben, W.L., Shunta, J.P., 1985. Design of distillation column control systems, 1st ed. Instrument Society of America, New York.
- Bullerdiek, E.A., Hobbs, J.W., 1995. *Advanced controls pay out in 6 weeks at Texas refinery*. Oil and Gas Journal.
- Calugaru, G., Danisor, E.A., 2016. *Dynamic matrix control used in stabilizing aircraft landing*, in: 2016 International Conference on Applied and Theoretical Electricity, ICATE 2016 - Proceedings. Institute of Electrical and Electronics Engineers Inc.
- Camacho, E.F., Bordons, C., 2007. Model Predictive Control, 2nd ed. Springer.
- Campo, P.J., Morari, M., 1987. *Robust Model Predictive Control*, in: American Control Conference. IEEE, Minneapolis.
- Canney, W.M., 2003. *The Future of Advanced Process Control Promises Benefits and Sustained Value*. Oil and gas journal.
- Cecil, L.S., 2012. Distillation Control: An Engineering Perspective, 1st ed. John Wiley and Sons.
- Charlton, W., 1968. *Linear System Identification using Pseudo Random Binary Signals*.
- Chatterjee, H.K., 1960. *Multivariable process control*. IFAC Proceedings Volumes 1, 142–151.
- Chen, C.T., Yen, J.H., 1998. *Multivariable Process Control Using Decentralized Single Neural Controllers*. Journal of Chemical Engineering of Japan 31, 14–20.

- Chevron, 2017. *Plt 63 No.2 FCCU Operation*.
- Chuong, V.L., Vu, T.N.L., 2017. *Identification and Dynamic Matrix Control algorithm for a heating process*, in: Proceedings - 2017 International Conference on System Science and Engineering, ICSSE 2017. Institute of Electrical and Electronics Engineers Inc., pp. 642–645.
- Cornieles, E., Saad, M., Gauthier, G., Saliah-Hassane, H., 2006. *Modeling and simulation of a multivariable process control*, in: IEEE International Symposium on Industrial Electronics. pp. 2700–2705.
- Cutler, C.R., Hawkins, R.B., 1987. *Constrained Multivariable Control of a Hydrocracker Reactor*, in: American Control Conference. IEEE, Minneapolis.
- Cutler, C.R., Perry, R.T., 1983. *Real time optimization with multivariable control is required to maximize profits*. Computers and Chemical Engineering 7, 663–667.
- Cutler, C.R., Ramaker, B., 1979. *Dynamic Matrix Control - A Computer Control Algorithm*. AIChE 86th National Meeting.
- Dai, L., Johan, K.A., 1999. *Dynamic Matrix Control of a Quadruple-Tank Process*. IFAC Proceedings Volumes 32, 6902–6907.
- Das, M., Banerjee, A., Ghosh, R., Goswami, B., Balasubramanian, R., Chandra, A.K., Gupta, A., 2007. *A study on multivariable process control using message passing across embedded controllers*. ISA Transactions 46, 247–253.
- Dasgupta, S., Sadhu, S., 2020. *Decoupling Controller Design for a Multivariable Time Delay System*. 2020 IEEE International Conference for Convergence in Engineering, ICCE 2020 - Proceedings 189–194.
- Davies, W.D.T., 1967. *Using the binary maximum length sequence for the identification of system dynamics*. Proceedings of the Institution of Electrical Engineers 114, 1582.
- Fatima, S.A., Ramli, N., Taqvi, S.A.A., Zabiri, H., 2021. *Prediction of industrial debutanizer column compositions using data-driven ANFIS- and ANN-based approaches*. Neural Computing and Applications 2021 33:14 33, 8375–8387.
- Fatima, S.A., Zabiri, H., Ammar Taqvi, S.A., Ramli, N., 2019. *System Identification of Industrial Debutanizer Column*. Proceedings - 9th IEEE International Conference on Control System, Computing and Engineering, ICCSCE 2019 178–183.
- Flowers, P., Theopold, K., Langley, R., Robinson, W.R., 2016. *Organic Chemistry - Hydrocarbons*, in: Chemistry. OpenStax.
- Forbes, M.G., Patwardhan, R.S., Hamadah, H., Gopaluni, R.B., 2015. *Model predictive control in industry: Challenges and opportunities*. IFAC - Papers Online 28, 531–538.
- Freitas, M.S., Campos, M.C.M.M., Lima, E.L., 1994. *Dual composition control of a debutanizer column*. ISA Transactions 33, 19–25.
- Froisy, B.J., 1994. *Model predictive control: Past, present and future*. ISA Transactions 33, 235–243.
- Fuentes, C., Luyben, W.L., 1983. *Control of High-Purity Distillation Columns*. Industrial and Engineering Chemistry Process Design and Development 22, 361–366.
- Gagnon, E., Pomerleau, A., Desbiens, A., 1998. *Simplified, Ideal or Inverted Decoupling ?* ISA Transactions 37, 265–276.
- Garcia, C.E., Morari, M., 1985. *Internal Model Control. 2. Design Procedure for Multivariable Systems*. Industrial and Engineering Chemistry Process Design and Development 24, 472–484.
- Garcia, C.E., Morari, M., 1982. *Internal Model Control - A Unifying Review and Some Results*. Industrial and Engineering Chemistry Process Design and Development 21, 308–323.
- Garcia, C.E., Morshedi, A.M., 1986. *Quadratic Programming Solution Of Dynamic Matrix Control (QDMC)*. Chemical Engineering Communications Chem. Eng. Common 46, 1–3.

- Garcia, C.E., Prett, D.M., 1986. *Advances in Industrial Model-Predictive Control*. Houston.
- García, C.E., Prett, D.M., Morari, M., 1989. *Model predictive control: Theory and practice-A survey*. *Automatica* 25, 335–348.
- Garrido, J., Vázquez, F., Morilla, F., 2014. *Inverted decoupling internal model control for square stable multivariable time delay systems*. *Journal of process control* 1710–1719.
- Georgiou, A., Georgakis, C., Luyben, W.L., 1988. *Nonlinear dynamic matrix control for high-purity distillation columns*. *AIChE Journal* 34, 1287–1298.
- González, J.R., Correa, G., Montoya, O.D., 2021. *Design of a control with multiple inputs multiple outputs by decoupling*. *Journal of Physics: Conference Series* 12002.
- Goodhart, S.G., 1998. *Advanced process control using DMCplus*, in: UKACC International Conference on Control (CONTROL '98). IEE, pp. 439–444.
- Graebe, S.F., Goodwin, G.C., 1992. *Adaptive PID Design Exploiting Partial Prior Information*. *IFAC Proceedings Volumes* 25, 41–46.
- Grega, W., 1999. *Hardware-in-the-loop simulation and its application in control education*, in: 29th Annual Frontiers in Education Conference. IEEE.
- Gulzar, M.M., Munawar, M., Dewan, Z., Salman, M., Iqbal, S., 2020. *Level Control of Coupled Conical Tank System using Adaptive Model Predictive Controller*. HONET 2020 - IEEE 17th International Conference on Smart Communities: Improving Quality of Life using ICT, IoT and AI 236–240.
- Gupta, Y.P., 1998. *Control of integrating processes using Dynamic Matrix Control*. *Chemical Engineering Research and Design* 76, 465–470.
- Halvarsson, B., 2010. *Interaction Analysis in Multivariable Control Systems: Applications to Bioreactors for Nitrogen Removal*.
- Hao, Y., Hau, Y., 2020. *Application of Dynamic Matrix Control in Liquid Level Control*, in: IEEE the 4th International Conference on Frontiers of Sensors Technologies. IEEE, Langfang.
- Hepburn, J.S.A., Wonham, W.M., 1982. *INTERNAL MODEL PRINCIPLE OF REGULATOR THEORY ON DIFFERENTIABLE MANIFOLDS.*, in: *IFAC Proceedings Volumes*. IFAC by Pergamon Press, pp. 319–323.
- Hilton, D., 1996. *A Practical Description of DMC and How DMC Works*.
- Holkar, K.S., Waghmare, L.M., 2010. *An overview of model predictive control*. *International Journal of Control and Automation* 3, 47–64.
- Hu Guolong, Sun Youxian, 2003. *Study and application of dynamic matrix control in refinery processes*, in: *Conference on Computers, Communications, Control and Power Engineering*. IEEE, pp. 1667–1671 vol.3.
- Hu, J., Shan, Y., Guerrero, J.M., Ioinovici, A., Chan, K.W., Rodriguez, J., 2021. *Model predictive control of microgrids – An overview*. *Renewable and Sustainable Energy Reviews*.
- Hu Xin, Wang Rui, Liu Yongchao, Du Jialu, 2015. *Dynamic matrix control for dynamic positioning system of ships*, in: 2015 34th Chinese Control Conference (CCC). Technical Committee on Control Theory, Chinese Association of Automation, pp. 1008–1013.
- Hugo, A., 2000. *Limitations of Model Predictive Controllers*. *Hydrocarbon processing*.
- IEC, 2003. IEC 61511: Functional Safety - Safety instrumented systems for the process industry sector - Part 1, International Electrotechnical Commission. Geneva, Switzerland.
- Isaksson, A.J., Graebe, S.F., 1999. *Analytical PID parameter expressions for higher order systems*. *Automatica* 35, 1121–1130.
- Isaksson, A.J., Graebe, S.F., 1993. *Model Reduction For PID Design*. *IFAC Proceedings Volumes* 26, 467–472.
- Joly, M., 2012. *Refinery production planning and scheduling: the refining core business*.



- Brazilian Journal of Chemical Engineering 29, 371–384.
- Kanna, R.A., Babu, A., Prakash, K.M., Xavier, R., 2017. Copper Strip Corrosion Test for Different Fluid Samples, International Refereed Journal of Engineering and Science.
- Kelly, S.J., Rogers, M.D., Hoffman, D.W., 1988. *Quadratic dynamic matrix control of hydrocracking reactors.*, in: Proceedings of the American Control Conference. Publ by American Automatic Control Council, pp. 295–300.
- Kim, W.G., Moon, U.C., Lee, S.C., Lee, K.Y., 2005. *Application of dynamic matrix control to a boiler-turbine system*, in: IEEE Power Engineering Society General Meeting. pp. 1595–1599.
- Kouro, S., Perez, M.A., Rodriguez, J., Llor, A.M., Young, H.A., 2015. *Model Predictive Control: MPC's Role in the Evolution of Power Electronics*. IEEE industrial electronics magazine 9, 8–21.
- Lee, P.L., Sullivan, G.R., 1988. *Generic model control — theory and applications*. IFAC Proceedings Volumes 21, 111–119.
- Li, H., Chu, H., Jiang, T., Liu, L., Luo, W., 2019. *Decoupling Control of Temperature and Vacuum in Molecular Distillation System Based on Expected Dynamic Method*, in: Proceedings - 2019 Chinese Automation Congress, CAC 2019. Institute of Electrical and Electronics Engineers Inc., pp. 2510–2515.
- Liang, W., Chen, H.B., He, G., Chen, J., 2020. *Model Order Reduction Based on Dynamic Relative Gain Array for MIMO Systems*. IEEE Transactions on Circuits and Systems II: Express Briefs 67, 2507–2511.
- Ljung, L., 1999. System identification : theory for the user. Prentice Hall PTR.
- Ljung, L., 1988. For Use with MATLAB® User's Guide System Identification Toolbox.
- Lopez-guede, J.M., Fernandez-gauna, B., Oterino, F., 2013. *On the Influence of the Prediction Horizon in Dynamic*. International Journal of Control Science and Engineering 3, 22–30.
- Lundström, P., Lee, J.H., Morari, M., Skogestad, S., 1995. *Limitations of dynamic matrix control*. Computers and Chemical Engineering 19, 409–421.
- Luyben, W.L., 1993. Practical Distillation Control. Springer US.
- Luyben, W.L., 1975. *Steady-State Energy Conservation Aspects of Distillation Column Control System Design*. Industrial and Engineering Chemistry Fundamentals 14, 321–325.
- Luyben, W.L., 1970. *Distillation Decoupling*. American Institute of Chemical Engineers 16, 198–203.
- Maarleveld, A., Rijnsdorp, J., 1970. *Constraint control on distillation columns*. Automatica (Oxford) 6, 51–58.
- Machacek, J., Kotyk, J., 1994. *Adaptive decoupling control of distillation column*, in: Proceedings of the IEEE Conference on Control Applications. IEEE, pp. 263–268.
- Marchionna, A., 2017. *Model Identification Process: from data collection to calibrated, empirical, dynamic, linear models*.
- Masheshri, J.C., Kotob, S., Yousuf, B.H., 2000. *Hydrocracker advanced control improves profitability*. Hydrocarbon processing.
- Mathworks, 1994. MATLAB.
- Matko, D., Arh, M., Skrjanc, I., Tomazic, T., 2013. *Self-tuning Dynamic Matrix Control of two-axis autopilot for small aeroplanes*, in: 2013 9th Asian Control Conference.
- Mayne, D.Q., Rawlings, J.B., Rao, C. V, Scokaert, P.O.M., 2000. *Constrained model predictive control: Stability and optimality*. Automatica 36, 789–814.
- Mcdonald, K.A., McAvoy, T.J., 1987. *Application of Dynamic Matrix Control to Moderate-and High-Purity Distillation Towers*. Industrial and Engineering Chemistry Research 26, 1011–1018.

- Ming, X., Chunyu, G., Baojie, L., Ze, D., 2020. *Design and Simulation of Adaptive Internal Model Control Algorithm*. 2020 5th International Conference on Power and Renewable Energy, ICPRE 2020 461–465.
- Mokhatab, S., Poe, W.A., 2012. *Process Control Fundamentals*, in: Handbook of Natural Gas Transmission and Processing. Elsevier, pp. 473–509.
- Morari, M., 1993. *Model Predictive Control: Multivariable Control Technique of Choice in the 1990s?* Control and Dynamical Systems Technical Reports.
- Morari, M., 1983. *Internal Model Control - Theory and Applications*. IFAC Proceedings Volumes 16, 1–18.
- Morari, M., Garcia, C.E., Prett, D.M., 1988. *Model predictive control: Theory and practice*. IFAC Proceedings Volumes 21, 1–12.
- Morari, M., Lee, J.H., 1999. *Model predictive control: past, present and future*. Computers and Chemical Engineering 23, 667–682.
- Morilla, F., Vázquez, F., Garrido, J., 2008. *Centralized PID Control by Decoupling for TITO Processes*, in: Proceedings of the 13th IEEE International Conference on Emerging Technologies and Factory Automation. pp. 1318–1325.
- Moro, L.F.L., Odloak, D., 1995. *Constrained multivariable control of fluid catalytic cracking converters*. Journal of Process Control 5, 29–39.
- Morshedi, A.M., Cutler, C.R., Fitzpatrick, T.J., Skrovanek, T.A., 1979. *Dynamic matrix control method*.
- Mort, N., 1994. *Multivariable Process Control*. IFAC Proceedings Volumes 27, 161–164.
- Muga, J.N., 2015. Design and Implementation of IEC 61499 Standard-Based Nonlinear Controllers using Functional Block Programming in Distributed Control Platform.
- Musch, H.E., Steiner, M., 1994. *Robust PID Control for an Industrial Distillation Control*, in: Third IEEE Conference on Control Applications. IEEE, Glasgow.
- Nakamoto, K., Watanabe, N., 1991. *Multivariable control experiments of non-linear chemical processes using non-linear feedback transformation*. Journal of Process Control 1, 140–145.
- National Instruments, 2018a. Numeric Controls and Indicators - LabVIEW 2018 Help [WWW Document].
- National Instruments, 2018b. Shared Variable Node - LabVIEW 2018 Help [WWW Document].
- National Instruments, 2018c. Summation Function - LabVIEW 2018 Help [WWW Document].
- National Instruments, 2018d. Types of Graphs and Charts - LabVIEW 2018 Help [WWW Document].
- National Instruments, 2018e. Pulse Signal Function - LabVIEW 2018 Help [WWW Document].
- National Instruments, 2018f. Transfer Function Function - LabVIEW 2018 Help [WWW Document].
- National Instruments, 2018g. Bundle Function - LabVIEW 2018 Help [WWW Document].
- National Instruments, 2015. NI cRIO-9063 Embedded Real-Time Controller with Reconfigurable FPGA for C Series Modules [WWW Document]. National Instruments.
- Neto, E.A., Rodrigues, M.A., Odloak, D., 2000. *Robust predictive control of a gasoline debutanizer column*. Brazilian Journal of Chemical Engineering 17, 967–977.
- Niederlinski, A., 1971. *A heuristic approach to the design of linear multivariable interacting control systems*. Automatica 7, 691–701.
- Nowakova, J., Pokorny, M., 2020. *Intelligent Controller Design by the Artificial Intelligence Methods*. Sensors 20.
- Ogata, K., 2010. Modern Control Engineering, 5th ed. Pearson Education, Inc, New Jersey.

- Ogunnaike, B., Ray, W.H., 1994. *Process Dynamics, Modeling and Control*, 1st ed. Oxford University Press.
- Ogunnaike, B.A., 1986. *Dynamic Matrix Control: A Nonstochastic, Industrial Process Control Technique with Parallels in Applied Statistics*. *Industrial and Engineering Chemistry Fundamentals* 25, 712–718.
- Ogunnaike, B.A., Lemaire, J.P., Morari, M., Ray, W.H., 1983. *Advanced multivariable control of a pilot-plant distillation column*. *AIChE Journal* 29, 632–640.
- Panwar, P., Mukhopadhyay, S., Bhatt, T.U., Tiwari, A.P., 2018. *Design of decentralized PI and LQR controllers for level and pressure regulation of steam drum of advanced heavy water reactor*. 2018 Indian Control Conference, ICC 2018 - Proceedings 2018-Janua, 258–263.
- Park, J.K., Choi, C.H., 1995. *Dynamic Compensation Method for Multivariable Control Systems with Saturating Actuators*. *IEEE Transactions on Automatic Control* 40, 1635–1640.
- Paulo Padrão, Fábio Coelho, Felipe Campelo, 2015. *Optimal Production Synthesis of Liquefied Petroleum Gas in a Debutanizer Tower*, in: *Proceedings of the 23rd ABCM International Congress of Mechanical Engineering*. ABCM Brazilian Society of Mechanical Sciences and Engineering.
- Pitta, R.N., Odloak, D., 2012. *Closed-loop re-identification of an industrial debutanizer column*. *IFAC Proceedings Volumes* 45, 862–867.
- Qin, S.J., Badgwell, T.A., 2003. *A survey of industrial model predictive control technology*. *Control Engineering Practice* 11, 733–764.
- Ramli, N.M., 2016. *Tuning and Control Strategies for a Debutanizer Column*, in: *4th International Conference on Process Engineering and Advanced Materials*. Elsevier.
- Ramli, N.M., Chandra Mohan, M.R., 2015. *Linear Model Predictive Control of a Debutanizer column*, in: *2015 4th International Conference on Software Engineering and Computer Systems, ICSECS 2015: Virtuous Software Solutions for Big Data*. Institute of Electrical and Electronics Engineers Inc., pp. 96–101.
- Ramli, N.M., Hussain, M.A., Jan, B.M., 2016. *Multivariable control of a debutanizer column using equation based artificial neural network model inverse control strategies*. *Neurocomputing* 194, 135–150.
- Ray, W.H., 1983. *Multivariable process control - A survey*. *Computers and Chemical Engineering* 7, 367–394.
- Reedy, J., Lunzmann, S., 2010. *Model Based Design Accelerates the Development of Mechanical Locomotive Controls*. SAE Technical Papers.
- Rijnsdorp, J.E., 1965. *Interaction in two-variable control systems for distillation columns-I. Theory*. *Automatica* 3, 15–28.
- Rivera, D.E., Morarl, M., Skogestad, S., 1986. *Internal Model Control: PID Controller Design*. *Industrial and Engineering Chemistry Process Design and Development* 25, 252–265.
- Roffel, B., Betlem, B.H.L., De Ruijter, J.A.F., 2000. *First principles dynamic modeling and multivariable control of a cryogenic distillation process*. *Computers and Chemical Engineering* 24, 111–123.
- Sadeghbeigi, R., 2000. *Fluid catalytic cracking handbook: design, operation, and troubleshooting of FCC facilities*. Gulf.
- Sågfors, M.F., Waller, K. V., 1998. *Multivariable control of ill-conditioned distillation columns utilizing process knowledge*. *Journal of Process Control* 8, 197–208.
- Saxena, S., Hote, Y. V., 2012. *Advances in Internal Model Control Technique: A Review and Future Prospects*. Technical review - IETE 29, 461–472.
- Seborg, D.E., Edgar, T.F., Mellichamp, D.A., 2004. *Model Predictive Control*, in: *Process Dynamics and Control*. John Wiley and Sons, New Jersey, pp. 534–565.

- Sharpe, P., Rezabek, J., 2004. *Embedded APC tools reduce costs of technology*. Hydrocarbon processing.
- Shen, D., Lim, C.C., Shi, P., 2020. *Robust fuzzy model predictive control for energy management systems in fuel cell vehicles*. Control Engineering Practice 98, 104364.
- Shen, Y., Cai, W.J., Li, S., 2010. *Multivariable Process Control: Decentralized, Decoupling, or Sparse?* Industrial and Engineering Chemistry Research 49, 761–771.
- Silberberg, M.S. (Martin S., 2015. Chemistry: the molecular nature of matter and change, Seventh ed. ed. McGraw Hill Education, New York, NY.
- Skogestad, S., 2007. *The Do's and Don'ts of Distillation Column Control*. Chemical Engineering Research and Design 85, 13–23.
- Skogestad, S., 2003. *Simple analytic rules for model reduction and PID controller tuning*. Journal of Process Control 13, 291–309.
- Sorensen, R.C., Cutler, C.R., 1998. *LP Integrates Economics into DMC*. Hydrocarbon processing.
- Stewart, M., Arnold, K., 2009. *Crude Stabilization*, in: Emulsions and Oil Treating Equipment. Gulf Professional Publishing, pp. 81–106.
- Tham, M.T., 1999. Multivariable control: an introduction to decoupling control.
- Travis, J., Kring, J., 2007. LabVIEW for Everyone: Graphical Programming Made Easy and Fun, National Instruments Virtual Instrumentation Series. Prentice Hall.
- Tyréus, B.D., 1979. *Multivariable Control System Design for an Industrial Distillation Column*. Industrial and Engineering Chemistry Process Design and Development 18, 177–182.
- Valve Developer Community, 2006. MDL [WWW Document]. Valve Corporation.
- Visioli, A., 2005. *Model-based PID tuning for high-order processes: when to approximate*. 44th IEEE Conference on Decision and Control, and the European Control Conference 7127–7132.
- Wade, H.L., 1997. *Inverted decoupling: a neglected technique*. ISA Transactions 36, 3–10.
- Waller, K.V.T., 1974. *Decoupling in distillation*. AIChE Journal.
- Wang, Q., Guo, X., Zhang, Y., 2001. *Direct identification of continuous time delay systems from step responses*. Journal of Process Control 11, 531–542.
- Weber, R., Gaitonde, N.Y., 1982. *Non-Interactive Distillation Tower Analyzer Control*, in: Proceedings of the American Control Conference. Institute of Electrical and Electronics Engineers Inc., pp. 87–90.
- Wilson, B., Das Biswas, B., 2004. *Advanced Control for Solvent Extraction*. Petroleum technology quarterly.
- Wojsznis, W.K., 2006. *Model Predictive Control and Optimization*, in: Instrument Engineers' Handbook. CRC Press, pp. 242–252.
- Wood, R.K., Berry, M.W., 1973. *Terminal composition control of a binary distillation column*. Chemical Engineering Science 28, 1707–1717.
- Yamuna Rani, K., Gangiah, K., 1991. *Nonlinear dynamic matrix control of an open-loop unstable process with least-squares minimization for constraints*. Chemical Engineering Science 46, 1520–1525.
- Yocum, F.H., Zimmerman, J.M., 1988. *Real time control of inverse response using dynamic matrix control*, in: Proceedings of the American Control Conference. Publ by American Automatic Control Council, pp. 266–267.
- Yongho, L., Moonyong, L., Sunwon, P., 1998. *PID Controller Tuning to Obtain Desired Closed-Loop Responses for Cascade Control Systems*. IFAC Proceedings Volumes 31, 613–618.
- Yu, C.C., Luyben, W.L., 1986. *Design of Multiloop SISO Controllers in Multivariable Processes*.



## APPENDICES

### Appendix A – MATLAB model transfer functions script file

```
%% In this script file, transfer functions obtained from the System
% Identification Toolbox are manually typed into this MATLAB script file
% and assigned variable names. This ensures the transfer functions can be
% instantiated in the MATLAB/Simulink environment for the development
% of a MIMO model.
```

```
%%
```

```
clc
```

```
clear
```

```
%% 1. Ambient Temp
```

```
% Ambient_Temp with Ovhd_Drum_Press
```

```
TF3D1 = tf([3.061],[1 5.35 1.275]);
```

```
% Ambient_Temp with Ovhd_Drum_Press_SV-PV
```

```
TF4D1 = tf([-3.061],[1 5.35 1.275]);
```

```
% Ambient_Temp with Reboiler_Valve_Pos
```

```
TF6D1 = tf([0.4528],[1 5.249 0.9055]);
```

```
%% 2. LCN Recycle Flow
```

```
TF17 = 0;
```

```
TF27 = 0;
```

```
% LCN_Recycle_Flow with Ovhd_Drum_Press
```

```
TF37 = tf([0.03129],[1 0.1977 0.016]);
```

```
% LCN_Recycle_Flow with Ovhd_Drum_Press_SV-PV
```

```
TF47 = tf([-0.03212],[1 0.2023 0.01679]);
```

```
% LCN_Recycle_Flow with Debut_Diff_Press
```

```
TF57 = tf([0.0132],[1 0.4215 0.06652]);
```

```
% LCN_Recycle_Flow with Reboiler_Valve_Pos
```

```
TF67 = tf([6.699],[1 7.781 0.957]);
```

```
TF77 = 0;
```

```
%% 3. De-Ethimizer Temperature
```

```
TF16 = 0;
```

```
TF26 = 0;
```

```
% Deeth_Temp with Ovhd_Drum_Press
```

```
TF36 = tf([-0.1775],[1 0.3455 0.01603]);
```

```
% Deeth_Temp with Ovhd_Drum_Press_SV-PV
```

```
TF46 = tf([0.1785],[1 0.3471 0.01612]);
```

```
% Deeth_Temp with Debut_Diff_Press
```

```
TF56 = tf([-0.001914],[1 0.1084 0.07097 0.002616]);
```

```
% Deeth_Temp with Reboiler_Valve_Pos
```

```
TF66 = tf([-0.04504],[1 0.649 0.03486]);
```

```
TF76 = 0;
```

```

%% 4. De-Ethanizer Pressure
TF15 = 0;
TF25 = 0;

% Deeth_Pressure with Ovhd_Drum_Press
TF35 = tf([0.004934],[1 0.5241 0.1822 0.00895]);

% Deeth_Pressure with Ovhd_Drum_Press_SV-PV
TF45 = tf([-0.004668],[1 0.47 0.1708 0.008437]);

TF55 = 0;

% Deeth_Pressure with Reboiler_Valve_Pos
TF65 = tf([0.002211],[1 0.4867 0.04347]);

TF75 = 0;

%% 5. De-Ethanizer Feed
TF14 = 0;

% Deeth_Feed_Flow with LPG_C5
TF24 = tf([-0.0007287],[1 0.6293 0.1123]);
TF34 = 0;
TF44 = 0;
TF54 = 0;

% Deeth_Feed_Flow with Reboiler_Valve_Pos
TF64 = tf([0.3628],[1 10.06 0.5412]);
TF74 = 0;

%% 6. Reboiler SIMO

% Reboiler_Temp with LCNRVP.PV
TF13 = tf([-0.004852],[1 0.3151 0.04709 0.00415]);

% Reboiler_Temp with Debut_Diff_Press
TF23 = tf([0.0009339],[1 0.3965 0.06791]);

TF33 = 0;

TF43 = 0;

TF53 = 0;

% Reboiler_Temp with Reboiler_Valve_Pos
TF63 = tf([0.6714],[1 5.496 0.6714]);

% Reboiler_Temp with Debut_Tray_24_Temp
TF73 = tf([0.01305],[1 0.5266 0.08758]);

%% 7. Reflux SIMO
TF12 = 0;

% Reflux_Flow with LPG_C5
TF22 = tf([-0.004903],[1 1.638 0.2383]);

TF32 = 0;

TF42 = 0;

```

```

% Reflux_Flow with Debut_Diff_Press
TF52 = tf([0.008285],[1 0.2468 0.02035]);

% Reflux_Flow with Reboiler_Valve_Pos
TF62 = tf([0.1951],[1 0.3764 0.3902]);

% Reflux_Flow with Debut_Tray_24_Temp
TF72 = tf([0.2693 -0.1926 -0.0219 -0.005952],[1 1.764 1.752 0.5189 0.09789
0.008874]);

%% 8. OVHD Pressure SIMO
% Ovhd_Press with LCNRVP.PV
TF11 = tf([0.001241],[1 0.8456 0.1968 0.01438]);

% Ovhd_Press with LPG_C5
TF21 = tf([-0.0001665],[1 0.3112 0.141]);

% Ovhd_Press with Ovhd_Drum_Press
TF31 = tf([0.3791],[1 1.451 4.211 0.6576]);

% Ovhd_Press with Ovhd_Drum_Press_SV-PV
TF41 = tf([4.536],[1 18.06 8.779]);

% Ovhd_Press with Debut_Diff_Press
TF51 = tf([-0.01348],[1 1.041 0.2387]);

% Ovhd_Press with Reboiler_Valve_Pos
TF61 = tf([-0.302],[1 6.456 2.517]);

% Ovhd_Press with Debut_Tray_24_Temp
TF71 = tf([0.0009007],[1 0.2369 0.0351]);

%% OVHD Pressure SIMO -
Overhead_Press_Model = tf([1],[5 1]);

Reflux_Flow_Model = tf([1],[5 1]);

Reboiler_Temp_Model = tf([1],[5 1]);

De_Eth_Feed_Model = tf([1],[5 1]);

C105_Press_Model = tf([1],[5 1]);

De_Eth_Temp_Model = tf([1],[5 1]);

LCNRecylce_Flow_Model = tf([1],[5 1]);

%%=====end=====%%

```



## Appendix B – MATLAB script file for the second order debutanizer model and IMC controller design

```
% In this script file, a second order debutanizer distillation process
% model is built from single-input single-output (SISO) transfer function
% models identified with the System Identification Toolbox.
% Furthermore, the PID controller gains are computed using the
% Internal Model Control (IMC) technique.

clc
clear

%% The SISO transfer function relating the O/H pressure with the LCN RVP.
num12 = [0.001241];
den12 = [1 0.8456 0.1968 0.01438];
TF12 = tf(num12,den12);

%The SISO transfer function relating the O/H pressure with the LPG C5
composition.

num22 = [-0.0001665];
den22 = [1 0.3112 0.141];
TF22 = tf(num22,den22);

%% The SISO transfer function relating the Reboiler with the LCN RVP.
num11 = [-0.004852];
den11 = [1 0.3151 0.04709 0.00415];
TF11 = tf(num11,den11);

%% The SISO transfer function relating the Reboiler with the LPG C5
composition.
num21 = [0.0009339];
den21 = [1 0.3965 0.06791];
TF21 = tf(num21,den21);

% The Decouplers for the MIMO model using simplified decoupling are
calculated
D12 = -TF12/TF11;

D21 = -TF21/TF22;

% The apparent plant following the implementation of decoupling controllers

Gp11 = zp(tf(TF11 + TF12*D21));
```

```

Gp22 = zpk(TF22 + TF21*D12);

%% Create the symbolic transfer function 's' to be used in the creation of
polynomials
s = tf('s');

%% The model is reduced using the method proposed by A.J. Isaksson and S.F.
Graebe
% Non-minimum phase part of the reduced model for Gp11.
Gp11_zero = (-0.806*s+1);

%Invertible minimum phase part of the reduced model is inverted.
Gp11_approx = 1/(43.103*s^2 + 5.784*s + 1);

%The inverse of the approximate model
Gp11_approx_inverse = 1/Gp11_approx;

%The lamda is used as a tuning parameter as part of the filter
Filter_lamda_11 = -50;

%The first order IMC filter
Filter_11 = 1/(Filter_lamda_11*s+1)^1;

% IMC Controller
IMC_Q11 = zpk(Gp11_approx_inverse*Filter_11);

%Feedback closed-loop controller
Controller_Gc11 =zpk(IMC_Q11/(1-Gp11_approx*IMC_Q11));

% Algebraic simplification of the controller to solve for the PID gains
Constant_1_11 = -0.86206;
Constant_2_11 = Constant_1_11*0.1342;
Constant_3_11 = Constant_1_11*0.0232;
Constant_4_11 = Constant_1_11*1;

%PID gains
Kp_11 = Constant_2_11;
Ki_11 = (Constant_3_11/Constant_2_11);
Kd_11 = Constant_4_11/Constant_2_11;

```

```

%% The model is reduced using the method proposed by A.J. Isaksson and S.F.
Graebe
% Non-minimum phase part of the reduced model for Gp22
Gp22_zero = (-0.806*s+1);

%Invertible minimum phase part of the reduced model is inverted.
Gp22_approx = 1/(6.798*s^2 + 2.182*s + 1);

%The inverse of the approximate model
Gp22_approx_inverse = 1/Gp22_approx;

%The lamda is used as a tuning parameter as part of the filter
Filter_lamda_22 = -0.015;

%The first order IMC filter
Filter_22 = 1/(Filter_lamda_22*s+1)^1;

% IMC Controller
IMC_Q22 = Gp22_approx_inverse*Filter_22;

%Feedback closed-loop controller
Controller_Gc22 = zpkm(IMC_Q22/(1-Gp22_approx*IMC_Q22));

% Algebraic simplification of the controller to solve for the PID gains
Constant_1_22 = -453.2;
Constant_2_22 = Constant_1_22*0.321;
Constant_3_22 = Constant_1_22*0.1471;
Constant_4_22 = Constant_1_22*1;

%PID gains
Kp_22 = Constant_2_22;
Ki_22 = (Constant_3_22/Constant_2_22);
Kd_22 = Constant_4_22/Constant_2_22;

%%=====End=====

```

## Appendix C – Hardware Specifications

Table C.1 shows the specifications of the Beckhoff PLC while Table C.2 shows the specifications of the CompactRIO both of which are utilized in the development of this thesis.

**Table C.1: Beckhoff Embedded Controller (PLC)** (Beckhoff, 2021)

Item	Specification
Power supply	24 V DC (-15 %/+20 %)
Current supply E-bus/K-bus	2 A
Max. Power loss	12.5 W (including the system interfaces)
Processor	Processor Intel® Atom™ Z530, 1.6 GHz clock frequency (TC3: 40)
Flash memory	128 MB Compact Flash card (optionally extendable)
Internal memory	512 MB RAM (optionally 1 GB installed ex-factory)
Interfaces	2 x RJ45, 10/100/1000 Mbit/s, DVI-D, 4 x USB 2.0, 1 x optional interface
Operating systems	Microsoft Windows Embedded CE 6 or Microsoft Windows Embedded Standard 2009
Control software	TwinCAT 3
Dimensions (W x H x D)	100 mm x 106 mm x 92 mm
Weight	approx. 575 g
Operating/storage temperature	-25...+60 °C/-40...+85 °C

**Table C.3: National Instruments Compact-RIO NI-cRIO-9063** (National Instruments, 2015)

Item	Specification
Processor	Xilinx Zynq-7000, XC7Z020 All Programmable SoC. ARM Cortex-A9 architecture. 667 MHz speed. 2 cores. 100,000 cycles flash reboot endurance.
Operating System	NI Linux Real-Time (32-bit)
Application software	LabVIEW 2014 SP1 or later, LabVIEW Real-Time Module 2014 SP1 or later, LabVIEW FPGA Module 2014 SP1 or later
Driver software	NI-RIO Device Drivers 14.5 or later
Memory	512 MB Nonvolatile memory 256 MB Volatile memory (DRAM)
Network	10Base-T, 100Base-T, 1000Base-T Ethernet Network interface IEEE 802.3 Compatibility 10 Mbps, 100 Mbps, 1,000 Mbps autonegotiated, half/full-duplex communication rates 100 m/segment maximum cabling distance
Power Requirements	9 VDC to 30 VDC voltage input range 30 VDC maximum reverse-voltage protection 18 W maximum power input, with four C Series modules 14 W maximum power input, without C Series modules